Vol 12 • No. 2 • October 2018

ISSN: 0976 - 1330

Journal of GEOMATICS

INDIAN SOCIETY OF GEOMATICS

Journal of Geomatics

(A publication of the Indian Society of Geomatics)

Editorial Board

Advisory Board

Indian Society of Geomatics
Executive Council 2017 – 2020

Secretary: (address for correspondence)
6202, SAC Bopal Campus, Ahmedabad – 380058, India
Email: secretary@isgindia.org; sasharma@sac.isro.gov.in

Journal of Geomatics

(A Publication of the Indian Society of Geomatics)

Vol. 12. No. 2 Research articles October 2018

Journal of Geomatics Vol 12 No. 2 October 2018

Assessment of the forest cover change in the Forest-Savannah transitional zone, Ghana between 1990 – 2013 using remote sensing and GIS

Alex Barimah Owusu and Faustina Essandoh-Yeddu
Department of Geography and Resources Development, University of Ghana, Legon
Email: owusuba@yahoo.com

(Received: Feb 21, 2018; in final form: Oct 08, 2018)

Abstract: Anthropogenic activities such as agriculture, mining, construction, and others have acted as alteration agents on landscapes and have over the years had an intense effect on forest cover. Since forest cover and its changes can dramatically affect soil, water quality, and water supply, Ghana faces difficult choices if it is to support rational and optimal use of its remaining forest resources. This study sought to draw attention to the major changes that have occurred in the forest cover of the forest-savannah transitional zone of Ghana over the past two decades (1990–2013). It also addresses causes and impacts and proposes approaches to address the root cause of the problems using multi-temporal remote sensing data and Geographic Information System-based techniques. The key findings include a big decline in forest of the area over the past 20 years. From the survey conducted, over 80% of respondents believe that the main driver of the declining forest cover is anthropogenic in nature. It is proposed that effective, sustainable, and environmental-friendly forest management policies be implemented through inclusive participation of key stakeholders in planning and management of forest and its resources.

Keywords: Forest cover, forest-savannah transitional zone, remote sensing, land-use and land-cover change (LULC)

1. Introduction

Large portions of forest landscapes on the Earth's surface have been significantly altered or tampered with, in some manner by humans (Yang, 2003). The leftover forest ecosystems in West Africa including Ghana, have a lot of natural endowments (e.g. wood and non-wood forest products) and provides regulating services (e.g. climate, water and disease regulation) that are important for economic development and for sustainability of livelihood supporting systems (Locatelli et al., 2008; Seppälä, 2009; Tachie-Obeng et al., 2009; Locatelli et al., 2011). The forests' ability to continue to provide these services and perform other functions is mostly determined by climatic conditions and human interference (Tachie-Obeng et al., 2009; 2010). Anthropogenic activities such as agriculture, mining, deforestation, construction, and shifting patterns of land use are primary components of many current environmental concerns as land-use and land-cover (LULC) change is gaining recognition as a key driver of forest cover change (Frimpong, 2011).

The condition of Ghana's forest cover is not different. It has been deteriorating for many years, particularly since the 1970. Gyasi (1993) argues that in Ghana, there is an evidence of accelerated environmental change. The change is most noticeable in the soils, flora and fauna, which appears to be increasingly endangered in the entire agroecological zones, including the mosaic of forest-savannah (Benneh et al., 1990). Over the years, there has been a progressive decline in size, quality and number of forest reserves. They are heavily encroached and degraded and the off-reserve carbon stocks are being rapidly depleted (GFIP, 2012). Many published works, national and international policy documents, suggest that Ghana's forest zone (roughly 8.6 million ha) was intact around 1880 (Fair, 1992; Ebregt, 1995; Parren and de Graaf, 1995). The fact that there is only about 1.7 million ha of forest today, which exists only in reserves and that only about half of these are themselves in "reasonably good condition" suggests a precipitous decline. Thompson (1910) found in a survey of Ghana's forests that, "comparatively few tracts are covered with so-called primeval or virgin forest; the majority consist of secondary irregular growth that has sprung up in areas previously cleared for farms" (Thompson, 1910). Land-use practices at the local and regional levels have had dramatic effects on soil condition as well as water quality and water supply, which in turn have shown impact on vegetation cover, particularly forest cover. According to Gyasi (1993) before 1850, most of the present southern sector of the forest-savannah zone consisted of virtually uninhabited virgin high forest owned largely by the Akyem people. However, most of the forests, in the late twentieth century were not in good condition.

Verbal accounts suggest that areas now well within the moist, semi-deciduous forest zone (e.g. 30 km south of Sunyani) had extensive grasslands everywhere (Fairhead and Leach, 1998; 2010).

Ghana faces difficult choices if it is to support rational and optimal use of the remaining forest resource. The problems are familiar to most stakeholders, including government, civil society, the private sector, and the donor community. The development and implementation of sound and effective responses have proved challenging. Perhaps a good graphical presentation of the spatial extent and a convincing argument on the destruction of the forest cover, particularly the transitional zones where likely regeneration of forest, when degraded is close to zero, will serve as a clarion call for action. This age of space technology (environmental remote sensing) provides an opportunity for visualizing and quantifying the extent of forest degradation that are compelling to generate action.

The study envisages therefore carefully articulating the major changes to forest cover of the forest-savannah transitional zone of Ghana, its causes and impact and

proposing approaches to address the root cause of the problems.

Questions addressed in this study are stated thus;

- What was the state of the forest 20 years ago?
- How much has the forest cover changed over the past 20 years?
- What are the primary drivers of the forest cover change within the study period?
- What is the impact of change on livelihood of the people?

It is therefore expedient that, this study tries to assess the forest cover change and trends in the forest-savannah transitional zone of Ghana from 1990- 2013.

1.1 Forest, forest cover change and implications for livelihood sustainability

The forest is known to be a valuable source of food, fibre, bio fuel, shelter and other bio-products. It provides the needs of the rapidly increasing world population, which is expected to reach 9 billion by 2050. Also, global records indicate that the total value of wood removals in 2005 was USD 64 billion whilst fuel wood brought in an additional USD 7 billion (FAO, 2005). Forest cover also plays an essential role for a country's economic growth and development but most often its importance is undermined and underutilized. Forests provide several raw materials for many industries including the paper and the construction industries. They also provide a multitude of raw materials for domestic industries and for export (FAO, 1994). In addition, forests play a critical role in regulating the world's climate and provide a variety of functions for people, including ecological, economic, social and aesthetic functions (Frumkin et al., 2017). A study found that the forestry sector provides employment for about 10 million people in the formal sector and 30 to 50 million people in the informal sector across the developing countries. Similarly, it is estimated that in Ghana, the forestry sector accounted for 2% of GDP in 2012, although it represented a decline from 8%, a decade ago.

The forest plays a crucial role in maintaining ecological balance on earth. It is among the most important repositories of terrestrial biological diversity and offers diverse habitats for various species of plants, animals and micro-organisms (FAO, 2017). Forest cover is also a major player in sustaining water sheds, carbon management, clean air and the conservation of critical species and ecosystems (United States Department of Agriculture, 2012). Hence, forests are crucial in maintaining biodiversity and the earth's ecosystem in general.

In spite of the quintessential role of forest, there is a growing concern about the rate and direction of forest cover change in recent years. The increase in population globally is presently at a rate of 1.11% estimated at 80 million per year (Worldometers, 2017) and has therefore attracted the need to clear up forest spaces and turn them to habitable and economic ventures for man. Due to population growth, there has been a drastic reduction in forest cover over the past century. Over 129 million ha of forest (an area almost equivalent in size to South Africa) have been lost since 1990, according to FAO (2015). Numerous studies used global remote sensing data to highlight the fact that during the last decade, forests in the tropics have been rapidly declining (DeFries et al., 2002). Recent estimates indicate a decline of 5.5m hectare of forests per year between 2010 and 2015 in the tropics (Romijn et al., 2015). However, Africa and South America had the highest net annual loss of forests in 2010-2015, with 2.8 and 2 million ha respectively (FAO, 2017).

The dominant causes of the changes in forest cover include: the clearing of forest lands for agriculture, especially for cash crops such as cocoa, coffee, oil palm and rubber plantations; the loss of forest lands to settlements and the exploitation of forests for timber and non- timber products (FAO, 2017). These changes in forest cover have various implications on livelihood sustainability and development. The changes in forest cover disrupt the global water cycle (Chakravarty et al., 2012). Hence the gradual depletion of the forest cover implies that the region cannot hold as much water thereby creating a drier climate. Water resources affected include drinking water, fisheries and aquatic habitats, flood/drought control, waterways and dams affected by siltation, less appealing water-related recreation, and damage to crops and irrigation systems from erosion and turbidity (Chakravarty et al., 2012). These are directly affecting agro biodiversity and aquatic life thereby affecting those that depend on it for livelihood and economic purposes. The mismanagement of our forest resources also inhibits potential future revenues and future employment that could be derived from their sustainable management for timber and non- timber products. These concerns have created a much wider global concern and the need to know attitude as a precursor to any effort at addressing forest cover change. Practitioners, researchers and politicians have all come to this realization and hence the renewed global efforts focusing on ways to know what and where of forest cover change.

Systematic field sampling and remote sensing technology have been the pillars of data collection in monitoring and assessing forest cover change. Field data collection is done continuously or periodically on permanently established sample sites to assess changes and trends of forest resources and characteristics. Remote sensing is used to map the extent and spatial distribution (fragmentation and contiguity) of the forests and land uses based on a stable classification system for change analysis and integration with field data (Tavani et al., 2009).

Traditional method of Surveying and taking inventory of trees originated in Europe in the late 18th century out of a fear that wood (the main source of fuel) would run out. The first information was organized into maps used to plan usage. In the early 19th century forest harvesters estimated the volume and dispersal of trees within smaller forests with their eyes. More diverse and larger forests were divided into smaller sections of similar type trees that were individually estimated by visual inspection. These estimates were related together to figure out the entire forest's available resources. Hence, these were not

effective since such surveys could not cover a wide area due to the impenetrability of the forest. Over the years, the inventory for forested regions has been greatly influenced by political agendas. For almost 40 years after the Second World War, ample forest inventory data were collected to provide information needed for forest management at the local level, but forest information at the national level was of secondary importance (Reddy et al., 2013).

Capacities of tropical countries to monitor forests and forest cover change were limited in the past change in the sustainable wood production capacity of the world's forests, including industrial wood and fuel wood at a global level of a potential is missing, as is knowledge about actual harvests and needs, to be compared to that potential. However, through capacity building efforts capacities are strengthening at technical, political and institutional levels (Herold and Skutsch, 2011; Romijn et al., 2015). A few countries like Mexico and India had well developed national forest monitoring systems even in past times. Other countries are in the process of developing capacities and are at various stages of development, they need considerable capacity improvements before they are able to produce accurate estimates of forest area, forest area change and carbon stock change (Tulyasuwan et al., 2012). In more recent years the use of remote sensing technology which involves measuring or acquiring information about surface properties using sensors typically found onboard aircraft or satellites has gained momentum. Remote sensing provides a systematic, synoptic view of earth cover at regular time intervals and useful for changes in land cover and to reveal aspects of biological diversity directly (Turner et al., 2003; Cohen and Goward, 2004; Alqurashi and Kumar, 2013). Estimates of change in forest cover based on satellite data can help researchers to understand the likely outcomes in terms of carbon dynamics**,** climate change and threats to biodiversity. Satellite data, particularly Landsat TM (Thematic Mapper) and ETM+ (Enhanced Thematic Mapper plus) series of sensor, have been important tools in the interdisciplinary study of tropical forests that are increasingly integrated into studies that monitor changes in vegetation cover within tropical forests and tropical protected areas and also applied with other types of data to investigate the drivers of land cover changes (Trigg et al., 2006; Kumar et al., 2010; Alqurashi and Kumar, 2013). Remote sensing technologies have been effective in monitoring forest cover changes in regions such as the Amazon basin (Skole and Tucker, 1993) and the Gunung Palung National Park in West Kalimantan, Indonesian Borneo (Trigg et al., 2006).

2. Methodology

2.1 Study area

The study area consists of six political administrative districts in the Brong-Ahafo region which fall within the Forest Transitional Zone of Ghana (Figure 1). The districts include: a) Berekum Municipal, b) Tano North, c) Dormaa East, d) Dormaa Municipal, e) Sunyani West, and f) Sunyani Municipal. The total land area covered by the study area is approximately 526,400.28 ha. It lies between Latitudes 7^0 20'N and 7^0 05'N and Longitudes 2^0 30'W. It falls largely within the Moist – Semi Deciduous Forest Vegetation Zone. The area forms the transitional zone between the forest zone of the south and the savanna zone in the north. The vegetation zone covers forests with timber species, tree crops such as cocoa, citrus, and others. Because of lumbering and farming practices, most of the forest areas have been degraded. Re-afforestation is therefore being undertaken in the forest reserves to reverse the trend.

The average rainfall between 2000 and 2009 was 88.987 cm. The area experiences a double maxima rainfall pattern. The main rainy season is between March and September with the minor between October to December. This offers two farming seasons in a year which supports higher agricultural production in the area. However, the rainfall pattern of the study area is decreasing over the years because of deforestation and depletion of water bodies caused by human activities. The area falls within the Wet Semi-Equatorial Climatic Zone of Ghana, with the mean monthly temperatures varying between 23 ºC and 33 ºC with the lowest around August and the highest being observed around March and April.

2.2 Data and data analysis

The use and management of forest resources need to be based on the mapping and inventory of the forestry environment. Similarly, the changing state of the forest, as a result of natural or human-induced causes (felling, clearing, fire, reforestation decline, regeneration, etc.), also need to be monitored. Remote sensing and GIS provide for the continuous monitoring of forest developments by detecting changes and integrating results into existing databases (FAO, 1999). The aim of this paper was to determine the forest cover change from 1990 through 2000 to 2012. Landsat images were used to determine the changes that have occurred. Secondary data was collected to aid in identifying land use or cover of the location and was also used in comparison and verification and to update to what was shown on the image.

In addition, primary data was collected from the field. About 40 key informants including the youth (both male and female) were interviewed. It was backed by focus group discussions to find out the state of the forest now and years back. The respondents were purposively selected, thus from among farmers or indigenes who had worked or lived in the community for over 10 years. Figure 2 is a workflow showing steps in involved in the processing of the satellite images for the study.

In addition, primary data was collected from the field. About 40 key informants including the youth (both male and female) were interviewed. It was backed by focus group discussions to find out the state of the forest now and years back. The respondents were purposively selected, thus from among farmers or indigenes who had worked or lived in the community for over 10 years. Figure 2 is a workflow showing steps in involved in the processing of the satellite images for the study.

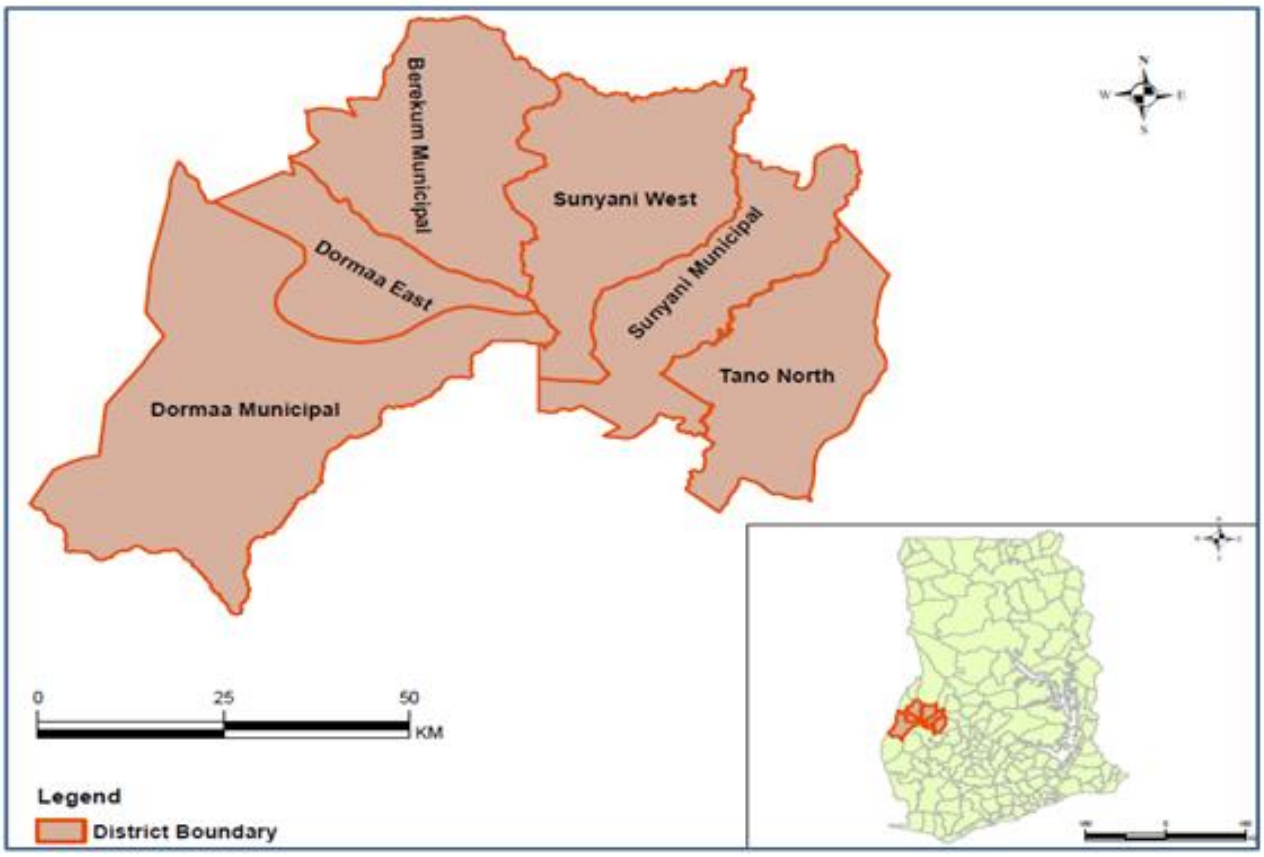

Figure 1: Map of the study area

Calibrations: Digital images collected from space borne sensors often contain systematic and unsystematic geometric errors. Geometric corrections are conversion of data to ground coordinates by removal of distortions due to the Earth's curvature and sensor motion. They are very necessary prior to any image analysis. If any measurement distortions are on an image (i.e. direction or distance) it must be rectified (Wireko, 2015). Radiometric calibration was also done. These calibrations were done in Envi 5.3 software using landsat calibration utilities. Further atmospheric calibration was done using FLAASH model in Envi 5.3. geometric calibration was performed using control points obtained from Survey and Mapping Division of Lands Commission. Ground truthing was performed to complement or validate the satellite images.

Development of a Classification Scheme: Based on prior knowledge of the study area, and a brief reconnaissance survey, with additional information from previous research in the study area, a classification scheme was developed for the study area. The classification scheme developed gives a rather broad classification where the land cover was identified by a single digit. Using Envi software, a supervised classification was employed in the classification. It is a procedure for identifying spectrally similar areas on an image by identifying 'training' sites of known targets and then extrapolating those spectral signatures to other areas of unknown targets. Small and discrete areas were used to "train" the classification algorithm to recognize land cover classes based on their spectral signatures, as found in the image. The training areas for any one land cover class need to fully represent the variability of that class within the image. There are numerous factors that can affect the training signatures of the land cover classes. Environmental factors such as differences in soil type, varying soil moisture, and health of vegetation, can affect the signature and affect the accuracy of the final thematic map. In each cover class, samples of between five (5) and eight (8) were selected.

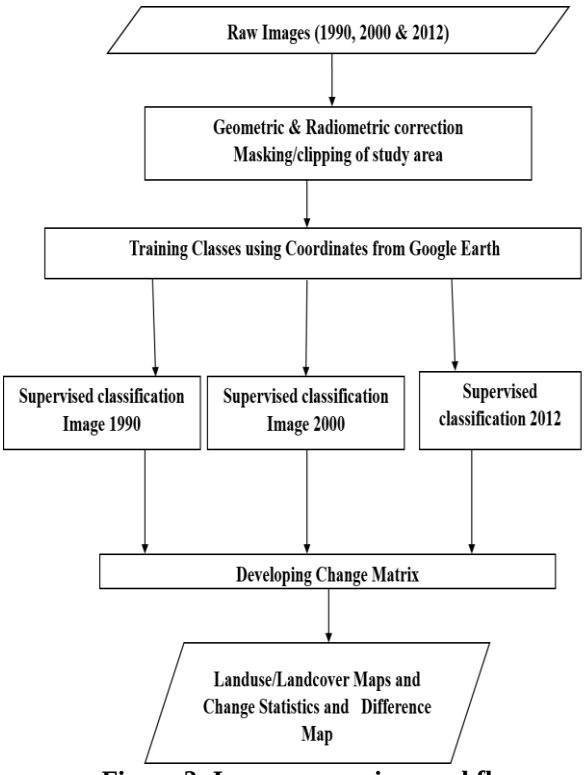

Figure 2: Image processing workflow

These factors were taken into cognisance to help give an accurate classification scheme. Numerous aspects were considered when supervised classification was being conducted. The first was developing an appropriate classification scheme. Training areas must be selected for each of the classes and statistics calculated for them. The appropriate classification algorithm must be selected, and once each pixel in the image (including the ones used as training areas) are evaluated and assigned to a land cover class, the accuracy of the classification has to be assessed. The classification algorithm used was the Gaussian Maximum Likelihood. The sampled training sites were converted into KML and opened in Google high resolution image for validation for accuracy. In all 98% of samples were accurately selected before the classification scheme was accepted and applied. A Gaussian Maximum Likelihood classifier was applied. This method evaluates the variance and co-variance of the various classes when determining in which class to place an unknown pixel. The statistical probability of a pixel belonging to a class is calculated based on the mean vector and co-variance matrix. A pixel is assigned to the class that contains the highest probability.

When the classification was conducted, an accuracy assessment was made to determine how correct the classified image is. An accuracy assessment involves the determination of the overall accuracy of the classification, errors of omission, errors of commission, producer's accuracy, and consumer's accuracy. All measures gave an indication of how well the classification of the image was conducted.

Image Classification: Classification is a process of sorting pixels into finite number of individual classes, or categories of data, based on their data file values. If a pixel satisfies a certain set of criteria, then the pixel is assigned to the class that corresponds to that criterion. Landsat TM/ETM+ image for 3 different years namely 1990, 2000 and 2012 was classified using the supervised classification scheme provided by the ENVI image processing software. This classification was guided by many observations made on the ground. Classified TM pixels were in four basic categories: Water Bodies, Settlement / Bare-grounds, Secondary Vegetation, and Primary Forest (Table 1). It is common practice to make two or more iterations of a classification process, to improve the accuracy of the result. However, with each iteration, the test sites would be edited to better reflect the representation of their class and to remove or reduce any class overlap. In this classification, we made six (6) iterations.

Change detection method was based on post-classification image differencing analysis where classified images of two intervals, are compared pixel by pixel. This method produces pixels under a particular land cover at the beginning year and compare the same pixel of the next year to determine whether the pixel has changed or not. The results are a change matrix of cover types showing from and to cover. The change statistics is a sum of pixels under the cover types at different years and this is interpreted as land cover type before and after, and which are often converted into percentage change.

Table 1: Land cover classification scheme

CODE	LAND COVER CLASS
1	Water Bodies
2	Settlement / Bare-ground
3	Secondary Vegetation
4	Primary Forest

In this study, the primary data from the key informants were analysed qualitatively, in the form of quotations, and samples were used in supporting the discussion

3. Results and discussions

3.1 Forest cover change analysis

The study focused on forest cover change using the 1990 cover as the base year. The comparison of land cover maps of 1990 and 2000 showed a considerable change in primary forest, secondary vegetation, bare ground and this is illustrated in Table 2. There is a clear decrease in primary forest coverage, but increase in land cover types like secondary vegetation, bare ground and water body. However, there are only some negligible changes in water bodies. In summary, there was a total of 169700.85 ha of primary forest in 1990 which reduced to 98574.21 ha, indicating a reduction of -71247.87 ha (-42%) from 1990 to 2000. Also, secondary vegetation changed from a total of 376172.01 ha to 325243.08 (about -13.5%) ha in 2000 to bare-ground or other settlements.

Specifically, as indicated in Table 2, 5.40 ha of water bodies turned to 'secondary vegetation' from 1990 to 2000. About 72619.29 ha of primary forest was maintained from 1990 to 2000, whilst 80130.6 ha and 16938.90 ha changed to secondary vegetation and bare ground respectively. This shows that, there is drastic change happening, mainly to forest vegetation cover. One important analysis that needs to be done is to probe whether these changes are to human and societal benefit. Interestingly, about 25315.47 ha of secondary vegetation was noted to have turned to primary forest, from 1990 to 2000. This could be argued that, some parts of the vegetation contained young trees and scrubs, which without any disturbances for over ten years built into thick vegetative cover. It could also mean that the area was possibly mostly covered with sparse forest in 1990, which now have grown into a dense forest, being a good example of forest improvement.

Dense forest, being a good example of forest improvement. The rate of deforestation is found to be considerably higher than forest improvement as shown table 2. Table 3 compares the cover types between 2000 and 2012. It shows that 18233.67 ha of primary forest changed to secondary vegetation whiles

Table 2: Land cover differencing statistics (1990 – 2000)

Year	1990 - Area (hectares)					
2000 (Final)	Land Cover Class / Cluster	Water body	Bare ground	Secondary Vegetation	Primary Forest	Total
	Waterbody	0.00 (0.00%)	31.59 (0.09%)	108.00 (0.03%)	12.06 (0.01%)	151.65
	Secondary Vegetation	5.40 (100%)	24426.99 (72.64%)	271609.02 (83.51%)	80130.6 (47.22%)	376172.01
	Bare ground	0.00 (0%)	8529.84 (25.37%)	28210.59 (8.67%)	16938.9 (9.98 %)	53679.33
	Primary Forest	0.00 (0%)	639.45 (1.90%)	25315.47 (7.78%)	72619.29 (42.79%)	98574.21
	Total	5.4	33627.87	325243.08	169700.85	528577.2

Table 3: Land cover status by class / cluster (2000 - 2012)

Year	2000 - Area (Hectares)					
2012 (Final)	Land Cover Class / Cluster	Water body	Bare ground	Secondary Vegetation	Primary Forest	**Total**
	Water body	3.24 (2.11%)	612.43 (0.16%)	260.45 (0.48%)	663.46 (0.67%)	**1539.58**
	Secondary Vegetation	14.67 (9.54%)	177745.53 (47.14%)	7565.33 (14.09%)	18233.67 (18.46%)	**203559.20**
	Bare ground	0.00 (0.00%)	10134.57 (2.69%)	26.55 (0.05%)	38145.34 (38.63%)	**48306.46**
	Primary Forest	135.81 (88.35%)	188553.64 (50.01%)	45857.55 (85.38%)	41713.00 (42.24%)	**276260.00**
	Total	**153.72**	**377046.17**	**53709.88**	**98755.47**	**529665.24**

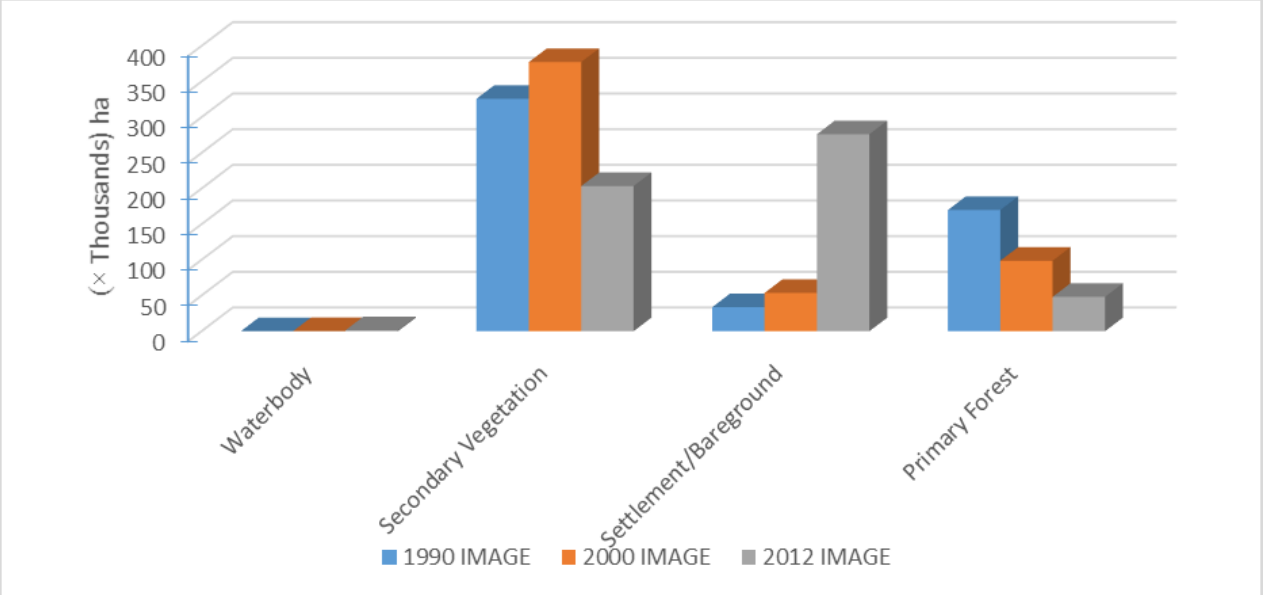

Figure 3: Bar graph comparing changes in land cover types for 1990, 2000 and 2012

The rate of deforestation is found to be considerably higher than forest improvement as shown table 2. Table 3 compares the cover types between 2000 and 2012. It shows that 18233.67 ha of primary forest changed to secondary vegetation whiles 38145.34 ha changed into bare lands. Remarkably, 14.67 ha of water bodies have turned to secondary vegetation and in some cases primary forest from 2000 to 2012. This could be due to growth of vegetation in wetlands and drying up of water bodies, galamsey (Illegal small-scale gold mining) activities destroying river sources etc.

Interestingly, as high as 41713.0 ha of primary forest remained forested for period of 12 years, extending between the year 2000 and 2012. It is remarkable to contend that, people are now appreciating the need to halt the felling of trees and growing new ones to replace already destroyed ones. Again, as high as 10134.57 ha of bare ground remained same between 2000 and 2012. Figure 3 is a bar graph showing comparison between the four land cover types over the years.

Figure 3 shows that in 2000, secondary vegetation increased. This may have been because a lot of forest had been cut down for farming activities like slash and burn', timber, or used for other purposes. It also indicates that primary forest and secondary vegetation are giving way seriously to settlements and bare-ground. Though, the changes in water body appears to be insignificant, key informant respondents were gripped with fear that the rate at which their water sources are drying up while the available few are also being seriously polluted by illegal miners, if care is not taken, may reach crises levels. These, according to the Community members, have led to them to depend on sachet water (filtered and bagged water) for drinking and cooking. The degradation is a big threat to sustainable biodiversity and food security of the country, there is therefore an urgent need for an effective land-use planning that stresses forest restoration and improvement practices. Below are the land cover classification maps of study area (1990, 2000 and 2012) showing the spatial pattern and change.

Figure 4 shows that in 2000, secondary vegetation increased. This may have been because a lot of forest had been cut down for farming activities like slash and burn', timber, or used for other purposes. It also indicates that primary forest and secondary vegetation are giving way seriously to settlements and bare-ground. Though, the changes in water body appears to be insignificant, key informant respondents were gripped with fear that the rate at which their water sources are drying up while the available few are also being seriously polluted by illegal miners, if care is not taken, may reach crises levels. These, according to the Community members, have led to them to depend on sachet water (filtered and bagged water) for drinking and cooking. The degradation is a big threat to sustainable biodiversity and food security of the country, there is therefore an urgent need for an effective land-use planning that stresses forest restoration and improvement practices. Below are the land cover classification maps of study area (1990, 2000 and 2012) figures 3, 4 and 5 respectively, showing the spatial pattern and change.

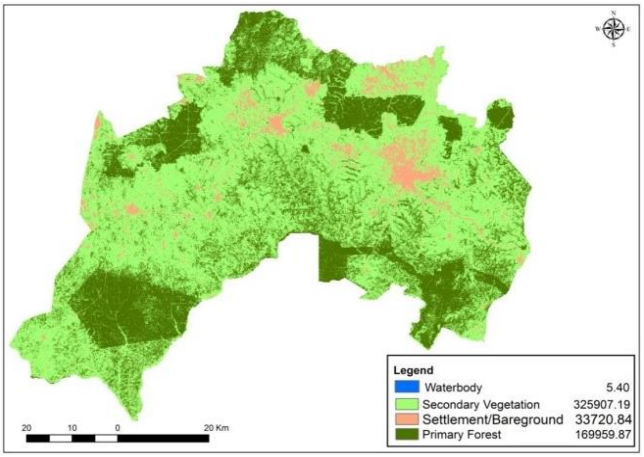

Figure 4: Land cover map of study area - 1990

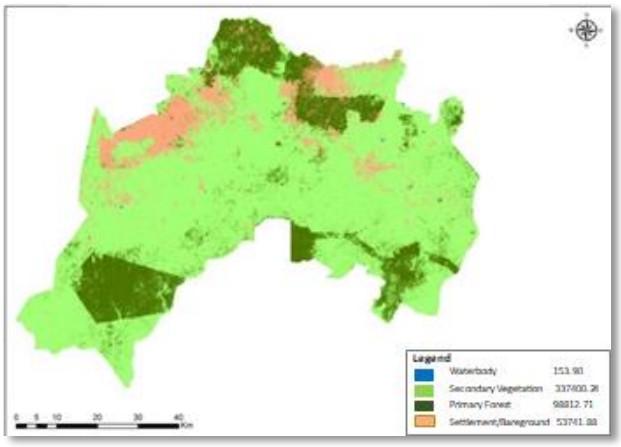

Figure 5: Land cover map for study area – 2000

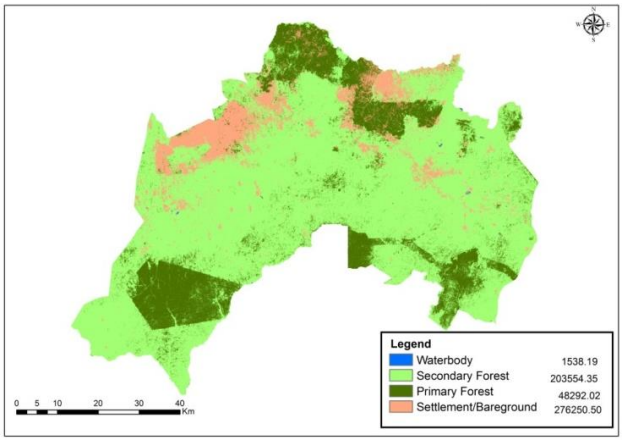

Figure 6: Land cover map of Study Area - 2012

From figure 7 above, a Change Difference Map was used to produce image difference between 1990 and 2012, initial state and final state images (that is, final - initial) and the classes were defined by change thresholds of 6. A positive change shows all areas above the threshold of 6 identifies pixels that became brighter meaning they gained vegetation (final state brightness was greater than the initial state brightness); while a negative change identifies pixels that became dimmer, meaning they lost vegetation (final state brightness was less than initial state brightness). It is clear that primary forest in the area has changed drastically (over 80%) to other forms of cover from 1990 to 2012. Some have turned into secondary vegetation and bare-ground etc. The causal factors include

climatic variations, shortage in rainfall pattern/ periods, increase in built up sections of the community etcetera. These all add up to the vegetation cover changes observed in the study community.

3.2 Local perception of the forest cover change

The study also sought the views and experiences of local residents concerning forest cover change in their area over the last 20 years (1990-2012). The study selected 40 key informants from 20 towns of two (2) participants from each town. Since this section was interested in historical change, the target was two older people of above 70 years; one (1) male and one (1) Female. The selected person was on the recommendation of the District Assembly Man of the town. The person must be a knowledgeable person who can and is willing to share his or her experience. The respondents' views were analysed qualitatively. Their narratives confirmed the observations from the satellite data analysis. It was found that there was a very big decline in forest and moreover, there has been a big change in the state of forest between 20 years ago and now. This is being confirmed by GFIP (2012), that over the years, there has been a progressive decline in size and quality of many forest reserves. They are heavily encroached and degraded and the off-reserve carbon stocks are being rapidly depleted. Furthermore, the condition of Ghana's forests has been in decline for many years, particularly since the 1970s. More than 90% of respondents testified that, in about 20 years ago, the area was within a very thick, heavy forest, with all kinds of timber species and wild animals, not forgetting wild fruits of all kinds.

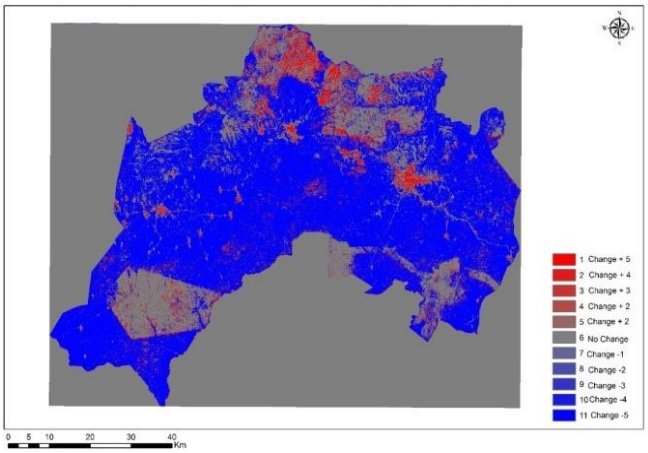

Figure 7: Land cover difference map indicating the changes and trend from 1990 to 2012

The study has been confirmed with the respondents testifying the presence of thick dark forest with many animals. The main crop was cocoa and big timber logs but now, it is said that one can't plant cocoa on large scale as before as the whole area is gradually turning into grass. Figures 8 and 9 show cocoa farms and the current forest cover outlook.

Figure 8 shows a typical cocoa farm in the area, a village about 30 km from Sunyani. It was a common scene and almost every household owned a cocoa farm. Majority (over 80%) of the people claimed they could walk throughout cocoa farms to Sunyani about 40 km and beyond. But now, as shown in Figure 9, the forest is degrading to scrubs and grassland within the last 20 to 30 years. Unfortunately, at present, over 80% of the people think, the forest is depleting and is gradually transiting to savannah and grassland. Majority believe that there is about 30% secondary forest left, which cannot be compared to the virgin forests they saw.

Figure 8: Forest with cocoa farm in study area

Figure 9: The forest is depleting to grassland

One of the respondent also testified the presence of thick forest of about 40 km and used to experience frequent heavy down-pours, that took several days before the ground could dry up while recently, after the rains, the whole place gets dried up quickly. The situation is buttressed by Gyasi (1993) who argues that in Ghana, there is evidence of accelerated environmental change. The change is most noticeable in the soils, flora and fauna, which appear to be increasingly endangered in the entire agro ecological zones, including the mosaic of forest-savannah (Benneh et al.,1990).

To them a larger part of the community forest is turning to shrubs, and some parts gradually becoming bare. They are of the view that, the root cause of the forest depleting is

poverty manifesting in different ways of land use and management practices. Poverty has led to over drawing of the environment as a way of ensuring survival.

3.3 Causes of forest cover change

Over 80% of respondents who said that the forest is seriously deteriorating also believe that the causes are anthropogenic in nature. The major human activities in their view, that are causing deforestation and land degradation in the area include lumbering activities, frequent cutting down of trees for farming thus 'slash and burn', use of chemicals (insecticides and weedicides) for farming, and bush fires among others. This is in line with the UNEP (2000) claim that major direct causes of forest degradation brought on by humans include overharvesting of industrial wood, fuel wood and other forest products, and overgrazing, though forests are also susceptible to natural factors such as insect pests, diseases, fire and extreme climatic events. Lumbering, which destroys hundreds of young trees and farms are of a big concern to the community members. Though, there are bye-laws guiding the mode of their operation currently in the country and in the district, most of the youth are surprisingly engaging in illegal chain-saw operation in felling trees even at night and at times in the middle of the deep forest. It came out that; some pupils drop out of school to indulge in this 'get-rich-quick' chain-saw business to the detriment of their education, which is a major concern for parents, head-teachers and some chiefs. It was found that, the head teacher of the only JHS in Berekum, had to go through the forest to look for school going children in JHS 2 to come and register for the Basic Education Certificate Examinations. There is the need for community forest watch dogs and monitors to control the rate of bush burning.

'Slash and burn', a traditional practice of clearing the land before planting is found to be degrading the land rapidly because of population pressure and land scarcity, 'a cleared piece of land' does not get enough fallow period to rejuvenate. The serious felling of trees and weeding too close to river banks are causing a lot of small streams to dry and the temperatures are too high especially at night. The findings confirmed the argument that, land-use and land-cover changes directly impact biotic diversity worldwide (Sala et al., 2000); contribute to local and regional climate change (Chase et al., 1996) as well as to global climate warming (Houghton et al., 1999).

The study found that the Extension Officers do not visit the farms regularly as expected to sensitize them on important farming practices. About 75% of farmers were of the view that the application of chemicals (insecticides and weedicides) on farms contributes to the deteriorating nature of soil. After the application of the weedicide for a long time, they see the soil looks too dry, with deep cracks and not manageable as before. One of the youth leaders said, he has adopted a strategy of applying the weedicide only once in the crop season, that is just after sowing, but weeds manually with hoes and cutlasses for the subsequent clearings for restoration of nutrients of the soil. They are of the view that, too much chemicals dry-up the soil and could possibly destroy useful bacteria and insects that might be contributing to natural restoration of soil.

Bush burning was also said be initiated by hunters for game meat during the harmattan season, palm-wine tappers, charcoal burners, and at time 'slash and burn' farm preparation strategies, which leads to spread of fires at times beyond control. This causes a lot of destruction of food, property, and at times even human lives. The land becomes very bare, open and dry, with its attendant famine, water shortages, and disease. The root cause of these malpractices was found to be poverty related. One man said, he often depends on hunting during harmattan to pay the school fees of his children, and to him, it is lucrative. He argued that in order to stop him from doing that, he would need to be offered an alternative livelihood source, which he is familiar with. This buttresses an existing position made that 'high rates of deforestation within a country are most commonly linked to population growth and poverty, and shifting cultivation in large tracts of forests (Mather and Needle, 2000). Further, Murphree, (1993) has also stressed that poverty is identified as both the cause and the effect of forest degradation.

Most people in rural settings especially women, still use fuel wood for cooking since they don't have access to liquefied petroleum gas. Most of them cannot afford and it appears not to be reliable because it could run short in supply at any time.

3.4 Impact of forest cover change on livelihood and eco-system services

The impact of deforestation and change in forest cover is huge. Almost, all respondents of key informant interviews mentioned that, the changes have made their farming activities difficult. There has been decline in yields due to low fertility in soil. This has led to poor sales and therefore income and grass took over all the farm produce.

Years back, there were a lot of ecosystem services like easy access to game, snails, mushrooms, and wild fruits according to their seasons. These served as reliable food security/ supplement, and reliable source of income for many families. It agreed with the philosophy that economic development is a prerequisite for sustainable natural resource use (Mellor, 1998). However, with depletion of the forest, all these services and benefits are being waded-off. Further, it came out clearly that, it was becoming extremely difficult for hunters to get animals during hunting.

There are reports of excessive heat, changes in temperature and rainfall pattern forcing farmers to adapt coping strategies and these are all signs of climate change and variability. This is also affecting the forest cover. Such changes also determine, in part, the vulnerability of places and people to climatic, economic or socio-political agitations (Füssel, 2010).

3.5 Specific recommendations

The forest is seriously depreciating/depleting, from all indications from the field report and satellite data analysis and as the adage goes, when the last tree dies, then the last

man dies, so the question is: what needs to be done to reverse the situation? As such the study recommends the need for all stakeholders to come together to strategize, prioritize and plan strategically for forest and environmental management for sustainable livelihoods and development. Below are some specific recommendations for sustainable forest management and development:

- There is the need for re-enforcement of the forest guard policy to protect the forest. The communities involved could also form watchdog committee to monitor, to strengthen policy efforts on illegal felling of trees, as well as show their commitment for a good cause.
- There is the need for a massive community sensitization and education on forest and environmental management. Community members should understand and appreciate the meaning and benefits of sustainable forest management, through participatory approaches to get them understand as well as to own the processes.
- Through participatory strategies, the government, NGOs, Development partners etc. should bring in feasible terms for farmers on input supply (for example, fertiliser, and weedicides), soft loans/ credit on flexible payment terms.
- Reforestation and afforestation programs with community participation on a profit sharing basis and improvement in technology and management of plantation are required.
- Agricultural Extension Officers should have regular days of visiting farmers at home or on farms to do educational programmes as well as creating access to good practices on the ground.
- There should be alternative livelihoods measures put in place, like gari processing, bread making for women, vocational skills for the youth, etc.
- It is important that policy considers 'social security scheme' for farmers, scholarships for the needy but brilliant children, especially farmers' wards.
- Putting in place laws to regulate tree cutting, bush fires - during the dry season, which destroys our forest, so that small trees/plants will grow to replace old ones in 10 years. Hunters should stop hunting for animals in bush through bush burning and they must be monitored.

4. Conclusion

In the interest of sustainable development, and forest sustainability, the study has been able to assess the change in the forest cover of the Forest-Savannah Transitional Zone of Ghana over the past two decades (1990–2013). It established that, there has been a big decline in forest cover over the study period. Larger part of the study areas was found to be in thick forest in 1990s but are now fast depleting into savannah, which should be a serious concern. About 90% of respondents testified that, about 20 years ago, dense forests covered larger parts of the study area, with all kinds of timber species and wild animals, and wild fruits. However, the forest is depleting and is gradually transiting to grassland. Majority also believe that only about 30% of virgin forests of the past exist in present days.

The main cause has been identified as anthropogenic, thus felling of trees, use of fire for land preparation and for hunting, use of agro-chemical, and infrastructural development. To them a larger part of the community's forest is turning to shrubs, and some parts are gradually becoming bare or being used for other purposes. In some few cases however, it was found that other vegetative areas got converted to forest, which may be due to good forest management practices. The best way in keeping our forest for generations to come, is through participatory forest management practices that is guided by environmentally friendly policies.

References

Alqurashi, A. F and L. Kumar (2013). Investigating the use of remote sensing and GIS techniques to detect land use and land cover change: A review. Advances in Remote Sensing, 2(02), 193.

Benneh, G., G.T. Agyepong and J.A. Allotey (1990). Land degradation in Ghana. Food Production and Rural Development Division.

Chakravarty, S., S. K. Ghosh, C. P. Suresh, A. N. Dey and G. Shukla (2012). Deforestation: causes, effects and control strategies. In Global perspectives on sustainable forest management. InTech.

Chase, T. N., R. A. Pielke, T. G. Kittel, R. Nemani and S. W. Running (1996). Sensitivity of a general circulation model to global changes in leaf area index. Journal of Geophysical Research: Atmospheres, 101(D3), 7393-7408.

Cohen, W.B and S. N. Goward. (2004). Landsat's role in ecological applications of remote sensing. Bioscience 54(6):535-545. Committee of Scientists. 1999. ... U.S. Department of Agriculture, Washington, DC [online]. Available: http://www.fs.fed.us/news/news_archived/ science/cosfrnt.pdf

DeFries, R. S., R. A. Houghton, M. C. Hansen, C. B. Field, D. Skole and J. Townshend (2002). Carbon emissions from tropical deforestation and regrowth based on satellite observations for the 1980s and 1990s. Proceedings of the National Academy of Sciences, 99(22), 14256-14261.

Ebregt, A. (1995). Report in Tropical Rainforest and Biodiversity Conservation in Ghana. The Netherlands: Dutch Government Ministry of Foreign Affairs Directorate General for International Cooperation, 42.

Fair, D. (1992). Africa's rain forests – retreat and hold. Africa insight 22(1), 23-28.

Fairhead, J and M. Leach (1998). Reframing deforestation: global analyses and local realities with studies in West Africa Psychology Press.

Fairhead J and M. Leach (2010). Ghana International Development Centre of the University of Oxford, UK, Reconsidering the extent of deforestation in twentieth century West Africa.

FAO, (1994). Year Book of Forest Products. https://www.fao.org/docrep/014/W04607/W0460T00.htm

FAO, (1999). Remote Sensing for Decision-makers Series, No. 15, "Satellite imagery to assist forest management - Pilot study in Morocco, FAO Publications.

FAO (2005). Global Forest Resource Assessment update 2005. The State of World's Forests. https://www.fao.org/3/a-y5574e.pdf
FAO, (2015). The Global Forest Resources Assessment 2015: Desk Reference. FAO. Rome, Italy.

FAO (2017). from http://www.fao.org/resources/infographics/infographics-details/en/c/325836/

Frimpong, A. (2011). Application of Remote Sensing and GIS for Forest Cover Change Detection. (A Case Study of Owabi Catchment in Kumasi, Ghana) (Doctoral dissertation).

Frumkin, H., G.N. Bratman, S.J. Breslow, B. Cochran, P. H. Kahn Jr, J. J. Lawler and S.A. Wood (2017). Nature contact and human health: A research agenda. Environmental Health Perspectives, 125(7), 075001-1. https://doi.org/10.1289/ehp1663

Füssel, H. M. (2010). Review and quantitative analysis of indices of climate change exposure, adaptive capacity, sensitivity, and impacts. Background note to the World Development Report, 34.

GFIP (2012). Ghana Forest Investment Plan. Ministry of Lands & Natural Resources and Forestry Commission in collaboration with: Ministries of Environment, Science & Technology and Finance & Economic Planning, Accra, Ghana.

Gyasi, E.A. (1993). Pilot study of production pressure and environmental change in the forest-savannah zone of southern Ghana, University Press.
https://doi.org/10.1016/0959-3780(95)00070-5

Herold, M and M. Skutsch (2011). Monitoring, reporting and verification for national REDD+ programmes: two proposals Environ. Res. Lett., 6, 1-10. 10.1088/1748-9326/6/1/014002

Houghton, R. A., J. L. Hackle and K. T. Lawrence (1999). The US carbon budget: contributions from land-use change. Science, 285(5427), 574-578. https://doi.org/10.1126/science.285.5427.574

Kumar, D., S. Borah and U. Shankar, (2010). Monitoring forest cover change using remote sensing in Amchang Wildlife Sanctuary, Assam, India. Communicated Data.

Locatelli, B., V. Evans, A. Wardell, A. Andrade and R. Vignola (2011). Forests and climate change in Latin America: linking adaptation and mitigation. Forests, 2(1), 431-450. https://doi.org/10.3390/f2010431

Locatelli, B., M. Kanninen, M. Brockhaus, C. P. Colfer, D. Murdiyarso and H. Santoso (2008). Facing an uncertain future: How forests and people can adapt to climate change. https://doi.org/10.17528/cifor/002600

Mather, A.S and C. L Needle (2000). The relationships of population and forest trends. The Geographical Journal, 166(1), 2-13. https://doi.org/10.1111/j.1475-4959.2000.tb00002.x

Mellor, D.H. (1998). The facts of causation. Psychology Press.
https://doi.org/10.4324/9780203302682

Murphree, M.W. (1993). Communities as resource management institutions (pp. 1-15). London: IIED.

Parren, M.P and N.R. de Graaf (1995). The quest for natural forest management in Ghana, Côte d'Ivoire and Liberia. Stitching Tropenbos.
https://doi.org/10.1080/00382167.1996.9629894

Reddy, C.S., C.S. Jha and V.K. Dadhwal (2013). Assessment and monitoring of long-term forest cover changes in Odisha, India using remote sensing and GIS. Environmental monitoring and assessment, 185(5), 4399-4415. https://doi.org/10.1007/s10661-012-2877-5

Romijn, E., C.B. Lantican, M. Herold, E. Lindquist, R, Ochieng, A. Wijaya and L. Verchot (2015). Assessing change in national forest monitoring capacities of 99 tropical countries. Forest Ecology and Management, 352,109-123.
https://doi.org/10.1016/j.foreco.2015.06.003

Sala, O.E., F.S. Chapin, J.J. Armesto, E. Berlow, J. Bloomfield, R. Dirzo and R. Leemans (2000). Global biodiversity scenarios for the year 2100. Science, 287(5459),1770-1774.
https://doi.org/10.1126/science.287.5459.1770

Seppälä, R. (2009). Adaptation of forests and people to climate change. IUFRO.
https://doi.org/10.1080/02827580903378626

Skole, D and C. Tucker, 1993. Tropical deforestation and habitat fragmentation in the Amazon: Satellite data from 1978 to 1988. Science, 260: 1905-1910 of the Secretary-General, March 1996.
https://doi.org/10.1126/science.260.5116.1905

Tachie-Obeng, E., M. Idinoba and J. Nkem (2009). Simulation of forest vulnerability to land use land cover and climate change in Ghana. In IOP Conference Series: Earth and Environmental Science (Vol. 6, No. 30, p. 302020). IOP Publishing. https://doi.org/10.1088/1755-1307/6/30/302020

Tachie-Obeng, E., E. Gyasi, S. Adiku, M. Abekoe and G. Zierrogel (2010). Farmers' adaptation measures in scenarios of climate change for maize production in semi-arid zones of Ghana. In 2nd International Conference: climate sustainability and Development in Semi-arid Regions, August (16-20).

Tavani, R., M. Saket, M. Piazza, A. Branthomme and D. Altrell (2009). Case studies on measuring and assessing forest degradation: measuring and monitoring forest degradation through National Forest Monitoring Assessment (NFMA).

Thompson, H.N. (1910). Gold Coast. Report on forests. https://doi.org/10.5962/bhl.title.27582

Thompson, S.P. (1910). A physiological effect of an alternating magnetic field. Proceedings of the Royal Society of London. Series B, Containing Papers of a Biological Character, 82(557), 396-398. https://doi.org/10.1098/rspb.1910.0032

Trigg, S.N., L.M. Curran and A.K. McDonald (2006). Utility of Landsat 7 satellite data for continued monitoring of forest cover change in protected areas in southeast Asia. Singapore J. Trop. Geo., 27, 49-66. https://doi.org/10.1111/j.1467-9493.2006.00239.x

Tulyasuwan, N., M. Henry, M. Secrieru, I. Jonckheere and S. Federici, S. (2012). Issues and challenges for the national system for greenhouse gas inventory in the context of REDD+. Greenhouse Gas Measurement and Management, 2(2-3), 73-83. https://doi.org/10.1080/20430779.2012.716298

Turner, B.L., J. A. Chudek, B.A. Whitton and R. Baxter (2003). Phosphorus composition of upland soils polluted by long-term atmospheric nitrogen deposition. Biogeochemistry, 65(2), 259-274. https://doi.org/10.1023/a:1026065719423

United Nations Environment Programme, (UNEP), (2000). Global Environmental Outlook (GEO-3)

United States Department of Agriculture (2012). Forests— and the USDA Forest Service— at Work for Minnesota. USDA, Minnesota.

Worldometers (2017). Current World Population. http://www.worldometers.info/world-population/ (10-06-2017).

Wireko, A. (2015). Impacts of Land Use/Cover Change on Water Quality in Lake Bosomtwi Basin of Ghana. (University of Ghana, MPHIL Dissertation)

Yang, X. (2003). Modeling urban growth and landscape changes in the Atlanta metropolitan area. Int. J. Geographical Information Science, 17(5), 463–488. 10.1080/1365881031000086965

Journal of Geomatics Vol 12 No. 2 October 2018

Hydrochemical characterization and ground water quality assessment over Southern Kashmir using Geographic Information System (GIS)

Mohammd Rafiq[1], Mir Shahid Gull[2], Anoop Kumar Mishra[1] and Kishan Singh Rawat[1]
[1]Centre for Remote Sensing and Geoinformatics, Sathyabama Institute of Science and Technology, Chennai, 600119
[2]Srinagar Development Authority, Jammu and Kashmir, email:shahidgis2011@gmail.com
Corresponding author: email: emidamls6@gmail.com. Phone no. 91-9469183781

(Received: Feb 25, 2018; in final form: Oct 08, 2018)

Abstract: We carried out a detailed Geographic Information System (GIS) based study on hydrochemistry of groundwater in Jhelum water basin of three southern Kashmir districts of India, namely, Shopain, Kulgam and Anantnag, to assess the quality of groundwater for determination of its suitability for various purpose. Sampling sites are selected in these three districts of Kashmir valley using various available attributes, wells and springs including their spatial coordinates. About 149 groundwater samples during post snow melt season and 201 groundwater samples during pre-snow melt season for the years 2012 and 2013 have been collected. Samples were collected from tube wells and natural springs and were analyzed for various physicochemical parameters using a field water testing kit. The physicochemical parameters have been compared with the standard guideline values as recommended by the Bureau of Indian Standards (BIS) and World Health Organization (WHO). Results show that physicochemical parameters of majority of water samples during post snow melt season fall in the desirable limit as recommended by WHO. We also estimated Water Quality Index (WQI) index using physicochemical parameters during pre and post snow melt season separately. We found that about 80% of the samples during the post snow melt season qualified as excellent category as defined by WHO on the other hand only about 19% of the water samples fell in this category during pre-snow melt season. This can be attributed to the precipitation and lithology as higher precipitation occurs during the pre-snow melt which enhance infiltration. This study shows that water quality is poorer during pre-snow melt season as compared to post snow melt season in these three districts of the valley.

Keywords: Ground Water Quality, Interpolation, GIS, Hydrochemistry, WQI

1. Introduction

Safe water is essential for health and development. However, the supply of safe water is still denied to millions of people in a developing country like India. Water related diseases caused by the consumption of polluted water supplies coupled with poor sanitation and hygiene cause 3.4 million deaths per year (Gehrig and Rogers, 2009). Despite various efforts by government, civil society and the international community, over a billion people still do not have access to safe water sources. Ground water is a fundamental source to provide water for drinking and irrigation purpose (Teli et al., 2014). The scale of the problem of ground water quality is very large. Groundwater quality depends on the various processes. Chemical and physical composition of the groundwater varies depending upon several factors like frequency of the rain, time of stay of rain water in the root-zone and intermediate zone and the presence of organic matter. Four kinds of substances, namely, organic waste, industrial waste, silt from degraded catchment and fertilizers are responsible for pollution of water sources. Some of the common water contaminations include Nitrates, Pathogens, Trace metals, inorganic constituents and organic compounds. Water quality assessment is crucial to observe its suitability for various purpose (Arumugam and Elangovan, 2009). Urbanization may introduce the impact of pollution in groundwater (Whittemore et al., 1989; Lone et al., 2018; Rafiq et al., 2018a). Geochemical analysis of groundwater helps to investigate the changes in water quality in the context of urbanization (Burston et al., 1993).

Various studies focused on evaluation of ground water quality over different parts of the globe (Som and Bhattacharya, 1992; Wicks and Herman, 1994; Raju, 1998; Arumugam and Elangovan, 2009; Rawat et al., 2013; Jacintha et al., 2016). Water quality over majority of districts in Southern Kashmir depends on the natural springs and tube wells for water supply. The major source of water in the region is the glacier melt (Rafiq and Mishra 2016, 2018, Mishra and Rafiq 2017, Romshoo et al., 2018, Rafiq et al., 2018b).

In this study, we investigate the hydrochemistry of groundwater in Jhelum water basin of southern Kashmir districts of India to assess the quality of groundwater for the determination of its suitability for various purpose.

2. Study area

The study area consists of three southern Kashmir districts, namely, Shopain, Kulgam and Anantnag, located between 33º17'20" and 34º15'30" North latitude and between 74º30'15" and 74º35'00" East longitude. The study area is shown in Figure 1. These districts are bounded by Poonch in the west, Srinagar in the North, Kargil in the North East, Doda in the East, Pulwama in the North West and Rajouri & Udhampur in the South & South East. The study area has a total geographical extent of 3,967 sq km, comprising of 605 villages. The population of study area is 11,70,013 and population density is 294 persons per square kilometer as per 2011 census.

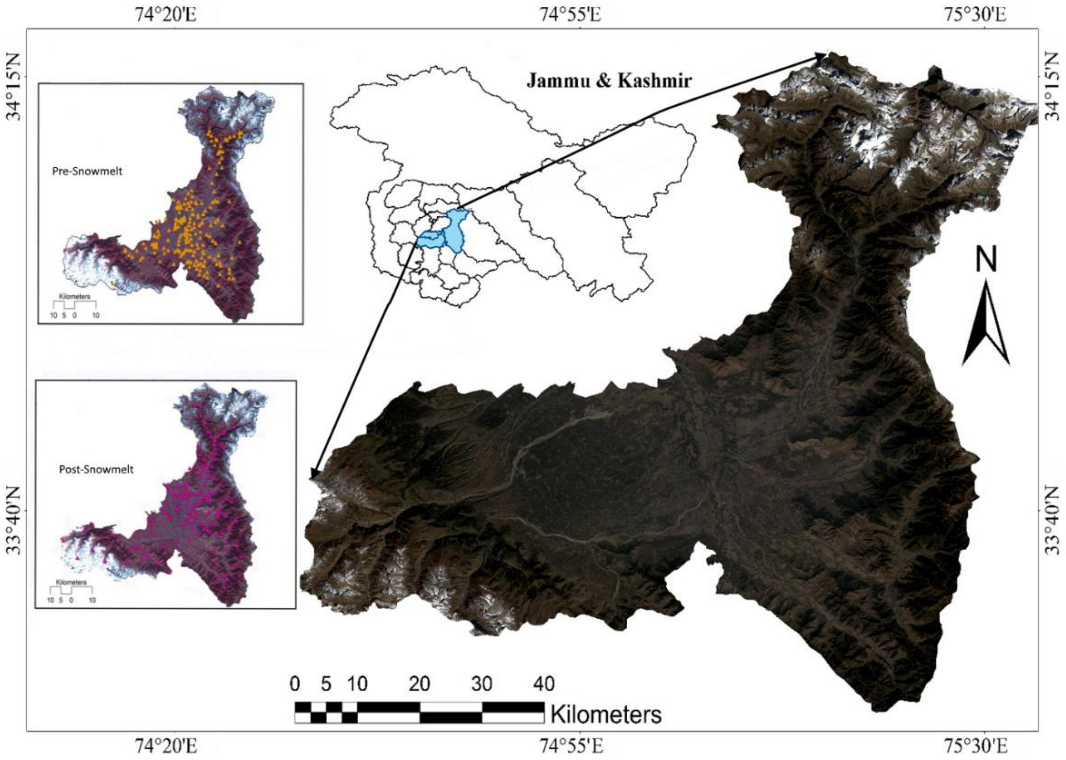

Figure 1: Study area showing the sample location for both pre and post snowmelt

3. Materials and methods

In present study, we have utilized Landsat 8 OLI data to extract the study area. We also used the water quality data from Central Ground Water Quality Board (CGWB) and Public Health Engineering (PHE) department, Jammu, India during 2012 and 2013 as shown in Figure 1. We have acquired 19 and 34 samples from PHE and CGWB for post-snowmelt and pre-snowmelt respectively. Similarly, 19 and 34 samples were collected for Pre-snowmelt from PHE and CGWB respectively. For the assessment of water quality, we also used a water testing Kit provided by Tamil Nadu Water Supply and Drainage Board (TWAD). Also a few parameters were tested at Centre Of Research for Development (CORD), at the University of Kashmir. Furthermore, the ancillary groundwater quality data was collected from the PHE and CGWB. The data was then organized and added to the point data in ArcGIS 10.2. Water quality parameters that were analyzed consists of pH, total hardness (TH), Chlorides, Calcium, Magnesium, Fluorides, Potassium, Sulphates (SO_4), Nitrates (NO_3), Fe, sodium, etc.

The ancillary data from CGWB and PHE included parameters such as pH, total dissolved solids (TDS), EC, alkalinity, residual chlorine hardness, Ca, Mg, Na, K, Fe, Cl, SO_4, NO_3, NO_2 and F were collected. About 149 groundwater samples during post-snow melt season and 201 groundwater samples during pre-snow melt seasons of years 2012 and 2013 were collected from public bore wells, private wells and springs at different. The samples in pre and post-snow melt were collected from the same location.

Then the samples were analyzed for various physicochemical parameters such as alkalinity, hardness, and pH, Fe, Cl, SO_4, NO_3, F and NO_2 on site with the help of TWAD water testing kit. Other parameters which include Calcium, Magnesium, Sodium and TDS were analyzed in laboratory. Spatial coordinates and levels of sampling points are measured using a hand held GPS instrument (Trimble Juno SB). Various attributes like co-ordinates (Lat/Lon), Altitude (height above ASL), Source (spring or tube well), location and photos were collected on the site. Various datasets generated in the field and the ancillary data were converted into a GIS format. For this, the groundwater ancillary data and field data was digitized in the ArcGIS 10.2 which resulted in the formation of the groundwater quality point layer. The resultant groundwater quality layer was bifurcated into two layers (i.e. pre and post-snow melt ground water quality layer). The water quality parameters of the both layers were interpolated individually to make spatial variation thematic maps for these parameters by using Inverse Distance Weighting (IDW) interpolation techniques. Furthermore, water quality parameters were compared with the international standards for understanding the suitability of groundwater for drinking.

The Water Quality Index (WQI) map was also prepared for all three districts (Shopain, Kulgam and Anantnag). For generating the WQI, we used the below mentioned algorithm (Equation 1) Chatterjee and Raziuddin, (2002).

$$WQI = \sum Q q_n w_n / \sum w_n \text{---------- (1)}$$

where,
Q_n = Quality rating of n^{th} water quality parameter.
W_n= Unit weight of n^{th} water quality parameter.

Q_n quality rating is calculated using the following equation 2

$$Q_n = [\frac{V_n - V_{id}}{S_n - V_{id}}] \times 100 \text{ ---------- (2)}$$

where,
V_n = Estimated value of n^{th} water quality parameter at a given sample location.
V_{id} = Ideal value for n^{th} parameter in pure water.
S_n = Standard permissible value of n^{th} water quality parameter.
W_n Unit weight is calculated as:

$$W_n = \frac{k}{S_n} \text{ ---------- (3)}$$

where,
S_n = Standard permissible value of n^{th} water quality parameter.
k = Constant of proportionality and it is calculated by using the equation (4).

$$k = [1/(\sum 1/S_{n=1,2.....n})] \text{----------(4)}$$

The ranges of Water Quality Index WQI, Corresponding status of water quality and their possible use as per International standards are summarized in table 1.

The water quality parameters were selected based on its direct involvement in deteriorating water quality. The standards for the drinking water, recommended by the Bureau of Indian Standards (BIS), Indian Council of Medical Research (ICMR), Indian Standards Institution (ISI) and World Health Organization (WHO) are considered for the computation of quality rating (Q_n) and unit weights (W_n). For the purpose of calculation of WQI, eleven water quality parameters have been selected. These parameters include pH, Hardness, Chloride, Fluoride, Nitrate, TDS, Calcium, Magnesium, Sulphate, Iron and Alkalinity. The values of some of these parameters are found to be high above the permissible limits in some of the samples of the study area. The standard values of water quality parameters and their corresponding ideal values and unit weights are given in table 2. The methodology followed is shown in figure 2 in the form for a flow chart.

Table 1: Water Quality Index (WQI) ranges and recommended usage as per international standards

S. No	WQI	Status	Possible Usage
1	0-25	Excellent	Drinking, Irrigation and Industrial
2	26-50	Good	Domestic, Irrigation and Industrial
3	51-75	Fair	Irrigation and Industrial
4	76-100	Poor	Irrigation
5	101-150	Very Poor	Restricted use for irrigation
6	>150	Unfit for Usage	Proper treatment required before use.

Table 2: Standard values of water quality, and their ideal values and unit weights

S. No	Parameters	Standard Value S_n	Ideal Value V_n	K value	Unit Weight W_n
1	pH	8.5	8.5	0.546	0.064312
2	Hardness	600	0	0.546	0.000911
3	Chloride	250	0	0.546	0.002186
4	Fluoride	1.5	0	0.546	0.364435
5	Nitrate	50	0	0.546	0.010933
6	TDS	500	0	0.546	0.001093
7	Calcium	200	0	0.546	0.002733
8	Magnesium	150	0	0.546	0.003644
9	Sulphate	250	0	0.546	0.002186
10	Iron	1	0	0.546	0.546653
11	Alkalinity	600	0	0.546	0.000911

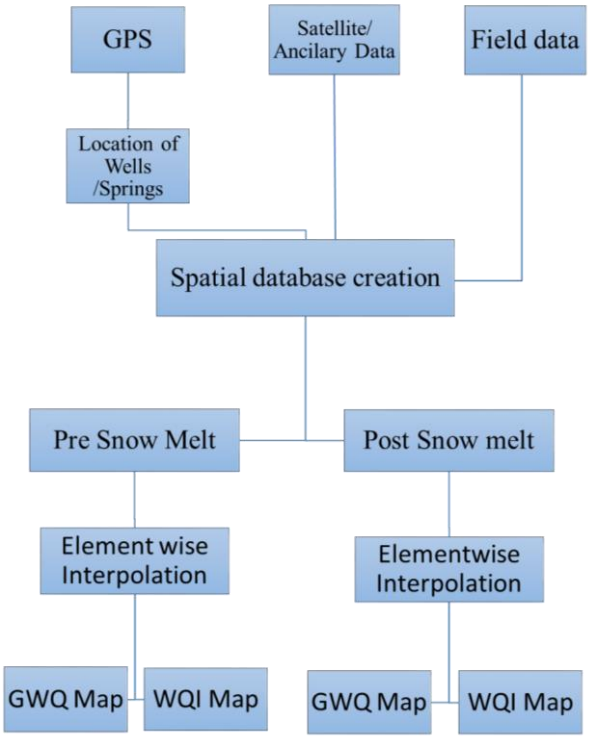

Figure 2: Flow chart of the scheme

4. Results and discussions

Interpolation technique was used to generate the thematic maps for the water quality parameters using 149 samples during post-snow melt season (April-October). Figure 3 illustrates the concentration of water quality parameters over study area during post-snow melt season. It is noted that southern tip of the study area shows highest concentration of sodium (56 mg/l), Magnesium (75mg/l), and Alkalinity (300mg/l). Northern tip of the study areas shows minimum concentration of Phosphate, Magnesium, and Nitrite. Central parts of the study areas show the minimum concentration of Chloride, Fluoride, and Nitrate. It is concluded that water quality parameters like Calcium, Magnesium, Sodium, Sulphate, Alkalinity, Hardness and Nitrite were found to be falling in desirable limits for post-snow melt data over majority of the study area (Table 3).

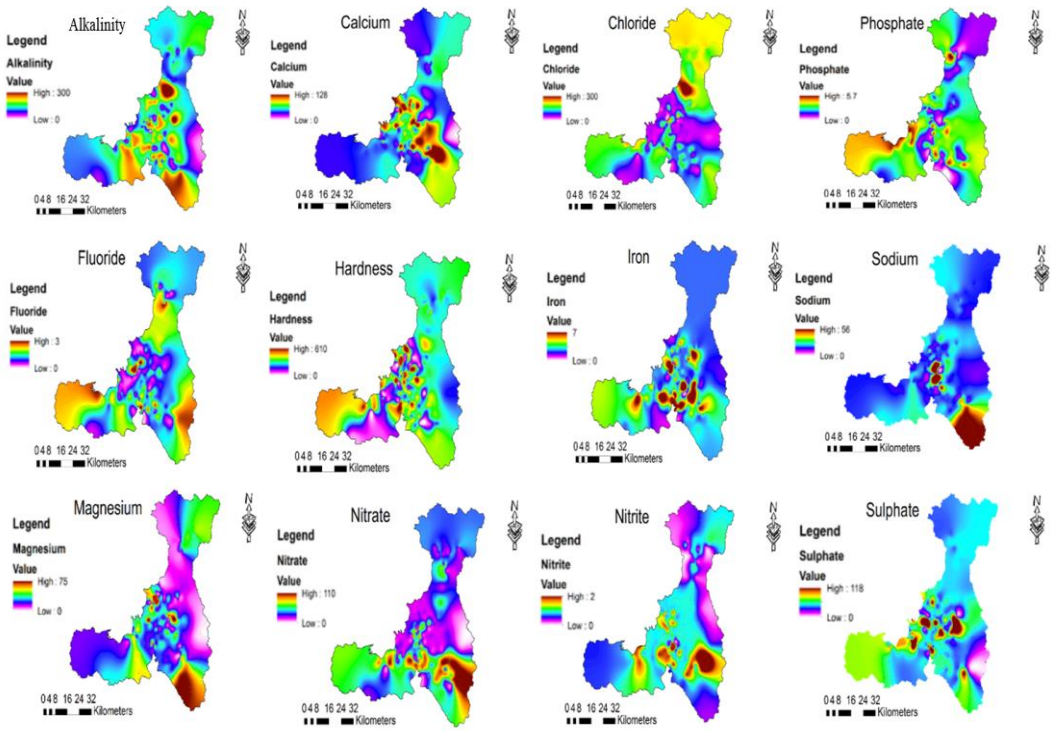

Figure 3: Concentration of water quality parameters during post snow melt season

Table 3: Area (%) under/beyond standard limit of water quality parameters during post-snow Melt season

Parameter	Standard BIS/WHO/CPHEEO	% Area in Standard limit	% Area beyond standard
pH	8.5	99.6	0.4
Hardness	600	100	0
Chloride_Cl	250	100	0
Fluoride_F	1.5	99.9	0.1
Iron_Fe	1	94	6
Nitrite_No_2	0.45	100	0
Nitrate_No_3	50	96.8	3.2
Phosphate	5	99.6	0.4
Alkalinity	600	100	0
TDS	500	93.7	6.3
Calcium_Ca	200	100	0
Magnesium_Mg	150	100	0
Sodium_Na	200	100	0

For pre snow melt season (November-March), 201 samples were analyzed. Figure 4 displays the concentration of the water quality parameters over study area during pre-snow melt season. It may be noted that southern tip of study area shows minimum concentration of Calcium, Iron and Sodium while western tip shows maximum concentration of Chloride (173 mg/l). Northern tip of study area shows minimum concentration of Magnesium, Sodium, Iron and Phosphate. Central part of study area shows variable concentration of water quality parameters. It may be noted that during pre-snow melt season, only 6 parameters (Calcium, Magnesium, Sodium Sulphate, Alkalinity and Hardness) were found under desirable limits (Table 4).

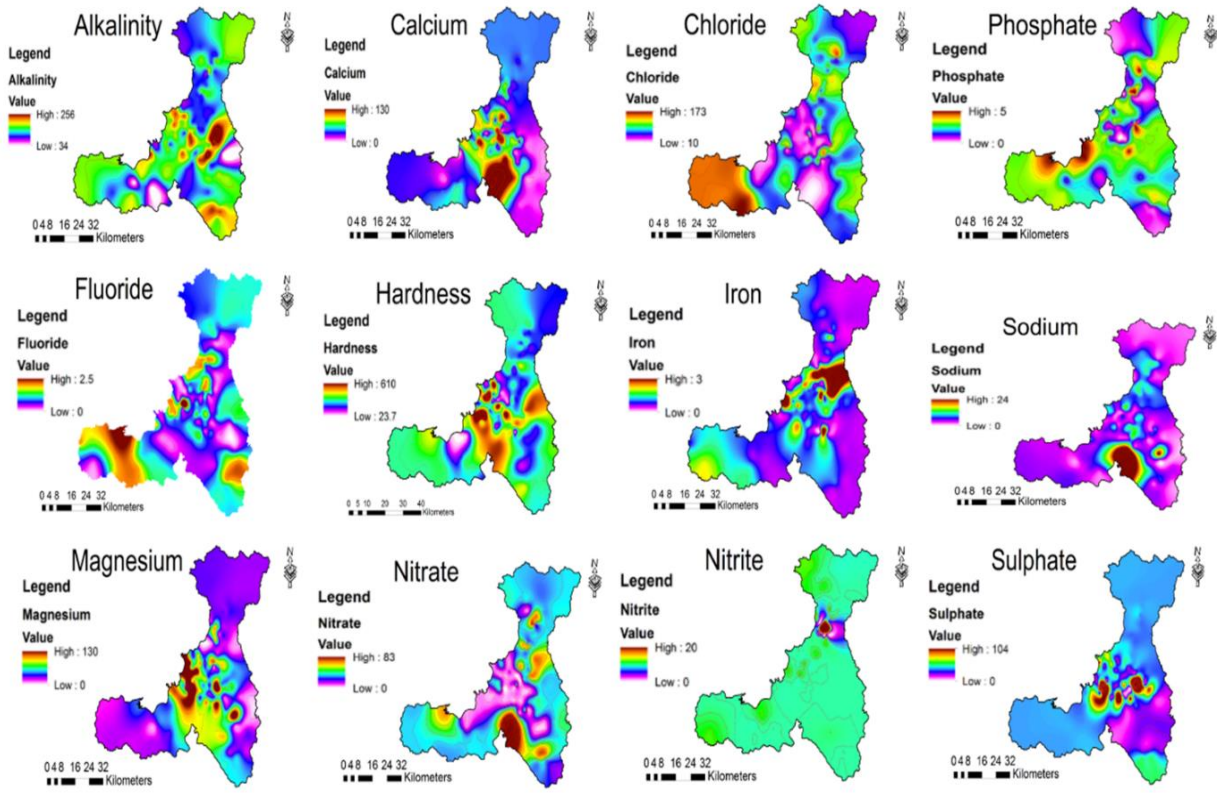

Figure 4: Concentration of water quality parameters during pre-snow melt season

Table 4: Area (%) under/beyond standard limit of water quality parameters during pre-snow Melt season

Parameter	Standard BIS/WHO/CPHEEO	% Area in Standard limit	%area beyond standard
Ph	8.5	99.9	0.1
Hardness	600	100	0.0
Chloride_Cl	250	99.6	0.4
Fluoride_F	1.5	99.4	0.6
Iron_Fe	1	92	8.0
Nitrite_No_2	0.45	94	6.0
Nitrate_No_3	50	96.1	3.9
Phosphate	5	99.2	0.8
Alkalinity	600	100	0.0
TDS	500	95.5	4.5
Calcium_Ca	200	100	0.0
Magnesium_Mg	150	100	0.0
Sodium_Na	200	100	0.0
Sulphate_So4	250	100	0.0

As described in methodology section, 11 water quality parameters were used to estimate Water Quality Index (WQI) over study area during pre and post-snow melt season separately. Figure 5 shows the concentration of WQI over study area during post-snow melt season. It may be concluded that majority of study area shows WQI in the range of 0-25. Few regions in the central part of study area shows maximum values of 70-150. Results also show that about 80% of study area possess excellent drinking water quality as per international standards. Figure 6 shows the concentration of WQI over study area during pre-snow melt season.

We have categorized the values based on previous study by Chatterjee and Raziuddin, (2002) (Table 5). It may be noted that southern tip of the study area shows a high concentration of about 100-150 of WQI while northern tip shows a minimum concentration of about 25-50. It may also be noted that only about 23% of study area shows excellent quality of drinking water during pre-snow melt season as compared to 80% during post-snow melt season. Furthermore, two samples were taken in different seasons (pre and post-snow melt) for the same location to check the variation of water quality and it was found that the water quality is poor during pre-snow melt than post-snow melt. This may be due to the fact that water impurities may get diluted after snow melt. The region is dominated by the western disturbances and most of the rainfall occurs during November to April. Also the lithology of the area is dominated by limestone which gets infiltrated due to the rain thus detonating the water quality. This can also be linked to an increasing trend of GW contamination due to anthropogenic activities in the area.

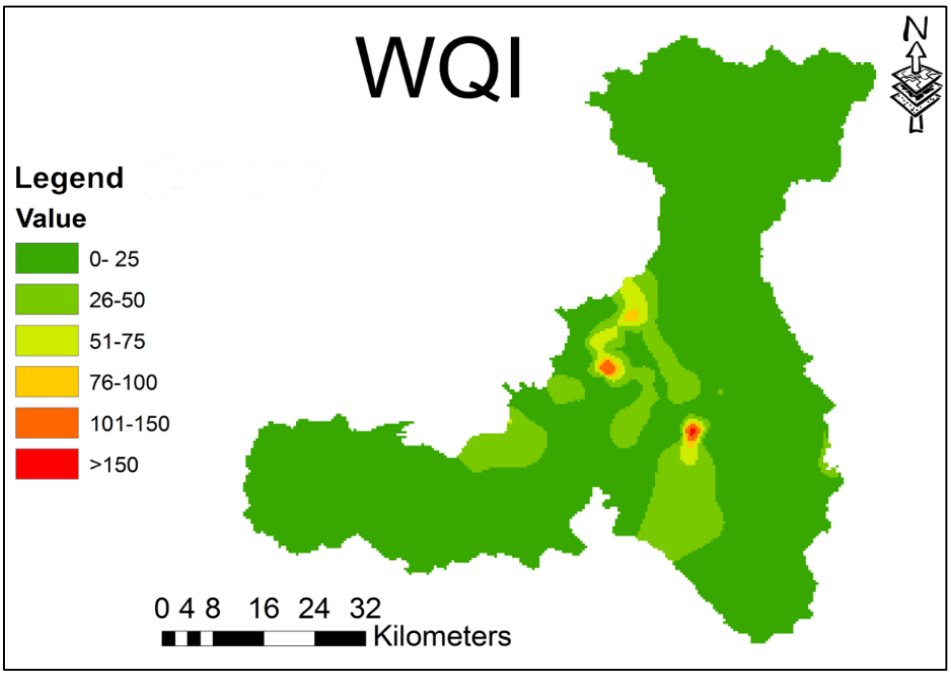

Figure 5: Concentration of Water Quality Index during post-snow melt season

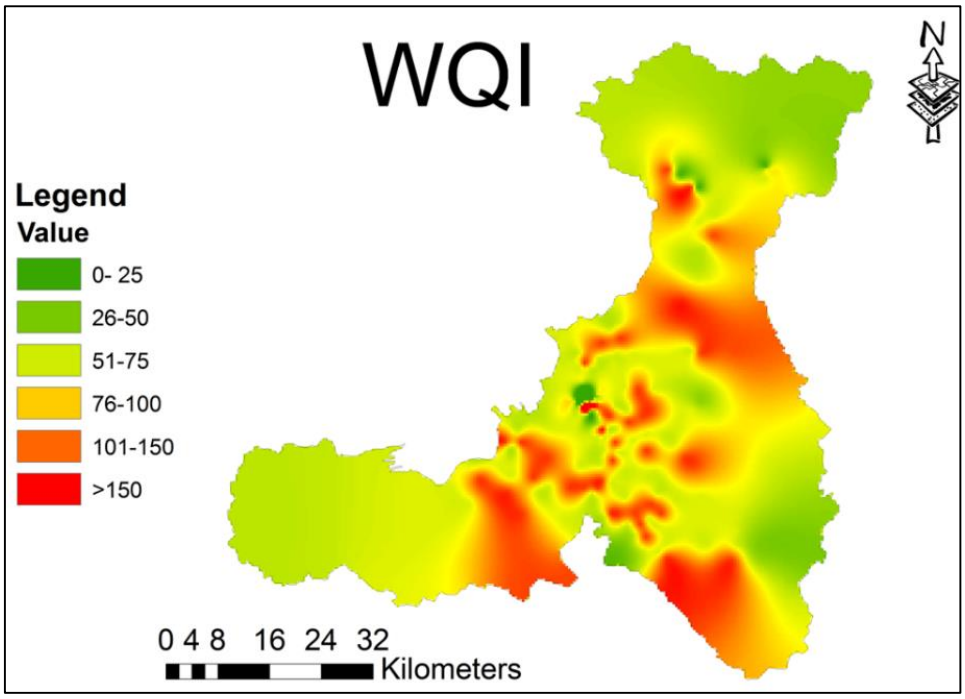

Figure 6: Concentration of Water Quality Index during pre-snow melt season

Table 5: WQI and status of water quality (Chatterjee and Raziuddin, 2002) for Post and Pre Snow melt season

S. No	WQI	Status	% Area(Post)	% Area(Pre)
1	0-25	Excellent	80.53945	23.56944795
2	26-50	Good	12.9821	76.38265692
3	51-75	Fair	5.596168	0.020166373
4	76-100	Poor	0.731031	0.005041593
5	101-150	Very Poor	0.12604	0.017645576
6	>150	Unfit for Usage	0.025208	0.005041593

5. Conclusion

The hydro-chemical analysis of groundwater samples over southern Kashmir shows that the groundwater quality over majority of the region is good for various purpose including human consumption. This study also reveals that groundwater quality during post-snow melt season is better as compared to the pre-snow melt season. WQI index shows that majority of the region shows groundwater samples suitable for drinking purpose. However, the concentration of few chemicals are increasing during pre-snow melt resulting in poor WQ. Overall the WQI revealed that the groundwater is suitable for human consumption. For sustainable use of groundwater in this region it's important to minimize the effects of anthropogenic activities and likely effects of climate change on ground water level (Mishra et al. 2016).

Acknowledgement

We are thankful to Prof Shakil Ahamd Romshoo, Central Ground Water Board and Public Health Department for their support during the field work. Landsat data from Earth Explorer is thankfully acknowledged**.** We would also like to extend gratefulness to The Council of Scientific and Industrial Research (CSIR) HRDG for providing financial support though order no. 24(0350)/17/EMR-II to carry out this research.

References

Arumugam, K. and K. Elangovan (2009). Hydrochemical characteristics and groundwater quality assessment in Tirupur Region, Coimbatore District, Tamil Nadu, India. Environmental Geology, 58, 1509-1520.

Burston, M.W., M.M. Nazaari, K.P. Bishop and D.N. Lerner (1993). Pollution of ground water in the Coventry region (UK) by chlorinated hydrocarbon solvents. Journal of Hydrology, 149, 137–161.

Chatterjee, C and M. Raziuddin (2002). Determination of Water Quality Index (WQI) of a degraded river in Asansol industrial area (West Bengal). Nature, Environment and Pollution Technology, 1(2), 181-189.

Gehrig, J. and M.M. Rogers. (2009). Water and conflict: incorporating peace, building into water development. Edited by Warner, D., Seremet, C., and Bamat T., Catholic Relief Services.

Jacintha, T.G.A., K. Rawat, A.K. Mishra and S.K. Singh (2016). Hydrogeochemical characterization of groundwater of peninsular Indian region using multivariate statistical techniques. Applied Water Science, 7(6), 3001-3013.

Lone, A., R. Shah, H. Achyuthan, and M. Rafiq (2018). Source identification of Organic Matter using C/N Ratio in freshwater lakes of Kashmir Valley, Western Himalaya, India. Himalayan Geology, 39(1), 101-114.

Mishra, A.K., J. Panda and M. Rafiq (2016). Increasing Risk of Droughts and Floods and Decline in Ground Water Level in Warming Environment. International Journal of Earth and Atmospheric Sciences, 4(2), 127-132.

Mishra, A.K. and M. Rafiq (2017). Analyzing snowfall variability over two locations in Kashmir, India in the context of warming climate. Dynamics of Atmospheres and Oceans, 79, 1-9.

Rafiq, M., A.K. Mishra and M.S. Meer (2018a). On land-use and land-cover changes over Lidder Valley in changing environment, Annals of GIS, DOI: 10.1080/19475683.2018.1520300.

Rafiq, M., S.A. Romshoo, A.K. Mishra and F. Jalal (2018b). Modelling Chorabari Lake outburst flood, Kedarnath, India, Journal of Mountain Sciences, doi.org/10.1007s11629-018-4972-8.

Rafiq, M and A.K. Mishra (2018). A study of heavy snowfall in Kashmir, India in January 2017. Weather, 73(1), 15-17.

Rafiq, M and A.K. Mishra (2016). Investigating changes in Himalayan glacier in warming environment: a case study of Kolahoi glacier. Environmental Earth Sciences, 75(23), 1469.

Raju, K.C.B. (1998). Importance of recharging depleted aquifers, State of the art of artificial recharge in India. Journal of Geological Society of India, 51, 429–454.

Rawat, K.S., A.K. Mishra, V.K. Sehgal and V.K. Tripathi (2013). Identification of geospatial variability of fluoride contamination in ground water of Mathura district, Uttar Pradesh, India. Journal of Applied and Natural Science, 4(1), 117-122.

Romshoo, S.A., M. Rafiq and I. Rashid (2018). Spatio-temporal variation of land surface temperature and temperature lapse rate over mountainous Kashmir Himalaya. Journal of Mountain Science, 15(3), 563-576.

Som, S.K and A.K. Bhattacharya (1992). Groundwater geochemistry of recent weathering at Panchpatmali bauxite bearing plateau, Koraput district, Orissa. Journal of the Geological Society of India, 5(40), 453– 461.

Teli, M.N., N.A. Kuchhay, M.A. Rather, U.F. Ahmad, M. A. Malla and M.A. Dada (2014). Spatial interpolation technique for groundwater quality assessment of district Anantnag J&K. International Journal of Engineering Research and Development, 10(3), 55-66.

Wicks, C.M and J.S. Herman (1994). The effect of a confining unit on the geochemical evolution of groundwater in the Upper Floridan aquifer system. Journal of Hydrology, 153, 139–155.

Whittemore, D.O., K.M.M. Greggor and G.A. Marotz (1989). Effects of variations in recharge on groundwater quality. Journal of Hydrology, 106, 131–145.

Journal of Geomatics Vol 12 No. 2 October 2018

Geo-spatial approach for mapping of field measurement books in Andhra Pradesh: a case study

Ch.Tata Babu, L. Sneha, M. Hari Krishna and K.V. Ramana
Andhra Pradesh Space Applications Centre, Planning Department, Vijayawada, Govt. of Andhra Pradesh
Email: tatababuapsac@gmail.com

(Received: Mar 08, 2018; final form: Oct 08, 2018)

Abstract: An effective and secure transaction of landed properties is essential for the welfare of any country's economy. Governments at all levels require accurate, easily retrievable land records for establishing the ownership rights. A Field measurement Book (FMB) provides data about land and ownership. It is the base for legal aspects like ownership as well as fiscal aspects like taxation of land. The main objective of the study is to regenerate a spatially accurate, legally supportive and operationally efficient sub divisional cadastral database. The definition and compilation of an accurate database is based on an analytical reconstruction of sub-division boundaries rather than the conventional field reconstruction process by using Collabland software. To attain this, village cadastral maps, Field Measurement Books and Adangal records have been used. This study mainly elaborates the methods used for producing and updating the FMB map. It investigates the use of High Resolution Satellite Imagery (HRSI) and Global Positional System (GPS) which are vital elements in timely maintaining many of the cadastral maps in GIS. The abilities of remote sensing imageries in sub parcel mapping are evaluated using World View-2 satellite data. The study reveals that the sub-parcel wise information serves the administrative mandates, maintaining up to date database, assigning values for taxation, addressing rural development, management and services to citizens. The study indicates that the adopted technology can be extended to other areas of the State and updation work can be done in a limited time.

Keywords: cadastral mapping, adangal, FMB, HRSI, GIS, Collabland

1. Introduction

The dynamically changing relationship of humankind to land has a great influence on the development of land administration systems. The individual survey number sketches are maintained as Field Measurement Book (FMB). It illustrates the dimensions of each field boundary of the sub-divisions in the particular FMB. Each sub-division number is owned by a property owner. Land records originated from Mughal period and later during British period, scientific cadastral surveys were conducted to determine boundaries and extent of each individual landholding. Now a day the land information in India is maintained at Block/Taluka/Mandal offices. Map data is stored in Field measurement book, Jamabandi, Khasra Girdawari, Adangal, Padigree Sheets etc. and land ownership detail is maintained using various registers (Mishra and Pal, 2000). Updating and searching for any land information in this type of system is very tedious work. Sub-division based information presents an accurate picture of land holdings, geographic location and their boundaries, make relevance, reliable, accurate, and up to date spatial land parcel data and information continuously available to the government, land authorities and communities. It provides consistency in reporting, reduce cost through the sharing of information technology, facilitate citizens, professionals, research, and build the land market.

1.1 About Field Measurement Book (FMB)

It contains pictorial representation of the survey fields and sub-divisions recorded in the Adangal Register. It depicts measurements of individual fields with sub-divisions at a scale of 1:1000 or 1:2000. Each survey number is divided into several sub-divisions. Each sub division is owned by an owner. Three copies are prepared by the Survey department. Original copy is preserved in State Archives, duplicate copy is supplied to Tahsildar office and triplicate copy is supplied to the Village functionary. A sample of FMB sketch is presented in Figure-1.

G-line (Guess): This is an imaginary line which converts the map into various sizes of triangles in order to accurately fix the boundary lines and various points in the map. This line is the foundation on which the entire map is built. Any error in a G-line will affect all calculations based on that G-line.

F-line / Boundary line: It is the outer boundary line in a sketch, which signifies the actual field boundaries of the sketch. The F-line points are fixed with reference to its offset distance from the G-line.

Sub-division lines: These lines demarcate a small parcel of land within a survey number. A sub-divisional polygon's extent is directly correlated to the extent found for the particular sub division. The sub division lines are generally defined through a ladder etc., except for the graphical representation in the FMB.

Ladder: The field line points are defined with reference to an offset distance from the G-line. The offset distance may be to the left or right side of the G-line. This left or right angle deviation (offset) is depicted by Ladder. By converting the ladder details into electronic data, one can produce the outline of the FMB sketch. The ladder details get attracted whenever there is a change in the field line, involving a bent.

Extension lines: Each survey number field is an integral part of the village map and hence other fields surround each sketch. The exact direction in which the subject field joins the neighbouring field is shown on the FMB as an extension line.

Neighbouring field survey numbers: As mentioned earlier, each survey sketch is surrounded by other fields. These surrounding field numbers are marked around each FMB. This enables mosaicing of FMBs into D-sketches, village maps and so on.

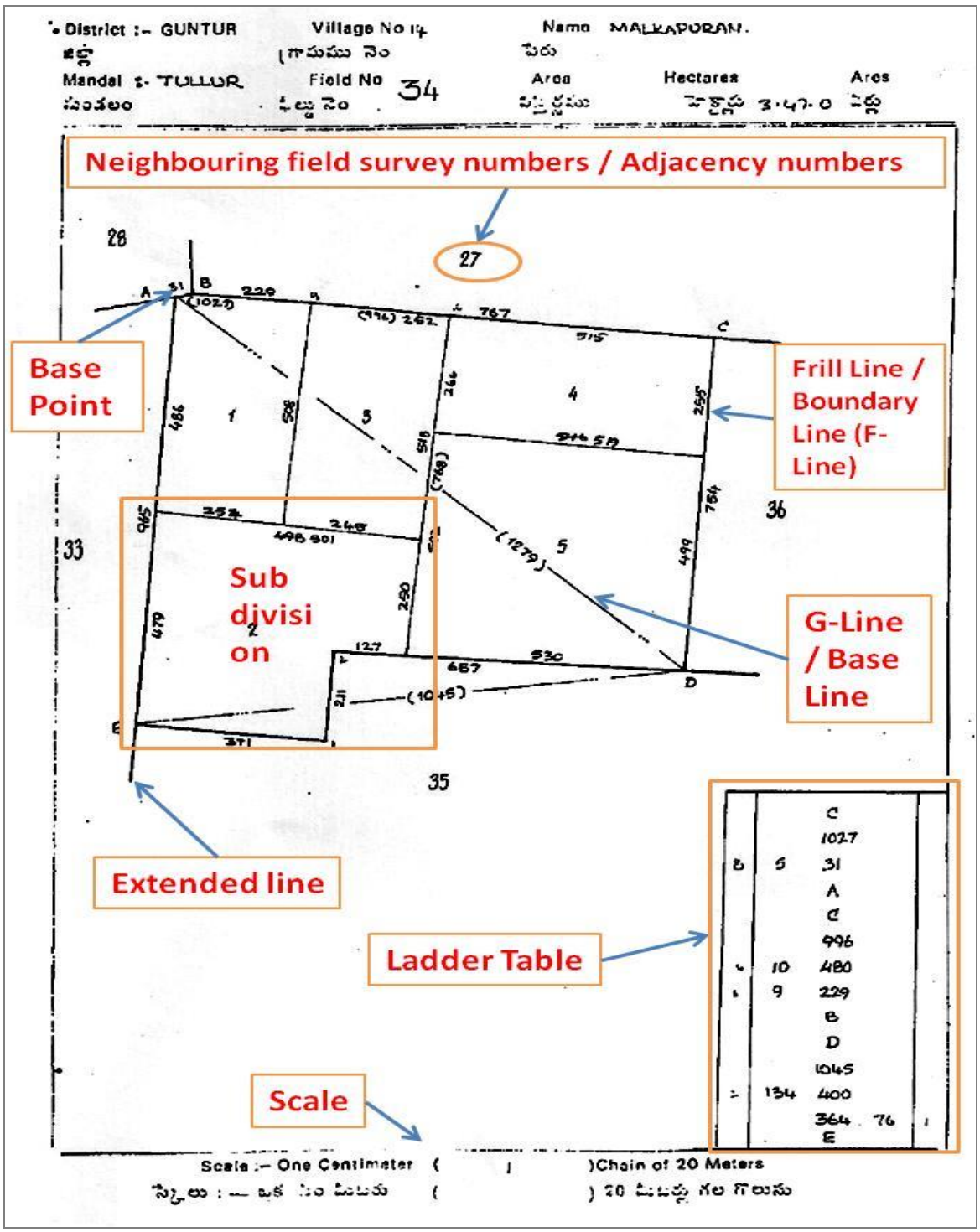

Figure 1: A Sample FMB sketch

1.2 FMB Scenario in Andhra Pradesh

The FMBs were surveyed during the period of Mughal and it reached its scientific form during the British rule. In Andhra Pradesh, during the initial survey, different survey systems were adopted such as Paimash system, Khasra method, Simple triangulation, Plane table, Block map, Punganur System and Diagonal and Offset (D&O) system (GoAP, 1980). The method of measurement of individual properties and holdings underwent several changes as the survey progressed. More than 96% of FMBs were surveyed by using D&O system in the state. Along with D&O system, Plane table and Block maps are found in Anantapuramu district. The available FMBs in Andhra Pradesh are either in Gunter Links or in Metric Links.

As per the records of Survey Settlements and Land Records (SS&LR) Department, Andhra Pradesh is having about 49 Lakh FMBs with different survey methods. Recently, state government has launched "MeeBhoomi" project which contains all land details along with Adangal/Pahani and 1-B/Record of Revenue (RoR) of the state. Government has made it available to the public for checking their land details online in the official website of MeeBhoomi anywhere/ anytime. MeeBhoomi portal contains the details of land owners, area, assessment, soil

type, water resources, and nature of possession of the land, liabilities and crops grown. It is very useful for land owners, tenants, administrators, etc.

Different systems of survey in Andhra Pradesh

Paimash system: It was started in first quarter of 19th century, in which, each land holding (plot) was numbered and named in this system. Measurements were taken from north to south and then east to west. Areas and boundaries were generally taken with a 24 feet chain at that time. This method underwent several changes as the survey techniques advanced.

Khasra method (1858-65): If the field was quadrilateral, four sides were measured in this method. All irregular fields were divided into quadrilateral or triangular portions called as taks and the field itself could be plotted only by piecing of taks. The areas were worked out by multiplying the means of lengths by the means of breadths. But no serious attempt was made for mapping of the details on ground.

Simple triangulation (1866-77): Triangulation is a surveying method that measures the angles in a triangle formed by three survey control points. Using trigonometry and the measured length of just one side, the other distances in the triangle are calculated. The shape of the triangles is important as there is a lot of inaccuracy in a long skinny triangle, but one with base angles of about 45 degrees is ideal. In triangulation, entire area to be surveyed is covered with a framework of triangles. For the triangle, the length of the first line, which is measured precisely, is known as Base line. The other two computed sides are used as new baselines for two other triangles interconnected with the first triangle. Each of the calculated distances is then used as one side in another triangle to calculate the distances to another point, which in turn can start another triangle. Triangulation with offsets method survey was used during 1878-1886.

Plane table (1887-91): Plane Table surveying is a graphical method of survey in which the field observations and plotting are done simultaneously. The plan is drawn by the surveyor in the field, while the area to be surveyed is before his eyes. Therefore, there is no possibility of omitting the necessary measurements. Under this system, the maximum area of survey fields was taken to be 6 acres in wetland and 12 acres in dry land.

Block map system (1892-96): In this method, the block was divided into large triangles and all survey fields and sub-divisions were correctly plotted by offsets from the sides of these triangles. Only a few stations of these triangles were theodolite stations, the rest being fieldstones or peg stations. This method was extremely cheap but results were inaccurate and the system was not suitable for maintenance.

Punganur system (1918-20): The system was first adopted in the Punganur zamindari of Chittoor district and then followed in Repalli taluk of Guntur district and Venkatagiri zamindari of Nellore district. Under this system, all points on the boundary of a field are offset from G-Line and field boundaries are not measured but computed.

Diagonal and Offset (D&O): This is the latest method and is being adopted for survey since 1902. Each field tri-junction is connected with the next field by a line called G-line and selecting convenient diagonals completes the triangles. Independent framework is provided for each survey field. Field and subdivision bends are offset on the G-lines and diagonals. The diagonal and offset system affords an independent check of a substantial amount of fieldwork done by the surveyor. The up-to-date diagonal and offset system is more accurate, less costly and quite easy for maintenance of framework of survey and land records.

1.3 Review of Literature

Rao et. al., (1996) demonstrated overlaying of cadastral maps over the merged product of IRS 1C PAN and LISS III data. Singh (1998) discussed different issues associated with Land Records and modernization of the same. Greenfield (2001) evaluated the accuracy of digital orthophoto quadrangle in the context of parcel based GIS. Similar study has been carried out by Raju et. al., (2008) who stated that the potential of very high resolution satellite data is high in urban cadastral mapping. Ali et. al., (2012) described the use of remote sensing data for updation of cadastral maps. Kumar et. al., (2013) demonstrated updation of cadastral maps using high resolution remotely sensed data. Kemiki et. al., (2015) discussed possibilities of implementation of cadastral information system and stated that it as useful for property valuation, resident's inventory and property leasing analysis. Padma et al, (2015) demonstrated updation of approximate sub-divisional parcel boundaries of a cadastral map by using World View-2 satellite data.

1.4 Objectives

The study is aimed at developing comprehensive landed database for sustainable development of the state with the following objectives.

- To reproduce the field measurement book sketches using Collabland software
- To develop comprehensive sub-division wise database of the State

2. Data Used

High resolution World View-2 satellite data of PAN (0.5m) and Multispectral (2m) were acquired on 15th January, 2015 over the study area. The FMB sketches were collected from SS&LR department and used to produce the digital sketches using Collabland software and generate village wise mosaics. These maps were geo-referenced and overlaid on the satellite imagery for further use. The study area comprises of Malkapuram village, which is located in Guntur District of Andhra Pradesh. GPS was used for Ground Control Points (GCPs) collection in the study area.

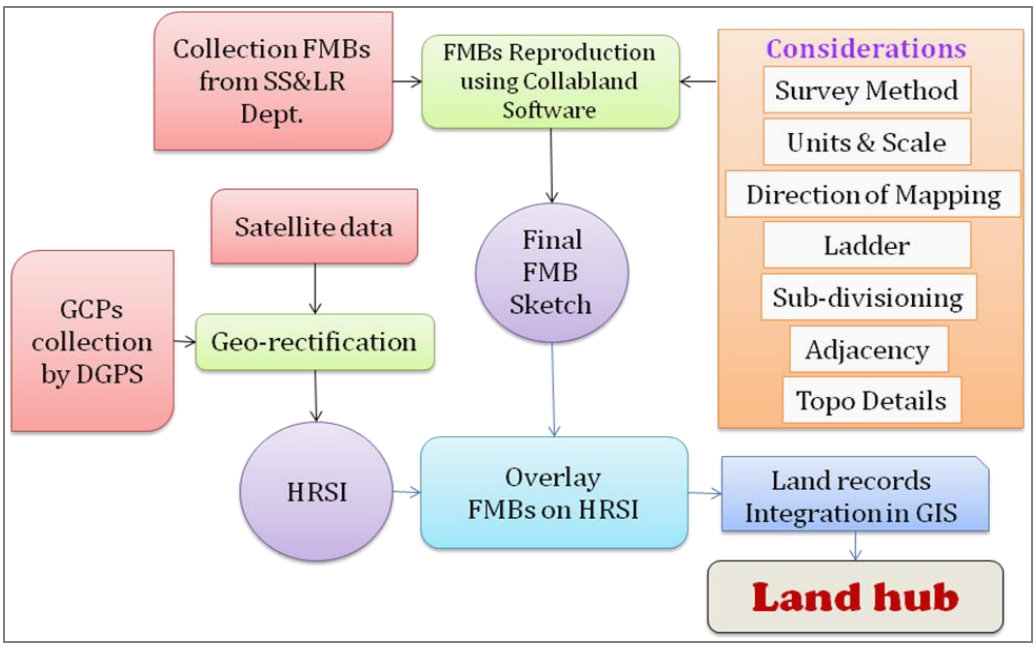

Figure 2: Methodology

3. Study Area

The study area comprises of Malkapuram village, which is situated on the Vijayawada - Amaravathi main road. It is located 31kms towards north from district headquarters. The study area lies to the north of Guntur district between 16º 29' - 16º 32' N latitudes and 80º 30' - 80º 32' E longitudes. This place is associated with the ancient historic culture of Kakatiyas and Golkonda Kings.

4. Methodology

An attempt has been made to reproduce the FMB sketches using Collabland software, which is developed by National Informatics Centre (NIC), Government of India. It is a software for digitization and mosaicing of survey maps for computerization of land records. It allows a variety of survey systems, extending from the conventional Chain and Theodolite method to the modern Electronic Total Station (ETS) system (APSAC, 2016). The software also supports in regional language and the interface sample in Telugu is given in the Figure 3. World view-2 multispectral image was geometrically corrected using the ground control points. Village wise FMB sketch mosaics were generated in Collabland software based on adjacency and boundary lines of the FMB. The high-resolution satellite images were rectified using collected Ground Control Points (GCPs). After the finalization of satellite data, the village wise mosaic FMBs were transformed on satellite data by using affine method of transformation tool in the GIS environment (NRSC, 2011). The comprehensive methodology used in the present study is shown in Figure-2.

5. Results & Discussion

The study has demonstrated that collabland software is capable of producing accurate computer aided field measurement book sketches. Traditionally, the surveyors in developing countries have given priority to implement accurate cadastral field surveys without giving much attention to the cost but since the turn of the new millennium, more cost-effective and flexible methodologies were utilized. However, modern cost-effective methodologies do not neglect the quality but focus more on required accuracy on the user point of view by using technical capacity and available equipment. In many developing countries the use of very high resolution satellite data with possible combination of different survey methodology depending on local quality requirements and characteristics of the land is implemented.

5.1 FMB Reproducing

To attain this, the FMBs have been collected from survey department in the form of hard copy. Collabland software has been used for digitization/reproduction of the FMB. It allows different survey maps for digitization and mosaicing of land survey maps. Initially, the FMB sketches were examined by the draughtsman/digitizer for reproduction; with respect to method of survey, scale, traverse direction, base distances, units, etc. Once confined with all these parameters, the input values (survey measurements) have been entered into the Collabland software in the form of tables i.e. Ladder, Boundary, Adjacency and Extended. The ladder table is very crucial for the reproduction of a field sketch and has all the survey details of FMB sketch. The adjacency and boundary tables have been used for demarcation of the adjoining field boundary and survey numbers of the FMB sketch. The sub-division points have been joined for sub-dividing the FMB sketch and titled in order to assign numbers for each individual sub-division. The extended table has been used as extension of ladder table. The topological details like Building, Culvert and Bridge, Sluice, Thatched house, River, Canal, Aqueduct, River flow direction, etc. have been drawn on the FMB sketch as per the specification on the original FMB. The digitized FMB sketch has been saved by selecting

corresponding district, mandal, village name, which are pre-defined in the software with regional language and is stored in the database with corresponding survey number. The quality assurance has been abided for reproduction of FMB in terms of measurements, tables, adjacency, sub-divisions, scale, title, completeness, etc. Cross verification has been made frequently for ensuring coherent consistency of the FMB. Thus, village level mosaic has been generated to piecing of individual FMBs by using mosaic tool in the software. Edge matching is done by fetching two different FMB sketches of the same village into the same file and matching their edges with reference to the adjacency, boundary and base lines. On-screen checking has been performed for checking the common edge between the sketches. The reproduced FMB map is presented in Figure-3 and village mosaic is presented in Figure-4.

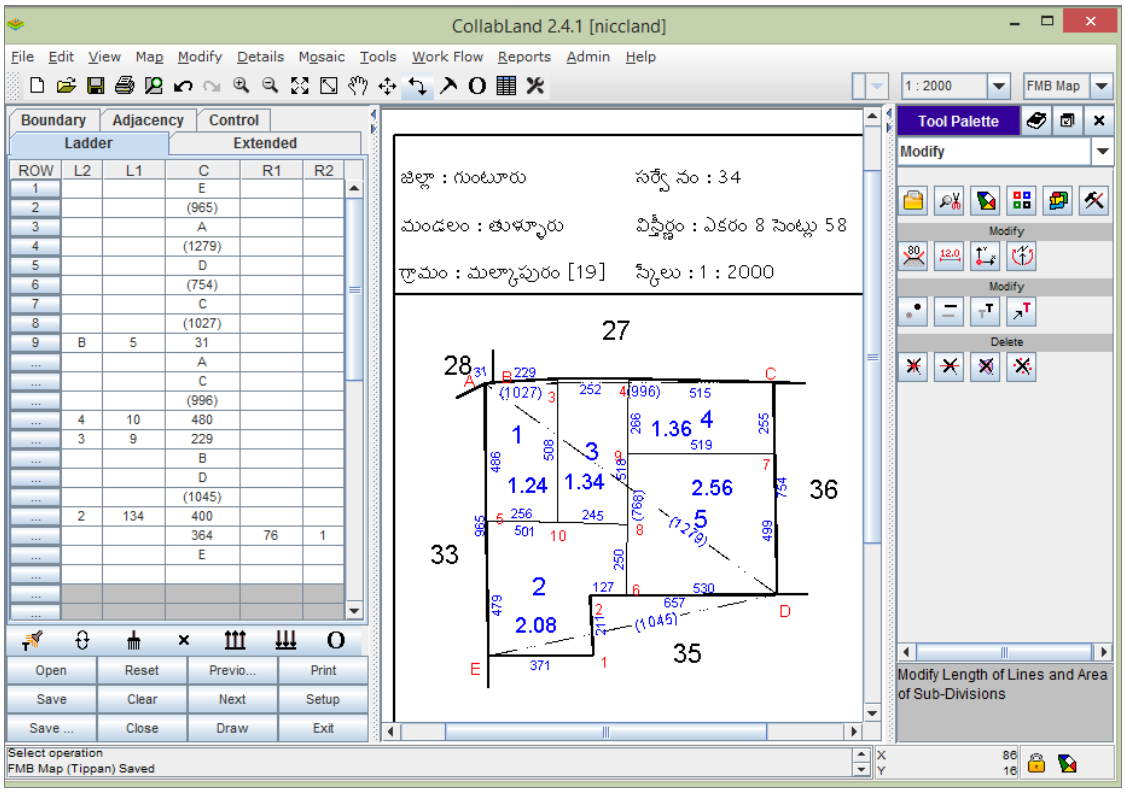

Figure 3: Reproducing FMB sketch in Collabland software

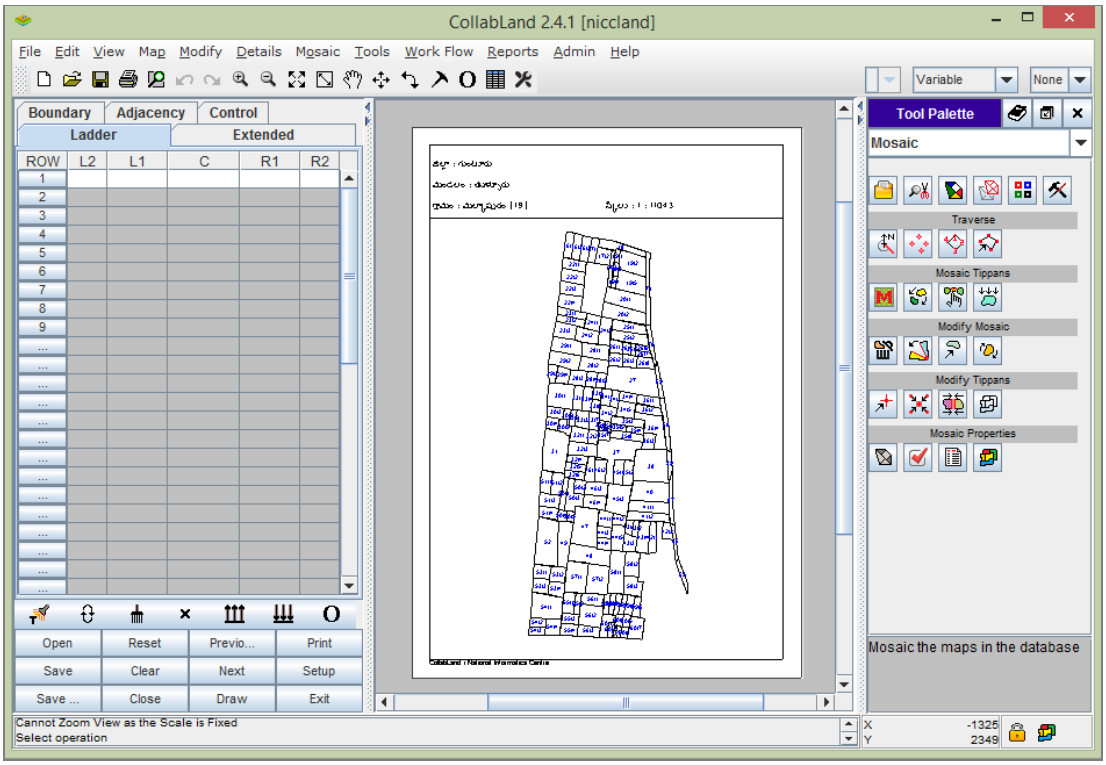

Figure 4: Village Mosaic of FMBs in Collabland software

Figure 5: Village mosaic overlaid on HRSI

5.2 Overlay on High Resolution Satellite Imagery (HRSI)

High resolution satellite images are considered as source of information to solve socio-economic problems in many contemporary fields of study. These images, together with remote sensing and GIS techniques support decision making in many ways. HRSI provides an alternative data for acquisition of spatial data by providing remote and inaccessible area survey details. World View-2 PAN & MSS images were acquired and separately geo-rectified with collected GCP's in conjunction with Digital Elevation Model (DEM). These two images were geo-rectified separately and merged for final fusion product generation using ERDAS Imagine software. After the finalization of satellite data, the digitized vector sub-divisions were geo-referenced by using GCP's and transformed on satellite data by using affine method of transformation tool in the GIS environment. Thus, the FMB village mosaics are overlaid on HRSI and it can be used for updating the sub-divisions, transferring the land ownership details easily and precisely. The village mosaic overlaid on HRSI is shown in Figure-5 and sub-divisions of the survey number 34 are presented in Figure-6.

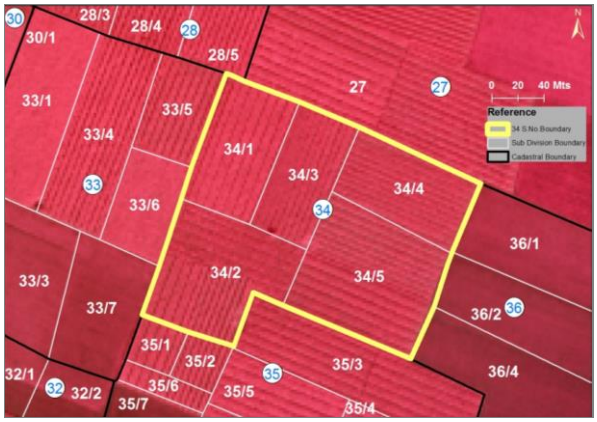

Figure 6: Survey number 34 is overlaid on HRSI

The Resurvey Settlement Records (RSR) data can be integrated with individual land holdings and make it as information system. This will serve the administrators in maintaining an up to date database, assigning values for taxation, calculating subsidies, addressing rural development and management and providing products and services to citizens and companies. The individual land holdings data (RSR) of survey number 34 is illustrated in Figure-7.

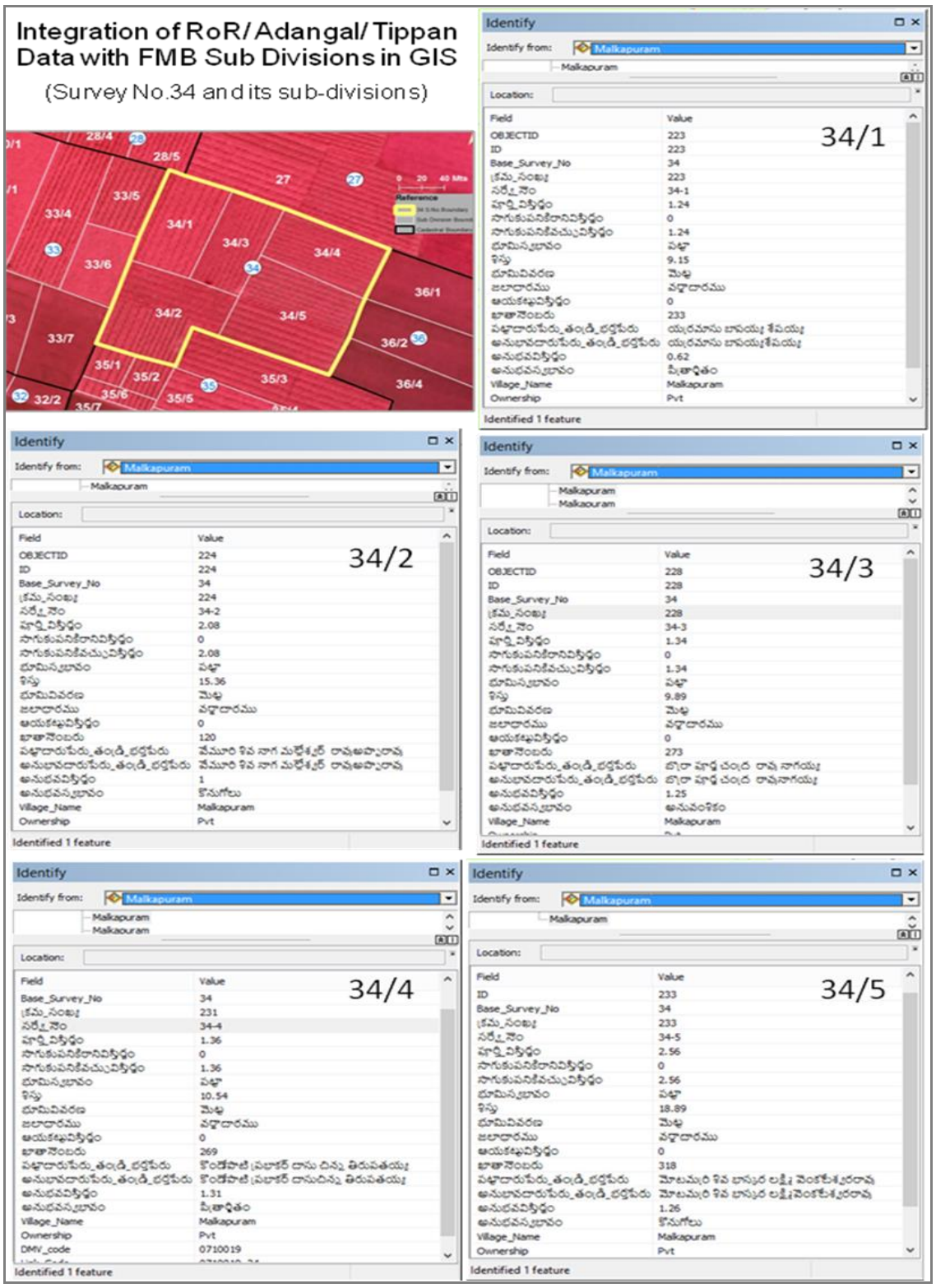

Figure 7: Integration of Adangal data with FMB sub-divisions from 34/1 to 34/5

6. Conclusions

The overall results suggest that the approach is more effective in reproducing FMBs by using survey measurements in the sketches. This study found that the CollabLand software is effective in regenerating accurate FMB sketches and has been adopted for Digital India Land Records Modernization Programme (DILRMP) project in the State of Andhra Pradesh. The FMBs are generally very old and need thorough updation as they have gone through various stages of manual settlement resulting in degradation of quality. The FMB sketches were perceived as a static, plain view of preselected areas, available at fixed scales, but due to the advances of the geospatial technology, it is now evolving into a dynamic, continually updated network of interrelated databases with volumes of geographically referenced information linked to a comprehensive digital land database. The integration of FMBs data with HRSI is more effective for further developmental planning and

management of the State. The village wise FMB maps have been overlaid on geometrically corrected image for development of applications in various sectors like urban planning, surveying, agriculture, property taxation, etc. This approach provided an effective technique for reproducing FMB data and facilitate to public dynamically. The FMB data can be easily updated, retrieved to do different calculations with less time and cost. This would be extended to the entire State in future. However, semi-automated procedure needs to be evolved for undertaking a gigantic task like digitization of all records pertaining to a State.

Acknowledgments

The authors are gratefully indebted to the Chief Commissioner, Land Administration, Revenue Dept., Govt. of Andhra Pradesh for his encouragement during the work. Authors are greatly acknowledged to shri Sanjay Gupta, E.O. Spl. Secretary to Planning department, Govt. of A.P. for his whole hearted support and constant encouragement during the work. Thanks are also due to the Commissioner and their staff, SS&LR Dept. for their extensive help, valuable suggestions and discussions. We also thank Shri C.J.Antony, Sr. Tech. Director and Shri K. Surendranath, NIC for providing necessary technical support for Collabland s/w. The authors wish to extend sincere appreciation of the encouragement given by the management and the staff of APSAC, Planning Dept., Govt. of Andhra Pradesh during the course of the study.

References

Ali, Z., A. Tuladharb and J. Zevenbergenb (2012) "An integrated approach for updating cadastral maps in Pakistan using satellite remote sensing data, International Journal of Applied Earth Observation and Geoinformation, 18, pp.386-398.

APSAC (2016). Manual of FMBs Digitization at District Level under DILRMP Project, Andhra Pradesh, Hyderabad.

Greenfield, J (2001) Evaluating the accuracy of Digital Orthophoto Quadrangle in the Context of Parcel based GIS, Photogrammetric Eng. & Remote Sensing, 67(2), pp. 199-205.

GoAP (1980). Manual of the Andhra Pradesh Survey Manual of Departmental Rules – Volume-I" GoAP, Hyderabad.

Kemiki, O. A., J. O. Odumosu, A. B. Ayoola and N. I. Popoola (2015). Cadastral Information System for M.I. Wushishi Housing Estate, Journal of Environment and Earth Science, 5 (16), pp. 54-61.

Kumar V. V. G., K. V. Reddy and D. Pratap (2013). Updation of Cadastral Maps Using High Resolution Remotely Sensed Data, International Journal of Engineering and Advanced Technology, 2 (4), pp. 50-54.

Mishra, A and D. J. Pal (2000). Land Record Information Management System (LRIMS) - A Conceptual Framework, Map India 2000 Conference, April 2000.

NRSC (2011). Manual of Space Based Information Support for decentralized Planning (SIS-DP) NRSC, Hyderabad.

Padma, G.V., P. V. Ramireddy, Ch. Tatababu, M. V. R. Murty and G. P. Rao (2015). A Geospatial Frame Work for Mapping of Approximate Cadastral Sub Divisions in Joniganuru Village, Santhipuram Mandal, Chittoor District, Andhra Pradesh - An Initiative, International Journal of Engineering Sciences & Research Technology, 4(7), pp. 200-208.

Raju, K. N. P., S. Kumar and K. Mohan (2008). Urban cadastral mapping using very high resolution remote sensing data, Journal of the Indian Society of Remote Sensing, 36, pp.283-288.

Rao, D. P., R. R. Navalgund and K. Y. V. N. Murthy (1996). Cadastral Applications using IRS 1C data. Indian society of Geomatics, 70, pp. 624-628.

Singh, R. B (1998). Land Records Application of Modern Techniques in preparation of Land Records, Udaipur, Shiva Publishers.

Journal of Geomatics Vol 12 No. 2 October 2018

Estimation of changes in ice thickness of Chhota Shigri glacier, Himachal Pradesh using DGPS and SRTM derived elevation profiles

Rupal M. Brahmbhatt[1], Ritesh Agrawal[2], B. P. Rathore[2], I. M. Bahuguna[2] and A.S. Rajawat[2]
[1] M. G. Science Institute, Ahmedabad - 380 009
[2] Space Applications Centre (ISRO), Ahmedabad - 380 015
Email: ritesh_agrawal@sac.isro.gov.in

(Received: March 20, 2018; in final form: October 10, 2018)

Abstract: Himalayan glaciers are animportant source of water and sensitive indicator of climate change, however, sufficient field based scientific database is lacking due toinaccessible and harsh climatic conditions. Field measurements on Himalayan glaciers are vital to understand glaciation-deglaciation processes, apart from validating satellite based analysis. This study has attempted to estimate changes in ice thickness of Chhota Shigri glacier, Himachal Pradesh using DGPS and SRTM derived elevation profiles. DGPS measurements were madeduring an expedition carried out in 2014. Around 1100 elevation observation points were collected in the non- glaciated region and 4800 on the glacier surface. Elevation profile generated over the glacier surface was compared with the corresponding profile extracted from DEM of SRTM data of the year 2000. SRTM DEM bias was estimated using non glaciated elevation points collected using DGPS. It observed that during14 years' period, there has been a loss in glacier ice thickness of around 6.7m (~0.5m per year). Rate of volume loss is estimated as0.002 km^3per year.The study suggests periodic DGPS observations over same elevation profile in subsequent field expeditions for improving accuracy of estimated changes in glacier ice thickness, which can be utilised for validating results derived from DEM differencing technique.

Keywords: DGPS, Chhota Shigri, Glacier, Elevation Profile

1. Introduction

Global warming is causing an apparent rapid retreat of many glaciers worldwide. Estimation of total glacial ice volume and ice-thickness distribution periodically are crucial for understanding the complex interactions between climate and the glacial system.Himalayan glaciers are not only important source of water, but are also sensitive indicator of climate change. It is extremely difficult to collect fieldbased observations due to inaccessible and harsh climatic conditions prevailing in Himalayan region. Limited field based scientific database is available. This database is general collected during various field expeditions for validating satellite based interpretations and analysis.

Changes in glaciers and ice caps are good indicators of climatic fluctuations (Zemp et. al., 2008) and the current trend shows that majority of the world glaciers have undergone a reduction in glacier mass at an accelerating rate. Monitoring changes in total ice-volume is significant for studies related to climate change and its consequences on global sea level rise (Jevrejeva et. al., 2008). UNESCO initiated the International Hydrological Decade (1965–74) to estimate the total volume of stored water worldwide. Many studies carried out regarding mass balance of mountain glaciers on global level are showing negative mass balance (Cogley, 2009; Zemp et. al., 2009), which may be due to global warming(Yadav et. al., 2004; Roy and Balling, 2005). Temperate glaciers are sensitive indicator of climate change as indicated by their changes in mass balance patterns (Vincent et. al., 2004; Ohmura et. al., 2007). Limited mass balance data in the Himalayan region is a major constrain to explain impact due to climatechange. Field based mass balance study was initiated for Gara glacier, Himachal Pradesh in September 1974 (Raina et. al., 1977). Mass balance were estimated for eight glaciers at least for one year during 1980s (Dyurgerov and Meier, 2005). These studies are scanty and insufficient and carried out for short period, not exceeding one decade (Dobhal et. al., 2008).

Mass balance of a glacier referred as the total loss or gain in mass at the end of the hydrological year. It estimated by measuring total accumulation and ablation of snow and ice during a specific year. Empirical relations were developed between field mass balance and Accumulation Area Ratio (AAR) by Kulkarni, 1992; Kulkarni et al., 2004, Kulkarni et. al., 2007 and Singh et al., 2013.

There are wide variations in glacier mass changes from time to time and place to place due to various factors such as elevation, latitude, orientation, precipitation, size, debris covered or debris free etc. Generally mass balance studies are carried out by using geodetic, glaciological, hydrological or AAR method (Benn and Evans, 2010; Bhambri et. al., 2011; Cuffey and Paterson, 2010; Gardelle et al., 2012).

Field based glacier mass balance estimations require large amount of efforts in terms of resources, logistics and accuracy in measurements. Remote sensing based methods have become an important alternative to conventional methods of mass balance estimation. These methods include monitoring of snow line at the end of ablation season and adopting AAR approach, DEM differencing, LIDAR techniques (Bahuguna et al., 2007; Berthier et al., 2007; SAC, 2011; SAC, 2016).This study has attempted to estimate changes in ice thickness of Chhota Shigri glacier, Himachal Pradesh using DGPS and SRTM derived elevation profiles.

2. Study area

The ChhotaShigri is typical valley type glacier located in the Chenab basin, Lahaul and Spiti Valley, PirPanjal Range, Western Himalaya in Himachal Pradesh. The glacier is located in the altitude range of 6263 m to ~4050 m a.s.l., is ~9 km long and covers 15.7 km^2 of area. The main glacier is a north facing, whereas trunk glaciers areeither east or west facing (Figure 1). Due to orographic position, this glacier is influenced by the monsoon-arid transition zone and two atmospheric circulation systems, viz., the Indian monsoon during summer (July–September) for wet precipitation and the northern-hemisphere mid-latitude westerlies during winter (January–April) (Singh et. al 1997; Bookhagen and Burbank, 2006; Gardelle et. al 2011) for dry precipitation.

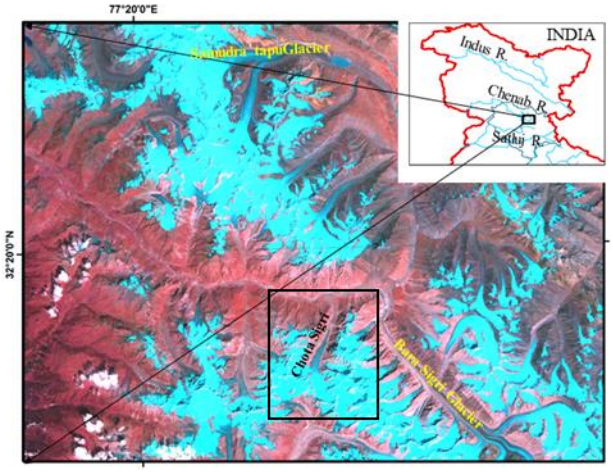

Figure 1: Location Map of study area (Chhota Shigri glacier)

3. DGPS measurements

The geodetic measurements were carried out with the help of GPS instrument. The dual frequency GPS instrument is equipped with Leica GPS500 instrument with SR520 receiver. The dual frequency instrument measures the GPS observable in dual (L1 and L2) frequency mode, which is utilized for the ionospheric correction. The GPS based observation were taken during the period 13th - 16th September 2014. Two base stations were established i.e., one in glaciated and other in non-glaciated region. These were used as reference points for collection of kinematic profiles over the glaciated and non-glaciated regions.

3.1. Elevation profile measurements

The kinematic observations using DGPS were made in two steps. In the first step, the kinematic observation was collected in the non-glaciated region while in the second step, measurements were collected in the glaciated region. In the non-glaciated region, the observations were made along the main stream of the Chandra River as well along a stream originating from snout of the glacier. The elevation profile was collected at an interval of 15 seconds. Over the glaciated surface, measurements were madeat a higher interval rate of 3 seconds. DGPS measurements were made from snout to accumulation zone of the ChhotaShigri glacier. In addition to elevation profile,locations of glacier features such as maulin, crevasses and erratics over ablation/accumulation zonewere also obtained using DGPS (Figure 2).

Figure 2: DGPS measurements over different glacier features of Chota Shigri glacier

4. Data analysis and results

The static GPS observations of the base stations were processed using six IGS stations namely (CHUM, COCO, LHAZ, HYDE, KIT3 and PBR2) and precise ephemeris using Gamit software developed by MIT. The established precise base station was used for the computation of the elevation profile using differential data processing with the help of the Track module developed by MIT. The total 1104 elevation observation points were collected in the non- glaciated region and 4878 elevation observation collected on the glacier surface are shown as blue and yellow color respectively in figure 3.

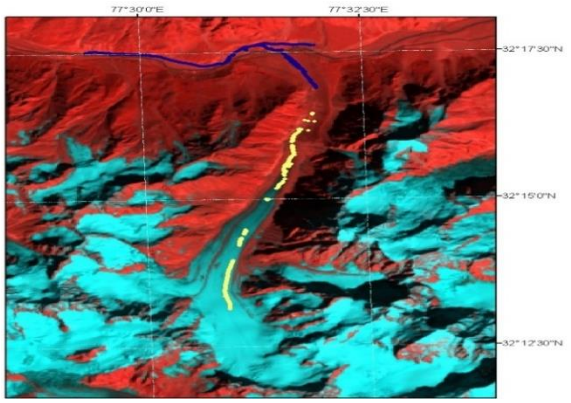

Figure 3: Location of DGPS measurements (Blue dots are over non-glaciated region and yellow dots are over glaciated surface)

The DGPS measurements are observed in the WGS84 ellipsoid whereas the SRTM DEM is in the Orthometric heights. In order to estimate changes in elevation of the glacier surface with respect to SRTM 30m DEM, the SRTM DEM was corrected to get the elevation information in the same GPS reference plane. The corrections were made by estimating the geoid height using EGM96 (Earth Gravity Model 1996). The EGM96 geoid height is used for the conversion of SRTM Orthometric height into ellipsoidal height according to the following formula

$$h = H + N$$

Where,
h = WGS84 Ellipsoid height
H = Orthometric height
N = EGM96 Geoid height

The non-glaciated elevation values between SRTM DEM and DGPS measurements were compared and used for the estimation of the Biases present in the SRTM DEM. Figure 4 shows that there is a strong correlation between elevation of SRTM and DGPS and there is an elevation offset of -2.5 m.

The elevation of the glaciated surface was further corrected by applying a computed offset value in the non-glaciated region. The elevation range measured over the glacier varies in the range of 3950 to 4850 m. DGPS based observations were taken both in the accumulation and ablation zone of the glacier.

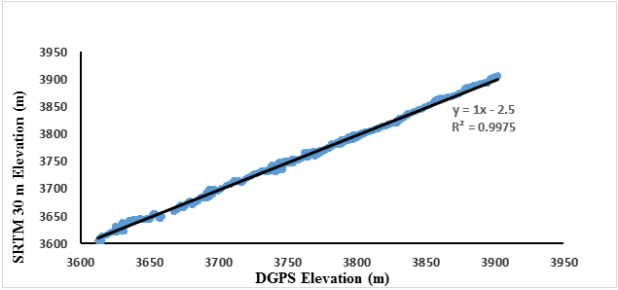

Figure 4: Correlation of DGPS and SRTM 30m DEM shows vertical offset of -2.5 m in non-glaciated region

While comparing DGPS and SRTM derived profiles over same transect, it is observed that change in ice thickness is about 6.7m for 14 years which is -0.5m per year (Figure 5). Total volume loss per year is estimatedas ~0.002 km^3 using standard method. These results are comparable with studies carried out by Azam et. al., 2012 and Engelhards et. al., 2016 who have estimated a negative mass balance of –0.67 ±0.40 m w e a^{-1}during the period 2002/2010 and -0.59±0.12 m w e a^{-1}during 2002-2013 of Chhota Shigri glacier using glaciological methods respectively.

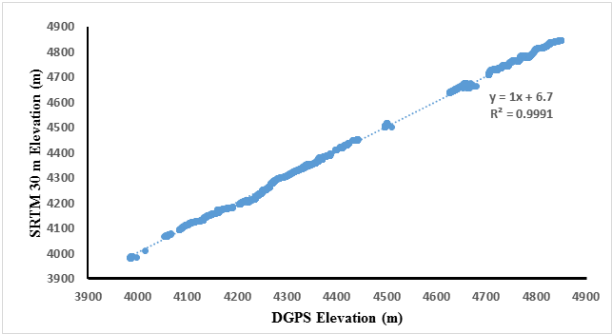

Figure 5: Correlation of DGPS and SRTM 30m DEM with vertical offset of -6.7 m in glaciated region of ChhotaShigri

5. Conclusions

The study has demonstrated potentials of DGPS measurements over glaciated region to derive elevation profile and its utility in estimating changes in glacier ice thickness, in conjunction with SRTM DEM derived elevation profile. The study shows that there has been a loss in glacier ice thickness of around 6.7m (~0.5m per year) over Chhota Shigri glacier during time frame 2000 - 2014.Rate of volume loss is estimated as 0.002 km^3per year. The study suggests periodic DGPS observations over same elevation profile in subsequent field expeditions for improving accuracy of estimated changes in glacier ice thickness, which can be utilised for validating results derived from DEM differencing technique.

Acknowledgements

Authors are grateful to Shri D. K. Das, Director, Space Applications Centre, (ISRO), Ahmedabad for his overall guidance during this study. Authors would like to sincerely acknowledge Dr. Raj Kumar, Deputy Director, EPSA for giving useful comments and suggestions to improve the manuscript.

References

Azam, M.F., P. Wagnon, A.L. Ramanathan, C. Vincent. and P. Sharma. (2012). From balance to imbalance: a shift in the dynamic behaviour of ChhotaShigri glacier, western Himalaya, India. Journal of Glaciology, International Glaciological Society, 58 (208), 315-324.

Bahuguna, I.M., A.V. Kulkarni, S. Nayak, B.P. Rathore, H.S. Negi. and P. Mathur. (2007). Himalayan glacier retreat using IRS 1C PAN stereo data, International Journal of Remote Sensing, 28(2), 437–442

Benn, D.I. and D.J. Evans. (2010). Glaciers and Glaciation, Hodder Education, London, 802; ISBN 9780340905791

Berthier, E., Y. Arnaud, K. Rajesh, A. Sarfaraz, A, P. Wagnon. and P. Chevallier. (2007). Remote sensing estimates of glacier mass balances in the Himachal Pradesh (Western Himalaya, India). Remote Sensing Environment, 108(3),327-338, doi:10.1016/j.rse.2006.11.017.

Bhambri, R., T. Bolch, R.K. Chaujar. and S.C. Kulshreshtha. (2011). Glacier changes in the Garhwal Himalayas, India 1968-2006 based on remote sensing. Journal of Glaciology, 57(203), 543-556.

Bookhagen, B. and D.W. Burbank. (2006). Topography, relief, and TRMM-derived rainfall variations along the Himalaya. Geophysical Research Letter, 33(8), L08405(10.1029/2006GL026037).

Cogley, J.G (2009). Geodetic and direct mass-balance measurements: comparison and joint analysis. Annals of Glaciology, 50(50), 96-100.

Cuffey, K. M. and W.S.B. Paterson (2010). The Physics of Glaciers, Fourth Edition,Academic Press,704ISBN 9780123694614

Dobhal, D. P., J.G. Gergan and R.J. Thayyen (2008). Mass balance studies of the Dokriani Glacier from 1992 to 2000, Garhwal Himalaya, India. Bulletins of Glaciological Research, 25,9-17.

Dyurgerov, M.B. and M.F. Meier (2005). Glaciers and the changing Earth System: a 2004 snapshot. Boulder, CO, Institute of Arctic and Alpine Research. Occasional Paper 58.

Engelhardset, M., P. Kumar, L. Li. and A. Ramanathan (2016). Mass-balance modelling of Chhota Shigri and Patsio glacier in western Himalaya, India,EGU General Assembly, 17-22 April, Vienna, Austria

Gardelle, J., Y. Arnaud and E. Berthier (2011). Contrasted evolution of glacial lakes along the Hindu Kush Himalaya mountain range between 1990 and 2009. Global Planet.

Gardelle, J, E. Berthier and Y. Arnaud (2012). Slight mass gain of Karakoram glaciers in the early twenty-first century,Nature Geoscience,5(5),322-325, doi: 10.1038/NGEO1450

Jevrejeva, S, J.C. Moore and A. Grinsted (2008). Relative importance of mass and volume changes to global sea level rise; Journal of Geophysical Research, 113, D08105.

Kulkarni, A.V. (1992). Mass balance of Himalayan glaciers using AAR and ELA method. Journal of Glaciolology, 38,101–104.

Kulkarni A.V., B.P. Rathore and S. Alex (2004). Monitoring of glacial mass balance in the Baspa basin using accumulation area ratio method, Current Science,86(1),185-190

Kulkarni, A.V. et al., (2007). Glacial retreat in Himalaya using Indian remote sensing satellite data, Current Science, 92(1),69–74.

Ohmura, A., A. Bauder, H. Muller and G. Kappenberger (2007). Long-term change of mass balance and the role of radiation, Annals of Glaciology, 46,367–374.

Raina, V.K., M.K. Kaul and S. Singh (1977). Mass balance studies of Gara Glacier. Journal of Glaciolology, 18(80), 415-423.

Roy, S.S. and R.C. Balling (2005). Analysis of trends in maximum and minimum temperature, diurnal temperature range, and cloud cover over India. Geophysical Research Letter, 32(12), L12702. (10.1029/2004GL022201).

SAC (2011). Snow and Glaciers of the Himalayas, Space Applications Centre, ISRO, Ahmedabad, India, 258 pages, ISBN: 978-81-90-9978-7-4

SAC (2016). Monitoring Snow and Glaciers of Himalayan Region, Space Applications Centre, ISRO, Ahmedabad, India, 413 pages, ISBN: 978-93-82760-24-5

Singh, P., S.K. Jain and N. Kumar (1997). Estimation of snow and glacier-melt contribution to the Chenab river, Western Himalaya, Mountain Research Development, 17(1),49-56. (10.1029/2004GL022201).

Singh S. K., I. M. Bahuguna, B.P. Rathore and Ajai (2013). Spatial distribution of glacier mass balance using remote sensing data in the Himalayan region. In: Climate Change and Himalaya, Natural Hazards and Mountain Resources (Eds: Sundaresen J, Gupta P, Santosh K M and Ram Boojh) Scientific Publishers (India), ISBN: 978-81-7233-881-7 1-6.

Vincent, C., G. Kappenberger, F. Valla, A. Bauder, M. Funk and E. Le Meur (2004). Ice ablation as evidence of climate change in the Alps over the 20th century. Journal Geophysical Research, 109(D10), D10104. (10.1029/2003JD003857).

Yadav, R.R., W.K. Park, J. Singh and B. Dubey (2004). Do the western Himalayas defy global warming? Geophysical Research Letter, 31(17), L17201. (10.1029/2004GL020201.)

Zemp, M., I .Roer, A. K¨a¨ab, M. Hoelzle, F. Paul and W. Haeberli (2008). WGMS: Global Glacier Changes: facts and figures, NEP, World Glacier Monitoring Service, Zurich, Switzerland, 88

Zemp, M., M. Hoezle and W. Haeberli (2009). Six decades of 497 glacier mass-balance observations: a review of worldwide monitoring network. Annals of Glaciology, 50(50), 101-111

Journal of Geomatics Vol 12 No. 2 October 2018

Development of an automated tool in GIS for generating action plans to combat desertification/land degradation

R.J. Bhanderi, Shashikant A Sharma and A.S. Rajawat
Space Applications Centre, Indian Space Research Organisation, Ahmedabad, India
Email: rjbhanderi@sac.isro.gov.in

(Received: Aug 21, 2018; final form: Oct 10, 2018)

Abstract: Increasing global land mass under various processes of desertification/land degradation is one of the most alarming issue. Desertification/land degradation combating action plan tool has been developed in GIS environment using model builder utility and inputs parameters like desertification/land degradation status, land use / land cover (LU/LC), ground water prospects, slope and land capability maps prepared for Bellary district, Karnataka, India using satellite data and ancillary data. Multi-criteria based integrated approach has been used in GIS. It is observed that in general north-eastern parts of the Bellary district requires no action as the land is under no apparent degradation. Most of the south-western parts of the Bellary district requires various measures for combating desertification/land degradation. Suggested measures may help planners to arrest and reverse land degradation processes. GIS tool developed in this study can be utilised in other study areas by altering criteria based on local specific requirements.

Keywords: GIS, Model, Thematic data, Combating Desertification

1. Introduction

Land degradation refers to reduction or loss of the biological or economic productivity, resulting from a combination process arising from human activities and habitation patterns (UNCCD, 1994). Desertification is land degradation in arid, semi-arid and dry sub-humid areas resulting from various factors, including climatic variations and human activities (UNCCD, 1994). There is an urgent need to stop and reverse the process of land degradation. Sustainable management of soil, water and biodiversity are required for protecting the land from further degradation.

Remote sensing and GIS techniques have been extensively utilised in mapping and monitoring desertification and land degradation in India (SAC, 2018; Dharmarajan et al., 2018; Nayak et al., 2017; SAC, 2016; Ajai et al., 2009) aimed at providing current status of desertification and land degradation to United Nations Convention on Combating Desertification (UNCCD) based on land degradation processes and severity. The outcome is useful in prioritising areas, where suitable remedial actions are required for arresting land degradation. Three level classification system (land use classes, land degradation processes and severity levels) have been standardized and used for mapping of land degradation and desertification at national and district level (SAC, 2018; SAC, 2016; Ajai et al., 2009). There is a requirement of regularly monitoring desertification / land degradation of the country for planning effective strategies and measures to combat desertification / land degradation.

Recent studies carried out at national level in India using digital IRS AWiFS data interpreted at 1:500, 000 scale shows that 96.40 mha area of the country is undergoing process of land degradation i.e., 29.32% of the Total Geographic Area (TGA) of the country during 2011-13, while during 2003-05 the area undergoing process of land degradation is 94.53 mha (28.76% of the TGA). There is a cumulative increase of 1.87 mha area undergoing process of desertification/land degradation in the country (constituting 0.57% of the TGA of the country) during the time frame 2003-05 and 2011-13 (SAC, 2016). The change analysis carried out for 2011-13 and 2003-05 time frames indicates that around 1.95 mha land has been reclaimed and 0.44 mha land has been converted from high severity to low severity degradation class, indicating improvement. On the other hand, around 3.63 mha productive land has degraded and 0.74 mha land is converted from low severity to high severity degradation class (SAC, 2016). Desertification/ Land degradation status mapping carried out for selected 76 districts and 2 sub-basins using digital IRS LISS-III data on 1:50, 000 scale revealed that out of 49.66 million ha area mapped, 22.80 million ha area (45.92%) is undergoing desertification/land degradation during timeframe 2011-13. The area under desertification/land degradation during time frame 2003-05 is 22.94 million ha (46.20%). A cumulative decrease of 0.14 million ha area (0.28%) in the area undergoing desertification/land degradation is observed (SAC, 2018).

Long term planning is required for arresting land degradation processes in particular for reclaiming degraded lands, conserving soil and moisture as well developing land and water resources in the region. It also includes mitigating measures such as preventing runoff, arresting soil erosion, stabilising sand dunes, moisture conservation measures and constructing rainwater harvesting structures. The preparation of local specific action plans to achieve these objectives require thematic data on natural resources, terrain and socio-economic conditions.

In this study, a tool has been developed to generate desertification/land degradation combating action plans in an automated way by using standard criteria in a GIS environment. It also has a provision to generate and manipulate the desertification/land degradation combating action plans by user defined criteria in an interactive manner.

2. Study Area

Bellary district, located in Karnataka in south India has been selected as study area (Figure 1). It covers an area of 8,461 sq. lm area. District has population of 24,52,595 with 290 population density, 983 sex ratio and a literacy rate of 67.43% (Census, 2011). Area is covered mainly with black cotton and red soil. The main river in the district is Tungabhadra. Bellary is observed with 41.88% and 41.82 % of total geographical area under land degradation/ desertification for the time frames 2011-13 and 2003-05 respectively as per IRS-LISS-III data interpretation carried out on 1:50, 000 scale, showing marginal increase (SAC, 2018). The processes of desertification/land degradation observed in the district are vegetation degradation, water erosion, man-made (mining/industry), salinity/alkalinity and settlements.

3. Data used

GIS database prepared on 1:50, 000 scale comprising Desertification/Land Degradation Status Map (DSM), land use / land cover, ground water prospects, slope and land capability available at SAC (SAC, 2018; SAC, 2013) have been used as inputs for generating desertification/land degradation combating action plan map.

4. Methodology

Overall methodology for generating action plans to combat desertification/land degradation is given in Figure 2. In order to integrate various themes, firstly, desertification/land degradation status layer was integrated with land use/ land cover layer. The resultant integrated output of these two layers was integrated with ground water prospect and resultant output of these three layers was integrated with slope and finally with land capability layer. The output composite layer has the basic information of all the five layers. Various combinations known as Composite Land Development Units (CLDU) are created in this composite layer. Decision rules (criteria) have been defined based on type of desertification/land degradation process, evaluation of existing landuse/land cover, ground water prospect, slope and land capability in the region (Table 1, modified from SAC, 2013). Suitable measures to combat desertification/land degradation are assigned based on above mentioned decision rules for each of the CLDU. ArcGIS based model (GIS based tool) developed for generating desertification/land degradation combating action plan in GIS environment is shown in Figure 3.

5. Results

Desertification/land degradation combating action plan generated based on integrated approach in GIS environment using different thematic parameters is shown in Figure 4. It is observed that in general north-eastern parts of the Bellary district requires no action as the land is under no apparent degradation. Most of the south-western parts of the Bellary district requires various measures for combating desertification/land degradation. This region is mostly affected by water erosion and vegetation degradation. In most of the region ground water targeting may help in getting double crop and thus help reduce exposure of land to processes of land degradation. Construction of farm ponds/rain water harvesting structures are also suggested in parts of this region for irrigation purpose as well to reduce water erosion. Agro-horticulture is suggested mostly in southern parts of the district to improve vegetation cover. Afforestation along with contour bunding is suggested in various parts of the south-western region of the district to improve vegetation cover as well reduce soil erosion.

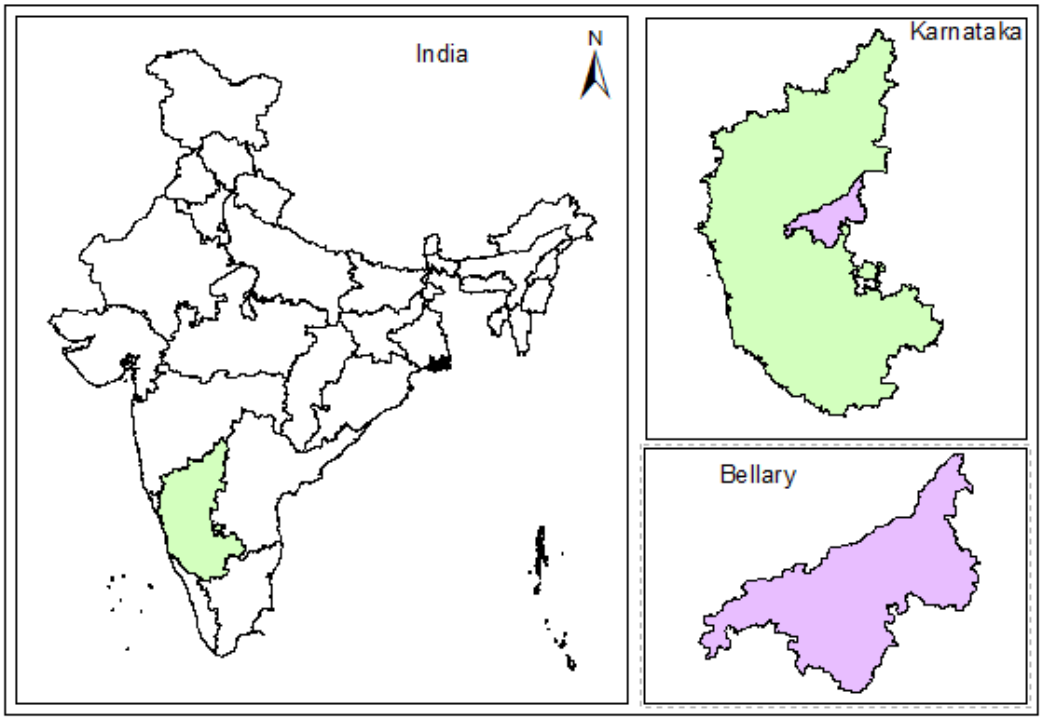

Figure 1: Location map

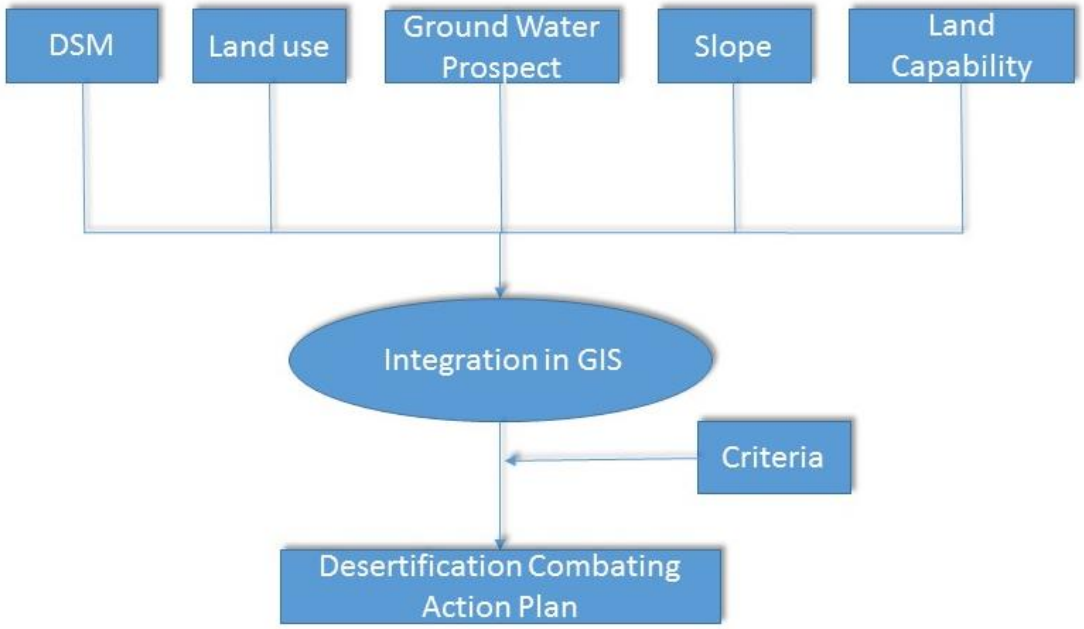

Figure 2: Methodology to generate desertification and land degradation combating action plan

Table 1: Decision rules for generation of desertification/land degradation combating action plan

Sr. No.	Desertification/land degradation Process	Land Use/ Land Cover	Ground water Prospect	Slope in per cent	Land Capability	Measures
1	Vegetation degradation	Open Forest	Moderate	3-5	VI	Afforestation
2	Vegetation degradation, Water erosion	Open Forest	Moderate - Poor	3-5	VI	Afforestation with contour bunding
3	Vegetation degradation, Water erosion	Scrub Forest	Poor	5-10	VI	Afforestation with proper soil and water conservation
4	Vegetation degradation	Open Forest	Moderate	>35	VI	Afforestation with staggered trenches
5	Vegetation degradation	Open Forest	Moderate-Poor	5-10	VI	Protection and Gap Filling
6	Water erosion	Kharif Crop	Moderate	3-5	IV	Agro-horticulture with groundwater irrigation
7	Water erosion	Kharif Crop	Moderate	0-3	III & IV	Double cropping with ground water usage
8	Water erosion, Salinity	Wasteland, Salt affected land	Moderate	3-5	III	Drainage treatment
9	Water erosion	Double Crop	Good- Moderate	0-1	III	Minimal action - farm ponds
10	Vegetation degradation, Waterlogging, Salinity	Land with scrub & Land without scrub	Moderate - Poor	10-15	IV	Silvipasture
11	Barren, Rockey	Barren rocky/Stony waste/ Sheet rock area	Poor	5-10 & 10-15	VIII	Natural regeneration
12	No Apparent Degradation	Kharif+Rabi, Dense Forest	Good	3-5	III	No action

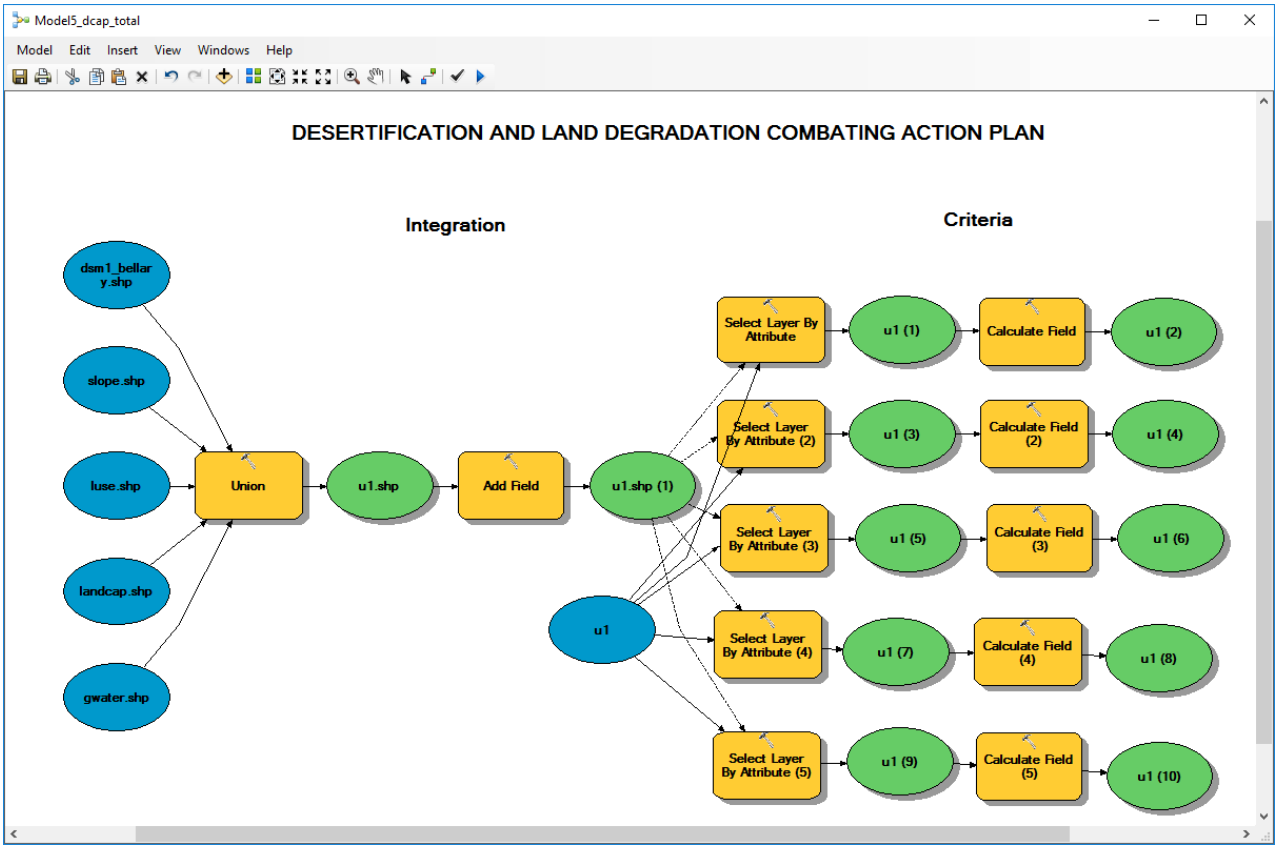

Figure 3: Model to generate desertification/land degradation combating action plan

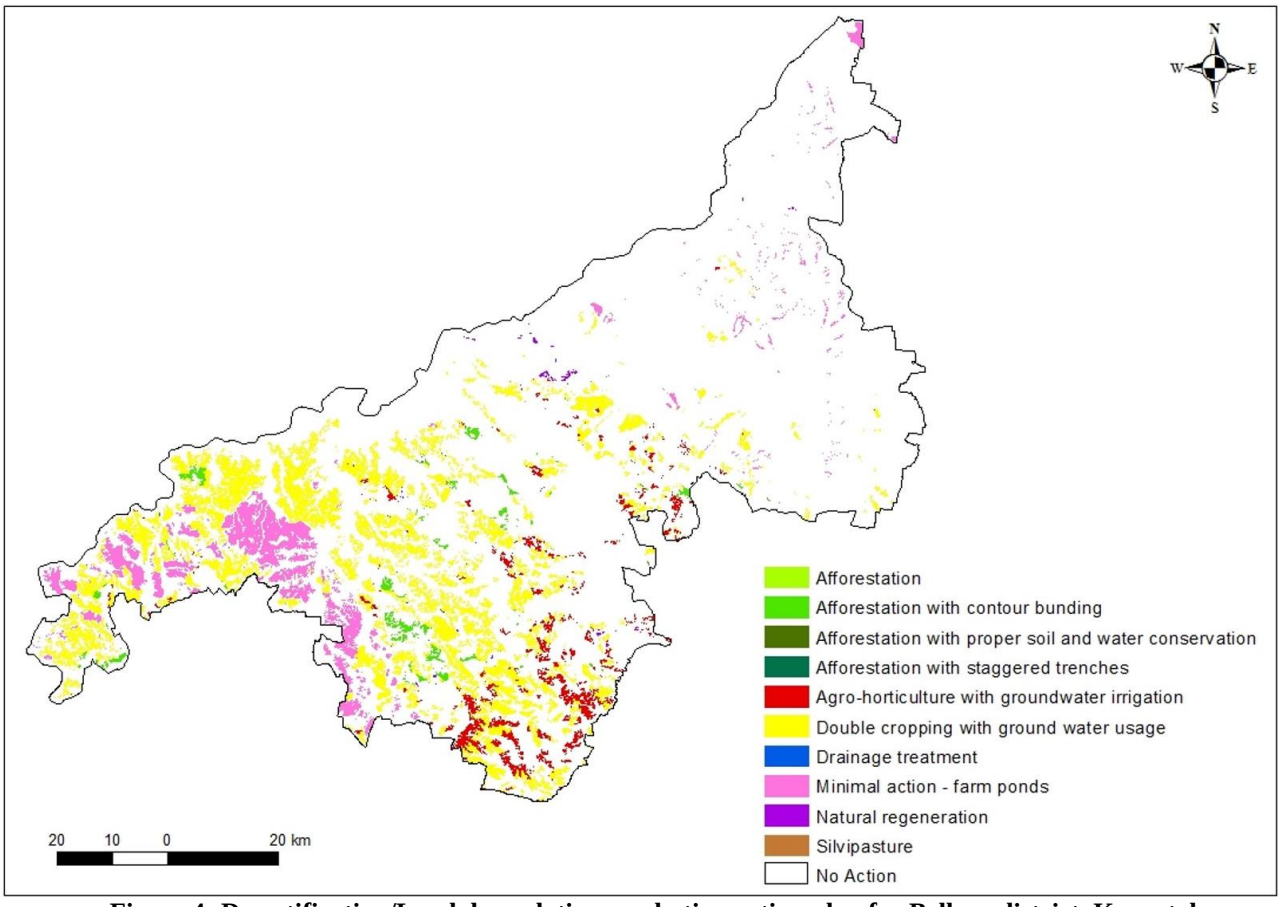

Figure 4: Desertification/Land degradation combating action plan for Bellary district, Karnataka

6. Conclusion

This study has demonstrated development of a tool in GIS environment to generate desertification/land degradation combating action plan automatically. Its utility has been demonstrated for a selected district. GIS tool developed in this study can be utilised in other study areas by altering criteria based on local specific requirements.

Acknowledgements

Authors are thankful to Shri D K Das, Director, Space Applications Centre (SAC) and Dr. Raj Kumar, Dy. Director EPSA/SAC for their kind support and encouragement.

References

Ajai., A. S. Arya, P. S. Dhinwa, S. K. Pathan and K. Ganesh Raj (2009). Desertification/land degradation status mapping of India, Current Science, 97(25), 1478- 1483.

Census (2011). www.census2011.co.in/states.php

Dharumarajan, S., M. Lalitha, Rajendra Hegde, N. Janani, A.S.Rajawat, K.L.N. Sastry and S.K. Singh (2018). Status of desertification in South India- Assessment, mapping and change detection analysis, Current Science, 115(2), 331-338.

SAC (2018). Desertification and Land Degradation Atlas of selected districts of India (Based on IRS LISS III data of 2011-13 and 2003-05), Space Applications Centre, ISRO, Ahmedabad, India, ISBN:978-93-82760-31-3, Volume-1, 148p, Volume-2, 145p. (http://envfor.nic.in/division/publications-and-working-papers) (https://vedas.sac.gov.in/vedas/node/60).

SAC (2016). Desertification and Land Degradation Atlas of India (Based on IRS AWiFS data of 2011-13 and 2003-05), Space Applications Centre, ISRO, Ahmedabad, India, ISBN:978-93-82760-20-7. 219 p. http://envfor.nic.in/division/publications-and-working-papers) (https://vedas.sac.gov.in/vedas/node/60).

SAC (2013). Desertification Status Mapping of India – 2nd cycle - Technical Guideline. Space Applications Centre, Ahmedabad, 49 p. (https://vedas.sac.gov.in/vedas/node/60).

Nayak, S.S., Binal Christian, P. S Dhinwa, J.K Garg and Ajai (2017). Desertification monitoring in Sojat taluka, Pali district, Rajasthan using satellite data. Journal of Geomatics, 11(2), 240-247.

UNCCD (1994). Elaboration of an international convention to combat desertification in countries experiencing serious drought and /or desertification , particularly in Africa (Paris: General Assembly of the United Nations), 58p.

Journal of Geomatics Vol 12 No. 2 October 2018

Spatio-temporal distribution and identification of Encephalitis disease hotspots: A case study of Gorakhpur Tehsil, Uttar Pradesh, India

Nutan Tyagi, Santanu Sahoo and Laxmikant Shukla
Department of Geography, D.D.U. Gorakhpur University, Gorakhpur
Email: nutan_tyagi@yahoo.com

(Received: Apr 27, 2018; in final form: Oct. 16, 2018)

Abstract: Encephalitis is a complex disease with a high mortality, morbidity and disability ratio. In India, it is a major pediatric problem, which has spread over many different areas ever since reporting of the first clinical case in 1955 in Vellore. Gorakhpur district is located in the eastern part of Uttar Pradesh and in low-lying region with tropical climate. It is mainly paddy growing area, with clay soil and high ground water table. Gorakhpur and its surrounding region have very conducive conditions for the breeding habitat of Encephalitis vector and this area has been experiencing the outbreak of Encephalitis since 1978. Every year from July to November, the outbreak of Encephalitis, causes many deaths and long term disability to children and young adults. The study aims to provide a database and thematic maps using geospatial tool for Gorakhpur tehsil. The database created on GIS platform has compiled and track information on the incidence, prevalence and spread of the encephalitis disease in Gorakhpur tehsil. The disease distribution pattern shows the clustering of the disease in the tehsil. Hotspots maps have been created for different years and for the whole period also. Most of these hotspots (very high risk areas) are located in the middle part starting from the northern part of the region and stretching from north to south. The geospatial database created through the study on Encephalitis will provide an effective platform, which can be utilized by the health care providers, public health managers and policy makers to generate policies that will best meet the need for prevention, control and management of Encephalitis in Gorakhpur tehsil.

Key words: Encephalitis Hotspots, Spatial Statistics, Statistically Significant, Spatial Autocorrelation.

1. Introduction

Encephalitis is a complex disease with a high mortality, morbidity and disability ratio. It is a seasonal epidemic disease with a 40-year recorded history in Gorakhpur region. Gorakhpur and its surrounding region have very conducive conditions for breeding habitat of encephalitis vector. This area has been experiencing almost every year the outbreak of Encephalitis. Gorakhpur and its surrounding region have been a known focus of encephalitis since 1978, when the first case was reported here. It is mainly a paddy growing area, with clay soil and high ground water table. Every year, particularly from July to November the outbreak of encephalitis causes many deaths and long-term disability to children and young adults. People at highest risk for encephalitis and its complications, include the very young, the very old and people with weakened immune systems. Since 1988, the disease manifestations have changed and apart from Japanese Encephalitis cases, unidentified categories of cases are also reported. These cases are now classified under the category of EVE (Entero-Viral Encephalitis). both types of cases occurring in Gorakhpur region are termed as AES (Acute Encephalitis Syndrome) cases since 2005. This paper is an attempt to identify high risk area of the disease. In medical geography geospatial analysis tool is an effective means of finding spatial distribution, areas of concentration, assessing trends, and decision making related to health and epidemiology. Spatial statistics empowers the user to answer questions confidently and make important decisions than the simple visual analysis, spatial statistics is one method for better understanding of geographical phenomena, pin pointing the causes of specific geographical patterns, summaries the distribution of single number and make decisions with a higher level of confidence (Chakraborty, 2013).

Spatial statistics is most powerful tool for describing and analyzing how various geographic objects or events occur and change across the study area. Spatial analysis tools such as GIS and spatial statistics, enable epidemiologists to address the spatial distribution and predict the outbreaks of disease more accurately (Chaput et al., 2002).

Identifying clusters is the process that follows basic series of steps. It can be done manually and by using tools. The aim is to investigate disease clusters and disease incidence near point source (Lawson and Denison, 2002). Automated tools which can do cluster analysis are Spatial Autocorrelation (Moran's I), Hotspots analysis, Cluster Outlier Detection, Interpolation IDW, Kernel Density Mapping, Anselin's LISA (local Indication of spatial Association) etc., are many methods which can provide the information whether there is clustering or statistical autocorrelation occurring (Anselin and Getis, 1992; Anselin, 1993; 1995; 1996).

2. Objectives

1 Spatial distribution of encephalitis at CD block, village and ward level in Gorakhpur tehsil during the period of 2006-2016.

2 Creation of occurrence map of the disease through this database.

3 To understand the statistically significant and spatial pattern of the encephalitis occurrence region using hotspots analysis to identify the priority areas, in order to formulate strategies that might help in reducing the burden of disease.

3. Methodology

Present paper intends to investigate the spatio-temporal pattern of Encephalitis and uses spatial statistical techniques and analysis to study the characteristics of spatial patterns of the distribution of encephalitis in Gorakhpur tehsil at village and ward level. Mapping of the disease for every year from 2006-2016, in GIS domain has been carried out using Arc GIS 10.1. A database has thus been generated with the help of line list data collected from the District Hospital of Gorakhpur and analyzed by tabulation, diagrams and mapping. Spatial auto-correlation analysis using Hotspots Analysis has been carried out with the Spatial Analyst extension (version 10) of Arc GIS 10.1 tool, which uses Getis-OrdGi* or G statistics (Getis and Ord, 1992) to identify the spatial pattern.

4. Study Area

Gorakhpur tehsil occupies the north eastern portion of the district of the same name. The study area lies between latitude $26^0$36'4' N to $26^0$57'3" N (40 km) and Longitude $83^0$13' 58" E to $83^0$37'26"E (41 km) and is spread over an area of 841 km.^{2}, which is about 25.32% of the district area (Figure 1). According to 2011 census, the tehsil has 16,30,731 population and contributes 36.72 per cent of the total population of Gorakhpur District (44,40,895). The district headquarters Gorakhpur city having the population 673,446 (2011census) is also located within the study area. Administratively Gorakhpur Tehsil, incorporates whole of Chargawan, Bhathat CD block and partial areas of Jungle Kaudiya, Pipraich, Piprauli and Khorabar CD blocks. Two villages of Sardarnagar CD block are also included in this Tehsil. It has 511 villages out of which 444 villages are inhabited and 67 villages are uninhabited.

Besides Gorakhpur City (Municipal Corporation) one Nagar Panchayat Pipraich and five census towns are also located within the limits of study area. Gorakhpur city is divided into 70 wards, while Nagar Panchayat Pipraich has been divided into 12 wards. Bansgaon tehsil forms the southern boundary of the study area, on the west and north-west the boundary marches along Sahjanwa tehsil and Campierganj tehsil respectively, on the north east study area adjoins Mahrajganj and Kushinagar districts and further south Chuari Chaura tehsil forms the dividing line. NH-28 running almost east-west passes through the southern portion of tehsil and NH 29 runs almost north-south in the western part and south of Gorakhpur city and connects the region with Varanasi. NH-24 connects the region to Saunauli (near Nepal border).

5. Encephalitis in Gorakhpur and its surrounding region

Acute Encephalitis is a clinical condition caused by the Japanese Encephalitis Virus (JEV) or other infectious causes (Kakkar et al., 2013). Encephalitis is a seasonal epidemic disease with a 40-year recorded history in Gorakhpur Region. The increasing number of encephalitis cases in the study region has become a priority health issue. Recent outbreak shows two trends- incidence of disease is reported not only in peak period but throughout the year and increasing outbreaks outside the endemic rural areas, particularly in urban area also.

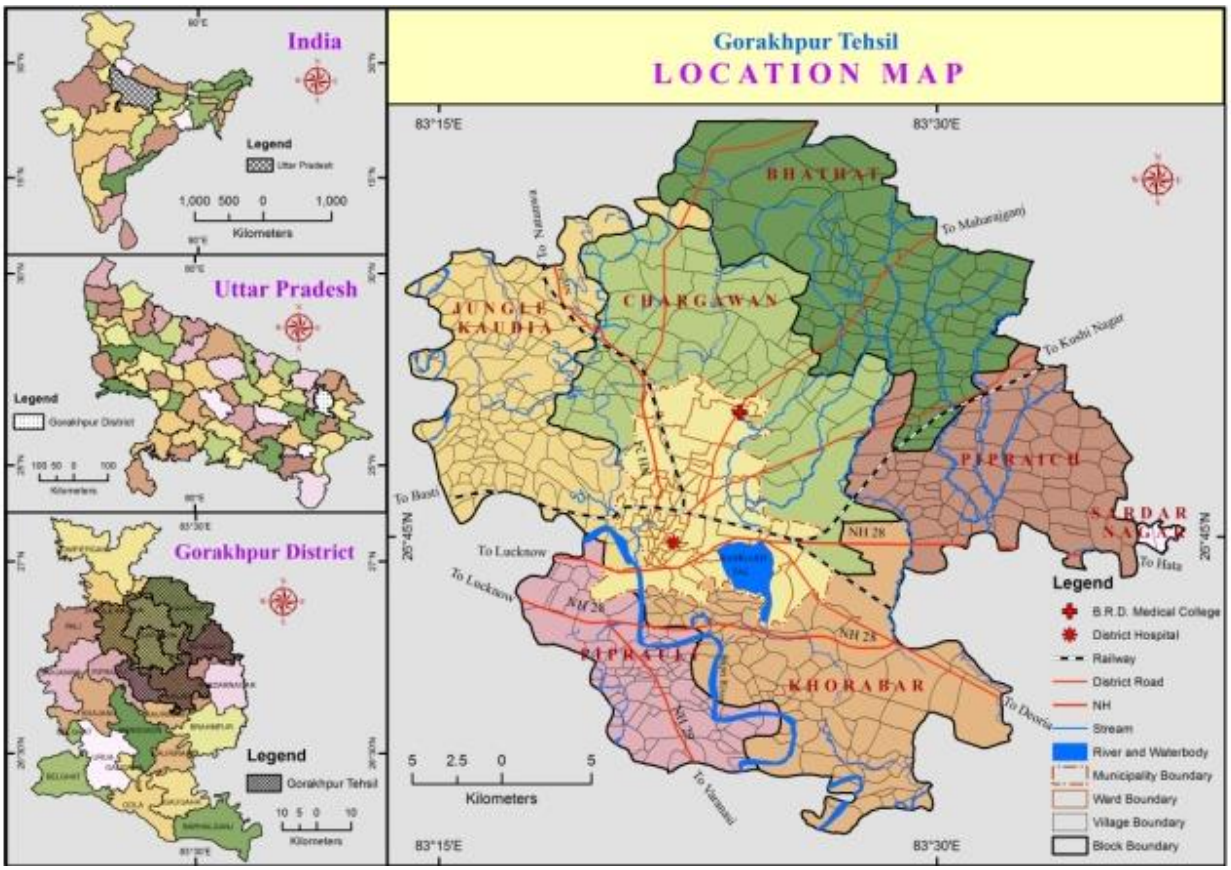

Figure 1: Location of study area

Gorakhpur and its surrounding region have very conducive conditions for breeding habitat of encephalitis vector. This area has been experiencing almost every year the outbreak of Encephalitis. The disease has been a public health burden in this region since 1978, when the first case was reported here. Overall 15 districts of surrounding region of Gorakhpur district are affected by encephalitis. Gorakhpur district remained the most affected district in the region.

Gorakhpur tehsil situated in the north eastern part of the district has highest concentration of the reported cases of encephalitis. During 2006-2016, nearly half (51.54 per cent) of the cases of the district are reported from here. During the span of study time, overall 3256 encephalitis cases are reported in Gorakhpur tehsil. It is very surprising fact that highest number (856 cases) of encephalitis cases are registered from the urban area, i.e., Gorakhpur city. The study area also includes the two most affected CD blocks (Chargawan and Khorabar) of the Gorakhpur tehsil and district. It is quite remarkable that at village level, all the villages are not affected by the outbreak this disease. It is concentrated in some villages, while others are absolutely free from the disease till now.

6. Spatial Pattern of Encephalitis in Gorakhpur Tehsil

6.1. Geographic Distribution of Encephalitis Cases, 2006- 2016

Distribution pattern of encephalitis cases reveals that distribution of the cases is concentrated in some parts of the tehsil. To analyse the spatial distribution pattern of encephalitis annual incidence of the disease, between 2006-2016 (eleven-year span) has been used and villages are grouped into seven classes (Table 1) according the reported cases and endemism (Figure 2). There is no definite trend in the incidence because cases appear in fluctuating manner.

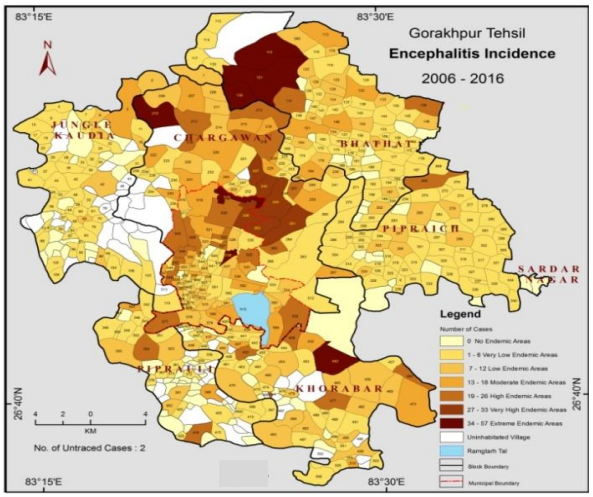

Figure 2: Encephalitis incidence

6.1.1 Non Endemic Areas

In this category villages which do not have reported cases during the study period are included. About 148 villages (28.63 per cent of the total) have never experienced the outbreak of encephalitis. Most of these villages are concentrated and distributed in the western and south western part of tehsil. Many of them are uninhabited ones. These villages are also scattered in north east and eastern areas of the region in Bhathat and Pipraich CD block. In the middle part non-endemic areas are found in patches. Three wards of Gorakhpur city have no reported cases of encephalitis, viz., Lohia Nagar, Jungle Tulsiram East and Kalyanpur.

6.1.2 Extremely High Endemic Areas (>34 Encephalitis Cases)

In these areas highest number of encephalitis cases (287 cases) have been reported, which ranges between 34-57 cases. Five villages (J. Janul Abden Urf Jainpur, Jungle Dumari No 2, Jungle Ramgarh Urf Chauri, Rampur Gopalpur and Jungle Dumari No1) and two wards (Manbela and Shahpur) fall under this category. Manbela ward of Gorakhpur city ranks first (with 57 cases) as far as the incidence of cases is concerned. Jungle Dumri No -1, situated in the north-western part of tehsil has 48 reported cases. These areas account for 8.82 per cent of the total incidence of disease. The combined population of these areas is 70,376 people, which is 4.32 per cent of the tehsil population.

6.1.3 Very High Endemic Area-(27-33 Encephalitis Cases)

This category area includes five villages, viz., Jungle Dhusar, Jungle Chatradhari, Harsewakpur No.2 (Census town), Bangai, Gulariha (Chargawan block) and are located in north middle area of the region. Semra ward of Gorakhpur city with total 29 cases is also in this class and out of total cases 5.41 per cent cases of the tehsil are reported from these areas. The combined population of these areas represents 3.21 per cent (52,306 people) of the tehsil population. Total 176 cases have been reported from these villages and wards.

6.1.4 High Endemic Areas (19-26 Encephalitis Cases)

High Endemic area includes the areas where 19-26 encephalitis cases have been reported during last eleven years and total 600 cases are reported from the areas included in this category. Ten wards of Gorakhpur city (Surya Kund, Engineering College, Chargawan, Shivpur Sahbaganj, Basharatpur, Lachhipur, Rajendra Nagar West, Nausarh, Rasoolpur, Rapti Nagar and Tiwaripur), 15 villages and Pipraich Nagar Panchayat are high endemic areas and located mostly in the adjoining areas of high endemic areas. 18.43 per cent of the total reported cases appear here. Fifteen villages, viz., Jungle Belwar, Dangipar, Sahookol Urf Mirzapur, Khorabar Urf Soobabazar, Motiram Adda (Khorabar CD block), Parmeshwarpur, Ekla No.2, Jungle Tinkonia No1, Bisunpur, Jungle Tinkonia No1, Jungle Pakri, Khuthan Khas, Karmaha Buzurg (Chargawan CD block), Jungle Ranee Suhas Kunwar urf Mahaveer Chappra, Bagha Gara (Piprauli CD block), Karmaha Buzurg and Bailo (Bhathat CD block) are under this category.

Table 1: Gorakhpur Tehsil: Distribution of Encephalitis cases 2006 – 2016

Sl. No.	Endemic Areas	No. of Cases	Percentage	No. of Villages	No. of City Wards
1	No Endemic Areas (0)	0	0	148 (28.63%)	3 (4.29%)
2	Very Low, <6 cases	855	26.25	256 (49.52%)	19 (27.14%)
3	Low, 7-12 cases	764	23.47	63 (12.19%)	20 (28.57%)
4	Moderate, 13-18 cases	574	17.63	24 (4.64%)	14 (20%)
5	High, 19-26 cases	600	18.43	15 (2. 90%)	11 (15.71%)
6	Very High, 27-33 cases	176	5.41	5(0.97%)	1 (1.43%)
7	Extremely High >34	287	8.82	5 (0.97%)	2 (2.86%)
	Total	3256	100	517 (100)	70 (100)

6.1.5 Moderately Endemic Areas (13-18 Encephalitis Cases)

Fourteen wards of Gorakhpur city and 24 villages are included in these areas, Total 574 cases (17.63% cases) are reported from these areas. Fourteen wards of the city are under this category and the distribution of the wards included in this category are scattered all over the city, while villages are distributed and concentrated in the middle part stretching from north to south.

6.1.6 Low Endemic Areas (7-12 Encephalitis Cases)

Low endemic areas are distributed in the eastern, western and southern fringe areas of the region. Encephalitis cases appear in 20 (28.57 per cent) wards and 63 (12.19 per cent) villages. Overall 764 (23.47 per cent) encephalitis cases are reported from the areas under this category.

6.1.7 Very Low Endemic Areas (<6 Encephalitis Cases)

Very low endemic areas are scattered all over the study area. 19 wards of the Gorakhpur city and 256 villages are included under this category and covers 26.25% of the total incidences (855 cases).

Distribution of these villages is more on eastern and western sides of the tehsil. From the analysis of annual incidence of encephalitis cases in Gorakhpur tehsil, it is clear that high endemic areas are located in north and mid part of the tehsil and also include the northern wards of the city. Rest of the high endemic areas are distributed in patches, while low endemic areas are scattered all over the tehsil.

7. Occurrence of Encephalitis cases (2006-2016)

According to the analysis of annual incidence of encephalitis data it is revealed that in some areas encephalitis is appearing almost every year, and some villages have reported cases sporadically (Figure 3; Table 2), while some villages do not have any incidence of the disease. During the study period about 148 villages of the tehsil were found to be unaffected by the annual outbreak of encephalitis. In 69 villages (18.65 per cent), the disease occurred only once and in 58 villages (15.68 per cent) twice. 70 villages (18.92 per cent) experienced the outbreak thrice and four and five times outbreak was recorded in 46 (12.43 per cent) and 28 villages (7.57 per cent) respectively. As the occurrence of the disease increases the number of villages in that category got reduced. Six, seven and eight times disease incidence occurred in 36 (9.73 per cent), 20 (5.41 per cent) and 17 (4.59 per cent) villages respectively. Disease incidence of nine times in eleven years appeared in 14 villages (3.78 per cent), out of which 4 villages are located in Chargawan CD block.

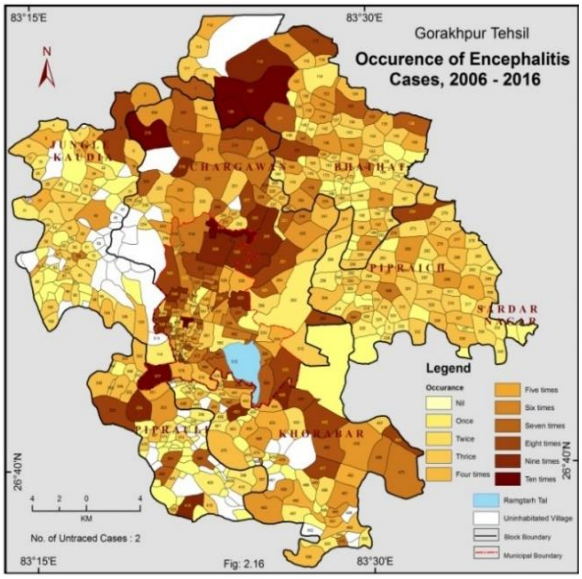

Figure 3: Occurrence of Encephalitis cases

Jungle Janual Abden urf Jainpur, Jungle Dumari No.-1 (Bhathat CD block) and Rampur Gopalpur (Chargawan CD block) have the incidence of disease every year. That is why these villages have highest number of encephalitis cases during the study period. Nagar Nigam Gorakhpur area shows a different trend. Lohia Nagar, Jungle Tulsiram and Kalyanpur are the three wards of the city which are not affected by encephalitis and no incidence of the disease was recorded here during the study period.

In Civil Lines II ward, only once in 2007, encephalitis cases were reported and after that it is free from the disease. 3 wards, viz., Janpriya Vihar, Narsinghpur and Raiganj have reported cases twice. Average of three times occurrence of encephalitis is reported from Jharna Tola, Jatepur Railway Colony, Civil Lines and Hansupur wards. Nine wards (Vikas Nagar, Chaksa Hussain, Netaji Subhash Chandra Bose Nagar, Jafara Bazaar, Dilezakpur,

Table 2: Gorakhpur Tehsil: Occurrence of Encephalitis cases at village and city level (2006-2016)

Occurrence	Bhathat	Chargawan	Jungle Kaudia	Pipr auli	Pipr aich	Khor abar	Sardar Nagar	Total Villages	Per cent	Gorakhpur City	Per cent
Once	14	2	19	7	14	13	-	69	18.65	1	1.49
Twice	11	6	14	4	15	8	-	58	15.68	3	4.48
Thrice	21	6	16	6	16	5	-	70	18.92	4	5.97
Four times	7	8	7	7	10	7	-	46	12.43	9	13.43
Five times	7	2	5	2	4	8	-	28	7.57	8	11.94
Six times	10	9	4	1	3	9	-	36	9.73	6	8.96
Seven times	4	4	1	4	2	5	-	20	5.41	11	16.42
Eight times	3	8	1	3	-	2	-	17	4.59	9	13.43
Nine times	2	4	1	1	1	5	-	14	3.78	8	11.94
Ten Times	1	4	-	2	-	2	-	9	2.43	5	7.46
Eleven Times	2	1	-	-	-	-	-	3	0.81	3	4.48
Total Cases	82	54	67	37	65	64	0	369	71.57	67	95.71
No cases	15	7	43	47	9	24	2	148	28.43	3	4.29

Purdilpur, Diwan Bazaar, Sheshpur and Mahui Sugharpur, of the city have the occurrence of the disease four times, while five times disease cases are reported from eight wards (Shaktinagar, Jungle Salikram, Mahadev Jharkhandi-2, Bhediagarh, Krishna Nagar, Humayunpur North, Alhadadpur and Mahewa). Six and seven times the disease appeared in 6 and 11 wards respectively. 9 wards recorded the incidence eight times and 8 wards nine times. 10 times incidence is recorded in 5 wards, viz., Chargawan, Shivpur Shabajgang, Semra, Tiwaripur and Rasoolpur, while cases are recorded every year in three wards, viz., Manbela, Alinagar and Nausarh wards and are also worst affected areas of the city

8. Hotspot delineation

Basically, "hotspot" refers to area with unusually high occurrence of point incidents. Hotspot analysis aims to assist identification of locations with unusually high concentration of occurrence in the form of hotspots and cold spots within a limit of geographical area that appear overtime. This method has the advantage of detecting the presence of hotspots and cold spot for each feature in a data set over the entire area. This tool works by looking at each feature with context to neighbouring features. It identifies spatial clusters of High values (Hotspots) and spatial clustered low values (Cold spot). These hotspots and cold spots can be thought of as spatial concentrations.

Hotspot analysis can identify that whether spatial variation in distribution is statistically significant and help to target those areas for further study. Delineation of these hotspots and cold spots helps in optimizing the use of resources for timely interventions (Handique, et al., 2011). Spatial autocorrelation is a statistical tool that can be used in epidemic study. Global Moran's I is used to establish the autocorrelation and Getis-ord. General G. (global) Hotspots Delineation (Moran, 1950). Density mapping can locate clusters in the dataset but cannot specify its significance.

9. Results

Getis-OrdGi* or G statistics method has the advantage of detecting the presence of hotspots and cold spot for each feature in a data set over the entire area. Gi* statistics returned for each feature in dataset is a Z score. For statistically significant positive Z score, the larger the Z score, more intense is the clustering of high value (hotspots). For statistically significant negative Z score, smaller the Z score more intense is the clustering of low values (cold spot). The resultant Z score tells the user where features with either high or low value cluster are spatially distributed. The resultant Z score values for Gorakhpur tehsil is between 5.97 to 11.51, which is significant at 99% confidence level indicating clustering pattern for each year during 2006 to 2016 (Table 3).

Table 3: Gorakhpur Tehsil: Spatial Autocorrelation

Year	Z-score	Moran's I	Pattern
2006	8.49	0.12	Clustering
2007	5.97	0.08	Clustering
2008	6.99	0.09	Clustering
2009	9.50	0.13	Clustering
2010	6.92	0.10	Clustering
2011	11.52	0.16	Clustering
2012	6.67	0.09	Clustering
2013	8.82	0.12	Clustering
2014	7.22	0.10	Clustering
2015	6.99	0.09	Clustering
2016	3.76	0.07	Clustering
2006-2016	12.13	0.22	Clustering

The value of Moran's I index range from -1 to +1. The value '1' means perfect positive spatial autocorrelation (This means values are clustered together), while close to -1 value suggests perfect negative autocorrelation. Moran's I is a spatial autocorrelation analysis tool which is used to measure the presence of clustering in similar value (Tsai et al, 2009).

Table 3 shows the calculated Z score and Global Moran's I for Gorakhpur tehsil from 2006-2016. The Moran's I index of 2006 shows that on the basis of encephalitis cases distribution this year Moran's I value calculated as 0.11. In 2009, 2011 and 2013 Moran's I index were found to be 0.13 (highest), .015 and 0.11 respectively and rest of the year, it remained below 0.1 ranging from 0.08 to .09. The average value for 2006-2016 period comes 0.22. The values of Moran's I suggest that the disease pattern could be a result of random chance. Z score values being between 5.97 to 11.51, which is significant at 99% confidence level indicate clustering pattern for each year.

Apart from the annual spatial distribution pattern of the disease, hotspots maps for each year and for whole study period (Figure 4 and 5) have been created. The analysis of this result shows that some areas of the tehsil have emerged as hotspots of encephalitis. The disease distribution is highly clustered and most of the region of tehsil is in no significant category.

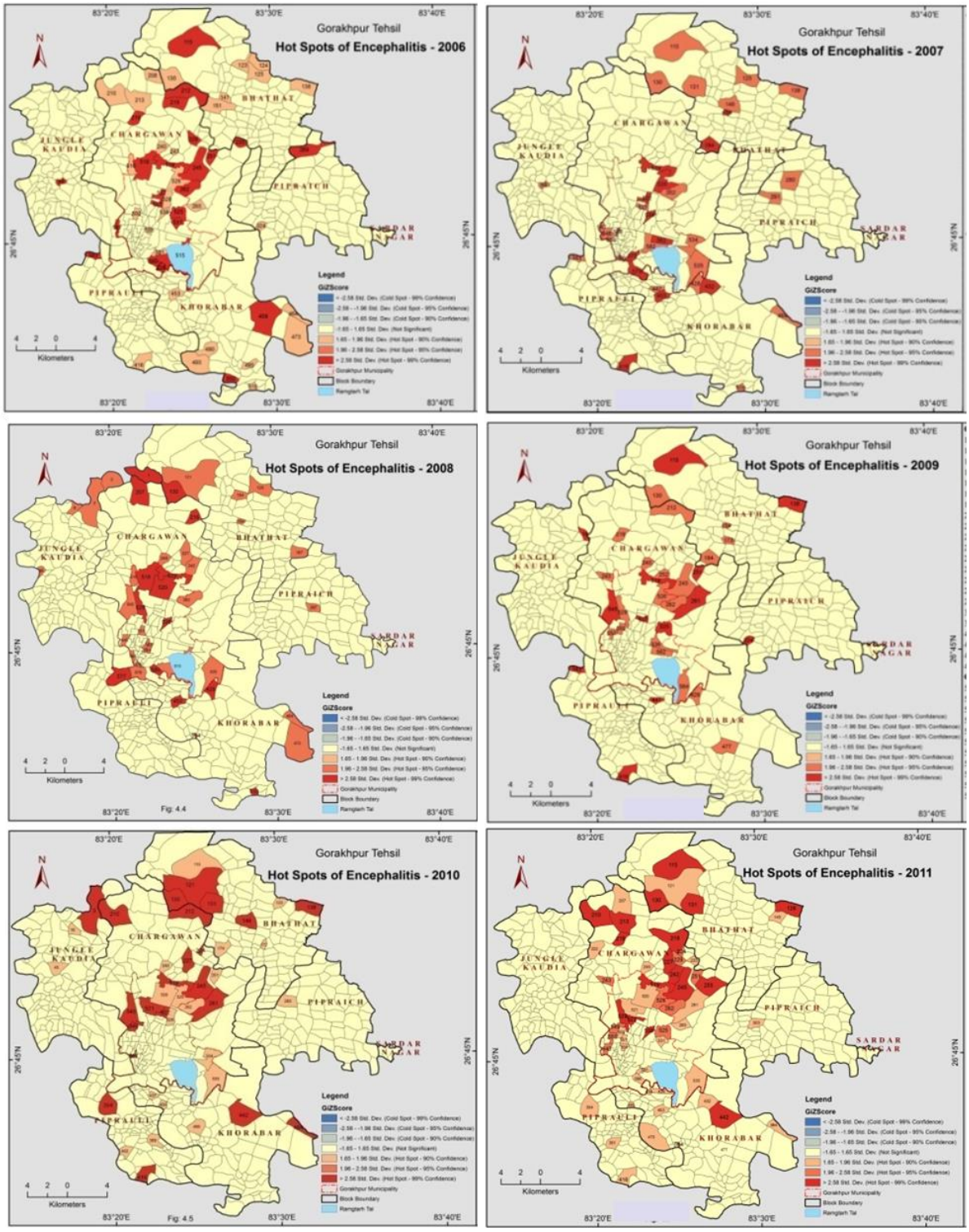

Figure 4: Hotspots of Encephalitis, 2006-2011

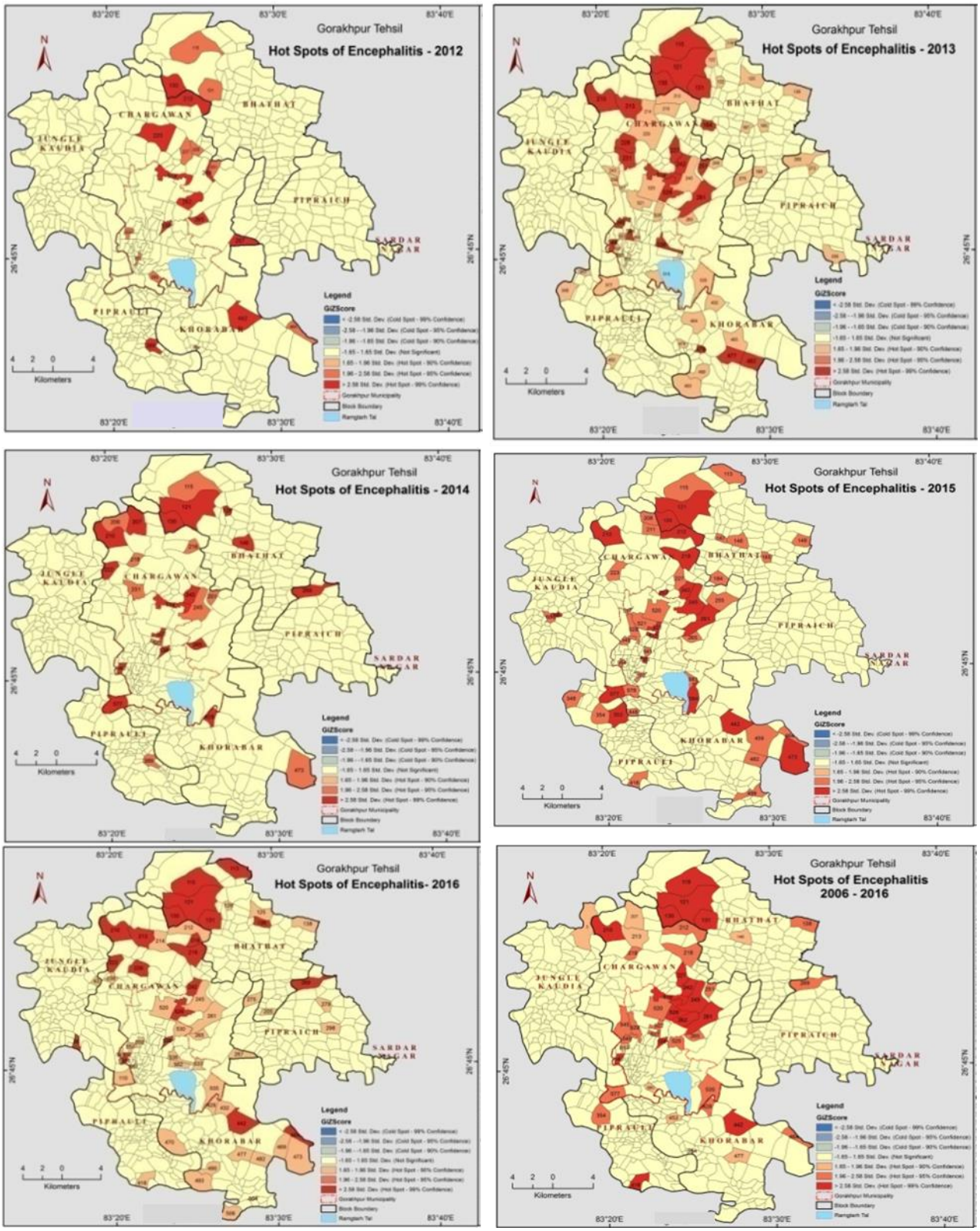

Figure 5: Hotspots of Encephalitis, 2012-2016 and 2006-2016

Z score which is > 2.58 has been considered to be significant at 99% confidence level ($p<0.01$) and put into Hotspots category. Areas. Areas having Z score between 1.65-1.96 (Significant at 90% confidence level) and P value<0.10 areas are categorized Low Risk Areas. Z score from 1.96-2.58 is considered significant at 95% confidence level ($p <0.05$) are High Risk and Z value <1.65 are under no significant category.

Most of these hotspots (very high risk areas) are located in the middle part starting from the northern part of the region and stretching from north to south. Two prominent clusters have been categorized as encephalitis hotspots. The biggest hotspots spreads in the central part of the region, covers 5 villages, viz., Bangai, Gulariha, Jungle Chatra Dhari and Jungle Dhoosar and two wards-Shahpur and Tiwaripur of Gorakhpur city. The second hotspots covering four big villages, viz., Jungle Dumari 1, Jungle

Dumari 2, Jungle Janaul Abden urf Jainpur and Kamraha Bujurg is located in the northern part of Gorakhpur Tehsil. This makes clear that these two regions in Chargawan and Bhathat CD blocks are highly sensitive region of the study area. Other four spots are scattered in north western, central, south east and south west part of the region, covering single village or ward and over all three villages and two wards. Overall 12 villages and 4 wards fall in the category of hotspots of encephalitis.

In High Risk Areas, 9 wards of the city are included. These wards are located in northern, south western and south eastern part of the city and also includes11 villages. All of these areas are mostly located adjacent to hotspots. 6 villages and two wards (Suryakund and Rustampur) are in Low Risk category.

It is revealed from the analysis that Jungle Kaudia and Pipraich CD block are not much affected by the outbreak of encephalitis. All remedial Areas. 55 wards (78.57 per cent) and 488 villages (94.39 per cent) are in no significant measures should be given priority for hotspots and high risk areas. As far as the cold spots are concerned, there are no cold spots as such in the study region.

The study shows that Encephalitis is concentrated in some areas tehsil and even in the wards of the city as well. This analysis helps to visualize the disease distribution pattern. The study can pin point the high risk areas and provide guidelines to administrators, planners, health department to prioritise their planning, monitoring and surveillance for the high risk areas. This kind of efforts will definitely helpful in the mitigation of Encephalitis occurring in this region. Thus, the result of the study is fulfilling the main objective of reducing the burden of the disease.

References

Anselin, L. (1993). Discrete space autoregressive models, in environmental modeling with GIS, Goodchild, M. F., B.O. Parks and L.T. Steyaert (eds.), Oxford University Press, New York, NY:454-469.

Anselin, L. (1995). Local indicators of spatial association – LISA. Geogr. Anal., 27(2), 93–116.

Anselin, L. (1996). The Moran scatter plot as an ESDA tool to assess local instability in spatial association, in Fisher M., Scholten H. and Unwin D. (Eds.) Spatial Analytical Perspectives on GIS, Taylor and Francis, London: 111-125.

Anselin, L. and A. Getis (1992). Spatial statistical analysis and Geographic Information Systems, The Annals of Regional Science,26,19-33.

Chakraborty, A. (2013). GIS in Epidemiological Spatial Dynamics, 14th ESRI India User Conference: 1.

Chaput, E.K., J. I. Meek. and R. Heimer (2002). Spatial analysis of human granulocytic Ehrlichiosis near Lyme, Connecticut,Emerg Infect Dis., Sep; 8(9), 943–948.

Getis, A. and J. K. Ord (1992). The analysis of spatial association by use of distance statistics, Geographical Analysis, 24, 189-206.

Handique, B.K., S.A. Khan, K. Chakraborty, J. Goswami and K.K. Sarma (2011). Spatial statistical analysis of Japanese encephalitis occurrence and identification of disease hotspots – Case studies in a JE endemic district of North East India, International Journal of Geoinformatics, 7(1), 7-14.

Kakkar, M., E.T. Rogawski, S S. Abbas, S. Chaturved, T. N. Dhole, S S. Hossain and S K. Krishnan (2013). Acute encephalitis syndrome surveillance, Kushinagar district, Uttar Pradesh, India, 2011–2012, Emerging Infectious Diseases www.cdc.gov/eid, 19(9), September.

Lawson, A.B. and D. G. T. Denison (2002). Spatial Cluster Modelling, CRC Press.

Moran, P. A. P. (1950). Notes on Continuous Stochastic Phenomena, Biometrika, 37, 17–23.

Tsai, P.J., M. L. Lin, C. M. Chu and C. H. Perng (2009). Spatial autocorrelation analysis of health care hotspots in Taiwan in 2006, BMC Public Health, 9, 464.

Journal of Geomatics Vol 12 No. 2 October 2018

Gridded Temperature generation using INSAT - Land Surface Temperature data and India Meteorological Department temperature data for Indian region

Ujjwal Gupta[1], Punit K. Patel[2], Shivangi Surati[2] and Markand Oza[1]
[1]Space Applications Centre-ISRO, Ahmedabad
[2]LDRP-ITR, Gandhinagar
email: ujjwal_gupta@sac.isro.gov.in

(Received: Aug 27, 2018; in final form: Oct 16, 2018)

Abstract: Gridded temperature generation is required in various domains of thematic applications such as crop growth simulation, forestry, hydrology and weather forecasting. The daily minimum and maximum gridded air temperature is generated for the Indian region using daily station-wise temperature data of 332 India Meteorological Department (IMD) ground stations. However, it is noted that there are many stations where temperature data is missing. In such cases, an attempt is made to generate accurate surface by estimating missing temperature of IMD stations data using various regression techniques. For this, Correlation Length Scale (CLS) is calculated using INSAT-3D and INSAT-3DR Land Surface Temperature (LST) satellite product. Neighbouring IMD stations data, which are falling within range of CLS radius, as well as respective satellite data are considered for estimating IMD station temperature using Linear Regression (LR) and Support Vector Regression (SVR) models. IMD stations temperature data values are estimated with indigenously developed weighted scheme given to LR and SVR. In order to validate the model and limit over fitting, Leave-One-Out Cross Validation (LOOCV) technique is used for April, August months for year 2017 and January month for year 2018 representing summer, monsoon and winter season respectively and corresponding results are reported in this paper. Root Mean Squared Percentage Error (RMSPE) values are used as measures for judging model goodness for various regression techniques. At the end, Thin Plate Spline (TPS) interpolation technique is used for gridded temperature generation. Deviation of temperature from actual temperature shows that TPS based gridded temperature with LST consideration performs better than without LST consideration.

Keywords: Gridded temperature generation, Correlation Length Scale, Regression, RMSPE, Thin Plate Spline

1. Introduction

Weather data simulation involves simulation of the conditions of the atmosphere for a given location and time. Applications of weather simulation are in various areas viz. agriculture, forestry, marine, air traffic, electricity and gas companies. Majority of these applications rely on weather simulations to anticipate demand that is highly driven by weather. Gridded temperature field is required for optimum use of temperature for various models of crop-growth analysis, geology, hydrology and many more. This gave motivation to generate gridded temperature for Indian region. In this paper, two sources of temperature data are used, Surface Air Temperature from India Meteorological Department (IMD) weather stations and INSAT-LST Land Surface Temperature (LST) satellite data.

IMD stations measure surface air temperature from its non-uniformly distributed 332 ground stations daily at 2 m above ground. Sparse coverage of weather stations as well as missing measured data affect gridded temperature generation.

Another source for temperature data is INSAT satellite data, which provides Land Surface Temperature (LST). The advantage of satellite data is that it provides uniformly gridded LST data for the whole region of India. LST measured from satellite is also error-prone because various atmospheric factors such as dust particles, moisture and wind speed as well as electronic factors such as sensor degradation, which are very difficult to correct for, affect it.

Existing interpolation techniques viz. Inverse Weighted Regression (IDW), Kriging and Thin Plate Spline (TPS) are used for gridded temperature generation (Yang et al. 2004, Tiengrod and Wongseree 2013). These techniques interpolate values at unknown points using available information at known points and require large number of measured sample points. In order to generate gridded temperature using these techniques with increased number of sampling points, estimation of missing IMD stations data becomes an important step.

There are several methods to estimate surface air temperature for LST that are categorised into five groups, viz. Statistical, Empirical solar zenith angle, Energy balance, TVX and Neural Network approach (Shah et al. 2013). Shah et al. (2013) discuss these approaches and estimate minimum and maximum air temperature using MODIS data over Indo-Gangetic Plain with RMSE of 2.2% and 2.16% for NDVI-T_{min} and NDVI-T_{max} regression respectively where T_{max} and T_{min} are maximum and minimum surface air temperature.

In this paper, an attempt is made to estimate missing daily IMD surface air temperature data of 332 stations using measured IMD temperature data as well as available satellite based LST data using statistical methods. After estimation of missing temperature for IMD station data, the estimated temperature values as well as IMD measured temperature values are used to generate gridded temperature using Thin Plate Spline (TPS).

Indian Institute of Tropical Meteorology (IITM) at Pune has categorised India into seven homogeneous temperature regions based on the spatial and temporal variations of

surface air temperatures across India (Figure 1). These regions are East Coast (EC), North Central (NC), Interior Peninsula (IP), North East (NE), North West (NW), West Coast (WC) and Western Himalaya (WH). Regions WH, NW, NC and NE located in northern part of the country whereas WC, IP and EC located in the southern part of the country. In the end, Root Mean Squared Percentage Error (RMSPE) is calculated and estimation error of surface air temperature is compared region wise as well as for the whole country.

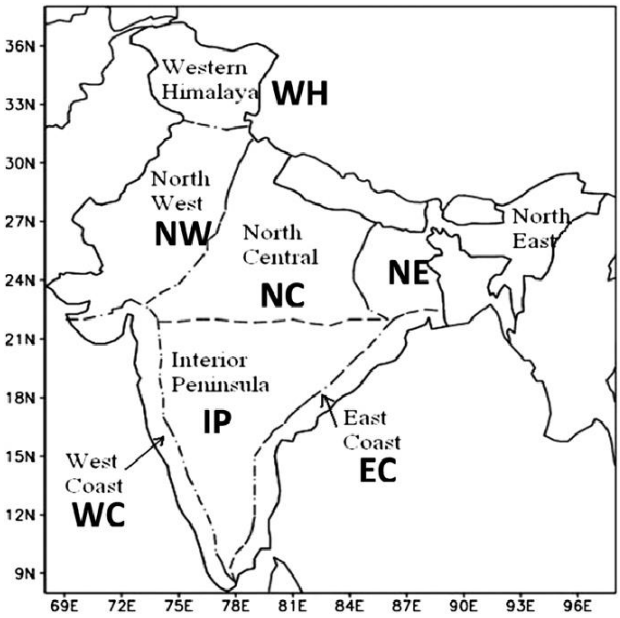

(source: www.tropmet.res.in)

Figure 1: Seven homogeneous temperature regions of India. Regions WH, NW, NC and NE are located in northern India whereas WC, IP and EC are located in southern India

2. Data Used

In this study, daily minimum and maximum surface air temperature data provided by India Meteorological Department (IMD) and LST data of geostationary satellite INSAT-3D and INSAT-3DR are used for gridded temperature generation.

IMD provides daily weather data viz. maximum temperature, minimum temperature, relative humidity, rainfall etc. for its 332 ground based weather stations (IMD; www.imd.gov.in). Out of these weather parameters, maximum temperature and minimum temperature are considered in this study.

For satellite data, INSAT-3D and INSAT-3DR Land Surface Temperature (LST) L2B product Imager data is taken from Meteorological and Oceanographic Satellite Data Archival Centre (MOSDAC; www.mosdac.gov.in). INSAT-3DR is a geostationary satellite which is a repeated version of INSAT-3D. The location of INSAT-3D is 82-degree east and the location of INSAT-3DR is 74-degree east. INSAT-3D and INSAT-3DR provide data with temporal resolution of 15 minutes at spatial resolution of 4km when combined. INSAT-3D carries an improved Very High Resolution Radiometer (VHRR). INSAT-3D is capable of capture data in six different wavelengths, viz. visible, shortwave infrared, middle infrared, water vapour and two bands in thermal infrared regions. Both INSAT-3D and INSAT-3DR LST products are generated using two thermal infrared bands of INSAT imager over India and come in form of Hierarchical Data Format (HDF). Both data products provided are processed by raw data extraction, radiometric corrections and geometric corrections by Meteorological and Oceanographic Satellite Data Archival Centre (MOSDAC).

3. Methodology

The main objective of the study is to estimate the missing IMD temperature values using satellite data that has its application in gridded temperature generation. In this paper, a methodology is developed for estimating missing temperature values and based on that, gridded temperature surface is generated. This methodology is carried out in three steps that are described below.

3.1 Processing INSAT-3D and INSAT-3DR data

INSAT-3D and 3DR provide Land Surface Temperature (LST) data in the form of Hierarchical Data Format (HDF) at temporal resolution of 15 minutes. From this, daily minimum and maximum LST is calculated in raster format. Both satellites data are used to improve quality of data in terms of temporal resolution.

LST data provided by satellite is in Kelvin (K) scale which is converted to Celsius (˚c) to make it compatible with IMD data. These daily temperature files are used further to calculate Correlation Length Scale (CLS) and for estimation of missing IMD stations data.

3.2 Calculation of Correlation Length Scale (CLS)

As next step of methodology, CLS is calculated for each station. Satellite data is used to find correlation length scale as satellite data has synoptic spatial coverage as compared to IMD data. To calculate CLS, correlation is calculated based on last five days of maximum and minimum LST data at pixels corresponding to geographic location of an IMD station with stations falling under 200 km. These correlation values are then binned with an interval of 10 km. For each bin, the mean correlation is estimated and second-degree polynomial function is fitted to mean correlation values.

Further, CLS is defined as a distance at which the value of the function representing mean correlation fell below 1/e, where e ~ 2.73 (Srivastava et al. 2009). CLS varies for each IMD station. Figure 2 shows second-degree polynomial function fitted to mean correlation values for an IMD station.

3.3 Use of regression models to estimate missing IMD stations data

CLS is used to identify neighbouring influencing stations for missing IMD stations. Last five days of IMD stations data as well as corresponding satellite data which are falling within the radius of influence are considered for making regression model. Linear Regression (LR) and Support Vector Regression (SVR) are applied to estimate

air temperature at IMD stations. In regression models, missing temperature station's satellite data along with IMD data and neighbouring stations satellite data with IMD data for previous 'd' days are used for capturing temporal and spatial relationship between LST and IMD temperature data. For estimating IMD temperature value of a particular day, IMD temperature values of neighbouring stations and LST values for same day are also considered in model making. While generating regression model, IMD station data is considered as dependent variable whereas INSAT LST data is considered as independent variable.

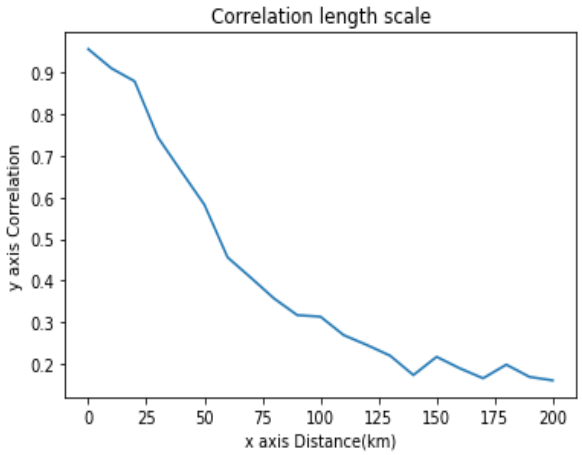

Figure 2: Correlation Length Scale (CLS) of a sample IMD station

A) Linear Regression (LR):

Linear regression is an approach to develop a linear model that depicts relationship between a scalar dependent variable and independent variables using training data. Simple linear regression equation is as shown below, (Cohen et al. 2003, Draper and Smith 1998).

$$y_i = w_0 + w_1 x_i + \varepsilon' \quad \text{.....(1)}$$

where, y_i = dependent variable
x_i = independent variable
w_0 = intercept
w_1 = slope coefficient
ε' = random error

B) Support Vector Regression (SVR):

SVR uses a different optimization objective as compared to the ones used in linear regression. There are various properties associated with cost function which gives a good solution with lesser computation. The cost function involves using a kernel, which could be linear, polynomial, radial basis function (RBF) kernel or sigmoid kernel. SVR estimates equation coefficients by minimizing the cost function $f(w)$,

$$f(w) = \frac{1}{2} w^T w \quad \text{.....(2)}$$

subject to: $\forall n \; |y_n - (x_n w + b)| \leq \varepsilon$

where, y_n = dependent variable
x_i = independent variable
w = weight vector
w^T = transposed weight vector, and
b, ε = bias and random error respectively.

With ε - incentive loss function, only the cost of samples that have residuals larger than ε is considered, while samples with smaller residuals have no effect on the regression. In this study, IMD stations data and satellite data used as training data to estimate missing IMD data using SVR with RBF kernel (Cohen et al. 2003, Draper and Smith 1998, Drucker et al. 1997).

In order to investigate the relationship between LST and IMD data, a weight based regression model is developed where for each sample; weights are assigned based on distance from missing temperature station and number of past days for which estimation is done. These weights are applied by varying polynomial order of weights. Distance weight and date weights are calculated to exploit spatial and temporal variations in temperature respectively.

$$distance\ weight = \left(\frac{CLS\ distance - x}{CLS\ distance}\right)^n \quad \text{.....(3)}$$

x = distance of sample point from missing temperature IMD station

$$date\ weight = \left(\frac{Total\ previous\ day - y}{Total\ previous\ day}\right)^n \quad \text{.....(4)}$$

y = previous day from missing temperature day of IMD station. For same day y=0, a day before missing temperature day y=1 and so on.

where, n = {1, 2, 3, 4} controls weights.

Maximum CLS distance is considered 200 km and total number of previous days affecting missing temperature day are taken as 5. Sum of distance weight and date weight is assigned to each corresponding sample point. Weighted Linear Regression and SVR are applied after assigning weights with varying degree i.e. n.

Performances of these regression techniques are evaluated by calculating Root Mean Squared Percentage Error (RMSPE) as measuring criteria (Nataliya et al. 2013). RMSPE is calculated by equation 5.

$$RMSPE = \sqrt{\frac{1}{n}\sum_{i=1}^{n}(100.|p_i|)^2} \quad \text{.....(5)}$$

where $p_i = \frac{(t_i' - t_i)}{t_i}$
t_i' = predicted temperature
t_i = actual temperature

Leave-One-Out Cross-Validation (LOOCV) is used to estimate how accurately a predictive model will perform. It

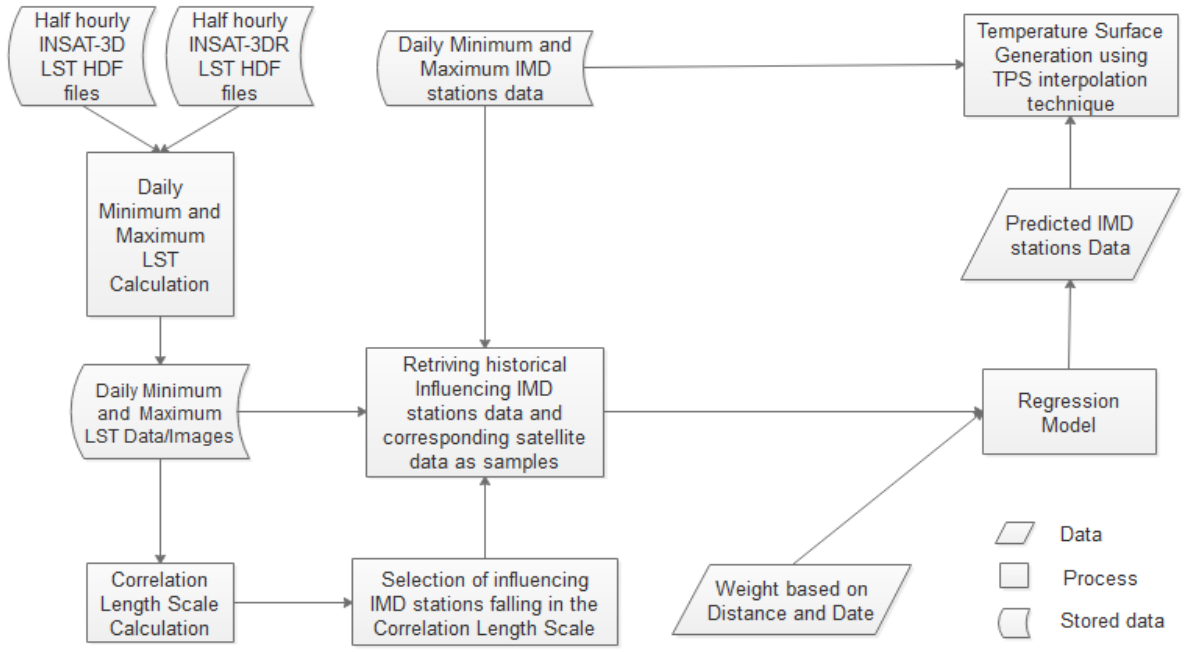

Figure 3: Flow diagram of proposed methodology

uses one observation as the validation set and remaining observation as a training set. In this paper, LOOCV is carried out by estimating temperature value of a station on a particular day while using other stations data as invariant. air temperature at IMD stations. A month-wise average RMSPE is reported for seven temperature homogeneous regions as well as Indian region.

In the end, TPS is applied to generate the gridded temperature for understanding effect on temperature interpolation without and with handling missing data as proposed. A flow diagram summarizing methodology is shown in Figure 3.

4. Results and Discussion

Performance of different regression techniques are compared by calculating Root Mean Square Percentage Error (RMSPE) in Leave One Out Cross-validation (LOOCV) manner for seasonal analysis. Seasonal analysis is carried out for seven temperature homogeneous regions in India namely, East Coast (EC), North Central (NC), Interior Peninsula (IP), North East (NE), North West (NW), West Coast (WC) and Western Himalaya (WH). April, August and January months data is used which represent summer, monsoon and winter seasons respectively. Results are computed up to four degree weighted linear and support vector regression methods to reduced model biasness towards nearest neighbour station with same day data. Various methods used in this study are summarized below in Table 1.

A) Summer Season

For summer, daily maximum and minimum temperature data of April, 2017 is taken to analyze the performance of different regression techniques as shown in Table 2 and Table 3. Based on daily data, average RMSPE is calculated and reported region wise. In study, it is found that for almost all temperature homogeneous regions fourth-degree polynomial weighted support vector regression gives best result. Results of regression methods for North Central (NC), East Coast (EC) and West Coast (WC) are seen to have less than other regions in summer. Lowest RMSPE for both maximum and minimum temperatures are reported for EC. In general, high RMSPE is noted for minimum temperature values over all regions as compared to maximum temperature values. North East (NE) and Western Himalaya (WH) show high RMSPE due to sparsity of stations in these regions and seasonal climatology.

Table 1: Various Regression techniques used in study with its abbreviations

AVG	Average of influencing IMD stations temperature data
LR	Simple Linear Regression
WLR	Weighted Linear Regression
WLR[n]	n - degree polynomial Weighted Linear Regression
SVR	Support Vector Regression
WSVR	Weighted Support Vector Regression
WSVR[n]	n - degree polynomial Weighted Support Vector Regression

B) Monsoon Season

Daily minimum and maximum temperature data of August, 2017 is taken for study of monsoon season. Estimation error for whole country is nearly 5.58% for maximum temperature and 5.49% for minimum temperature. The estimation error for West Coast (WC) is 4.85% for maximum temperature and 5.25% is for minimum temperature. For East Coast (EC), RMSPE is 4.17% for maximum temperature and 4.29% for minimum temperature. For WH estimation error is 7.81% and 7.90% for maximum and minimum respectively, which is highest among all other regions. A 4.22% for maximum temperature and 3.83% for minimum temperature estimation error is noted for NW region. In most of the

temperature homogeneous regions fourth degree polynomial SVR estimation results best as shown in Table 4 and Table 5.

C) Winter season

Daily minimum and maximum temperature data of January, 2018 is used for winter season. Average RMSPE is calculated for different temperature homogeneous regions and for the whole country. It is noted that for WH region the results are not as good as other regions because of the winter climatology. WH region also performs worst in all seasons. The estimation error for East Coast (EC) is reported lowest in winter season i.e. 1.52% for maximum temperature and 3.55% for minimum temperature. For Indian region, estimation error is noted as 5.40% for maximum temperature and 11.97% for minimum temperature. Results for all regions are reported in Table 6 and Table 7.

Table 2: Average maximum temperature RMSPE for summer

	WH	NW	NC	NE	WC	EC	IP	INDIA
AVG	28.11	9.84	5.80	11.43	7.36	7.69	6.57	9.37
LR	18.09	7.59	4.99	9.04	5.99	6.44	5.70	7.34
SVR	22.83	7.99	4.70	9.58	6.04	5.38	5.78	7.69
WLR	17.17	6.77	4.38	8.30	5.24	5.76	5.03	6.63
WLR2	16.43	6.24	3.99	7.84	4.71	5.29	4.61	6.18
WLR3	15.87	5.89	3.73	7.54	4.35	4.97	4.34	5.88
WLR4	15.43	5.66	3.55	7.34	4.12	4.74	4.16	5.67
WSVR	18.13	6.19	3.46	7.85	3.99	3.51	4.82	6.11
WSVR2	17.07	5.63	2.98	7.09	3.28	2.96	4.52	5.59
WSVR3	16.34	5.26	2.73	6.52	2.84	2.57	4.37	5.24
WSVR4	15.91	5.00	2.53	6.11	2.55	2.30	4.24	5.00

Table 3: Average minimum temperature RMSPE for summer

	WH	NW	NC	NE	WC	EC	IP	INDIA
AVG	78.51	16.45	12.42	15.56	8.54	4.78	9.81	13.77
LR	47.62	11.82	9.51	12.52	6.41	4.11	7.53	10.16
SVR	55.58	12.44	9.45	13.01	6.18	3.51	8.11	10.67
WLR	44.62	10.93	8.55	11.38	5.79	3.64	6.86	9.32
WLR2	42.38	10.29	7.88	10.60	5.42	3.37	6.35	8.73
WLR3	40.85	9.85	7.45	10.08	5.18	3.20	6.03	8.34
WLR4	39.76	9.55	7.18	9.71	5.00	3.09	5.83	8.07
WSVR	43.58	10.39	7.36	10.65	4.55	2.70	6.26	8.61
WSVR2	41.00	9.53	6.35	9.75	3.99	2.44	5.70	7.88
WSVR3	39.03	8.89	5.67	8.95	3.53	2.24	5.34	7.33
WSVR4	37.43	8.40	5.22	8.35	3.29	2.11	5.07	6.93

Table 4: Average maximum temperature RMSPE for monsoon

	WH	NW	NC	NE	WC	EC	IP	INDIA
AVG	13.25	7.69	7.04	9.72	9.10	6.52	10.09	8.93
LR	10.23	6.40	6.49	8.25	8.07	6.31	9.44	7.82
SVR	11.04	6.35	5.63	8.79	7.73	5.27	9.50	7.87
WLR	9.63	5.99	5.93	7.69	7.26	5.95	8.58	7.24
WLR2	9.12	5.72	5.58	7.27	6.70	5.72	7.95	6.83
WLR3	8.71	5.52	5.34	6.99	6.29	5.56	7.52	6.54
WLR4	8.37	5.36	5.17	6.82	6.01	5.45	7.23	6.34
WSVR	9.15	5.28	4.39	7.23	6.23	4.64	8.45	6.66
WSVR2	8.54	4.83	3.92	6.62	5.80	4.42	8.14	6.23
WSVR3	8.17	4.46	3.62	6.12	5.43	4.26	7.87	5.87
WSVR4	7.81	4.22	3.46	5.78	4.85	4.17	7.57	5.58

Table 5: Average minimum temperature RMSPE for monsoon

	WH	NW	NC	NE	WC	EC	IP	INDIA
AVG	12.86	7.23	6.75	9.39	8.90	6.40	9.58	8.58
LR	10.37	6.47	6.45	8.22	8.41	6.20	8.29	7.61
SVR	11.08	6.08	5.88	8.29	7.63	5.34	8.83	7.56
WLR	9.81	6.05	5.98	7.62	7.51	5.94	7.69	7.07
WLR2	9.27	5.72	5.63	7.16	6.85	5.69	7.22	6.66
WLR3	8.80	5.47	5.41	6.86	6.41	5.49	6.86	6.36
WLR4	8.41	5.29	5.25	6.66	6.11	5.33	6.59	6.14
WSVR	9.35	4.97	4.46	6.84	6.35	4.80	7.74	6.42
WSVR2	8.68	4.46	3.95	6.32	6.00	4.56	7.49	6.02
WSVR3	8.25	4.10	3.68	5.95	5.66	4.39	7.27	5.73
WSVR4	7.90	3.83	3.44	5.71	5.25	4.29	7.03	5.49

Table 6: Average maximum temperature RMSPE for winter

	WH	NW	NC	NE	WC	EC	IP	INDIA
AVG	37.90	12.98	11.55	12.23	7.21	4.48	8.34	10.87
LR	24.60	9.45	8.52	8.90	5.92	3.84	6.25	7.99
SVR	28.13	9.27	8.41	9.22	4.91	3.50	7.70	8.32
WLR	23.03	8.77	7.74	7.89	5.13	3.37	5.55	7.24
WLR2	21.55	8.27	7.18	7.28	4.61	3.09	5.04	6.70
WLR3	20.43	7.92	6.78	6.89	4.28	2.90	4.70	6.34
WLR4	19.58	7.66	6.51	6.63	4.07	2.77	4.46	6.08
WSVR	23.95	7.62	6.37	7.16	3.64	2.30	6.07	6.64
WSVR2	23.08	7.03	5.57	6.45	3.07	1.88	5.45	6.07
WSVR3	22.34	6.59	5.07	5.95	2.68	1.65	5.01	5.67
WSVR4	21.74	6.27	4.78	5.57	2.32	1.52	4.78	5.40

Table 7: Average minimum temperature RMSPE for winter

	WH	NW	NC	NE	WC	EC	IP	INDIA
AVG	204.23	36.96	34.09	28.09	17.76	11.31	19.80	25.42
LR	99.91	32.09	32.15	20.47	12.84	8.86	16.12	20.23
SVR	108.94	30.42	29.74	20.72	13.34	7.97	16.55	19.85
WLR	89.82	29.42	29.29	18.64	11.05	7.76	14.32	18.23
WLR2	85.69	27.28	27.07	17.33	9.91	6.99	13.06	16.79
WLR3	83.05	25.73	25.57	16.44	9.22	6.52	12.24	15.82
WLR4	81.06	24.61	24.53	15.79	8.78	6.22	11.70	15.15
WSVR	73.19	25.11	24.86	16.67	9.63	5.31	12.90	15.76
WSVR2	68.55	22.17	22.31	14.96	7.65	4.40	11.36	13.90
WSVR3	66.32	20.45	20.57	13.79	6.61	3.88	10.33	12.75
WSVR4	64.30	19.19	19.57	12.97	5.82	3.55	9.70	11.97

To understand effects of missing temperature data values on estimation over gridded temperature generation, thin plate spline interpolation is carried out using with and without estimating missing temperature values. Also, one station each from the seven temperature homogeneous regions is taken to study the deviation of estimated temperature from actual temperature. IMD stations viz. Srinagar, Amritsar, Agra, Shilong, Mangalore, Chennai and Hyderabad are selected from the regions WH, NW, NC, NE, WC, EC and IP respectively. Figures 4 to 9 show deviation of TPS Surface Air Temperature interpolation with and without estimation of missing IMD stations temperature data for minimum and maximum temperature for a sample day in summer, winter and monsoon seasons.

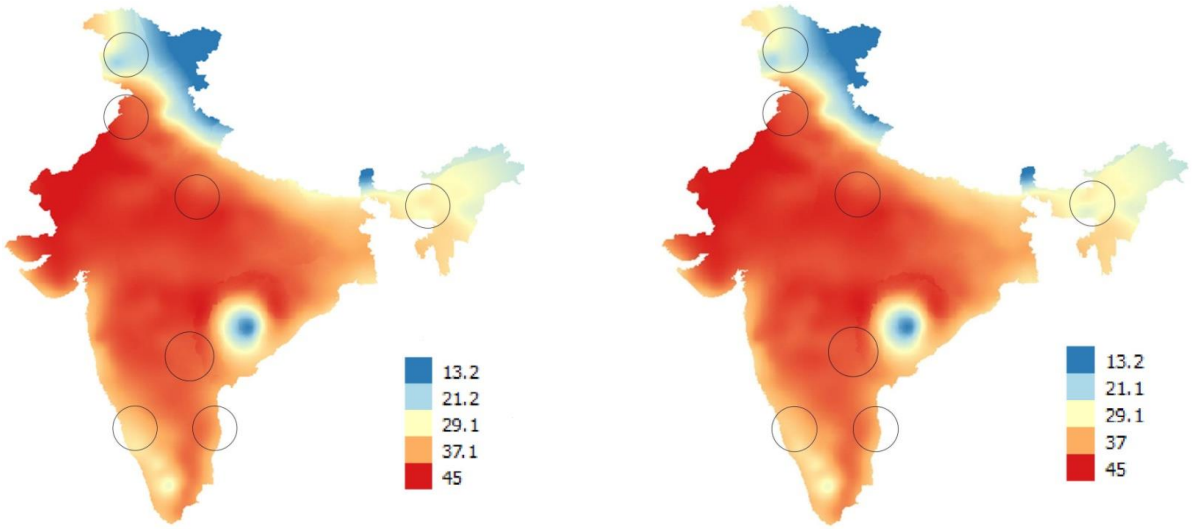

Figure 4: TPS interpolation of IMD stations Maximum Surface Air Temperature data for Summer (15 April); (a) With missing IMD stations data (Left), (b) After estimation of missing IMD stations data (Right)

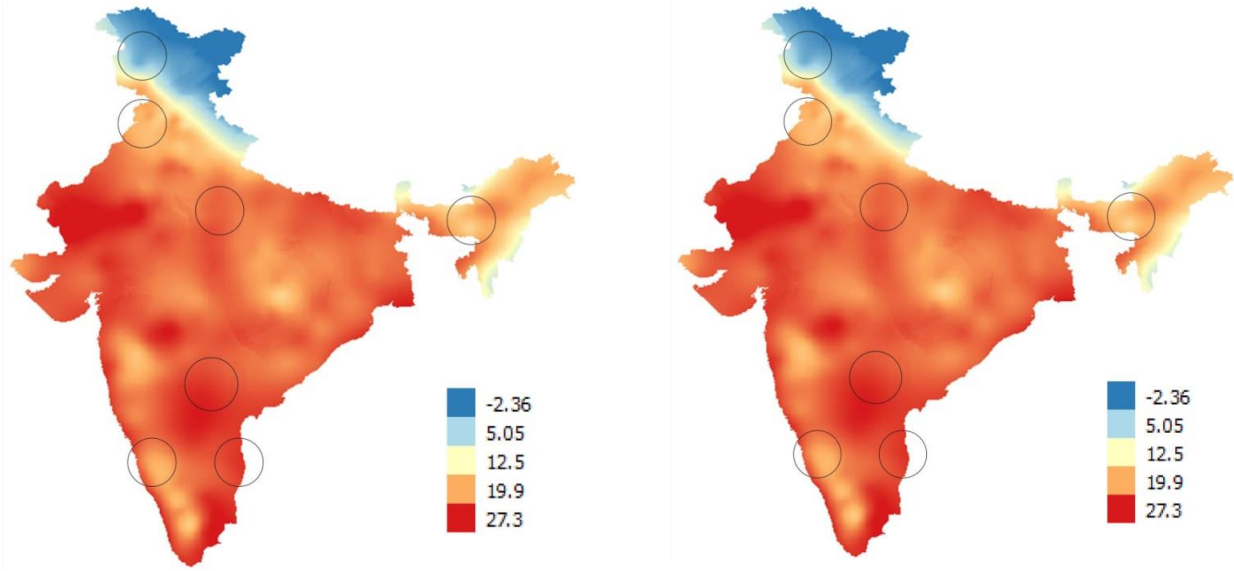

Figure 5: TPS interpolation of IMD stations Minimum Surface Air Temperature data for Summer (15 April); (a) With missing IMD stations data (Left), (b) After estimation of missing IMD stations data (Right)

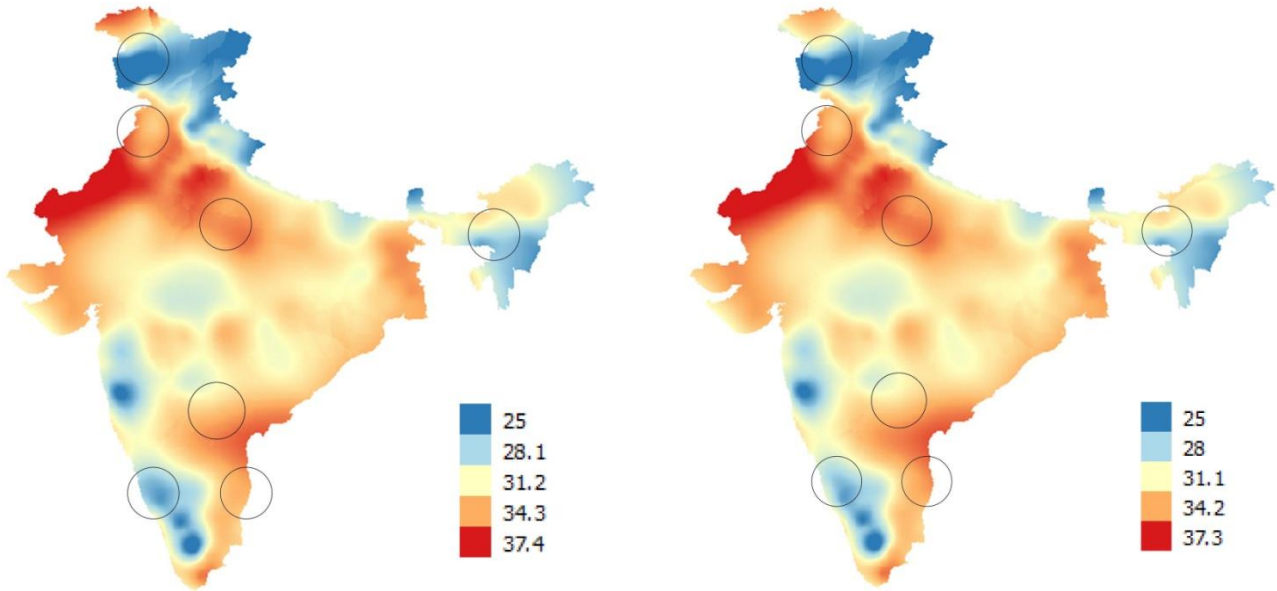

Figure 6: TPS interpolation of IMD stations Maximum Surface Air Temperature data for Monsoon (15 August); (a) With missing IMD stations data (Left), (b) After estimation of missing IMD stations data (Right)

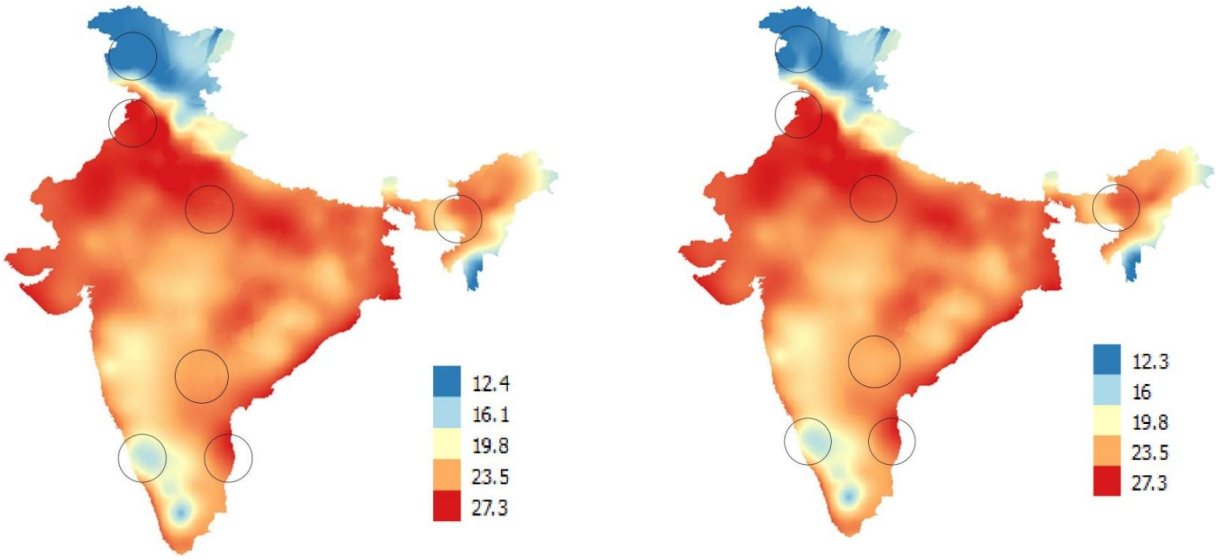

Figure 7: TPS interpolation of IMD stations Minimum Surface Air Temperature data for Monsoon (15 August); (a) With missing IMD stations data (Left), (b) After estimation of missing IMD stations data (Right)

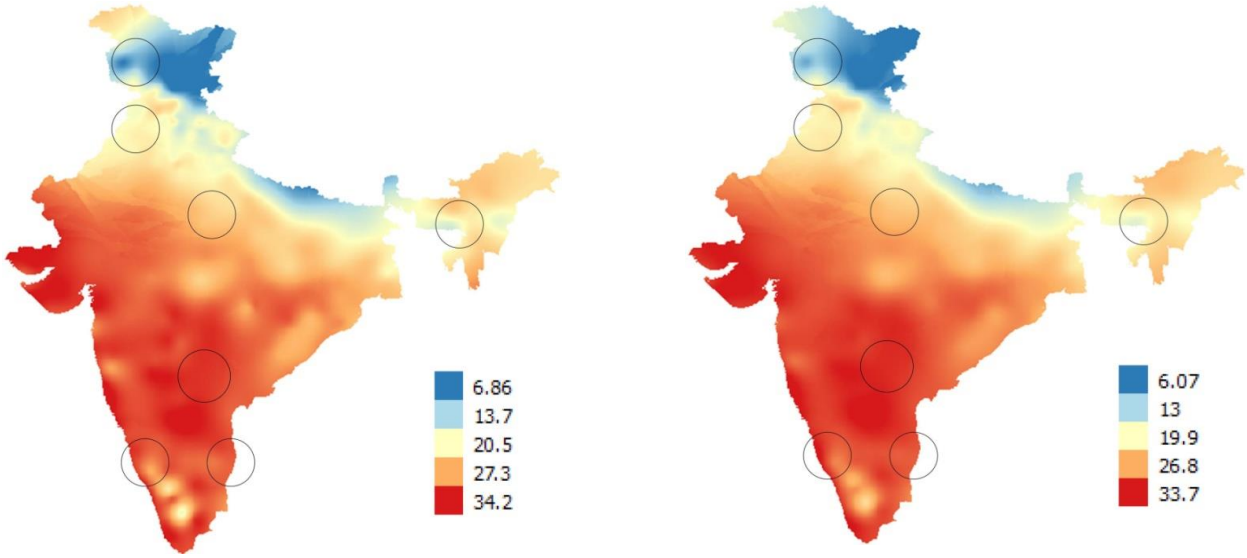

Figure 8: TPS interpolation of IMD stations Maximum Surface Air Temperature data for Winter (15 January); (a) With missing IMD stations data (Left), (b) After estimation of missing IMD stations data (Right)

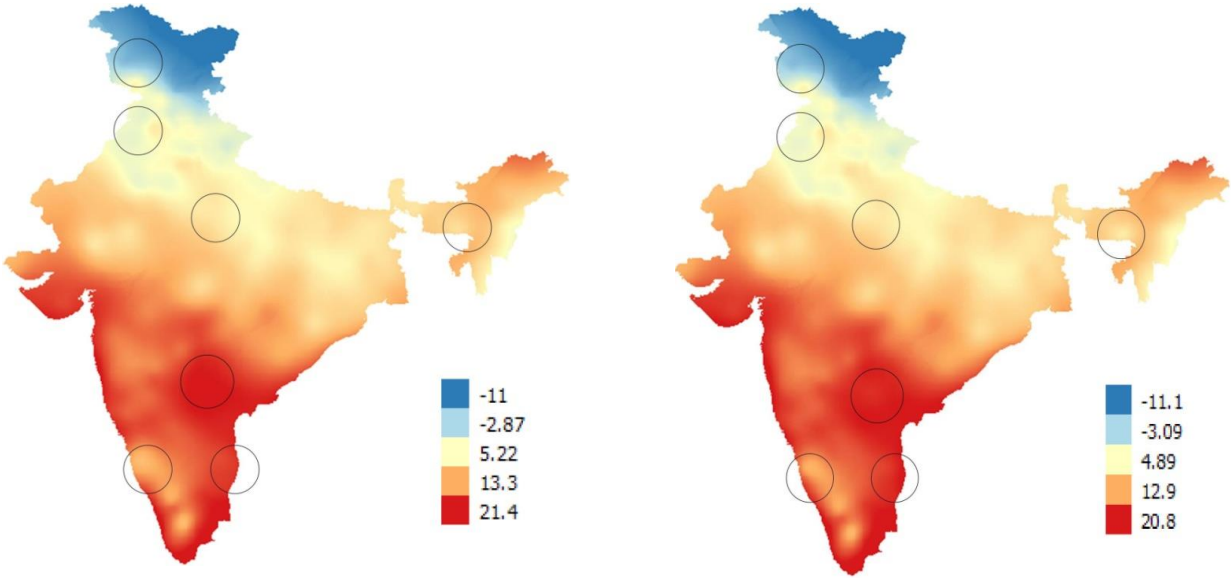

Figure 9: TPS interpolation of IMD stations Minimum Surface Air Temperature data for Winter (15 January); (a) With missing IMD stations data (Left), (b) After estimation of missing IMD stations data (Right)

For almost all the regions, the results show that TPS temperature interpolation with LST consideration is closer to actual temperature than TPS temperature interpolation without LST consideration. The deviation of maximum and minimum temperature from actual temperature with and without LST consideration for a sample day for three seasons is reported in Tables 8 to 13.

Table 8: Deviation of Maximum Temperature from Actual Temperature with and without LST Consideration for Summer (15 April)

Station Name	Region	Actual temperature	TPS temperature interpolation without LST consideration	Deviation of temperature from actual temperature without LST consideration	TPS temperature interpolation with LST Consideration	Deviation of temperature from actual temperature with LST consideration
Srinagar	WH	27	21.47	5.53	24.68	2.32
Amritsar	NW	41.6	41.77	0.17	41.62	0.02
Agra	NC	43	43.03	0.03	42.95	0.05
Shilong	NE	23.4	29.34	5.94	26.45	3.05
Mangalore	WC	35.5	31.64	3.86	34.46	1.04
Chennai	EC	34.6	35.58	0.98	34.92	0.32
Hyderabad	IP	41.6	41.27	0.33	41.52	0.08

Table 9: Deviation of Minimum Temperature from Actual Temperature with and without LST Consideration for Summer (15 April)

Station Name	Region	Actual temperature	TPS temperature interpolation without LST consideration	Deviation of temperature from actual temperature without LST consideration	TPS temperature interpolation with LST Consideration	Deviation of temperature from actual temperature with LST consideration
Srinagar	WH	0	2.00	2.00	4.27	4.27
Amritsar	NW	17.8	18.97	1.17	18.53	0.73
Agra	NC	23.6	23.21	0.39	22.24	1.36
Shilong	NE	12.6	16.12	3.52	16.14	3.54
Mangalore	WC	25.6	24.65	0.95	24.56	1.04
Chennai	EC	26.3	26.03	0.27	26.11	0.19
Hyderabad	IP	25.9	25.80	0.1	24.96	0.94

Table 10: Deviation of Maximum Temperature from Actual Temperature with and without LST Consideration for Monsoon (15 August)

Station Name	Region	Actual temperature	TPS temperature interpolation without LST consideration	Deviation of temperature from actual temperature without LST consideration	TPS temperature interpolation with LST Consideration	Deviation of temperature from actual temperature with LST consideration
Srinagar	WH	27.6	19.79	7.81	24.45	3.15
Amritsar	NW	33.4	34.36	0.96	34.23	0.83
Agra	NC	36.8	35.04	1.76	35.69	1.11
Shilong	NE	25	27.77	2.77	27.96	2.96
Mangalore	WC	31.7	27.66	4.04	30.17	1.53
Chennai	EC	35.2	34.24	0.96	34.79	0.41
Hyderabad	IP	31.9	32.34	0.44	31.99	0.09

Table 11: Deviation of Minimum Temperature from Actual Temperature with and without LST Consideration for Monsson (15 August)

Station Name	Region	Actual temperature	TPS temperature interpolation without LST consideration	Deviation of temperature from actual temperature without LST consideration	TPS temperature interpolation with LST Consideration	Deviation of temperature from actual temperature with LST consideration
Srinagar	WH	16.3	11.13	5.17	14.02	2.28
Amritsar	NW	26.8	27.78	0.98	26.99	0.19
Agra	NC	26.4	26.56	0.16	26.57	0.17
Shilong	NE	14.7	21.98	7.28	22.92	8.22
Mangalore	WC	24.5	19.33	5.17	20.47	4.03
Chennai	EC	26.2	26.47	0.27	26.18	0.02
Hyderabad	IP	22.1	23.74	1.64	23.07	0.97

Table 12: Deviation of Maximum Temperature from Actual Temperature with and without LST Consideration for Winter (15 January)

Station Name	Region	Actual temperature	TPS temperature interpolation without LST consideration	Deviation of temperature from actual temperature without LST consideration	TPS temperature interpolation with LST Consideration	Deviation of temperature from actual temperature with LST consideration
Srinagar	WH	13.7	9.56	4.14	11.87	1.83
Amritsar	NW	22.3	9.77	12.53	21.48	0.82
Agra	NC	22.9	24.78	1.88	24.36	1.46
Shilong	NE	14.8	19.49	4.69	18.36	3.56
Mangalore	WC	35.9	32.54	3.36	34.47	1.43
Chennai	EC	30.7	31.11	0.41	30.63	0.07
Hyderabad	IP	33	33	0	32.87	0.13

Table 13: Deviation of Minimum Temperature from Actual Temperature with and without LST Consideration for Summer (15 January)

Station Name	Region	Actual temperature	TPS temperature interpolation without LST consideration	Deviation of temperature from actual temperature without LST consideration	TPS temperature interpolation with LST Consideration	Deviation of temperature from actual temperature with LST consideration
Srinagar	WH	-3.3	-5.67	2.37	-4.83	1.53
Amritsar	NW	1.2	3.51	2.31	3.91	2.71
Agra	NC	5.7	7.15	1.45	6.32	0.62
Shilong	NE	3.8	9.02	5.22	6.94	3.14
Mangalore	WC	20.5	14.04	6.46	18.23	2.27
Chennai	EC	22.2	19.82	2.38	21.51	0.69
Hyderabad	IP	18.8	20.05	1.25	19.59	0.79

Proposed methodology relies on quality of satellite data product to a large extent. Estimation from this methodology depends upon cloud free and clear sky environment as well as regional climatology. For current study, cloudy pixel handling is not performed on INSAT LST data. RMSPE for summer is low as compared to other seasons as winter season is affected by fog conditions for most of the India and monsoon season is cloudy.

5. Conclusions

This paper exploits the relationship between satellite derived LST and surface air temperature provided by IMD to estimate the missing IMD stations temperature data. This paper also reports performance of various regression techniques for estimation. Fourth degree polynomial regression performed best for most of the regions as well as for the whole country. RMSPE for WH region reported highest compared to other regions due to lack of stations and seasonal climatology. The southern part of India (WC, EC and IP) shows better accuracy as compared to northern part of India. The RMSPE reported for India is 5 and 6.93% for summer, 5.40 and 11.97% for winter and 5.58 and 5.49% for monsoon for maximum and minimum temperature respectively. At the end, the deviation of estimated temperature from actual temperature shows that,

TPS based gridded temperature with LST consideration is closer to actual temperature than TPS based gridded temperature without LST consideration.

Acknowledgments

The authors sincerely thank Director, Space Applications Centre (SAC), Shri D. K. Das for his constant encouragement during this study. Authors owe their sincere thanks to Shri Shashikant Sharma, Group Head, VRG, SAC for providing us necessary suggestions and infrastructure for this study.

References

Cohen P., S. G. West. and L. S. Aiken. (2003). Applied multiple regression/correlation analysis for the behavioral sciences. (2nd ed.), Hillsdale, NJ: Lawrence Erlbaum Associates.

Draper, N. R. and H. Smith. (1998). Applied Regression Analysis (3rd ed.)., John Wiley.

Drucker, H., C. J. Burges, L. Kaufman, A. J. Smola. And V. Vapnik. (1997). Support vector regression machines, In Advances in Neural Information Processing Systems, pp. 155-161.

INSAT-3D Imager L2B Land Surface Temperature (LST) product, DOI:10.19038/SAC/10/3DIMG_L2B_LST, MOSDAC (http://www.mosdac.gov.in)

INSAT-3DR Imager L2B Land Surface Temperature (LST) product. DOI:10.19038/SAC/10/3RIMG_L2B_LST, MOSDAC (http://www.mosdac.gov.in)

Nataliya, L. S., P. T. Anton, V. T. S. Maxim, B. Adriaan, A. J. Timur. and A. K. Valeriy. (2013). A Survey of Forecast Error Measures. World Applied Sciences Journal 24, 171-176, ISSN 1818-4952.

Shah, D. B., M. R. Pandya, H. J. Trivedi. and A. R. Jani. (2013). Estimating minimum and maximum air temperature using MODIS data over Indo-Gangetic Plain. Journal of earth system science, 122(6), 1593-1605.

Srivastava, A. K., M. Rajeevan. and S. R. Kshirsagar. (2009). Development of a high resolution daily gridded temperature data set (1969–2005) for the Indian region. Atmospheric Science Letters, 10(4), 249-254.

Tiengrod, P. and W. Wongseree. (2013). A comparison of spatial interpolation methods for surface temperature in Thailand. In Computer Science and Engineering Conference (ICSEC), 2013, pp. 174-178.

Yang, C. S., S. P. Kao, F. B. Lee. And P. S. Hung. (2004). Twelve different interpolation methods: A case study of Surfer 8.0. In Proceedings of the XXth ISPRS Congress, 35, pp. 778-785)

Journal of Geomatics Vol 12 No. 2 October 2018

Site suitability analysis for establishing soil and water conservation structures using Geoinformatics - A case study of Chinnar watershed, Tamil Nadu, India

Tushar Lohar[1*], K Balasubramani[2] and Bindu Bhatt[3]
[1, 3] The Maharaja Sayajirao University of Baroda, Vadodara, Gujarat, India -390002
[2] Central University of Tamil Nadu, Thiruvarur, Tamil Nadu, India - 610005
*Email: tusharlohar740@gmail.com

(Received: Jul 25, 2018; in final form: Oct 17, 2018)

Abstract: Watershed is an ideal unit for management of soil and water resources. Water harvesting structure is one of the important components of watershed management to conserve these resources. Determination of potential sites for water harvesting structures is essential for proper conservation which requires thorough understanding of rainfall-runoff characteristics and detailed evaluation of surface topography, soil characteristics, geomorphology and land use/land cover. To demarcate suitable zones for soil and water conservation structures, these characteristics need to be integrated in a weighted manner. In the present study, an attempt has been made to identify potential sites for construction of soil and water conservation structures in Chinnar watershed - located in Dharmapuri and Krishnagiri districts of Tamil Nadu. The study uses thematic layers such as runoff, slope, land cover/ land use, lineament, drainage density, soil texture and geomorphology. All these layers were prepared with the help of remote sensing images and toposheets and integrated using weighted overlay techniques in GIS environment to derive suitable sites for soil and water conservation structures. The lower value of one was assigned to the factor that is not favorable for the conservation structures and the higher value of nine was assigned to the factor that is highly suitable for conservation structures. All the factor values were summed up and overall site suitability score was computed. The computed score was classified finally into four suitability classes. The results show that only less than one percent area is highly suitable for implementing soil and water conservation structures. About 34 percent of the study area is moderately suitable and about 65 percent area is less suitable for soil and water conservation structures. Based on site suitability results and topographic characteristics, locations for conservation structures including check dams, stop dams, percolation tanks and farm ponds were identified. These locations are ecologically sound and economically viable and this will sustain the productivity of the watershed.

Keywords: Watershed, Runoff, Weighted Overlay Analysis, SCS-CN Method, GIS, Remote Sensing

1. Introduction

Site suitability evaluation in the watershed is a subset of watershed management wherein the objective is to conserve water for watershed use, sediment reduction, and improved productivity for all land uses (Rao and Raghavendra, 2009).

Soil and water conservation are activities that maintain or enhance the productive capacity of land in areas affected by or prone to soil erosion. There are many methods offered for soil and water conservation and rainfall runoff modeling. Soil Conservation Services and Curve Number (SCS–CN) technique is one of the primogenital and simplest method to measure the runoff. The curve number is a function of land use and Hydrologic Soil Group (HSG). It is a method that can incorporate land use for the computation of runoff from rainfall. The SCS-CN method provides a rapid way to estimate runoff change due to land use change (Zhan and Huang 2004).

Integrated analysis of all thematic maps and their respective weightage in GIS platform could be utilised to prepare a map showing potential zones for water conservation structures and their appropriate measures (Varade et al., 2017; Anbazhagan et al., 2005). Different water conservation structures and measures are recommended for an effective site- specific soil and water conservation plan of the study area (Varade et al., 2017).

The present study of Chinnar watershed of Cauvery river basin covers the western part of Krishnagiri and upper part Dharmapuri district in Tamil Nadu. This watershed comes under Hosur, Denkanikottai (Krishnagiri), Pennagram and Palacode taluks (Dharmapuri). Chinnar watershed is covered by 2/4 part of the hilly area. Therefore, topography act as a barrier for agriculture activities but nearly 70% of the workforce is dependent on agriculture and allied activities. The important crops of the watershed which are cultivated especially in monsoon season are paddy, maize, ragi, banana, sugarcane, cotton, tamarind, coconut, mango and groundnut. The district is one among most backward and drought prone area in the state. As the area is drought prone, it has become essential to conserve soil and water resources of the watershed in a proper manner.

1.1 Study area

The area of Chinnar watershed is 1564.36 sq. km., it extends between 12º4’41” N to 12º40’31’’ N latitude and 77º36’14’’ E to 78º04’41’’ E longitudes. The Karnataka State is located in the north and northwest side, Krishnagiri in west and Dharmapuri is located in south of the watershed. The river originates on the northwest slope of Vattalaimalai (1195m AMSL) in Krishnagiri district and meets river Cauvery at Hogenikkal waterfalls in Dharmapuri district (Venkateswaran, 2013) (Figure 1).

The study area is affected by drought due to scanty rainfall. The annual average rainfall over the study area is about 700 mm to1100 mm. The soil texture of the study area is clay, sand, sandy clay loam, sandy loam and loamy sand. The soil texture is governed by physiography of the study area.

Figure 1: Location map of study area

1.2 Aim and objectives

The aim of the study is to find out suitable sites for establishing soil and water conservation structures in Chinnar Watershed using GIS and Remote Sensing techniques. Specific objectives are:

- To study physical parameters of the watershed.
- To analyze rainfall-runoff depth during northwest monsoon season (2005-2013).
- To perform site suitability analysis using weighted overlay techniques.
- To locate suitable sites for different structures for conservation of soil and water.

1.3 Methodology

The Chinnar watershed area is generated using ArcSWAT tool and is 1,564 sq.km. in its extent. The stream network is generated from the SOI topographic maps on 1:50,000 scale. The generated stream network has been used for stream ordering based on Strahler method. The satellite data for the study are downloaded from Bhuvan Data Archive including Digital Elevation Model (DEM) from Cartosat-1 satellite (Figure 2). The DEM data is used for generating slope map of the study area. The LISS-III of Resourcesat –I have been used for the preparation of landuse/land cover map.

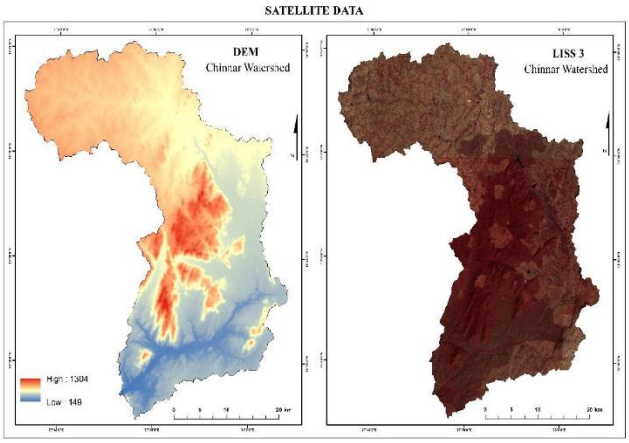

Figure 2: Cartosat DEM and LISS-III FCC of the Chinnar watershed

Figure 3 shows the flow chart of methodology adopted for identifying suitable sites for soil and water conservation structures. Geomorphology and lineaments features are extracted from Bhuvan thematic services by adding the WMS server in ArcGIS software. Lineaments features are used to applying the multi-ring buffer with a distance of 100, 200, and 500 and more than 500 m for assigning weightage for site suitability analysis. Geology map is created using the data collected from Geological Survey of India (GSI). Soil map is created from the data published by National Bureau of Soil Survey (NBSS).

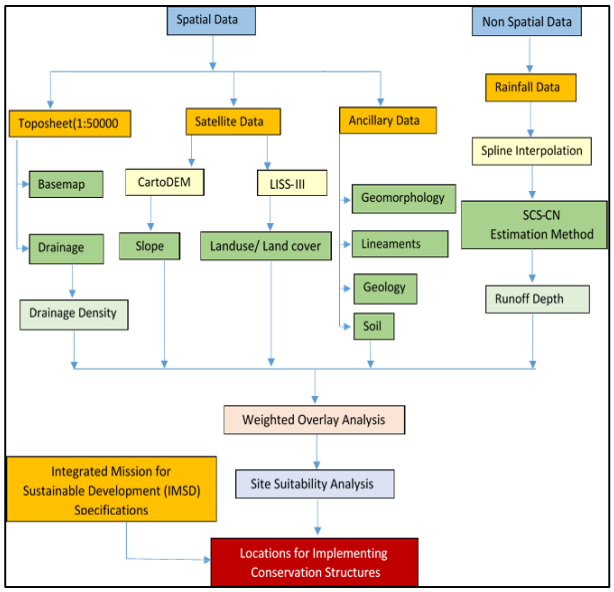

Figure 3: Flow chart showing the methodology adopted for identifying suitable sites for soil and water conservation structures

2. Physical environment

2.1 Climate

The climate of the study area is sub-humid to semi-arid. The mean temperature varies from 24°C to 40°C. The hottest period of the year is generally from March to May and the highest temperature rises to 40°C in April. The climate becomes cool in December and continuous up to February. The annual average rainfall over the study area is about 700 mm to1100 mm.

The highest rainfall occurs in upper part of the study area. Thally and Denkanikottai stations situated in the upper part of the watershed receive more rainfall. The middle part of the study area is affected by drought due to scanty rainfall. Hoganikkal, Pennagaram, Palacode, Panchppalli and Marandhalli stations receive very less to moderate rainfall (Figure 4).

2.2 Drainage

The drainage pattern of the watershed is dendritic. Drainage density is high in the hilly area and it is decreasing from central part to northern side. Lowest drainage density is found in upper part of the study area. Based on Strahler's system of stream ordering the watershed is 7th order (Figure 5 & 6).

2.3 Geology

Figure 7 shows the geology of Chinnar watershed. In various rock types, depth of weathering ranges from 2.2 to 50 m, while the fractures in rocks extend up to 50 m depth. The thickness of weathering in the rocks varies from 5 to 15 m near hills and 3 to 30 m in the plain area.

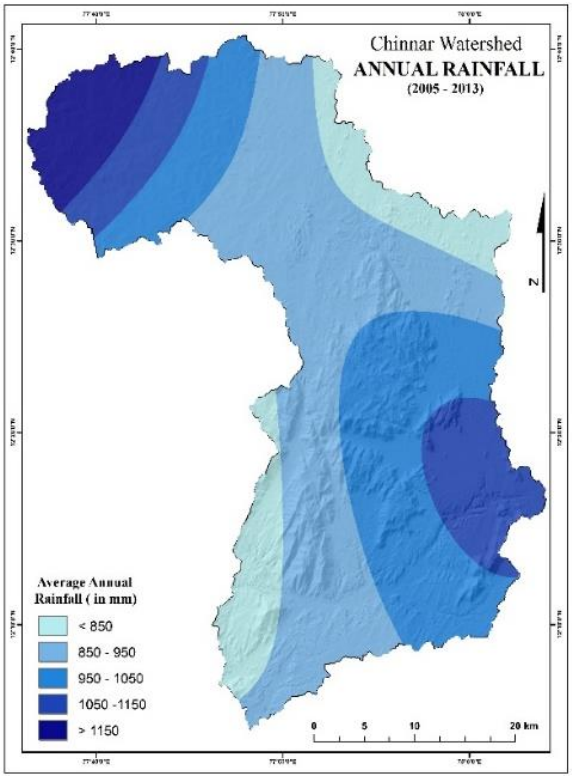

Figure 4: Rainfall distribution (2005-2013)

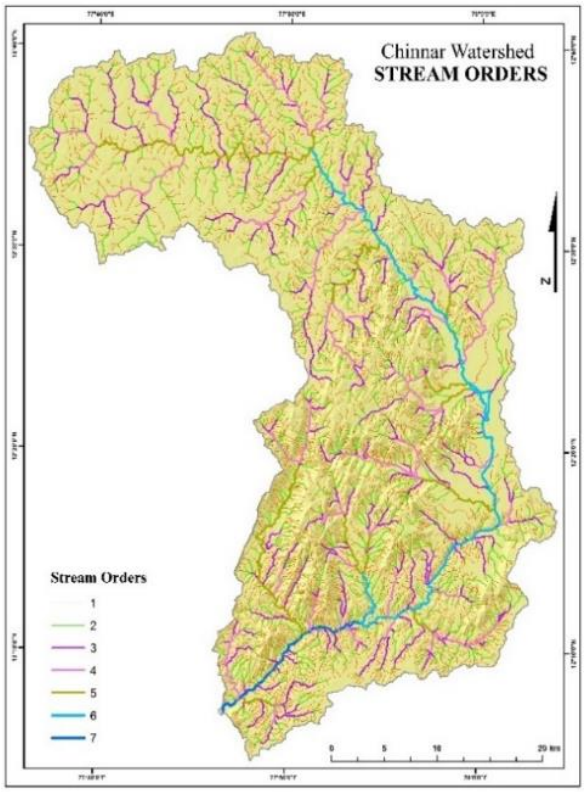

Figure 5: Stream ordering using Strahler's system

Groundwater occurs in the weathered residuum under unconfined conditions as well as in the fractured rocks under semi-confined condition (Venkateswaran, 2013). Groundwater fluctuation ranges from 3.52 m to 11.38 m below ground level (BGL). It reaches the lowest level during summer (March-June) and subsequently rise until the end of monsoon season (August–January) (Figure 7).

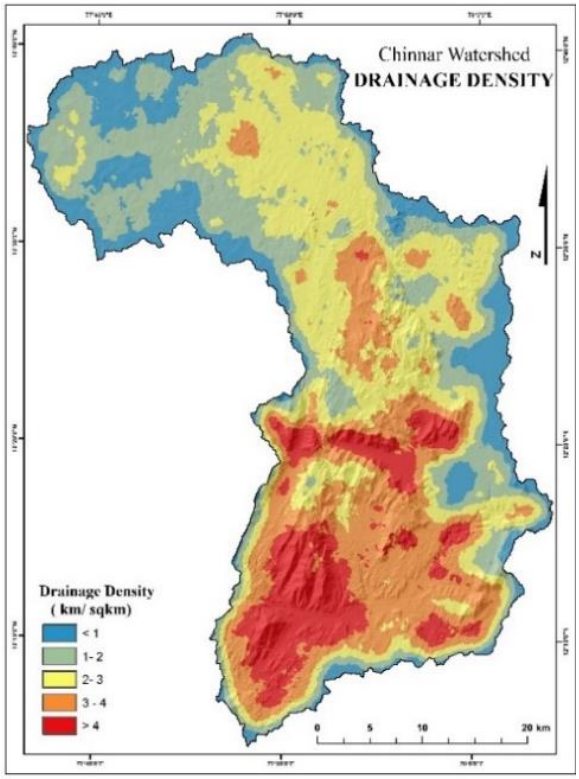

Figure 6: Drainage density of the watershed

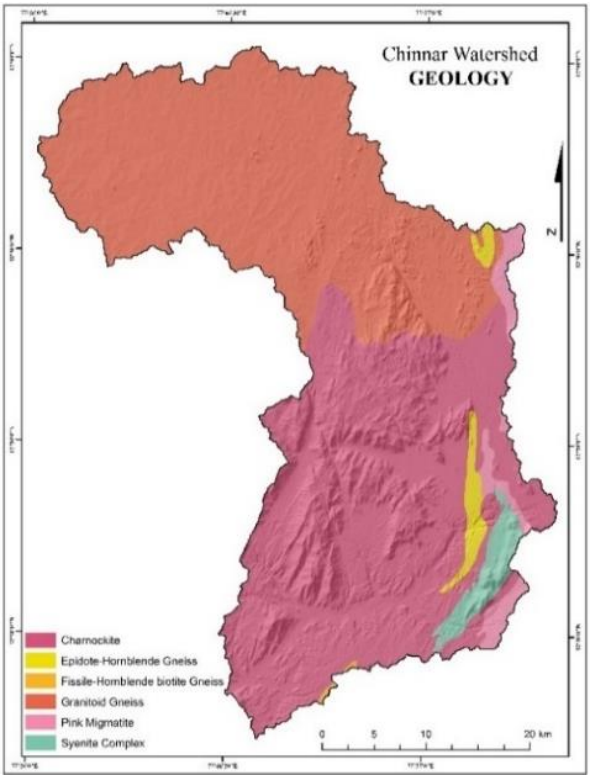

Figure 7: Geology of the watershed

2.4 Geomorphology

The study area is dominated by landforms of structural origin and denudational origin. The study area has been divided into two units each depending upon the degree of dissections namely, 1) Low dissected hills and valleys and 2) Moderately dissected hills and valleys. The pediment-pediplain complex is along the Chinnar River. The upper plateau adjoins hilly topography (Figure 8).

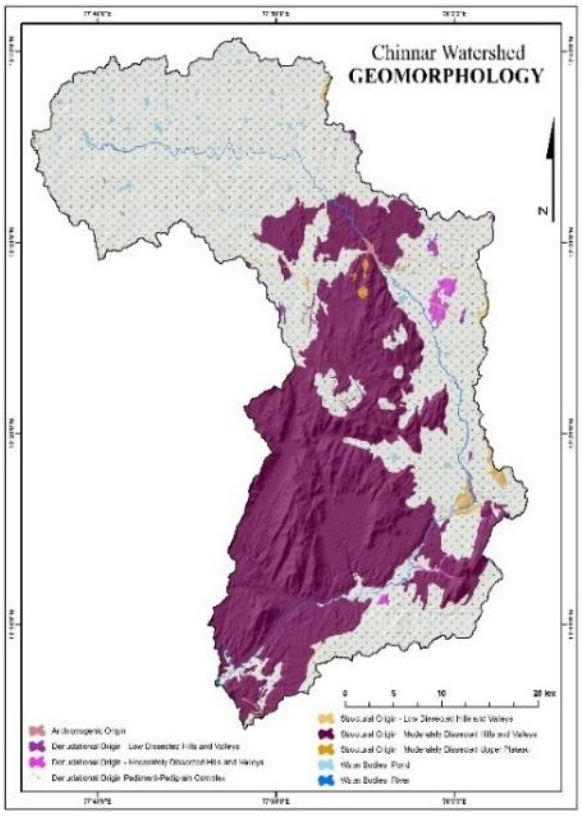

Figure 8: Geomorphology of the watershed

2.5 Lineaments

The lineament of the study area is of two major types viz., geomorphic lineaments and structural lineaments. Drainage parallel and scrap parallel are considered as geomorphic lineaments, observed in the western part of the study area and joint/Fracture are considered as structural features observed in entire study area (Figure 9).

2.6 Soil

The soil of the study area can be classified into clay, sand, sandy clay loam, sandy loam and loamy sand. The classification depends on the climate, rainfall, drainage, characteristics and geology of the area. Sand is a naturally occurring granular material composed of finely divided rock and mineral particles. Most of the upper part of the study area is covered by sand because of the erosion. Sandy clay loam is observed along the banks of the river and along the channel. The sandy loam is observed over the hilly area in the central part of the watershed, and loamy sand is observed in the upper western part of the study area (Figure 10).

2.7 Slope

The slope is a measure of the steepness of a line. The slope of the study area varies from 0 to 60 degrees. The slope map is generated from CartoDEM (30m) which was collected from Bhuvan. The slope values are classified in five classes such as <4, 4-8, 8-16, 16-24, and more than 24 degree (Figure 11).

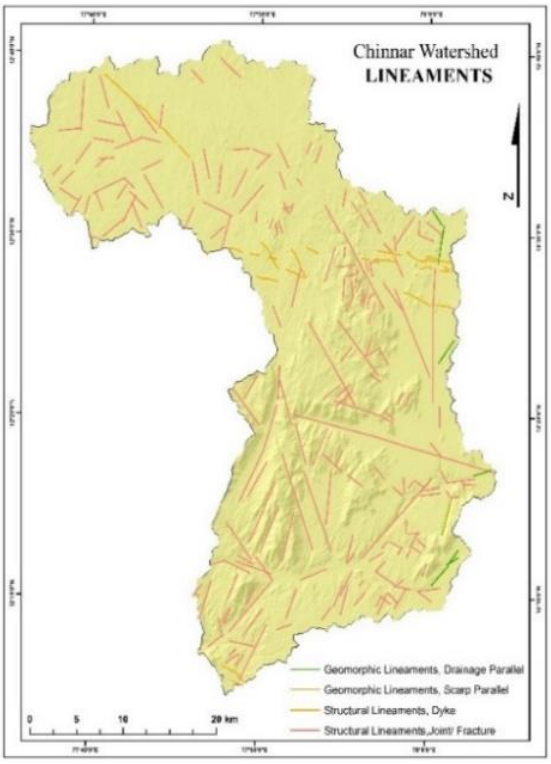

Figure 9: Lineaments in the watershed

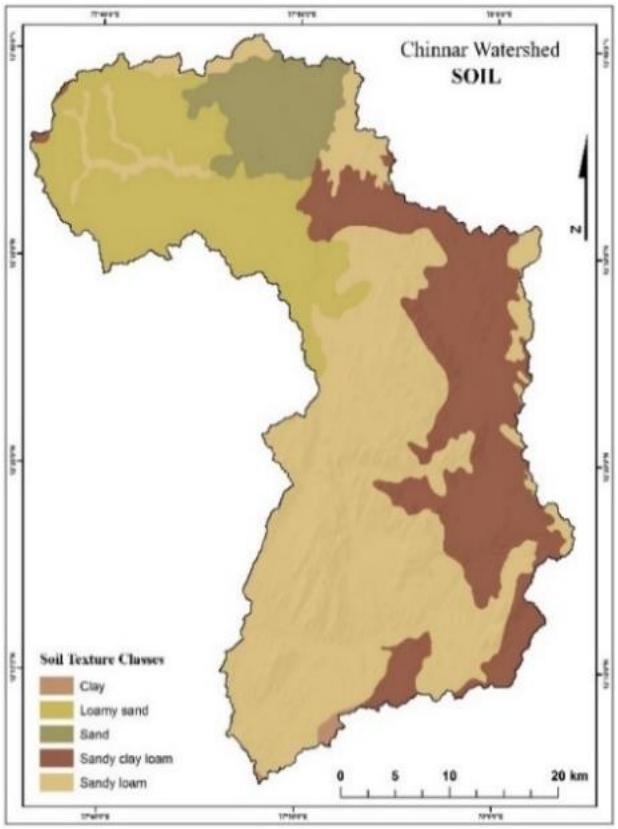

Figure 10: Soil texture of the watershed

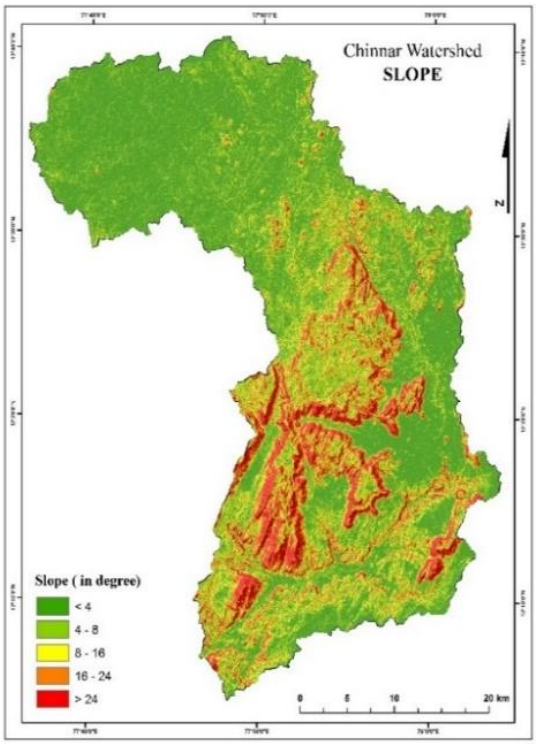

Figure 11: Slope of the study area

3. Social environment

3.1 Landuse/Land Cover

Agriculture and forest covers more area than other landuse classes. These classes cover approximately 573 sq km of study area. Hilly area is covered by forest in form of deciduous, evergreen, and scrub forests. Scrublands are observed in the eastern part of watershed (Figure 12). Table 1 shows distribution of landuse /land cover of the study area.

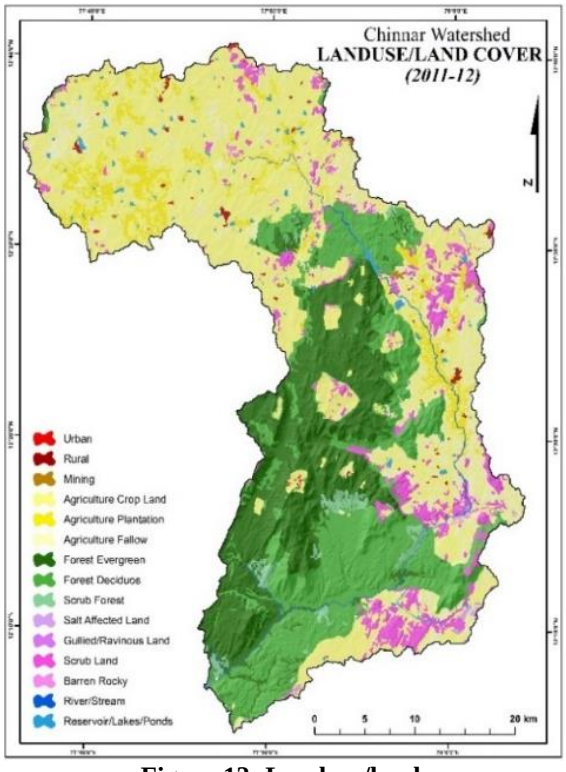

Figure 12: Landuse/land cover

Table 1: Area under landuse land cover

LULC features	Area in sqkm
Built-up	7.33
Agriculture	573.74
Plantation	81.54
Fallow	132.24
Forest (Deciduous)	323.67
Forest (Evergreen)	298.16
Scrub Forest	21.95
Wasteland	105.28
Waterbody	20.46

4. Rainfall-Runoff estimation

Runoff is a loose term that covers the movement of water to a channelized stream, after it has reached the ground as precipitation. The run-off of a stream is influenced by many complex conditions as, for instance, the amount of rainfall, its intensity, nature of soil, slope of the surface, area and configuration of catchment basin (Jain and Singh, 2003). It is also influenced by geologic structures, forests, wind, force of vapor pressure and few other elements.

When, intensity of the rainfall exceeds the infiltration rate, the excess rainfall begins to pond on the soil surface. When the rainfall ceases, the water held in surface storage either infiltrates into the soil or evaporate (Assefa and Wendy 2004). The volume of water that exceeds the volume of surface storage becomes surface runoff. Rainfall-runoff modeling may be used for a variety of purposes. The use of relatively simple rainfall-runoff models has become common over the years for designing detention storage or for design projects in medium to large watersheds where channel and floodplain storage are important factors in evaluating the flood hydrograph (Rao et al., 2001). Rainfall-runoff modeling may also be used as a management tool, for example, in the management of storm water runoff for water quality and urban development.

4.1 Rainfall

Rainfall is measured using rainguages. During a given storm, it is likely that depth measured by two or more rainguage will not be the same, therefore it is often necessary to determine the spatial average of the rainfall depth over the watershed area (Rafter, 1903). The study area has 10 rainfall gauging stations viz., Hosur, Thally, Denikanikottai, Rayakottai, Panchapalli, Marandahalli, Anchetty, Palacode, Pennagaram and Hoganikkal. The daily rainfall data from 2005 to 2013 was collected from Department of Economics and Statistics, Tamilnadu. The average rainfall was calculated from August to November, and it has been interpolated. Table 2 shows the distribution of rainfall during this period.

4.2 Rainfall-Runoff modelling

Rainfall-runoff estimation is very much required for identifying a suitable location for impounding harvesting structures. The report on the quantitative measurement in hydrology published by Perrault (1974) compared the measured annual rainfall (Pa) and the estimated annual streamflow (Qa) of the seine river in Paris. In order to estimate, amount of direct runoff that will be produced

from a given precipitation from a watershed, various hydrologic models can be used (Jonathan, 2003).

Table 2: Average rainfall distribution during northeast monsoon season (2005-2013)

RF Station.	Aug	Sep	Oct	Nov	Seasonal
Pennagaram	122.70	86.39	152.79	114.4	476.25
Heganikkal	108.07	79.97	168.26	116.9	472.48
Palacode	115.99	144.72	194.37	148.2	603.28
Thally	218.46	153.67	207.10	124.2	703.40
Marandahalli	120.96	95.65	206.00	151.6	574.23
Anchetty	114.10	98.63	148.12	90.43	451.29
Panchapalli	100.28	102.12	216.80	122.9	542.17
Rayakotta	95.67	100.23	147.76	106.1	449.79
Denikanikotti	113.02	116.74	189.26	110	529.93
Hosur	104.26	133.24	175.02	95.27	507.79

These models range from complex to simple, having different structures and input data requirements. Amongst these models, soil conservation service (SCS) model is most widely used for the estimation of direct run-off**.**

4.2.1 SCS-CN Rainfall estimation method

The Soil Conservation Service - Curve Number (SCS-CN) method is one of the most popular methods for computing the runoff volume from a rainstorm. The SCS-CN method was originally developed for its use on small agricultural watersheds and has since been extended and applied to rural, forest and urban watershed. In this study for calculating CN values and runoff, average rainfall data for the year 2005-2013 was used. Instead of using the annual rainfall, only the rainfall occurs between August and November has been used in this study because these month's receives comparatively more amount of rainfall and soil is almost wet in condition. Runoff curve number equation estimates total runoff from rainfall events and this relationship excludes time as a variable and rainfall intensity. Its stability is ensured by the fact that runoff depth (Q) is bounded between the maximum rainfall depth (P). This implies that as rainfall amount increase the actual retention (P-Q), approaches a constant value; the maximum potential retention (USDA, 2007). The runoff estimation related runoff (Q) to precipitation (P) and the curve number (CN) which is in turn related to storage (S). CN is based on the following parameters; hydrologic soil group, land use and treatment classes and hydrologic surface conditions. Following equation gives the relationship (Prasad et al., 2014):

$$Q = \frac{(P - Ia)^2}{(P - Ia) + S}$$

where; Q = runoff depth (mm); P = rainfall (mm); Ia = initial abstraction (mm); S = potential maximum retention after runoff start.

Initial abstraction consists mainly of interception and infiltration during early parts of the storm and surface depression storage. Its determination is not easy due to the variability of infiltration during the early part of the storm. Since it depends on conditions of the watershed at the start of a storm such as the land cover, surface conditions and rainfall intensity; thus, it is assumed as a function of the maximum potential retention as mentioned below (USDA, 2007)

$$Ia = 0.2S$$

The Curve Number can be calculated using potential maximum retention (S).

$$S = \frac{25400}{CN} - 254$$

The model is mainly depending on the runoff Curve Number. Curve number is estimated via the effect of soil and land cover on the rainfall runoff processes. The range of the Curve Number is between 1 (100 % rainfall infiltration) and 100, lower values of the Curve Number indicate lower runoff, while higher values of Curve Number refers to higher values of runoff (Mishra and Singh, 2003).

4.3 Hydrological soil group

Soils are assigned to hydrologic soil groups based on measured rainfall, runoff, and infiltrometer data. Since the initial work was done to establish these groupings, assignment of soils to hydrologic soil groups has been based on the judgment of soil scientists. Assignments are made based on comparison of the characteristics of unclassified soil profiles with profiles of soils already placed into hydrologic soil groups. Most of the groupings are based on the premise that soils found within a climatic region that are similar in depth to a restrictive layer or water table, transmission rate of water, texture, structure, and degree of swelling when saturated, will have similar runoff responses. The classes are based on the following factors (USDA, 2007):

- Intake and transmission of water under the conditions of maximum yearly wetness (thoroughly wet)
- Soil not frozen
- Bare soil surface, and
- Maximum swelling of expansive clays the slope of the soil surface is not considered when assigning hydrologic soil groups.

The four hydrologic soil groups (HSGs) are described by USDA (2007) as follows:

- ***Group A***: Soils in this group have low runoff potential when thoroughly wet. Water is transmitted freely through the soil. Group A soils typically have less than 10 percent clay and more than 90 percent sand or gravel and have gravel or sand textures. Some soils having loamy sand, sandy loam or silt loam textures may be placed in this group if they are well aggregated, are of low bulk density, or contain greater than 35 percent rock fragments.
- ***Group B***: Soils in this group have moderately low runoff potential when thoroughly wet. Water transmission through the soil is unimpeded. Group B soils typically have between 10 percent and 20 percent clay and 50 percent to 90 percent sand and have loamy sand or sandy loam textures.

Some soils having loam, silt loam, silt, or sandy clay loam textures may be placed in this group if they are well aggregated, are of low bulk density, or contain greater than 35 percent rock fragments.

- ***Group C***: Soils in this group have moderately high runoff potential when thoroughly wet. Water transmission through the soil is somewhat restricted. Group C soils typically have between 20 percent and 40 percent clay and less than 50 percent sand and have loam, silt loam, sandy clay loam, clay loam, and silty clay loam textures. Some soils having clay, silty clay, or sandy clay textures may be placed in this group if they are well aggregated, are of low bulk density, or contain greater than 35 percent rock fragments.
- ***Group D***: Soils in this group have high runoff potential when thoroughly wet. Water movement through the soil is restricted or very restricted. Group D soils typically have greater than 40 percent clay, less than 50 percent sand, and have clayey textures. In some areas, they also have high shrink-swell potential. All soils with a depth to a water impermeable layer less than 50 centimeter's [20 inches] and all soils with a water table within 60 centimeter's [24 inches] of the surface are in this group, although some may have a dual classification, as described in the next section, if they can be adequately drained.

Table 3 was used to find the hydrologic soil group of the study area depending upon the soil texture. Curve number is used to characterize the runoff properties for a certain soil and land cover/ land use. The soil conservation service runoff equation uses the curve number value as input parameter. Curve Numbers were evaluated for the study area on pixel basis using the land cover/land use and soil map that are reclassified to hydrologic conditions and hydrologic soil group. Curve numbers were thus generated using land cover and Hydrological Soil Group (HSG) classification system. A high value of the curve number (such as 100) refers to an area that has a high runoff potential and low infiltration.

Infiltration depends on the soil property, which effects the relation between rainfall and runoff (Arun, 2003). The soil conservation service model divides all soils into four Hydrologic Soil groups according to the United States Department of Agriculture (USDA) and the classification of soil to hydrologic soil group depends on infiltration rates and the soil texture composition. Only classes A, C and D are observed in the study area (Figure 13). Table 4 shows runoff curve number for combinations of different land cover and hydrological soil groups based on the USDA classification system.

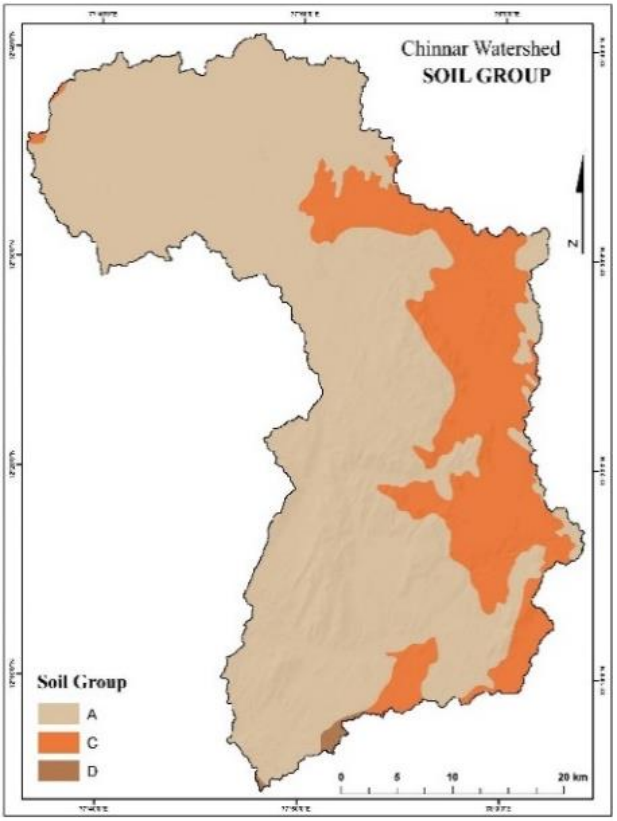

Figure 13: Hydrological soil group

Table 4: Runoff curve numbers

Landuse/ Land cover Classes	Hydrological Soil Group			
	A	B	C	D
Built-up	48	66	78	83
Agriculture Land	67	78	85	89
Plantation	65	73	79	81
Fallow Land	76	85	90	93
Forest (Deciduous)	68	79	86	89
Forest (Evergreen)	48	67	77	83
Scrub Forest	48	67	77	83
Wastelands	64	75	83	85
Waterbody	90	94	98	100

Table 3: Soil group and corresponding soil texture (Source: USDA, 1986; Rao et al., 2010)

Soil Group	Runoff Description	Soil Texture
A	Low runoff potential because of high infiltration rates	Sand, Loamy sand and Sandy loam
B	Moderately infiltration rates leading to moderately runoff potential	Silty loam and Loam
C	High/moderately runoff potential because of slow infiltration rates	Sandy clay loam
D	High runoff potential with very low infiltration	Clay loam, silty clay loam, sandy clay, silty clay and Clay

A low value to the curve number (such as 48) indicates an area that has a low runoff potential and high infiltration. (USDA, 1986).

4.4 Rainfall-Runoff depth

The rainfall runoff depth was calculated using SCS-CN method. Land use/land cover and hydrological soil groups curve numbers with average annual rainfall were estimated using raster calculator in ArcGIS 10.1. The high runoff potential is observed in the northern part of the study area (fallow land). The soil texture is loamy sand and sandy loam. A moderate runoff potential occurs in the eastern part of the study area (undulating hills and moderately sloppy terrain (Figure 14).

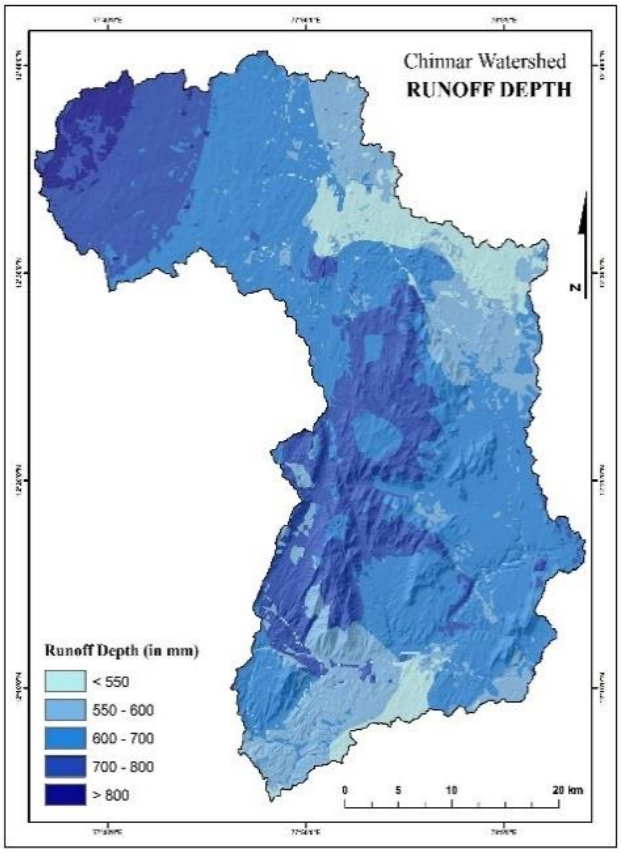

Fig 14: Runoff depth of the study area

5. Results and Discussion

Site suitability analysis is a type of analysis used in GIS to determine the best place or site for something (Patel et al., 2012). Potential sites used in suitability analysis can include the location of check dams and rainwater harvesting structures. Site selection analysis can be performed with vector or raster data but one of the most widely used types of site selections is weighted overlay site selection using raster data. Weighted overlay site selection analysis allows users to rank raster cells and assign a relative importance value to each layer. The result is a suitability surface which ranks potential sites from 1 to 9. Sites with a value of 1 are least suitable and those with a value of 9 are most suitable (Table 5).

Table 5: Weight determination of different Layers

Raster Layers	% influence	Feature Classes	Weightage
Slope	25	< 4 (Gentle Sloping)	5
(in degree)		4 - 8 (Moderately Sloping)	9
		8 - 16 (Strongly Sloping)	7
		16 - 24 (Moderately Steep Sloping)	3
		> 24 (Very Steep Sloping)	1
Runoff	15	< 550	1
(in mm)		550 - 600	3
		600 - 700	5
		700 - 800	7
		> 800	9
Soil Texture	10	Clay	1
		Loamy Sand	9
		Sand	5
		Sandy clay loam	7
		Sandy Loam	9
Geomorphology	15	Anthropogenic Origin	1
		Denudational Origin – Low Dissected Hills and Valleys	5
		Denudational Origin – Moderately Dissected Hills and Valleys	7
		Denudational Origin Pediment-Pediplain Complex	3
		Structural Origin - Low Dissected Hills and Valleys	5
		Structural Origin - Moderately Dissected Hills and Valleys	9
		Structural Origin - Moderately Dissected Upper Plateau	2
		Water Bodies- Pond	1
		Water Bodies- River	1
Drainage Density	10	< 1	1
(in sqkm)		1 - 2.	3
		2 - 3.	5
		3 - 4.	7
		> 4	9
Landuse/Land cover	10	Built up	1
		Agriculture	2
		Plantation	3
		Fallow	3
		Forest (Deciduous)	5
		Forest (Evergreen)	3
		Scrub Forest	9
		Wasteland	7
		Waterbody	1
Lineaments	15	Lineament buffer < 500 m	9
		Lineament buffer 500 - 1000 m	5
		Lineament buffer 1000 - 2000 m	3
		Lineament buffer > 2000 m	1

5.1.1 Weighted Index Model

Weighted Index Model represent weighting the multiple parameters. In this study, weighted index model was used for data integration. All thematic layers prepared for Chinnar watershed are classified with reference to the site suitability for water harvesting structures. In this study, most important aspect is to assess the area of high potential zones of water as it would help to prepare a plan for sustainable development of soil and water resources. This is carried out keeping in view that all the parameters are dependent on each other with respect to the study (Prasad et al., 2014).

5.2 Site suitability analysis

Identification of suitable sites for soil and water conservation structures are based on slope, runoff, geomorphology, soil, drainage density, landuse/land cover and lineaments (Prasad et al., 2014).

All the layers were generated in the ArcGIS- 10.1 software were in the vector format. In weighted overlay analysis, the rasterization of each physiographic unit was performed by using the conversion tools in the ArcToolbox Window. So, the first step of data conversion is rasterization for converting different lines and polygon into raster data format. After this, reclassification of all the raster files was performed using scale values of each unit. All the layers were ranked based on their influence following Lynn, (2009). For the site selection of soil water conservation structures in Chinnar Watershed, the weightage overlay analysis was used. Depending upon the influencing factors, weightages were assigned from rank 1 to 9. The lower value 1 represents the low or not suitable sites whereas the high values 9 represents highly suitable site over the Chinnar watershed. Further, using the Spatial Analyst Tool, weighted overlay function has been processed and suitability zones are identified (Figure 15). The resulted values range from 2 to 9. These are classified into highly suitable (7 - 9), moderately suitable (5 - 7), less suitable (3 -5) and not suitable (2 - 3) classes.

5.2.1 Highly suitable areas

The site having favorable location for construction of soil and water conservation structures is considered as highly suitable. These locations will not significantly effect on benefits and will not raise inputs above an acceptable level. The southwest part of the study area especially foots of hills are highly suitable for soil and water conservation. About 0.80% of the study area is highly suitable for implementing soil and water conservation structures.

.5.2.2 Moderately suitable areas

The site having moderately favorable location for construction of soil and water conservation structures is considered as moderately suitable. These locations will reduce some benefits and increase the required inputs to the extent that the overall advantage gained from use. The most part of the study area is moderately suitable for soil and water conservation. About 31 % of the study area is moderately suitable for implementing soil and water conservation structures.

5.2.3 Less suitable areas

The site having less favorable location for construction of soil and water conservation structures is considered as less suitable. Structures constructed in such area shall not be beneficial. The upper part of the study area is less suitable for soil and water conservation due to plain topography. About 65 % of the study area is less suitable for implementing soil and water conservation structures.

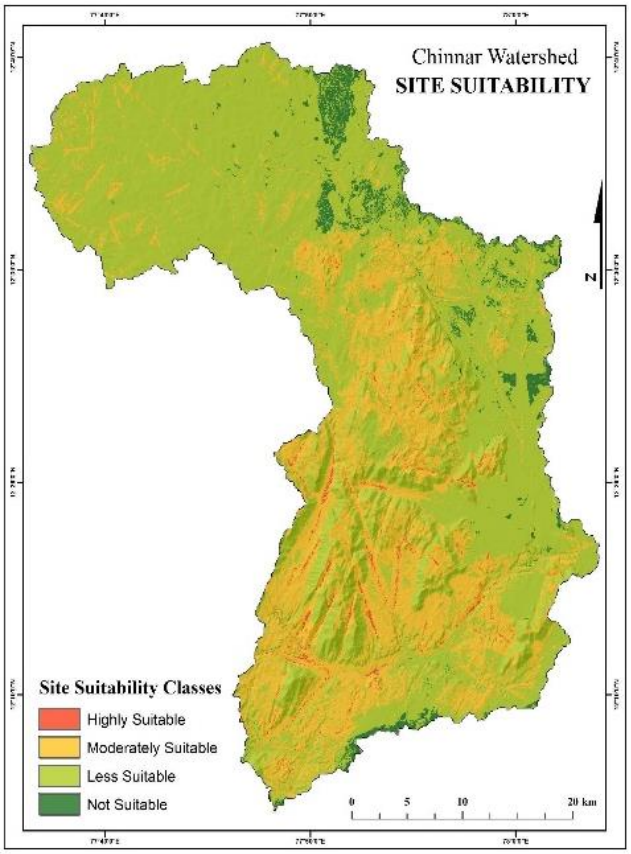

Figure 15: Site suitability for implementing soil and water conservation structures in the watershed

5.2.4 Not suitable areas

The site having severe limitations for the construction of soil and water conservation structures is considered as not suitable. Construction of any water conservation structure in these regions are not cost and time effective (Chopra et al, 2005). The areas that are not suitable are observed in the eastern part of the study area. About 3 % of the study area is not suitable for implementing any soil and water conservation structure.

5.3 Water conservation structures

The multi-layer integration through land use/cover, slope, flow direction, drainage density and rainfall depth gave the suitability units for identifying water-conservation sites for check dams, stop dams, percolation tank and farm ponds (Khare et al., 2013). Factor layers were incorporated in ArcMap, using weighted overlay function in the ArcGIS analyst and provided final suitability map. This map was used to identify potential sites (Figure 16) for different water harvesting structures in study area. Technical guidelines suggested by IMSD (1995) and INCOH (1995) were used for selecting suitable sites for conservation structures. Availability of water depends on many

variables like slope, landuse, soils, drainage, runoff potential, proximity to utility points, etc. These guidelines are used as a knowledge base for identifying sites (Perumal et al., 2003). The decision rules used in the present study for identifying suitable zones for water conservation structures are shown in Table 6.

Table 6: Soil and water conservation structures

Type of Structure	Slope	Runoff	Lineament Buffer (m)	Stream Order
Check Dams	Medium or Gentle Slope	High to Low	100 - 200	3rd,4th
Stop Dams	Very Gentle Slope	Moderate to low	200 - 500	3rd ,4th & 5th
Percolation Tanks	Gentle Slope	High to Low	< 100	4th & 5th
Farm Ponds	Flat or Gentle Slope	Moderate	> 500	3rd 4th & 5th

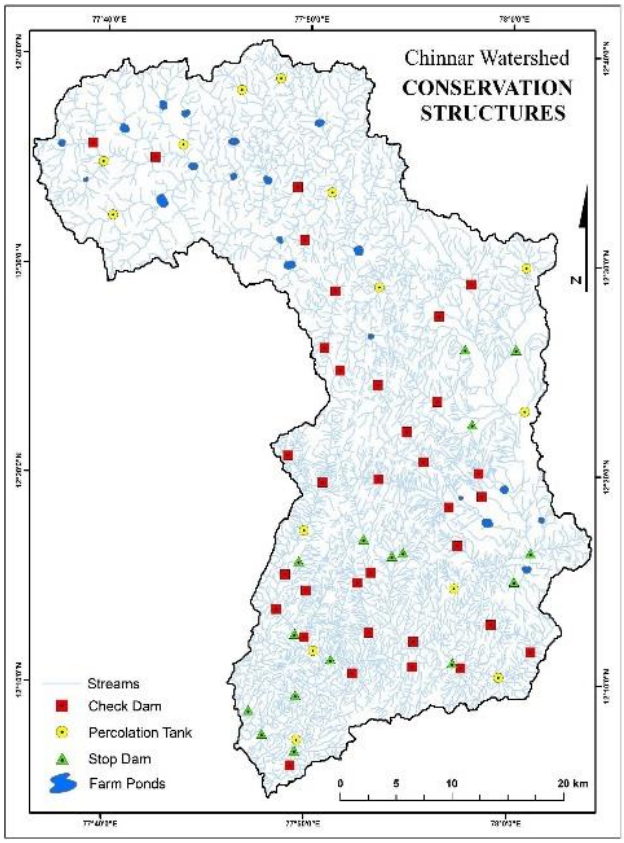

Figure 16: Optimal locations for soil and water conservation structures

5.3.1 Check dams

Check dams are very popular type of water harvesting structures and have greater importance since it has got a complimentary benefit of controlling soil erosion (IMSD, 1995). Check dams are structures constructed of rock, sediment retention fibre rolls, gravel bags, sandbags, or other proprietary product placed across a natural or manmade channel or drainage ditch. In Chinnar watershed, medium or gentle slope and 3rd and 4th orders streams are considered suitable sites for constructing check dams. There are 41 suitable sites identified for construction of check dam in the Chinnar watershed. These sites are fulfilling all the necessary conditions needed for construction of check dams.

5.3.2 Stop dams

Stop Dam is constructed across the direction of water flow on shallow rivers and streams for the purpose of water harvesting for irrigation as well as for domestic and animal use. In the study area deciduous forest, high to low runoff gentle slope and 3rd, 4th or 5th stream order is considered for selecting suitable sites for constructing stop dams. Thirteen sites have been identified suitable for the construction of stop dams in Chinnar watershed.

5.3.3 Percolation tanks

Percolation tanks are the structures for recharging ground water. These are generally constructed across streams and bigger gullies in order to impound a part of the run-off water (IMSD, 1995). In Chinnar watershed, moderate slope and proximity to lineaments (<100) are considered as suitable for percolation tank. There are 14 sites identified as suitable for construction of percolation tanks in Chinnar watershed.

5.3.4 Farm ponds

Farm ponds are made by either constructing an embankment across a water source or by excavating pits or the combination of both. These are the low-cost structures constructed in agricultural land located on higher reaches (IMSD, 1995). The farm ponds are used for protective irrigation in a prolonged dry spell in monsoon season.

Most part of the study area is highly suitable for construction of farm ponds. Sixteen favourable sites were identified for the construction of farm ponds based on rainfall pattern, heavy texture soil and agriculture lands,

6. Conclusions

Watershed is an ideal unit for management and sustainable development of its natural resources. The appropriate use of land and water resources of a watershed requires suitable engineering measures for conservation. Potential sites for water harvesting structures are identified normally based on the rainfall characteristics and rainfall runoff processes. Rainfall- runoff modeling of the watershed could be estimated using the soil conservation service-curve number (SCS-CN) method. Remote sensing and GIS provides an appropriate platform for estimating runoff using SCS-CN method. These methods play a significant role in generation of input parameters and spatial analysis. The SCS-CN method was applied in this study using average annual rainfall for the period 2005 to 2013 to estimate the runoff depth. The result indicates that significant amounts of annual runoff can be harvested through potential soil and water conservation structures.

As Chinnar watershed is drought-prone region and mainly depends on agriculture, it has become essential to conserve soil and water resources in a proper manner. Hence, site suitability analysis was carried out based on runoff, drainage density, slope, soil, land use/land cover, geomorphology and lineaments features. The weightage overlay analysis was used to delineate potential zones for

establishing conservation structures because the approach gives relative importance to the influencing parameters. Based on the suitable zones, locations for constructing check dams, stop dams, percolation tanks and farm pond were identified. These locations are ecologically sound and economically viable and this will sustain the agriculture productivity of the watershed.

References

Khare, A.M., N.C. Mondal, M. Sarang, W. Pawan. and R. Priti. (2013). Identification of water conservation sites in a watershed (WRJ-2) of Nagpur District, Maharashtra using Geographical Information System (GIS) technique. Journal of the Indian Society of Remote Sensing 41(3), 619-630.

Varade, A.M., Y.D. Khare, K.P. Dongre and G.W. Muley. (2017). Integrated Geographical Information System (GIS)-Based Decision Support System (DSS) approach to identify the site-specific water conservation structures in a watershed of Nagpur District, Central India, Sustainable Water Resources Management, ISSN 2363-5037.

Anbazhagan S., S.M. Ramasamy and D.S. Gupta. (2005). Remote sensing and GIS for artificial recharge study, runoff estimation and planning in Ayyar basin, Tamil Nadu, India, Environmental Geology 48(2), pp.158-170.

Arun, W. D. (2003). Runoff estimation for Darewadi Watershed using RS and GIS. International Journal of Recent Technology and Engineering 1(6), pp.46-49.

Assefa, M and M.D.G. Wendy (2004). Storm Runoff Prediction Based On a Spatially Distributed Travel Time Method Utilizing Remote Sensing and GIS. Journal of the American Water Resources Association 40(4), pp.863-879.

Chopra, R., R. Dhiman and P.K Sharma. (2005). Morphometric analysis of sub watersheds in Gurdaspur District. Punjab using remote sensing and GIS Technique. Journal of the Indian Society of Remote Sensing 33(4), 531–539.

Patel, D.P., B.D. Mrugen, N. Naresh and K.S. Prashant. (2012). Water harvesting structure positioning by using geo-visualization concept and prioritization of mini-watersheds through morphometric analysis in the lower Tapi Basin. Journal of the Indian Society of Remote Sensing 40(2), 299–312.

Rao, D.K.H.V., V. Hari Prasad and P.S. Roy. (2001). A suitable site: Geographic Information Systems and remote sensing technology, making water everybody's business (Ed. Agarval et al). Centre for Science and Environment, New Delhi. eng.warwick.ac.uk/ircsa/12th.html.243-245.

Elewa, H.H., E.M. Ramadan, A.A. El-Feel, E. Abu El Ella and A.M. Nosair. (2013). Runoff water harvesting optimization by using RS, GIS and watershed modelling in Wadi El-Arish, Sinai. International Journal of Engineering Research & Technology 2(12), pp.1635-1647

Geographical Information Technology Training Alliance: http://www.gitta.info/Suitability/en/html/WeightOverlaylearningObject1.html.

Prasad, C.P., B. Parul and P. Sarvesh. (2014). Site suitability analysis of water harvesting structures using remote sensing and GIS – A case study of Pisangan Watershed, Ajmer District, Rajasthan. The International Archives of the Photogrammetry, Remote Sensing and Spatial Information Sciences. DOI: 10.5194(8), 1471-1482.

IMSD, (1995). Integrated mission for sustainable development technical guidelines, National Remote Sensing Agency, Department of Space, Government of India, Hyderabad.

Jain, S and V. Singh. (2003). Water Resources Planning and Management, Development in Water Science 51, pp.68-76.

Jonathan, D.J (2003). Spatially distributed watershed mapping and modeling: GIS- based storm runoff response and hydrograph analysis: Part 2. Journal of Spatial Hydrology 3(2, 1-26.

Lynn, E.J (2009). Geographic Information Systems in Water Resources Engineering, New York . pp.94-102.

Mishra, S.K and V. Singh (2003). Soil conservation service curve number (SCS-CN) methodology, Dodrecht. DOI 10.1007/978-94-017-0147-1. 1-8, pp. 84-85.

Perumal, A., K. Rao and N. Rafter. (2003). A synergistic approach towards sustainable land resources management using remote sensing and GIS techniques an Indian experience in the semi-arid tropics. National Project Integrated Mission for Sustainable Development, Energy and wetland research.Hyderabad.http://www.ces.iisc.ernet.in/energy/paper/researchpaper.html.

Rafter, G W. (1903). The relation of rainfall to run-off. Department of the Interior, United States of Geological Survey (USGS), Washington.16, pp.21-26.

Rao, K and Raghavendra (2009) Soil erosion inventory and micro watershed modeling using digital technologies a case study of Mula Basin Maharashtra, Thesis. http://shodhganga.inflibnet.ac.in/bitstream/10603/126537/16/14_chapter%205.

State Ground and Surface Water Resources Data Centre Water Resources Department, Chennai, Tamil Nadu. http://www.groundwatertnpwd.org.in/weathergis.html
USDA (1986). Natural Resources Conservation Service, Urban Hydrology for Small Watersheds, Technical Release 55, Washington, DC. pp.2-11.

USDA (2007). Hydrology Part 630 National Engineering Handbook, Natural Resources Conservation Service,

United States Department of Agriculture, Washington. pp.7.1.-7.5.

Venkateswaran, S. (2013). Assessment of groundwater quality with a special emphasis on irrigational utility in Chinnar Watershed, Cauvery River, Tamil Nadu, International Journal of Recent Scientific Research 1(3), pp.01-09.

Zhan, X and M.L Huang. (2004). ArcCN-Runoff: an ArcGIS tool for generating curve number and runoff maps, Environmental Modelling & Software 19, 875–879.

Journal of Geomatics Vol 12 No. 2 October 2018

Suitability analysis for siting oil and gas filling stations using multi-criteria decision analysis and GIS approach – A case study in Tarkwa and its environs

M. S. Peprah[1], C. B. Boye[1], E. K. Larbi[1] and P. Opoku Appau[2]
[1]University of Mines and Technology, Tarkwa, Ghana
[2]Research Institute of Enhanced Oil Recovery, China University of Petroleum, Beijing, P. R. China
Email: mspeprah@st.umat.edu.gh

(Received: Jun 20 2018; in final form: Oct 18, 2018)

Abstract: Oil and gas stations are indispensable in the current technological society, however explosions from such fuel stations often cause loss of lives and properties within the surrounding communities thereby posing great concern to government and the citizenry. This condition calls for research that would provide meaningful solutions to mitigate this menace. Unlawful siting of oil and gas stations, non-consideration of environment impact on growing human population, competition for customers and lack of enforcement of standards are some of the causes of these explosions. This study investigated the level of compliance to standards set by the Ministry of Energy, and the Town and Country Planning Department by existing oil and gas stations in the study area. Primary and secondary data were used for the study. The primary data consist of locations of oil and gas filling stations picked with the Garmin handheld GPS whilst the secondary data comprise of topographic and soil maps from which soil types, roads, water bodies, terrain slope and land-use features of the area were extracted and used. The dataset was reclassified and Analytical Hierarchy Process was used to assign weights to the selection criteria. Spatial analyses were carried out using ArcGIS software to show areas suitable or otherwise for siting stations in the study area. The results showed 75% of oil and gas operators in the study area were compliant with the required standards while 25% were not. The integration of GIS techniques with multi criteria decision analyses has proved to be an effective tool for selecting suitable sites for filling stations and very useful in determining places of high fire risk for proper planning of the area. It is recommended that the authorities put measures in place to combine education and enforcement of the set standards through prosecution of offenders to bring sanity in the oil and gas filling station business.

Keywords: Analytical Hierarchy Process, Fire Risk, GIS, Oil and Gas Filling Stations

1. Introduction

The frequent reports of oil and gas explosions in the Republic of Ghana and its associated loss of lives, properties and national assets is an issue of concern receiving much attention by geospatial professionals (Saraei and Ghanei, 2011; Aslani and Alesheikh, 2011). The growing number of oil and gas stations operating along main roads, and settlement areas in some developing countries, especially Ghana calls for the need to control and manage the operations of such activities in the country (Uzochukwu *et al*., 2018). It is therefore imperative that government with the support of non-governmental agencies enforce set of rules and standards to manage the operations of oil and gas stations in the country (Tah, 2017).

As human population increases, there is commensurate surge in the number of automobiles working on the road leading to increasing demand for oil and gas (Njoku and Alagbe, 2015). This creates the need for filling station services and consequently the establishment of oil and gas stations within the communities. The permit required to operate oil and gas filling stations in Ghana is usually obtained from the Ministry of Energy and the Town and Country Planning Department. Some operators however, ignore seeking licenses from these bodies prior to establishing their businesses, perhaps to avoid payment of the required fees. Hence, some of these stations find themselves operating in unsuitable areas (Uzochukwu *et al*., 2018). The siting of environmentally sensitive commercial and service activities in rural or urban areas are guided by rules and standards (Tah, 2017). Accessibility for maneuvering in times of danger is key to safe operations of oil and gas stations.

In recent years, there have been several concerns regarding provision of licenses and indiscriminate siting of oil and gas stations (Aslani and Alesheikh, 2011). These fuels can give off flammable vapour at very low temperatures and can result in high risks of explosions if an ignition source is close (Njoku and Alagbe, 2015). In the Republic of Ghana, there have been several cases of wildfires and explosions of oil and gas filling stations as presented in literature with thousands of lives and millions of dollars lost each year (Norman *et al*., 2015; Kusimi and Appati, 2012; Addai *et al*., 2016; Amissah *et al*., 2010). As the health, safety and protection of people is a major concern to all, hence, the need to assess a site suitability for operating these activities in spatial contest of the study area concerned.

Geographic Information Systems (GIS) has proven to be very relevant in solving spatially related problems (Guler and Yomralioglu, 2017; Njoku and Alagbe, 2015). GIS has been applied in solving majority of problems in geoscientific discipline. Notably among them are; siting oil and gas stations (Tah, 2017; Njoku and Alagbe, 2015; Aslani and Alesheikh, 2011), forest risk mapping (Akay and Erdogan, 2017), selection of suitable sites for growing rice (Kihoro *et al*., 2013), landfill site selection (Guler and Yomralioglu, 2017), and planning of primer transportation of forest products (Akay and Yilmaz, 2017). Multi-criteria Decision Analysis (MCDA) and GIS are very useful tools for solving problems in spatial context because various decision variables can be evaluated and weighted

according to their relative importance to attain the final optimal decision (Broekhuizen *et al*., 2015; Kihoro *et al*., 2013). Also, MCDA has the ability to judge qualitative criteria along with quantitative criteria (Boroushaki and Malczewski, 2008). Moreover, it is simple to understand, easy to implement, modify, and suitable for problems which have a hierarchical framework (Aslani and Alesheikh, 2011). Hence, MCDA and GIS techniques were adopted in the present study. This study aims at finding out whether or not oil and gas operators in Tarkwa and its environs comply with the standard rules and regulations set by the Ministry of Energy and Town and Country Planning Department in Ghana. Furthermore, a propose map for siting oil and gas stations for future development and planning in suitable areas has been produced.

2. Study area

The study area (see Figure 1) is a mining community situated in the southwestern part of the Republic of Ghana. It is located on latitude 5º 18´ 00″ N and longitude 1º 59´ 00″ W with topographic elevation of about 78 m above mean sea level (Peprah *et al*., 2017). It is a semi urban area with high demand of oil and gas products for their daily operations. Some of the renowned mining companies include AngloGold Ashanti Iduapriem, Goldfields Ghana Limited, Ghana Manganese Company Limited and several mining services companies such as BCM Limited, Liebherr Limited, Africa Mining Services, Mantrac Company, Volvo Company, Hyundai Company Limited, Maxam Limited, Geodrilling Limited, Maxmass Limited, African Resource Management, SGS Geochemical Laboratory Limited and Cummins Limited. Most homes, offices, factories, hospitals and schools in the study area have power plants that provide alternative source of electric power due to the power fluctuations in the country's national grid. Moreover, other minor business services depend on private power produce by oil and gas products.

3. Resources and methods used

3.1. Resources

The data used for the study comprise primary and secondary data. The primary data consist of the location of some of the oil and gas filling stations in the study area picked with the Garmin Handheld GPS while the secondary data consist of topographic maps containing features such as contours, land use, vegetation, roads, soil types, and water bodies of the study area. Table 1 is a sample location of the oil and gas filling stations.

3.2. Methods used

3.2.1 Field data collection

A reconnaissance survey was carried out to inspect the vicinity of the stations and to determine appropriate methods to adopt for the survey. The locations of the oil and gas filling stations in the study area were captured using the Garmin Handheld GPS receivers. Geographic features within the surroundings of each station was measured and recorded. The measurements made included distance from green areas, distance of pump station to road, size of the filling stations, distance to neighbouring stations, and distance to any public facility (such as schools, banks, churches, hospitals, lorry stations, market, *etc*.).

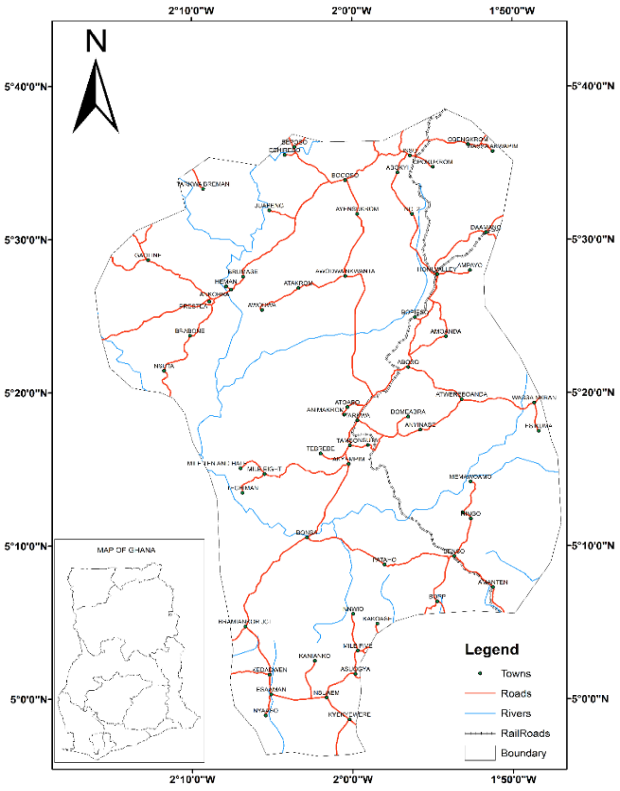

Figure 1: Study area

Table 1: Sample of oil and gas filling stations (units in meters)

ID	Northings (m)	Eastings (m)	Filling Stations	Location
1	580793.600	610277.400	Total 2	Akyempim
2	580836.500	610340.800	Star oil	Akyempim
3	581597.900	610299.700	Crown	Bankyim
4	584067.900	610525.900	Champion	Tamso
5	589204.300	613030.500	Shell	Tarkwa
6	588994.700	612859.600	Goil	Tarkwa
7	587577.600	611941.400	Allied	Tarkwa
8	586873.600	611533.400	Total 1	Tarkwa

3.2.2. Proximity analysis

Buffer analyses of fuel pumps distance to road, distance between neighbouring stations, distances between stations to any public facilities were done in ArcGIS environment. This was to assess the stations' compliance to the set standards by the Ministry of Energy, and Town and Country Planning Department. Filling stations that fell within the specified buffer distances complied with the set standards and are more likely to pose less hazard to the environment while those that fell outside the buffer zone are expected to pose hazards to the surroundings. The set standard of pump stations to roads is to be at least 15 m, and hence a buffer of 15 m was generated in ArcGIS environment. Again using set standard distance of at least 100 m and 400 m from any public facility and water bodies respectively, buffers were generated for each of the oil and gas stations to assess the level of compliance.

Buffer analyses were also performed to assess the proximity of oil and gas stations to populated areas and firefighting stations. Proximity analysis was carried out to determine the spatial relationship between the selected stations and their neighbouring features with regards to distances (Sara *et al*., 2011). It also allowed the spatial feature to be reclassified based on distance that meet the set criteria (Njoku and Alagbe, 2015; Tah, 2017; Aslani and Alesheikh, 2011).

3.2.3. Selection of suitable site for oil and gas stations

The suitable sites were selected based on spatial analyses of the following dataset: slope, land use, vegetation, roads, soil type and water bodies. As the dataset are of varying relative importance, Analytic Hierarchy Process (AHP) based on pairwise comparisons was used to generate weights for each criterion. The relative importance between two criteria was measured based on a numerical scale from 1 to 9 (Saaty, 1980). Figure 2 shows the flowchart of the MCDA. The AHP, which was first developed by Myers and Alpert (1968) and remodified by Saaty (1977), was used because the technique assesses a set of evaluation criteria and search for the optimal solution among a set of alternative options (Akay and Erdogan, 2017; Akay and Yilmaz, 2017). In the solution process of AHP, the study area was classified into low, moderate, and high.

3.2.4 Model generation

The suitability and restriction model was created in ArcGIS environment according to Equation 1 given as:

$$S = \sum_{i=1}^{n} w_i * c_i \prod_{j=1}^{m} r_j \qquad (1)$$

Where; S is suitability site for oil and gas; w_i is weight for criteria; c_i is criteria for suitability; r_j is restriction. Most restriction will include a minimum and maximum buffer distances for suitable selection of a site. Table 2 is the standards set for suitability selection and Table 3 is the relative importance values. The following procedure was adopted for creating the final raster map:

- Buffer creation for the criteria (slope, land use, roads and water bodies).
- Conversion of vector layers to raster.
- A restriction is created using the null tool so as to show areas viable for siting the oil stations.
- The various restrictions are combined to give the final restriction.
- The Restriction model and the suitability model are combined to give the final suitability of locations appropriate for siting the oil stations.

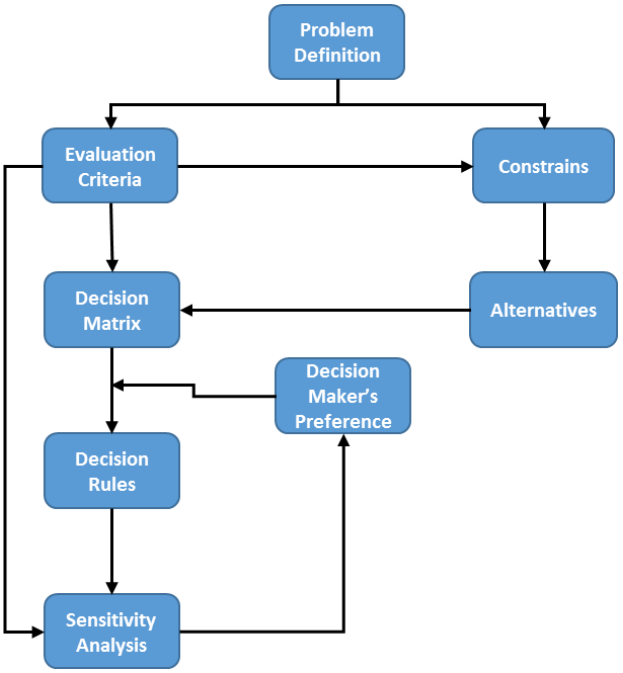

Figure 2: Flowchart of the MCDA process (Malczewski, 1999)

Figure 3 and 4 show the suitability and restriction model generated respectively for the suitable site selection. The combined model for the final output raster map is shown by Figure 5.

From Table 3, the values assigned to the sub-criteria were evaluated with regards to suitable site selection. Higher score was given when the criterion was more important (Akay and Yilmaz, 2017). The derived matrix was normalized to obtain the Eigen vectors (weights) which were assigned to the selection criteria.

Table 2: Restriction standards for suitability selection

Restriction source	Minimum buffer distances / degree	Maximum buffer distances / degree	Analysis buffer distances / degree
Slope	0°	20°	≤ 20°
Built-up areas	500 m	1000 m	500 m
Roads	100 m	500 m	100 m
Surface water	100 m	500 m	100 m

Table 3: The relative importance values (Saaty, 1980)

Importance Scale	Definitions of Scale
1	Equal Importance
3	Weak importance of one over another
5	Essential or strong importance
7	Demonstrated importance
9	Absolute importance
2, 4, 6, 8	Intermediate values between the two adjacent judgements

Each entry $a_{ji} = 1/a_{ij}$ of the matrix represents the importance of the *i*th criterion relative to the *j*th criterion. If $a_{ji} > 1$, the *j*th criterion is more important than the *i*th criterion. The column vector was produced by using Equation 2 given as (Gulci, 2014; Akay and Erdogan, 2017):

$$x_{ji} = \frac{a_{ji}}{\sum_{j=1}^{n} a_{ji}} \quad (2)$$

Where x_{ji} is each entry at the column, and *n* is the number of criteria. The weighted averages of the criteria w_{ji} were computed by averaging the entries (c_{ji}) on each row using Equation 3 given as (Aslani and Alesheikh, 2011):

$$w_{ji} = \frac{\sum_{i=1}^{n} c_{ji}}{n} \quad (3)$$

The ratio of consistency index (CI) and random index (RI) were also computed to check the consistency of the evaluations made for the pairwise comparison matrices. The smaller value of this ratio (< 0.1) the better the assigned weights (Kihoro *et al*., 2013; Broekhuizen *et al*., 2015). This was done to prevent bias through criteria weighting according to Equation 4 and Equation 5 given as:

$$CI = \lambda_{max} / n \quad (4)$$

$$CR = CI / RI \quad (5)$$

Where λ_{max} is the maximum Eigen value, *CI* is the consistency index, *CR* is the consistency ratio, *RI* is the random index, and *n* is the number of criteria or sub-criteria in each pairwise comparison matrix.

After consistency analysis, spatial analyst extension in the ArcGIS environment was used to assign weighted values (w_{ji}) to the corresponding criteria. Finally, a weighted overlay operation was carried out to sum up the weighed criteria together according to their relative importance to produce a weighted overlay map.

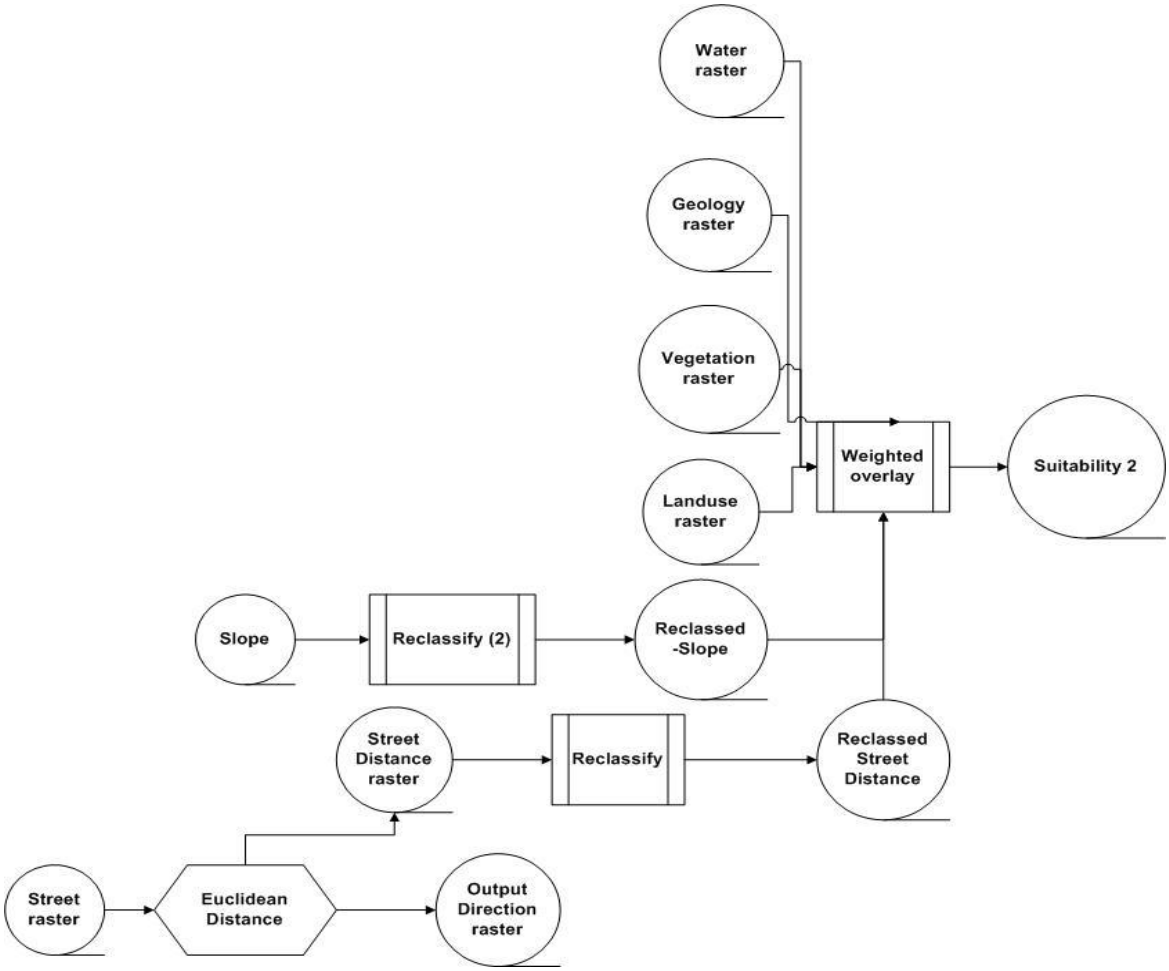

Figure 3: Suitability model of criteria used

Figure 4: Restriction model

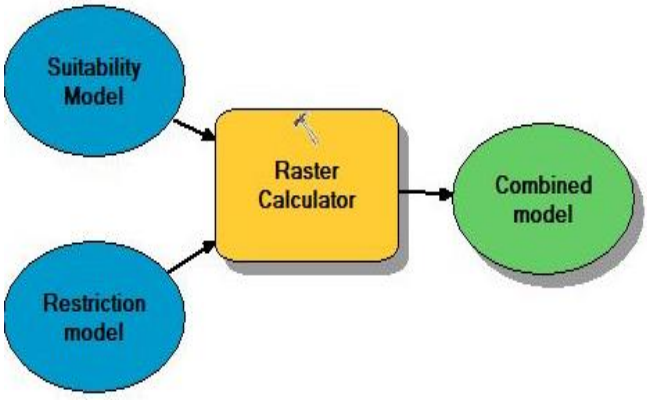

Figure 5: Combined model

4. Results and Discussion

4.1. Results

The outcome of the buffer analyses is presented in Figure 6, 7, 8 and 9 show the land use analyses. Table 4 and 5 are the suitability description and search distance to neighbouring stations. The required size of any station should be of a minimum area of 1080 m^2.

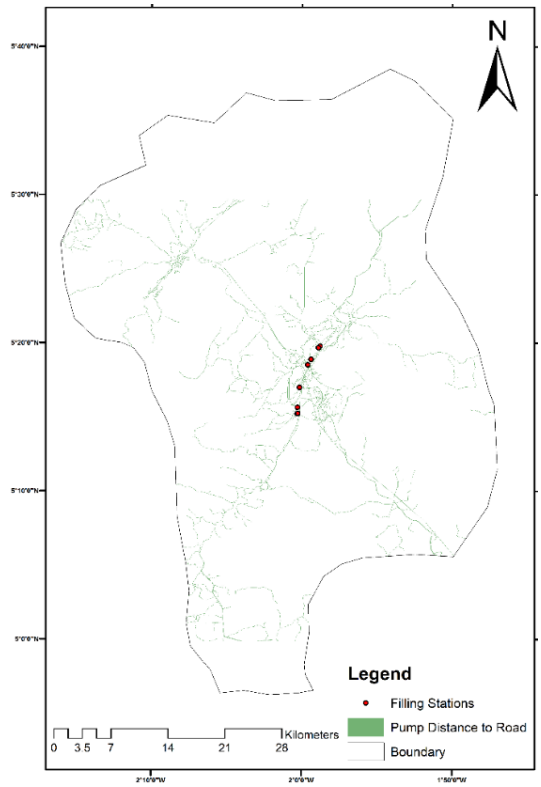

Figure 6: Distance of pump station to road buffer analysis

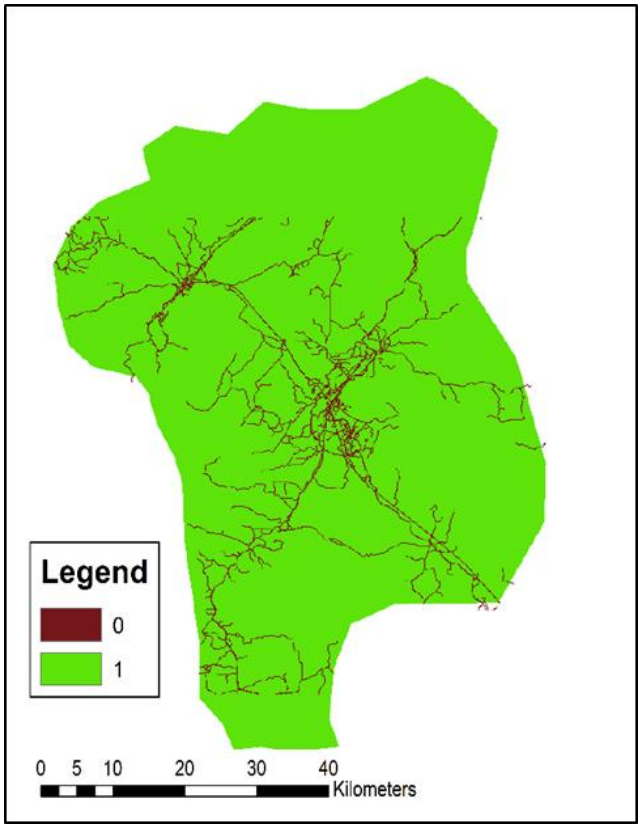

Figure 7: Map of street restriction

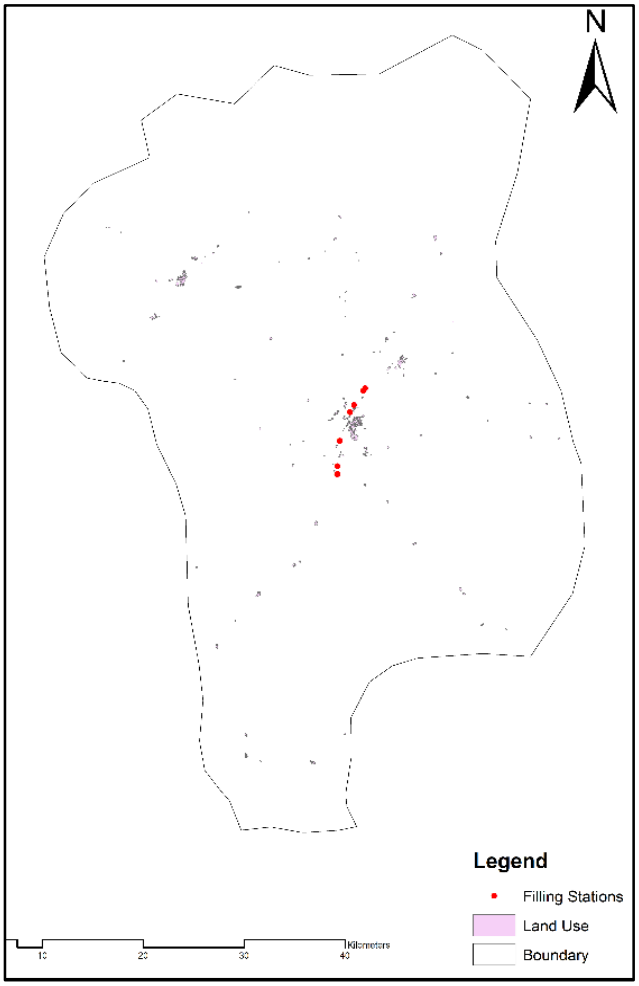

Figure 8: Distance to public facilities analysis

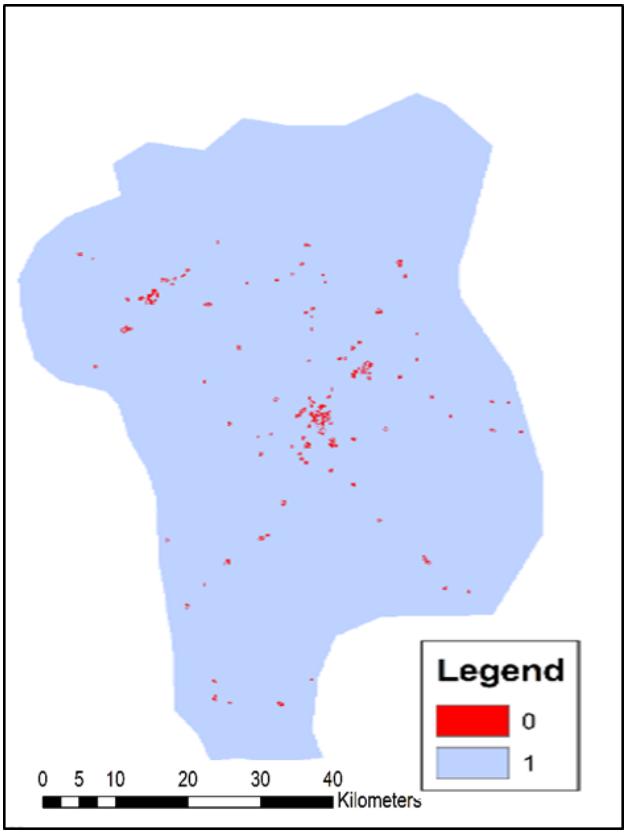

Figure 9: Map of land use restrictions

Table 4: Suitability description

Range of Value	Colour Code	Description
0.0 – 1.0	Red	Not Suitable
1.1 – 2.0	Yellow	Moderate Suitability
2.1 – 4.0	Green	Most Suitable

Table 5: Distance to neighbouring stations (units in meters)

From	To	Linear Distance (m)
Total 2	Star Oil	76.4921
Star Oil	Crown	762.6709
Crown	Champion	2480.6839
Champion	Total 1	2981.5189
Total 1	Allied	813.8200
Allied	Goil	1688.8023
Goil	Shell	270.4306

Figure 10 is the water restriction map. Figure11 is the slope analysis. From the restriction results (see Figure 7 and 9), the 0 represents the restricted region and 1 represents a viable region

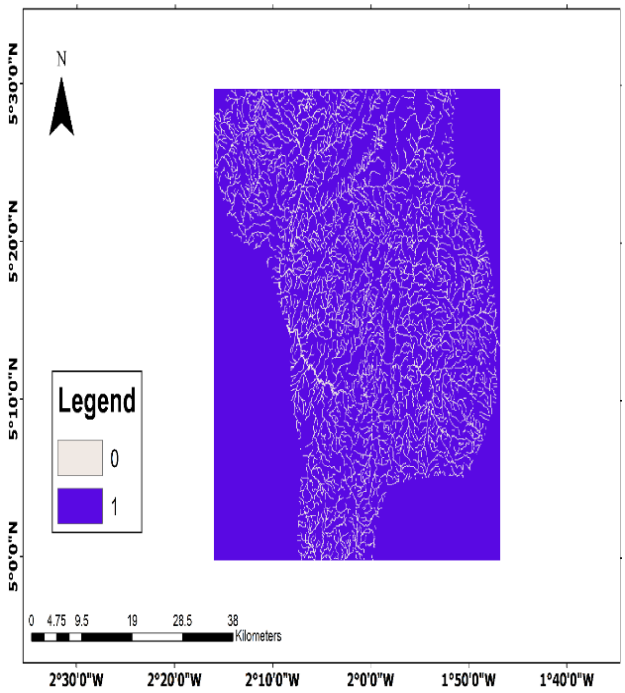

Figure 10: Map of water restriction

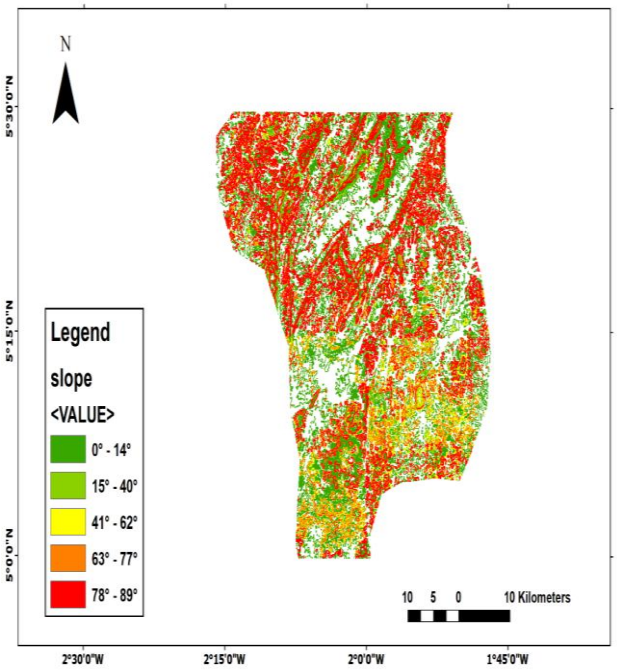

Figure 11: Slope analysis

The outcome of the pairwise comparison from which the weight for the criteria and their sub-criteria were generated is shown in Table 6. Also, Table 7 presents the normalized matrix and the computed weights from AHP. The calculated CI and CR were found to be less than 0.105, which implies there was consistency in the assigned weights. The suitability map for siting oil and gas stations is represented by Figure 12 and 13 shows the map of the combined model thus, suitability and restriction model for siting oil and gas stations including all the various criteria (slope, Land use, water bodies, forest, roads, and soil type). Figure 14 is also a map of the existing stations on the combined model map to check whether or not they are within acceptable region.

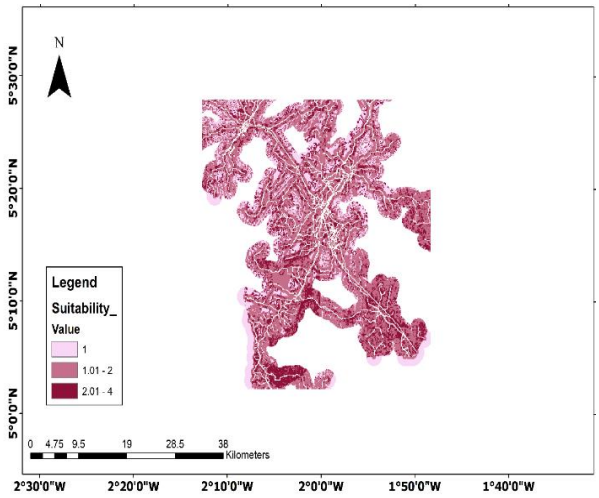

Figure 12: Suitability map

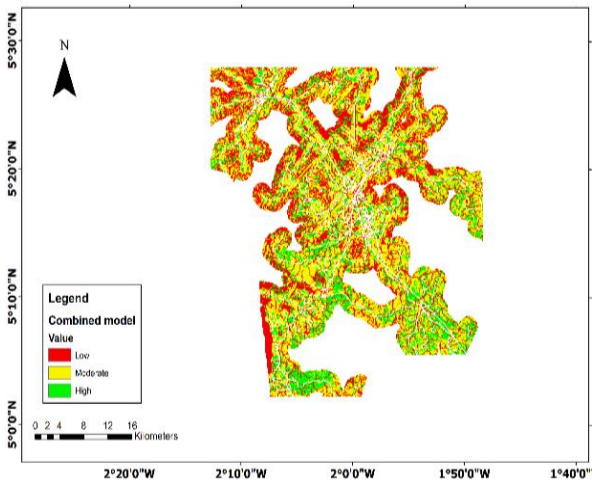

Figure 13: Map of combined model

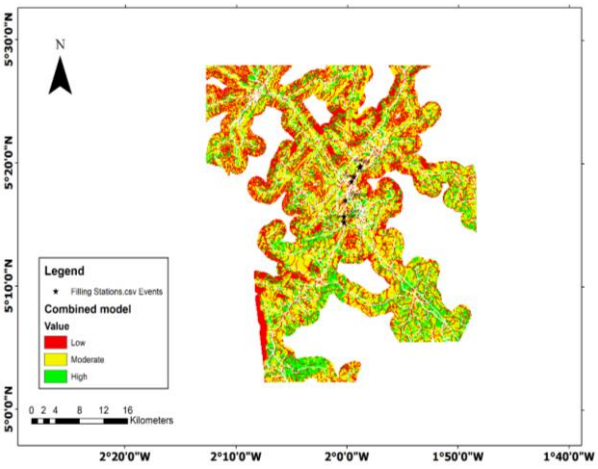

Figure 14: Map of combined model and existing filling stations

4.2. Discussion

All the oil and gas stations were found to be sited along the main highway in the study area. Some were also found close to settlements and public facilities (see Figure 8). 75% of the oil and gas filling stations in the study area meet the set standard while 25% do not. In terms of the pump distance to road analysis (see Figure 6), Star oil pump station does not meet the 15 m to major road criteria.

Table 6: A pairwise comparison

Criteria(n)	Land use	Slope	Soil types	Forest	Roads	Waterbodies
Land use	1	0.33	3	3	0.33	0.33
Slope	3	1	3	5	3	3
Soil types	0.33	0.33	1	0.33	0.33	0.33
Forest	0.33	0.2	3	1	0.33	0.33
Roads	3	0.33	3	3	1	0.33
Waterbodies	3	0.33	3	3	3	1

Table 7: Normalized data with weights

Criteria(n)	Land use	Slope	Soil type	Forest	Roads	Waterbodies	Weights
Land use	0.0938	0.1310	0.1875	0.1957	0.0413	0.0620	0.11855
Slope	0.2814	0.3968	0.1875	0.3262	0.3755	0.5639	0.3552
Soil types	0.0310	0.1310	0.0625	0.0215	0.0413	0.0620	0.0582
Forests	0.0310	0.0794	0.1875	0.0652	0.0413	0.0620	0.0777
Streets	0.2814	0.1310	0.1875	0.1957	0.1252	0.0620	0.1638
Waterbodies	0.2814	0.1310	0.1875	0.1957	0.3755	0.1880	0.2265

The major road within the vicinity of this station happens to have heavy traffic for most parts of the day making it difficult for vehicles to enter and exit the station. From Table 5, it was observed that, although a distance of 400 m is required between any two stations, longer distances were found between one station and the next with a distance of 2981.52 m being the longest distance found between Champion and the next filling station (*i.e.* Total 1). Only 25% of the filling stations were located at a distance of at least 400 m away from water body criteria. This can be attributed to the fact that management of some stations did not comply with the set standards before the establishment of the station as a result of improper planning. The study also revealed that all the filling stations in the study area were far away from firefighting stations, and some were not having all the required firefighting equipment. Some stations were also found to be located few meters from churches, lorry parks, and gas operating stations. Again, it was found that some filling stations had large land area for vehicles to enter and exit the station whiles others did not meet the set criteria. From Fig. 14, it was obvious that some of the existing filling stations are operating in an uncongenial environment and as such require much attention to prevent any future casualties.

It was furthermore observed that, the general topography of the study area is undulating with steep sloping terrains which make most portions unsuitable for operating oil and gas filling stations as previous studies have shown that, fire risk is relatively higher on steep terrains (Akay and Erdogan, 2017; Jaiswal *et al*., 2002). Moreover, some soil types and their engineering properties are not suitable for construction purposes (Aysen, 2003; Budhu, 2011; Frost and Frost, 2014), this is particularly true for sites close to the hilly part of the study area. This serves as a limitation as most oil filling stations store their oil in deep drenches.

5. Conclusions and Recommendations

From the study, it has been found that, 75% of the filling stations in the study area comply with the laid down standards set by the Ministry of energy and Town and Country Planning Department of Ghana. The study has revealed the spatial distribution of oil and gas stations along the main road of the study area for future planning purposes. The proximity analyses point to the fact that, some of the existing stations are sited in an uncongenial environment and therefore poses threat to the lives and properties within their vicinity. It was also realized that, there were no firefighting stations close to the locality of these stations. The study has again demonstrated the usefulness of multi-criteria decision analysis and GIS tools in solving spatially related pertinent problem.

It is recommended that the suitability map produced for the study area should be used and further environment impact assessment should be carried out by the authorities to assess the significant impacts the sited stations have on the environment. It is also recommended that site suitability analyses be incorporated in the Town and Country Department's planning scheme for future development and policy formulation. Measures should be put in place to enforce the set standards and prosecute offenders to bring sanity in the oil and gas filling station business. Finally, it is recommended that this study be replicated in other parts of the country or be adopted for future redevelopment of the study area.

Acknowledgement

The authors would like to thank the Departments of Geomatic and Environmental and Safety Engineering of UMaT, Tarkwa for the provision of secondary data and information used for the study.

References

Addai, E.K., S.K. Tulashi, J.S Annan and I. Yeboah. (2016). Trend of fire outbreaks in Ghana and ways to prevent these incidents, Safety and Health at Work, 7, pp. 284-292.

Akay, A.E and A. Erdogan. (2017). GIS-Based multi-criteria decision analysis for forest fire risk mapping,

ISPRS Annals of the Photogrammetry, Remote Sensing and Spatial Information Sciences, Vol. IV-4/WA, 2017 4th International GeoAdvances Workshop, 14-15 October 2014, Safranboln, Karabuk, Turkey, 25-30.

Akay, A.E and B. Yilmaz. (2017). "Using GIS and AHP for planning primer transportation of forest products", ISPRS Annals of the Photogrammetry, Remote Sensing and Spatial Information Sciences, Vol. IV-4/WA, 2017 4th International GeoAdvances Workshop, 14-15 October 2014, Safranboln, Karabuk, Turkey, pp. 19-24.

Amissah, I., B. Kyereh and V.K. Agyemang. (2010). Wildfire incidence and management in the forest transition zone of Ghana: Farmers' Perspectives, Ghana Journal of Forestry, 26, 61-73.

Aslani, M and A.A. Alesheikh. (2011). Site selection for small gas stations using GIS. Scientific Research and Essays, 6(15), 3161-3171.

Aysen, A. (2003). Problem solving in soil mechanics, A.A. Balkema Publishers, Lisse, Abingdom, Exton (PA), Tokyo, Japan, pp. 1-77.

Boroushaki, S and J. Malczewski. (2008). Implementing and extension of the analytical hierarchy process using ordered weighted averaging operators with fuzzy quantifiers in ArcGIS, Comput. Geosci., 34, 399-410.

Broekhuizen, H., C.G.M. Groothuis-Oudshoorn, J.A. Van Til, J.M. Hummel and M.J. Ijzerman. (2015). A review and classification of approaches for dealing with uncertainty in multi-criteria decision analysis for healthcare decisions, Pharmaco Economics, 33, 445-455.

Budhu, M. (2011). Soil mechanics and foundations, 3rd Edition, John Wiley and Sonc, Inc., USA, pp. 1-43.

Frost, B.R and C.D. Frost. (2014). Essentials of igneous and metamorphic petrology, Cambridge University Press, UK, pp. 1-40.

Gulci, N. (2014). Researches on precision forestry in forest planning. PhD Thesis, KSU, Kahramanmaras, pp. 1-264.

Guler, D and T. Yomralioglu. (2017). A GIS-Based landfill site selection approach using spatial multi-criteria decision-making methods, International Symposium on GIS Applications in Geography and Geosciences, 2017, Istanbul, Turkey, pp. 1-8.

Jaiswal, R.K., S. Mukherjee, D.K. Raju and R. Saxena. (2002). Forest fire risk zone mapping from satellite imagery and GIS, International Journal of Applied Earth Observation and Geoinformation, 4, 1-10.

Kihoro, J., N. J. Bosco and H. Murage. (2013). Suitability analysis for rice growing sites using a multi-criteria evaluation and GIS approach in Great Mwea Region, Kenya, Springerplus, 2(365), pp. 1-9.

Kusimi, J.M., and J.W. Appati. (2012). Bushfires in the Krachi District: The socio-economic and environmental implications, International Archives of the Photogrammetry, Remote Sensing and Spatial Information Sciences, XXXIX-B8, 2012 XXII ISPRS Congress, 25 August – 01 September 2012, Melbourne, Australia, pp. 39-44.

Malczewski, J. (1999). GIS and Multicriteria Decision Analysis, John Wiley and Sons, New York, pp. 1-40.

Myers, J. H. and M. I. Alpert. (1968). Determinant buying attitudes: meaning and measurement, Journal of Marketing, 32, 13-20.

Njoku, C.G. and A.O. Alagbe. (2015). Site suitability assessment of Petrol Filling Stations (PFSs) in Oyo Town, Oyo State, Nigeria: A Geographic Information Systems (GIS) approach, IOSR Journal of Environmental Science, Toxicology and Food Technology (IOSR-JESTFT), 9(12), 8-19.

Norman, I.D., B.M. Awiah, M.K. Aikins. and F.N. Binka. (2015). Review of catastrophe fires and risk communication, Ghana, Advances in Applied Sociology, 5, 167-177.

Peprah, S.M., Y.Y. Ziggah and I. Yakubu. (2017). Performance evaluation of the earth gravitational model (EGM2008) – A case study, South African Journal of Geomatics, 6(1), 47-72.

Saaty, T.L. (1977), A scaling method for priorities in hierarchical structures, Journal of Math Psychol., 15, 234-281.

Saaty, T.L. (1980), The Analytic Hierarchy Process: Planning, Priority Setting, Resource Allocation, McGraw-Hill, New York, USA, pp. 641-658.

Saraei, M.H and B.R. Ghanei. (2011). Evaluation and site selection of public parking's in Yazd City Central Tissue, Geographical Landscape (Human Studies), 6(15) 13-16.

Sara, R.G., C. Christine, G. Donn and J. Brad. (2011). The benefits of using Geographic Information Systems as a community assessment tool, Public Health Rep., 126(2) 298-303.

Tah, D. S. (2017). GIS-Based locational analysis of petrol filling stations in Kaduna Metropolis, Science World Journal, 12(2) 8-13.

Uzochukwu, O.C., O.O. Lilian, O.T. Uchenna and U.O. Ugbomhe. (2018). Business development and sustainability of selected petrol stations in Anambra State of Nigeria, Africa Journal of Business Management, 12(1) 11-20

Journal of Geomatics Vol 12 No. 2 October 2018

Land use and land cover change detection through spatial approach: A case study of Mangaluru Taluk, Karnataka

Sanjith S Anchan[1], Ateeth Shetty[2], H Gangadhara Bhat[2] and Mohandas Chadaga[3]
[1]Department of Civil Engineering, Sahyadri College of Engineering & Management, Mangalore
[2]Department of Marine Geology, Mangalore University, Mangalore
[3]Civil Engineering Department, Manipal Institute of Technology, Manipal
Email: sanjith.civil@sahyadri.edu.in

(Received: Apr 03, 2018; in final form: Oct 22, 2018)

Abstract: Land cover is a physical appearance of land and represents its ecological status. Land use/land cover changes are due to human intervention, natural disturbance and succession. The present study aimed at monitoring the land cover changes in Mangalore region during the period 1997 to 2017. Remote sensing and Geographical Information System (GIS) techniques were used to determine the land use and land cover changes based on the analysis of temporal Landsat-5 and Landsat-8 satellite imagery. Ground truth observations were performed to check the accuracy of the classification. The present study brought to light that the forest area that occupied 37% of the Taluk's area in 1997 has reduced to 31% in 2017. Other classes like agricultural land, built up area, water bodies and barren land have also experienced changes. Built-up lands (settlements) have increased from 6 per cent to 23 per cent of the total area. The high land vegetation and forest cover areas are disappearing rapidly; water bodies like lakes are also diminishing. Mangalore city is one of the fastest developing cities in India. Proper land use planning is essential for a sustainable development of Mangalore Taluk.

Keywords: Land use, Land cover, Change Analysis, GIS, Mangaluru

1. Introduction

Land Use/Land Cover (LU/LC) is an important component in understanding the interactions of the human activities with the environment and thus it is necessary to understand the changes in it. The land use/land cover pattern of any region is influenced by natural and socio-economic factors and their utilization by human in time and space (Aspinal and Hills, 2008; Feranec et al., 2007). Degradation of land is mainly due to population pressure that leads to intense land use without proper management practices. Over population makes people to relocate themselves towards sensitive areas like highlands. Usually such areas lack planning strategies. The influence of road and other constructions in such terrain will disturb the landscape that intern may lead to landslides/other mass movements. These changes have to be analysed for better understanding of interactions and relationships between human activities and natural phenomena. It also helps us to understand the necessity for improving resource management and decision making (Lu et al., 2004; Seif and Mokarram, 2012).

Proper information on land use/cover and outcome for their optimal use is essential at planning phase to meet the increasing demands of basic human needs and welfare very effectively. Land use and Land cover are inter related i.e., Land use affects land cover and changes in land cover affect land use. Every time changes in land cover by land use do not necessarily imply that there will be degradation of the land. However, many changing land use patterns driven by a variety of social causes, result in land cover changes that affects biodiversity, water and radiation budgets, trace gas emissions and other processes that come together to affect climate and biosphere (Riebsame et al., 1994). Remote sensing and GIS can be effectively used as a source or tool for rational planning of any area or region. With the invent of these techniques, land use/cover mapping has given a useful, economical and detailed way to improve the selection of areas designed to agricultural, urban and/or industrial areas of a region (Selcuk et al., 2003). Remote Sensing tool has been used to classify and map land use and land cover changes with different techniques and data sets. Remotely sensed data has made it possible to study changes in land cover in less time, at low cost and better accuracy (Kachhwaha, 1985). Various methods of supervised classifications have been applied widely for the land use change analysis throughout the world. These techniques depend on a combination of background knowledge and personal experience with the study area to a greater extent than other areas. Information on LU/LC is important in regional and urban planning and management (Chen et al., 2006; Crainic et al., 2009; Flotterod et al., 2011). An attempt is made in this study to map status and changes in LU/LC of Mangalore region, Dakshina Kannada district of the Karnataka State.

2. Study area

Mangalore region is located at Dakshina Kannada District of the Karnataka state, India and lies in between Arabian Sea towards west and Western Ghats mountain ranges towards east side. The study area (Figure 1) has been divided into three zones by having the river boundary as a reference. It extends between 12°25' N to 13°25' N latitude and 74°25' E to 75°25'E longitude and encompasses an area of 664 km^2. Climatically, the study area experiences humid hot temperate conditions. The annual mean maximum, minimum and average temperature of the study area stands at 36.6, 20.1 and 28.3 °C, respectively. On an average, the study area receives about 4030 mm of rainfall per year. Few rivers flowing in these regions are Nethravathi, Kumaradhara, Phalguni, Shambhavi, Nandini or Pavanje and Payaswini

Rivers. The region has a total population of 20,89,649 (Census of India, 2011).

Source: https://dk.nic.in/en/map-of-district/

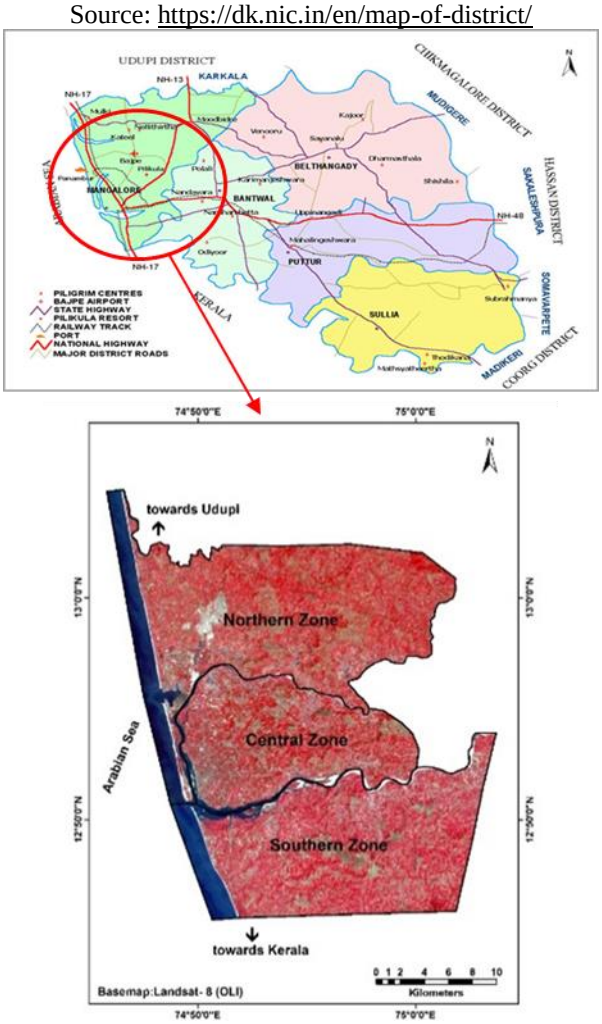

Figure 1: Study area showing the three zones along Mangalore, Dakshina Kannada District.

3. Objectives

The main objective of the present paper is to analyse the nature and the extent of land use/land cover changes in the study area over the past 20 years and to identify the main causes behind the changes.

4. Material and methods

4.1. Satellite data pre-processing

Landsat-5 (Thematic Mapper) and Landsat-8 (Operational Land Imager) satellite imagery with the resolution of 30 m, covering the path-146 and row-51 during February 1997 and January 2017 were used for land use/cover mapping. It was downloaded from the USGS Earth Explorer image database (Landsat Imagery Archive). It has a solar elevation angle of 63.13 degrees and a cloud cover lower than 10%.

4.2. Database preparation

Figure 2 shows the flow chart of methodology adopted for this study. The data sets were imported in ERDAS Imagine version 10.0, satellite image processing software to create a False Colour Composite (FCC). The layer stack option in image interpreter tool box was used to generate FCCs for the study areas. The sub-setting of satellite images was performed for extracting study area from both images by taking geo-referenced out line river boundary of Mangalore region as AOI (Area of Interest). For better classification results, indices such as Normalized Difference Vegetation Index (NDVI) were also used.

4.3. Land use/cover detection and analysis

Acquisition of land use/cover by traditional method takes several months or years; Remote sensing has proved an efficient technique for monitoring the spatial changes in local and global scales (Loveland et al., 2000; Foody, 2002). To work out the land use/cover classification, supervised classification method with maximum likelihood algorithm was applied using the ERDAS Imagine (v.2010) Software. Maximum likelihood Classifier (MLC) algorithm is one of the most popular supervised classification method for analysing satellite data. This method is based on the probability that a pixel belongs to a particular class. The basic theory assumes that these probabilities are equal for all classes and that the input bands have normal distributions. However, this method takes long time of computation, relies heavily on a normal distribution of the data in each input band and tends to over-classify signatures with relatively large values in the covariance matrix. The spectral distance method calculates the spectral distance between the measurement vector for the candidate pixel and the mean vector for each signature and the equation for classifying by spectral distance is based on the equation for Euclidean distance. It takes least computational time among other supervised methods, however, the pixels that should not be unclassified become classified, and it does not consider class variability. Ground verification was done for doubtful areas. Based on the ground truthing, the misclassified areas were corrected using recode option in ERDAS Imagine. The land use Land cover classes were taken as per the International Geosphere Biosphere Program (IGBP) LULC classification scheme.

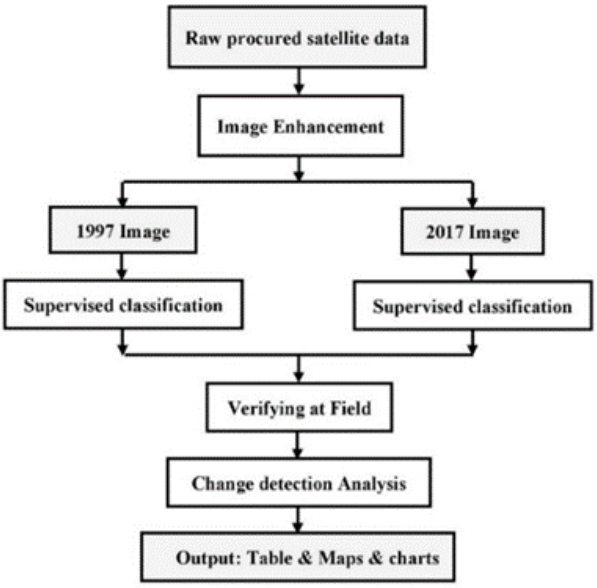

Figure 2: Methodology flowchart

5. Results and discussion

5.1. Land use mapping and distribution

A supervised maximum likelihood classification was implemented for the three images and the final classification products provided an overview of the major land use / land cover features of Mangalore region for the years 1997 and 2017. Six categories of land use / land cover were identified are described in Table 1.

Table 1: Classification scheme used for preparing the decadal land use and land cover datasets

Level - 1	Level - 2	Description
Built-up	Built-up (both urban & rural) BU	Urban, rural, residential, and industrial areas.
Agriculture	Crop Land	These include agriculture area delineable on satellite images in different seasons and the areas which are primarily agriculture but may be fallow.
Mixed Forest	Shrub land (SL)	Stunted height degraded forest.
	Grass Land (GL)	Land covered with grasses, notified or otherwise.
	Permanent wetland (PW)	Water saturated area having land-water interface.
Dense Forest	Forest (FO)	Included evergreen broad leaf forest (EBF), Deciduous Broad leaf forest (DBF), mangrove forest (MF).
	Plantation (PL)	Primarily commercial plantation outside forest, protected areas and wildlife sanctuaries.
Barren Land	Barren Land (BL)	Rocky or exposed rocky areas, Soil filled surfaces.
	Mining (MN)	Mining areas
Water bodies	Water bodies (WB)	Surface water delineable on satellite data in the form of river, lakes, pond, reservoirs/dams, canals.

Based mainly on International Geosphere Biosphere Program (IGBP)

The Figures 3, 4 and 5 illustrate the land use / land cover maps of Mangalore region for the year 1997 and 2017. For each zone separate supervised classification was performed and then the results are analysed. Above mentioned (Table 1) six classes of classification are adopted during supervised classification of three zones.

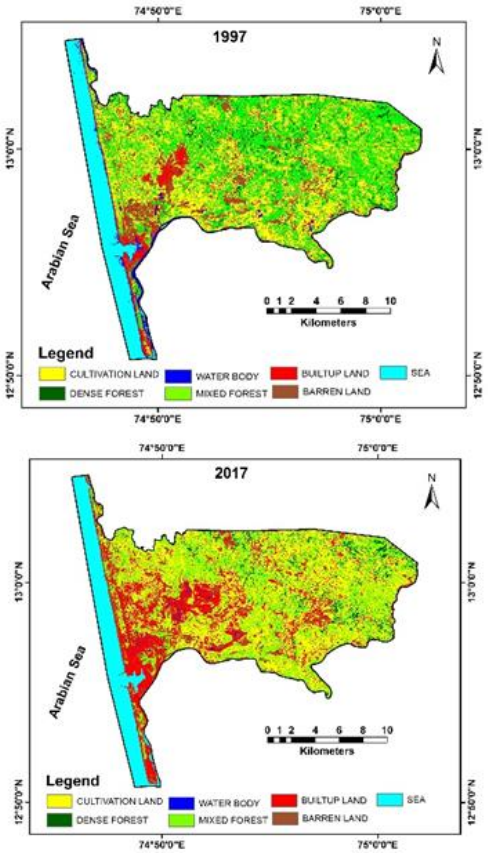

Figure 3: Land use / Land cover in the northern zone during 1997 and 2017

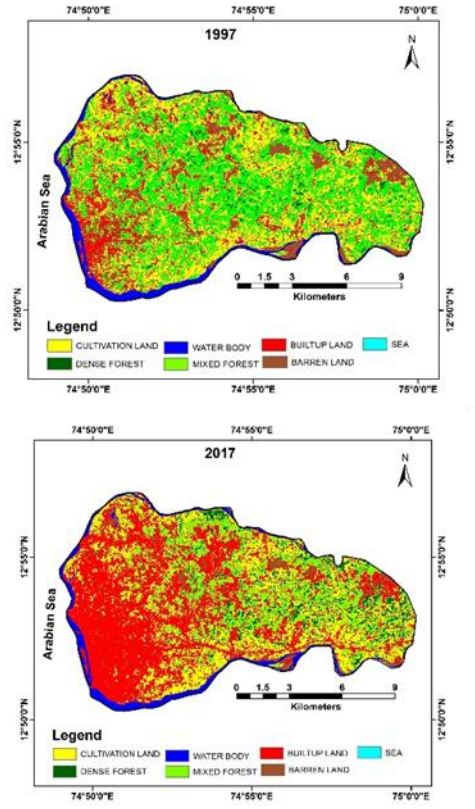

Figure 4: Land use / Land cover in the central zone during 1997 and 2017.

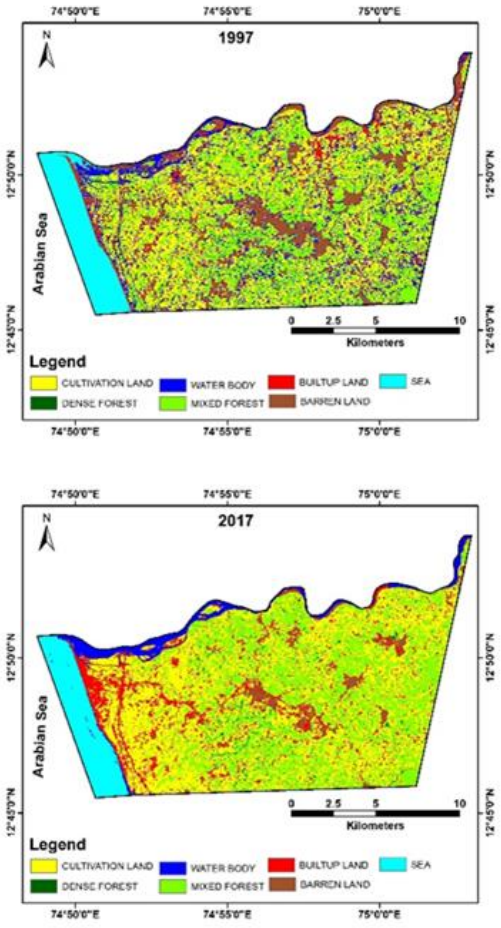

Figure 5: Land use / Land cover in the southern zone during 1997 and 2017.

Table 2 and 3 illustrate the areas under six classes of three zones (Northern, Central and Southern zone) for the year 1997 and 2017 respectively.

Table 2: Landuse/land cover area (km²) during 1997

Classes	North	Central	South
Cultivation Land	100.59	55.504	84.089
Dense Forest	16.506	4.769	4.607
Water Body	6.659	8.856	46.475
Mixed Forest	99.175	54.404	62.091
Built-up Area	10.557	20.076	9.539
Barren Land	40.129	17.613	22.951

Table 3: Landuse/land cover area (km²) during 2017

Classes	North	Central	South
Cultivation Land	97.506	39.157	100.921
Dense Forest	12.223	10.521	3.104
Water Body	1.503	8.028	9.065
Mixed Forest	82.528	26.656	71.696
Built-up Area	58.529	68.166	22.148
Barren Land	18.735	7.729	11.922

Table 2 and 3 provides data of spatial extent of the land cover in square kilometres for the three zones of study. Cultivation area at the north and central zone was 100.59 km² and 55.504 km² during 1997, but has reduced to 97.506 km², 39.157 km² respectively, in the year 2017. Whereas the cultivation land at the south zone has increased from 84.089 km² (1997) to 100.92 km² (2017). Built-up area at all the zones increased tremendously. During 1997 it was 10.557 km², 20.076 km² and 9.539 km² for north, central and south zone and in 2017 it was found to be 58.529 km², 68.166 km² and 22.148 km² respectively. Also water bodies have decreased drastically at north and south zone and quite stable at central zone since there were no much water bodies existing at central zone. It was found to be 6.659 km² and 46.475 km² (1997) at north and south zone and reduced to 1.503 km² 9.065 km² (2017) respectively. At central zone the water bodies area coverage was 8.856 km² (1997) and 8.028 km² (2017). Likewise, the barren land has reduced in all the zones. It was 40.129 km², 17.613 km² and 22.951 km² (1997) and 18.735 km², 7.729 km² and 11.922 km² (2017) at north, central and south zone respectively. The rapid increase in built-up land in the southern coastal Karnataka is due to the intensive urban growth and industrial revolution (Usha et al., 2014; Silambarasan et al., 2014; Usha et al., 2015; Kale et al., 2016).

Table 4 shows the percentage increase and decrease of land use land cover during 1997 – 2017 for all the three zones. It is observed that there is a large decrease in area of water bodies and barren land by 70.011% and 52.428% respectively. There is slight decrease in areal extent of mixed forest and negligible decrease in area of dense forest i.e., 16.131% and 0.123% respectively. While built up area has tremendously increased by 270.506% whereas the cultivation land has decreased by about 1.078%. Residential and commercial buildings were constructed in the barren land and beside the shores of the river bodies; Farming activities are observed to be stable. This is pictorially depicted in the figure 6.

The figure 7 illustrates the areal coverage of land use/land cover for six classes in the three zones (North, central and South) during 1997 and 2017 respectively. Cultivation area is more on the north and south zone compared to central zone. Also mixed forest cover area is high at north and south when compared to the central zone. Whereas built up area is large at central zone compared to the other two zones. Water bodies are slightly more in the south zone compared to other two zones.

Table 4: Changes in Land use/land cover classes

Classes	Increase (%)	Decrease (%)
Cultivation Land	-	1.0783
Dense Forest	-	0.1236
Water Body	-	70.0117
Mixed Forest	-	16.1311
Built-up Area	270.5068	-
Barren Land	-	52.4289

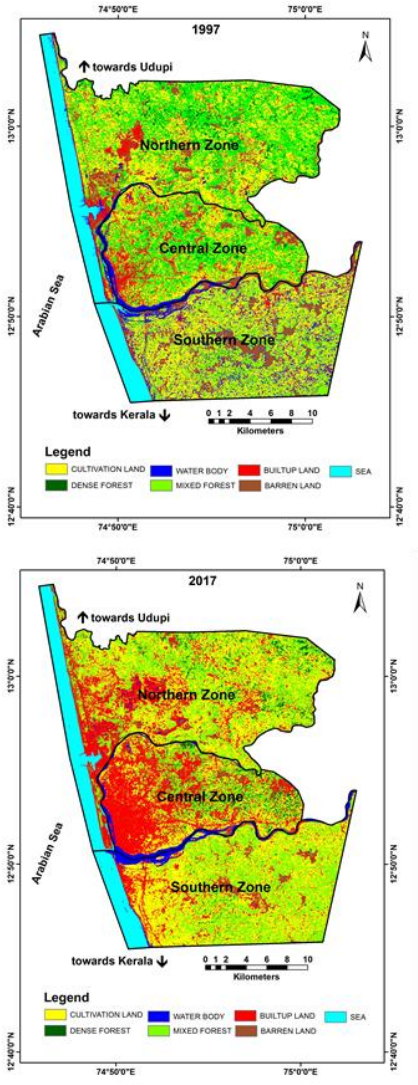

Figure 6: Land use / Land cover in the study area during 1997 and 2017

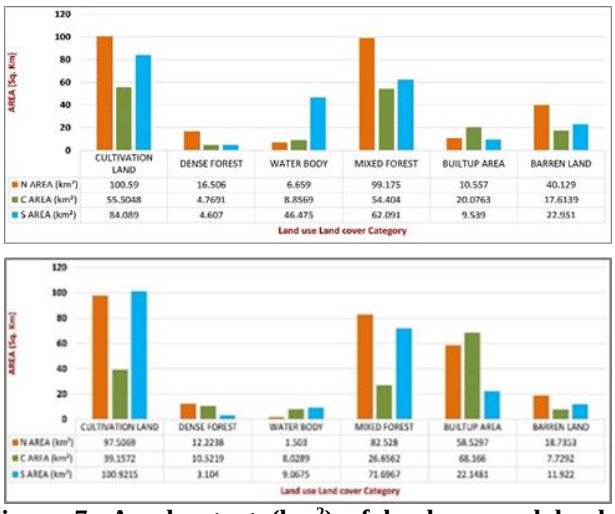

Figure 7: Areal extent (km^2) of land use and land cover in the three zones during 1997 and 2017

Each zones discrete study was conducted to understand evidently the land use/land cover change in respective three zones of interest. The data list of the increase and decrease in area of land use/land cover classification for the 20 years span of study is given in Table 5. It is clearly observed that the built up area have increased tremendously in all the three zones (North, Central and South). There is enormous increase in built up area at North zone by 454.45%. The noticeable change is increase in dense forest area at central zone region by 120.63%. North and south zone regions have significant decrease in water body's area of 77.43% and 80.49% respectively compared to central which is almost same for year 1997 and 2017. At all zones the barren land area in 2017 has decreased by half in its occurrence of 1997. Mixed forest has decreased by 16.79% and 51.01% at North and central zone and 15.47% a slight increase in area at south zone region.

The effect of increasing human population on land cover can be clearly noticed in the study. More the populations mean more the changes taking places in order to support the human activities and needs. Hence these activities will lead to land cover changes that was also similar to the result of this study. The population of Mangalore Taluk was 2,73,304 in 1991 and 4,25,725 in 2001 and recent Census of India, (2011) says it was 9,94,602 with an average Annual growth rate of ~ 4.55% and ~ 8.85% per year during the years 1991-2001 and 2001-2011 respectively. It could be suggested that population has an effect on land cover change to meet their need for pace and land in order to support human life such as development settlements and agricultural lands including rice fields. The figure 8 illustrates the decrease and increase in land use/land cover area with graphical representation for the year 1997 and 2017 respectively.

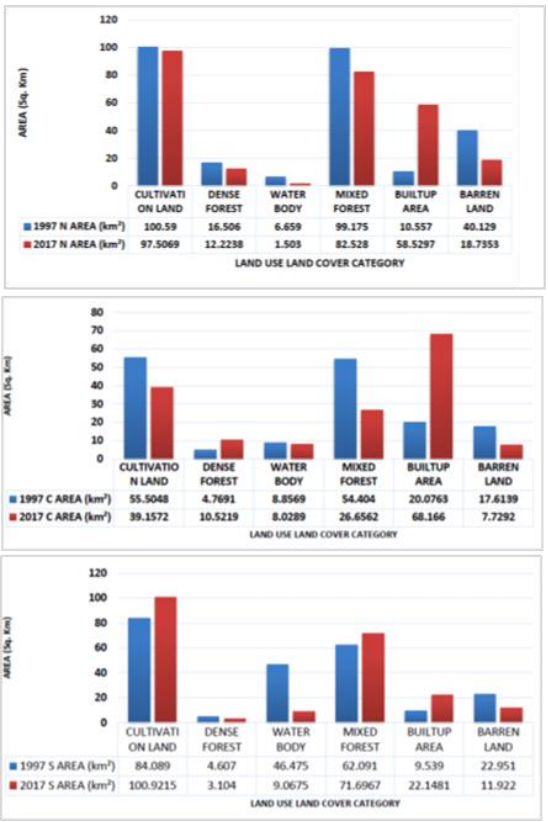

Figure 8: Areal extent (km^2) of land use and land cover in north, central and south zones during 1997 and 2017

The mean changes per year was also analysed to examine how fast the increase or decrease took place each year (Table 6). The mean increase per year of cultivation land, dense forest, water body, built-up area and barren land were analysed for the three respective zones. In north zone mean increase of built-up area was 2.40 km^2/year and mean reduction of land cover class of cultivation land, dense forest, water bodies, mixed forest and barren land were 0.15 km^2/year, 0.21 km^2/year, 0.26 km^2/year, 0.83 km^2/year and 1.07 km^2/year respectively. Similarly, in central zone mean increase of dense forest and built-up area were 0.29 km^2/year and 2.40 km^2/year respectively and mean reduction of land cover class of cultivation land, water bodies, barren land were 0.82 km^2/year, 0.04 km^2/year and 1.39 km^2/year respectively. In South zone the mean increase of land cover of cultivation land, mixed forest and built-up land were 0.84 km^2/year, 0.48 km^2/year and 0.63 km^2/year respectively while the mean reduction of land cover class of dense forest, water bodies and barren land were 0.08 km^2/year, 1.87 km^2/year and 0.55 km^2/year respectively.

The graphical representations of the mean changes per year was also examined to understand how fast the increase or decrease took place every year (Figure 9). The representation of mean was obtained by considering all six classifications in the same order as mention in table 6. The six classes represented in x-Axis are 1- CL, 2 - DF, 3 - WB, 4 - MF, 5 - BL, 6-BA. The peak variations in areal extent and the mean changes per year in built up area and barren land could be clearly observed through this representation.

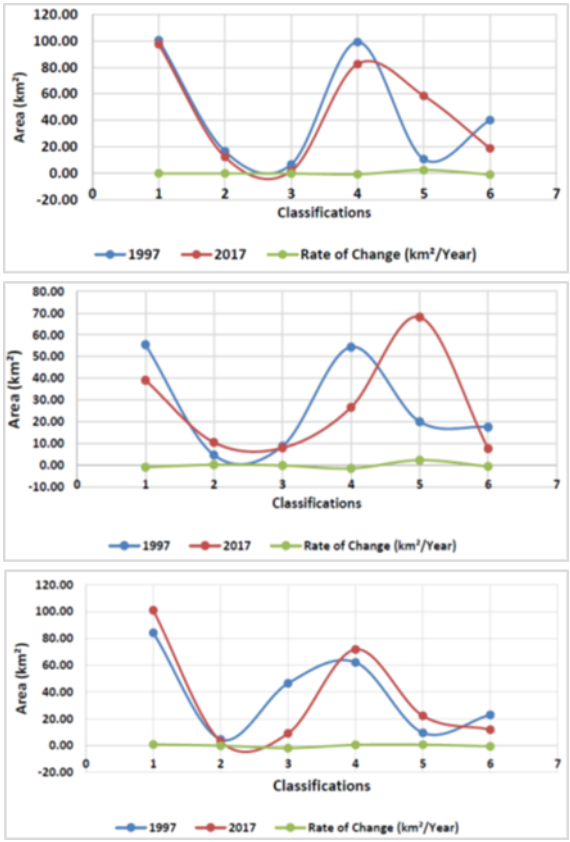

Figure 9: Mean changes in areal extent (km^2) of land use and land cover per year at north, central and southern zones during 1997 and 2017

Table 5: Increase and decrease in land use and land cover classes in all the three zones (km^2)

	NORTH				CENTRAL				SOUTH			
Class.	1997	2017	I (%)	D (%)	1997	2017	I (%)	D (%)	1997	2017	I (%)	D (%)
CL	100.59	97.51	-	3.07	55.50	39.16	-	29.45	84.09	100.9	20.10	-
DF	16.51	12.22	-	25.94	4.77	10.52	120.63	-	4.61	3.10	-	32.62
WB	6.66	1.50	-	77.43	8.86	8.03	-	9.35	46.48	9.07	-	80.49
MF	99.18	82.53	-	16.79	54.40	26.66	-	51.01	62.09	71.7	15.47	-
BL	40.13	18.74	-	53.31	17.61	7.73	-	56.12	22.95	11.92	-	48.05
BA	10.56	58.53	454.45	-	20.08	68.17	239.53	-	9.54	22.2	132.2	-

CL- Cultivation Land, DF- Dense forest, WB- Water bodies, MF- Mixed forest, BL- Barren Land, BA- Built up area, I – Increase, D – Decrease.

Table 6: Rate of land cover change per year (1997-2017)

	1997	2017		1997	2017		1997	2017		
ZONES	N AREA (km²)	N AREA (km²)	Rate of Change (km²/Year)	C AREA (km²)	C AREA (km²)	Rate of Change (km²/Year)	S AREA (km²)	S AREA (km²)	Rate of Change (km²/Year)	Overall Changes in entire Area
CULTIVATION LAND	100.59	97.51	-0.15	55.50	39.16	-0.82	84.09	100.92	0.84	-1.0783
DENSE FOREST	16.51	12.22	-0.21	4.77	10.52	0.29	4.61	3.10	-0.08	-0.1236
WATER BODY	6.66	1.50	-0.26	8.86	8.03	-0.04	46.48	9.07	-1.87	-70.0117
MIXED FOREST	99.18	82.53	-0.83	54.40	26.66	-1.39	62.09	71.70	0.48	-16.1311
BUILTUP AREA	10.56	58.53	2.40	20.08	68.17	2.40	9.54	22.15	0.63	270.5068
BARREN LAND	40.13	18.74	-1.07	17.61	7.73	-0.49	22.95	11.92	-0.55	-52.4289

6. Conclusion

The study has revealed that remotely sensed data (imageries) are important and extremely useful in mapping and monitoring the dynamics of land use / land cover changes. GIS analysis has shown the capabilities to analyse spatial data and to provide information that aid in the decision making. Northern and central zone of the study area has experienced drastic increase in built up area thereby decreasing the mixed and dense forest. Southern zone has very slow rate of change in land use / land cover. Necessary action has to be taken in order to restrict the rapid growth of built up area leading to the distraction of fertile Agriculture / Forest land.

7. Recommendation

Settlement expansion, subsistence farming and illegal logging are the major factors behind the land use/land cover changes observed in the area. These findings highlight the need for comprehensive assessment of human activities and adaptation of sustainable forest management practices such as close supervision of forest reserves and making more arable lands available through restoration of already degraded and impoverished lands.

References

Aspinal, R.J. and M.J. Hill (2008). Land use change: science, policy and management. Boca Raton: CRC Press.

Census of India, (2011). Primary Census Abstract Data Source.

Chen, X.L., H.M. Zhao, P.X. Li and Z.Y. Yin (2006). Remote sensing image-based analysis of the relationship between urban heat island and land use/cover changes. Remote Sensing of Environment 104 (2), 133–146.

Crainic, T. G., N. Ricciardi and G. Storchi (2009). Models for evaluating and planning city logistics systems. Transportation Science 43 (4), 432–454.

Feranec, J., G. Hazeu, S. Christensen et al. (2007). Corine land cover change detection in Europe (case studies of the Netherlands and Slovakia). Land Use Policy 2007, 24(1), pp. 234-247.

Flotterod, G., M. Bierlaire and K. Nagel (2011). Bayesian demand calibration for dynamic traffic simulations. Transportation Science 45 (4), pp. 541–561.

Foody, G. M. (2002). Status of land cover classification accuracy assessment. Remote Sensing of Environment 80 (1), pp. 185–201.

Kachhwaha, T.S. (1985). Temporal monitoring of forest land for change detection and forest cover mapping through satellite remote sensing. In: Proceedings of the 6th Asian Conf. on Remote Sensing. Hyderabad, pp. 77–83.

Kale. M.P., M. Chavan, S. Pardeshi C. Joshi, P.A. Verma, P.S. Roy, S.K. Srivastav, et al. (2016). Land-use and land-cover change in Western Ghats of India. Environmental monitoring and assessment 188 (7), pp. 387.

Lu, D., P. Mausel, E. Brondı´zio and E. Moran. (2004). Change detection techniques. Int. J. Remote Sens. 25, pp. 2365–2407.

Loveland, T.R., B.C. Reed, J.F. Brown, D.O. Ohlen, Z. Zhu, L. Yang and J.W. Merchant. (2000). Development of a global land cover characteristics database and IGBP Discover from 1 Km AVHRR Data. International Journal of Remote Sensing 21 (6–7), pp. 1303–1330.

Riebsame, W.E., W.B. Meyer and B.L. Turner. (1994). Modeling land-use and cover as part of global environmental change. Clim. Change 28, pp. 45–64.

Selcuk, R., R. Nisanci, B. Uzun, A. Yalcin, H. Inan and T. Yomralioglu (2003). Monitoring land-use changes by GIS and remote sensing techniques: case study of Trabzon. 2nd FIG Regional Conference Marrakech, Morocco, December 2-5.

Seif and Mokarram (2012). Change detection of Gil Playa in the Northeast of Fars Province, Iran Am. J. Sci. Res., 86(1), pp. 122-130.

Silambarasan, K., M.S. Vinaya and S. Suresh Babu (2014). Urban sprawl mapping and landuse change detection in and around Udupi Town: A remote sensing based approach. International Journal of Scientific Research Engineering & Technology 2 (12), 815-820.

Usha, M. Thukaram, M. Chadaga and B. Naveenchandra (2014). An integrated approach of Satellite Remote Sensing technology and Geographical Information system for the land use land cover change detection studies for urban planning of Mangalore taluk of Karnataka - published at: International Journal of Scientific and Research Publications 4 (5), 1-7.

Usha, B. Naveenchandra, M. Thukaram and M. Chadaga (2015). The study of impact of urbanization on urban heat island with temperature variation analysis of MODIS data using remote sensing and GIS technology. International Journal of Advanced Remote Sensing and GIS 4(1), 944-952.

Journal of Geomatics Vol 12 No. 2 October 2018

Comparison of Global Geoid Models Against the GPS/Levelling-Derived Geoid Heights in Tanzania

Method J. Gwaleba
Department of Geospatial Sciences and Technology, Ardhi University, Dar es Salaam, Tanzania
Email: gwalebamj@gmail.com

(Received: Aug 03, 2018; in final form: Oct 22, 2018)

Abstract: This paper compares the geoid heights from the Global Models – EGM2008, and EGM1996 against the GPS/Levelling-derived geoid heights in Tanzania. For the sake of comparison, the existing Preliminary African Geoid Model (AGP03) and the Tanzania Geoid Model (TZG13) are also tested against the GPS/levelling derived geoid heights at 13 benchmarks selected within the Tanzania Primary Levelling Network (TPLN). The comparisons of geoid heights obtained from these geoid models against the GPS/levelling geoid heights have been performed in absolute sense. Due to the fact that the ellipsoidal heights (h) obtained from the GPS do not provide the actual positions of points on the geoid, the orthometric heights (H) are needed. Broadly speaking, the orthometric heights are obtained through traditional sprit levelling which is a labour intensive work. In order to convert the ellipsoidal height (h) determined from GPS applications to orthometric height, the Geoid heights are needed. The spatial positions of these benchmarks have been recently determined at cm-level accuracy (with respect to ITRF2005) through a GPS campaign. The statistics of the differences between GPS/levelling-derived geoid heights (N_{GPS}) and the corresponding geoid heights obtained from the available three geoid models (N_{model}) suggests that, AGP03 model is the most suitable at this moment. The Root Mean Square (RMS) fit of the AGP03 geoid model against the GPS/levelling data is 53.8 cm, which is a 2 times better fit compared to the Global Geopotential Models (EGM08 and EGM96) in the area of interest. On the other hand, the RMS of the height differences between the TZG13 and the GPS/leveling derived heights was 74.7cm. The study suggests that AGP03 geoid model is closer to the GPS/levelling geoid observations in comparison to EGM08 model in Tanzania.

Key words: Geoid Models, GPS/Levelling, Geoid, TPLN, Tanzania

1. Introduction

The demand for height information from the satellite users based positioning techniques, mostly Global Positioning System (GPS), has increased interest on determination and use of precise geoid models. The knowledge of the local geoid surface allows the transformation of ellipsoidal heights to physically meaningful orthometric heights which are essential in most of the geodetic applications. Thus, GPS measurements in combination with a precise geoid model are preferred in obtaining orthometric heights instead of spirit levelling measurements, which is labour-intensive and costly (Sideris et al., 1992). Normally, for the purpose of GPS/levelling, in the absence of a publicly available geoid model, it is beneficial to select a Global Geopotential Model (GGM) which is a best fit to the local gravity field as the basis for local or regional geoid model (Kiamehr and Sjöberg, 2005). The Global models have a long and important history in the geodetic community, specifically as a tool for computing geoid heights.

On the other hand, many applications in geodesy, geophysics and engineering require physically defined heights related to the earth's gravity field (orthometric or normal heights), typically produced by spirit leveling. Therefore, for the conversion and combination of these fundamentally different height systems, the geoid must be known with accuracy comparable to the accuracy of GPS and leveling. Because more Global Geoid Models (GGMs) have now been released into the public domain, particularly those including data from the CHAMP and GRACE satellites dedicated gravimetry missions, and new gravity-field-related datasets, it is important to make validations in order to select the most appropriate geoid model. The development of the Earth Gravitational Model 2008 (EGM08) by the US National Geospatial-Intelligence Agency (NGA), (Pavlis et al., 2008) and other recent models revealed a major achievement in global gravity field mapping. The model is complete up to degree and order 2159 and contains additional spherical harmonic coefficients extending up to degree 2190 and order 2159, respectively. The EGM08 can provide long and medium wavelength information of the earth's gravity field to a higher resolution of wavelengths equivalent to 10' of arc. However, there are various recent models developed including EIGEN-6C2, EIGEN6C4, EIGEN6S4, GGM05C, GECO, GOCO05c etc. which have high precision and spatial resolutions of gravity data (Pal et al., 2016). This paper compares EGM2008 and local geoid models with the GPS/levelling observations in Tanzania.

Since the release of the global geoid models including the EGM2018 to the earth science community, there has been a strong interest among the geodesists to quantify its actual accuracy with different validation techniques and external datasets independently of the estimation and error estimation procedures that were used for its development (Yilmaz, and Karaali, 2010). Yilmaz and Karaali attempted over Turkey Landmass/Ocean and observed that the global geoid that best fits the GPS/leveling derived geoid heights was EGM08. As currently in Tanzania there is no comprehensive national geoid model which has been released for the public use, several attempts have been done to develop and validate models that best fit in the Tanzania region. Mayunga

(2016, p. 268, cited in Silyvester, 2013) indicates the developed model which was used to compute point values of a gravimetric geoid using short wavelength which later on were compared with GPS/leveling derived geoid heights. The differences obtained and the biases between the geometric and gravimetric geoid models were recorded. Ulotu (2009) developed the gravity database using sparse gravity data with varying density, distribution and quality. Assessment of this model was done by using KHT method and Least Squares Modification of Stokes to compute geoid of Tanzania, and the accuracy obtained was 29.7 cm.

In selection of suitable geoid model for application purposes, Kiamehr & Sjöberg (2005) cautioned and verified that published error estimates for the geoid models, particularly the global models should not be used directly to judge the most suitable Global Geopotential Model (GGM) for a certain regional/local geoid model representation, but rather as performance indicator. The reason is that such performance evaluations sometimes tend to be too pessimistic and global statistics are not necessarily true representatives in a particular region.

Therefore, the user of a GGM should perform his own accuracy and precision verifications, such as comparing the GGM-derived gravity field quantities with local data (Lambeck & Coleman, 1983). The global geoid model data have never been validated in Tanzania for public purposes. In this context, there is a need of validating the global models so that, it can be used in local areas to serve the communities. The validation process should be done by comparing geoid heights obtained from the global models against the GPS/levelling derived geoid heights. However, it is worth mentioning that though many researchers have reviewed the need of National Geoid Model in Tanzania, such as Ulotu (2009) and Mayunga (2016), the validation context has always remained a research area of interest due to lack unified geodetic network.

This paper checks the compatibility of the EGM08, EGM96, AGP03 and the TZG13 geoid models against the existing GPS/levelling - derived geoid in Tanzania by using the weighted mean approach. The purpose of this paper is to present the global geoid (EGM08 and EGM96) and local geoid (AGP03 and TZG13) heights validation on a certain part of the Tanzania Primary levelling Network (TPLN) by GPS/leveling.

2. Geoid, Ellipsoid and Orthometric Heights: A theoretical framework

2.1. Geoidheight

To understand what geoid heights mean, it is imperative to know what does geoid entails. The geoid is an equipotential surface of the earth's gravity field which, a least square sense coincides with mean sea surface in the open ocean. It is a best fit mean sea level surface. The geoid serves as a reference surface for height systems such as orthometric heights. It is a physical surface which represents the size and shape of the earth, by describing origin surfaces for point heights, determining mean earth ellipsoid, determining the horizontal and vertical datum of reference systems, examining changes in the earth and sea surfaces (Yilmaz and Karaali, 2010).

In this context, its physical realization is usually the mean sea surface as determined by ocean tide gauges (Hofmann and Moritz, 2006). In sum, the geoid surface is the closed surface going under the land which coincides with stable sea surface that is free of effects like temperature, pressure, density, salinity differences, currents and tides, and it is defined by its potential value (Yilmaz and Karaali, 2010). The geoids' height, N can therefore be defined as the separation of the ellipsoid surface with the geoid surface measured along the ellipsoidal normal as illustrated in Figure 1.

Geoid heights from the Global Geopotential Models (EGM96 and EGM08) are given as a set of spherical harmonic coefficients (Pavlis et al, 2008). Different datasets are often used to determine these coefficients ranging from satellite observations, which give the so-called satellite-only solutions, to data which incorporate satellite altimetry and surface gravity data (Rapp, 1996). For the African Geoid Project model (AGP03), geoid height is derived from the combination of Stokes's formula and the geopotential coefficients implied by EGM96 model (Merry, 2003).

2.2. Ellipsoid height

The ellipsoid is a geometric surface which approximates the geoid in a least squares sense. For geodetic purposes, the ellipsoid of revolution is produced when an ellipse is rotated about its semi minor axis, provides a well-defined mathematical surface whose shape and size are defined by two parameters viz., Size of a reference ellipsoid can be described by semi-minor axis, **b** or semi-major axis, **a;** Shape of a reference ellipsoid can be described by its flattening, **f** or its eccentricity, **e**.

The ellipsoid surface as a regular surface can be determined mathematically. It is for this reason that, as a reference surface, it is widely used for horizontal co-ordinate computations. Nevertheless, it is traditionally taken to be of limited use in heights as it ignores the flow of liquids (Hofmann & Moritz, 2006). The ellipsoid, h above the surface of ellipsoid is shown in Figure 1.

2.3. Orthometric height

Orthometric heights (H) are more desirable, because they better relate to mean sea level in the geophysical sense. Orthometric height refers to a vertical datum that is usually taken to be a best fit to mean sea level, either in a global sense or simply adopted from a local tide gage. Such a surface of equal potential of gravity (geopotential) best serves for describing height changes, because water will flow and self-level to the lowest geopotential surface (Roman et al., 2010). Theoretically, both ellipsoidal

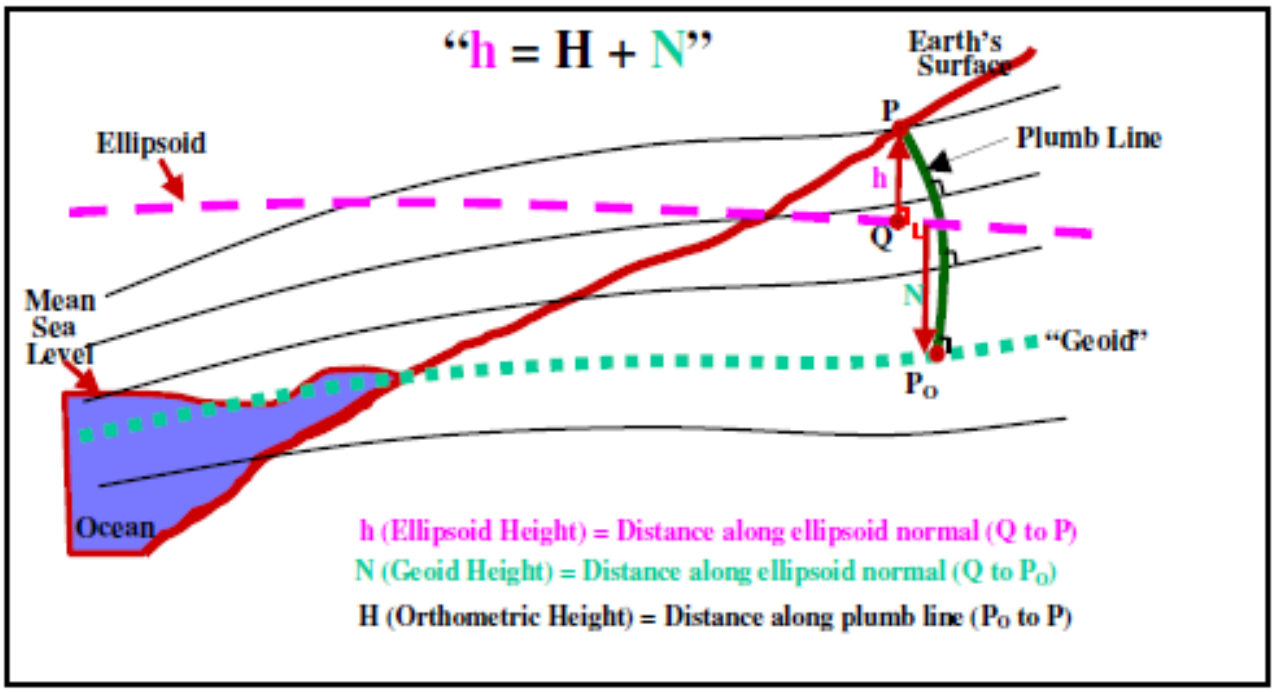

Figure 1: Relationship between geoid, ellipsoid and orthometric heights (Source: Roman et al., 2010)

height and orthometric heights are measured along the normal to the ellipsoid and along the direction of the plumb line (vertical), respectively. The actual gravity plumb line (over exaggerated in drawing) along which H is reckoned is a curved distance due to effects of direction of gravity, known as deflection of the vertical. For engineering purposes, the error produced by this approximation can normally be ignored. Figure 1 provides the relationship between geoid, ellipsoid and orthometric heights.

2.4 TPLN Orthometric heights

The Tanzania Primary Levelling Network (TPLN) was designed in the 1960 and implemented between 1961 and 1964 (Mayunga, 2016). It is comprised of 53 fundamental benchmarks (FBM) made up on loops based on local Mean Sea Level. The measurements were made on land in such a way that the misclosures between forward and back leveling between successive benchmarks is less than ± 3mm$\sqrt{k}$ where 'k' is the leveled distance in kilometers. The distribution of the misclosures of the levelling data in the loops was done loop-wise after the completion of observations on each loop. At present the TPLN consist of eight (8) loops namely, loop A, B, C, D, E, F, G and H. The leveled orthometric heights in the TPLN are corrected for gravity effects on the basis of the normal gravity computed by means of the International Gravity Formula, 1930 (Deus, 2007). The establishment of the TPLN was referred to tide gauge measurements at the Tanga harbour whose mean sea level was used as a reference. The value for the mean sea level (MSL) at Tanga harbour was deduced from tide gauge readings taken during a 28 months' period from August 1962 to November 1964, both months inclusive. The MSL was used to determine the elevation of the Reference Fundamental Benchmark at Maweni. The other in land benchmarks were connected to the Maweni FBM through the observations of loop 'A' and the other loops of TPLN.

3. Materials and methods

The Weighted Mean Method was devoted to validate the positional accuracy of the model, the height accuracy or both positional and height accuracy of the models in absolute sense. In order to determine the Global Geoid Model that best fit with the GPS/Leveling in Tanzania, the geoid heights from EGM08, EGM1996, AGP03 and the TZG13 models were calculated. Generally, the EGM08 model incorporates satellite data (GRACE), terrestrial gravity data and altimetry data (Pavlis et al., 2008). The accuracy of the EGM08 equating to a degree and order 2160 model is claimed to be ± 15 centimeters worldwide. The EGM96 model that incorporates surface gravity data, altimeter-derived free air gravity anomalies from ERS-1 and from the GEOSAT Geodetic Mission Global Positioning System (GPS) data, NASA's Tracking and Data Relay Satellite System (TDRSS), the French DORIS system, and the US Navy TRANET Doppler tracking system as well as direct altimeter ranges from TOPEX/POSEIDON (T/P) and the accuracy for the EGM96 geoid was ± 50cm worldwide (Lemoine et al., 1998; Pavlis et al., 2008). The AGP03model incorporates terrestrial gravity data filled at the 5' grid terrestrial gravity data set using gravity anomalies implied by the EGM96 model, with same accuracy as of EGM96 (Merry, 2003) and the TZG13 that involves the use of spherical harmonic expansion of the Earth's geo-potential derived from the GRACE satellite mission (Ulotu, 2009). The TZG13 model has an accuracy of 29.7cm.

The EGM08 geoid heights used were obtained at 5' x 5' grid values for the area of interest and those computed directly on benchmarks from the geopotential coefficients using software supplied with the model. The EGM96

geoid height at each of the 13 benchmarks was obtained at 5' x 5' grid values by using NIMA EGM96 calculator program for Windows 95/NT downloaded from http://earthnfo.nima.mil/GandG/wgs84/gravitymod/egm96/egm96.html. The EGM96 geopotential coefficients using spherical harmonic representations by the following expansion that is complete to degree 360 was used to compute the geoid heights. The data files for the AGP03 geoid heights were downloaded at 5' x 5' gridded free air gravity anomalies.

3.1. Position of selected benchmarks on part of the TPLN

GPS observation was done at 13 benchmarks. The 13 points of GPS observation were made on TPLN as possible in accordance with latitude, longitude and ellipsoid heights as indicated in Figure 2. The geodetic coordinates (ϕ, λ, h) data in ITRF2005 at the 13 TPLN benchmarks from the processing of GPS data and the correction values (σ) were collected as illustrated in Table 1.

Table 1: ITRF2005 data based on curvilinear coordinates and their accuracies with published orthometric heights on 13 benchmarks from the TPLN

Benchmark Name	Geodetic coordinates	Precision (σ) in meters
FBM Dar-Aux	Latitude: -06 46 42.041181	0.0039
	Longitude: 39 17 07.006124	0.0052
	Ell. Height: -15.510m	0.0091
	TPLN Height: 11.012m	-
FBM Kwala	Latitude: -06 47 54.041181	0.0039
	Longitude: 38 34 42.510094	0.0052
	Ell. Height:54.951m	0.0091
	TPLN Height:79.983m	-
IBM3/54_kilosa-Aux	Latitude: -06 49 53.346951	0.0080
	Longitude: 36 59 09.370195	0.0055
	Ell. Height:469.00m	0.0102
	TPLN Height:489.145m	-
IBM5/47_Dodoma-Aux	Latitude: -06 11 00.250444	0.0034
	Longitude: 35 44 50.885173	0.0023
	Ell. Height:1112.557m	0.0047
	TPLN Height:1131.415m	-
FBM Kondoa	Latitude: -04 54 06.245608	0.0020
	Longitude: 35 48 31.521179	0.0035
	Ell. Height:1373.695m	0.0060
	TPLN Height:1391.300m	-
FBM Tabora	Latitude: -05 01 55.066958	0.0067
	Longitude: 32 49 12.393679	0.0043
	Ell. Height:1218.728m	0.0079
	TPLN Height:1235.726m	-
FBM Shinyanga	Latitude: -03 40 13.552474	0.0019
	Longitude: 33 26 02.314643	0.0042
	Ell. Height:1103.618m	0.0064
	TPLN Height:1122.014	-
FBM Mwanza-Aux	Latitude: -02 31 22.411311	0.0051
	Longitude: 32 53 51.559420	0.0033
	Ell. Height:1122.052m	0.0092
	TPLN Height:1138.444m	-
FBM Makuyuni	Latitude: -03 33 12.367130	0.0042
	Longitude: 36 05 49.065398	0.0061
	Ell. Height:1051.145m	0.0095
	TPLN Height:1069.00	-
IBM A 24/5_Moshi-Aux	Latitude: -03 22 45.000000	0.0033
	Longitude: 37 19 22.800000	0.0028
	Ell. Height:787.442m	0.0008
	TPLN Height:805.051m	-
IBM Korogwe-Aux	Latitude: -05 09 58.796850	0.0018
	Longitude: 38 27 38.421593	0.0030
	Ell. Height: 276.375m	0.0048
	TPLN Height: 298.854m	-
FBM Maweni	Latitude: -05 07 12.424007	0.0046
	Longitude: 39 00 49.658730	0.0058
	Ell. Height: 37.447m	0.0079
	TPLN Height:63.237m	-
IBM 15/31_ Wami-Aux	Latitude: -06 12 43.842551	0.0012
	Longitude: 38 42 44.531514	0.0015
	Ell. Height: -12.316m	0.0028
	TPLN Height: 13.020m	-

Table 2: GPS/levelling derived geoid heights (m) at the selected 13 TPLN benchmarks from the GPS measurements.

Benchmark Name	Ell. Height, h (m)	Levelled Height, H_{SMD} (m)	$N_{GPS} = h - H_{SMD}$ (m)
FBM Dar-Aux	-15.510	11.012	-26.522
FBM Kwala	54.951	79.983	-25.032
IBM3/54_kilosa-Aux	469.00	489.145	-20.145
IBM5/47_Dodoma-Aux	1112.557	1131.415	-18.858
FBM Kondoa	1373.695	1391.300	-17.605
FBM Tabora	1218.728	1235.726	-16.998
FBM Shinyanga	1103.618	1122.014	-18.396
FBM Mwanza-Aux	1122.052	1138.444	-16.392
FBM Makuyuni	1051.145	1069.00	-17.855
IBM A 24/51_Moshi-Aux	787.442	805.051	-17.609
IBM Korogwe- Aux	276.375	298.854	-22.479
FBM Maweni	37.447	63.237	-25.79
IBM 15/31_ Wami-Aux	-12.316	13.020	-25.336

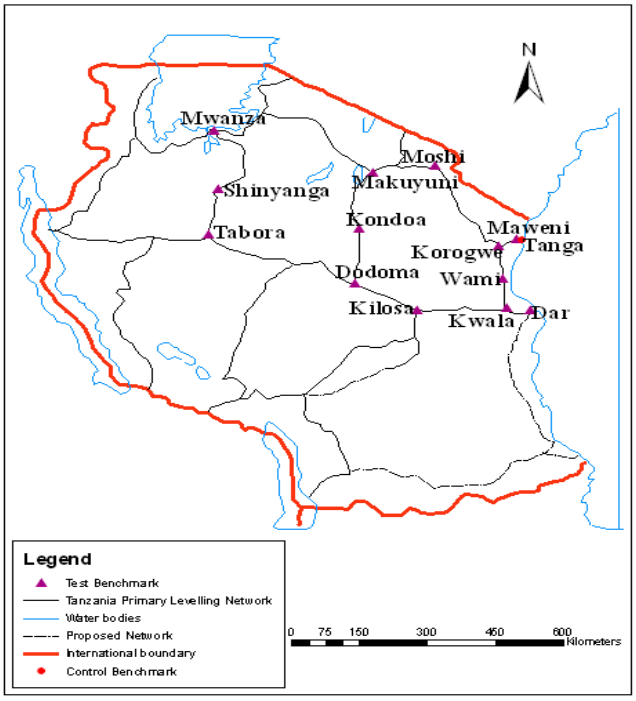

Figure 2: Selected 13 benchmarks for validation of Geoid Models from TPLN

4. Computations and discussion of results

4.1 GPS/Levelling-derived geoid heights (N_{GPS})

The geoid heights from GPS - derived ellipsoidal heights and the TPLN orthometric heights are referred to as GPS/levelling. The GPS/levelling geoid height results are shown in Table 2. The Pro-fix "Aux" after a benchmark name indicates that an auxiliary point had to be established to enable GPS observations.

4.2. Prediction of 5'x 5' geoid heights from geoid models

Predictions of geoid heights on the 13 TPLN benchmarks by using Weighted mean Method was done. The Weighted Mean approach is the method that makes the use of the weighted functions which reflect the fact that data points closer to the prediction points contribute to the accuracy of the value of the predicted geoid heights more than the distant ones. The method has proved to be economical and sufficiently accurate (John and Ulotu 2009, personal communication). The prediction is handled according to point-wise approach using the formula:

$$N_P = \frac{\left[\sum_{i=1}^{n}\left(N_i W_i\right)\right]}{\left[\sum_{i=1}^{n} W_i\right]} \quad \ldots\ldots\ldots\ldots\ldots\ldots\ldots\ldots (1)$$

The weight W_i is the reciprocal of the distance between point P and the corner points, N_i (i = 1, 2, 3, 4) such that:

$$\left.\begin{aligned} W_i &= L_i^{-1} \\ L_i &= \left(x_i^2 + y_i^2\right)^{1/2} \end{aligned}\right\} \quad \ldots\ldots\ldots\ldots\ldots\ldots (2)$$

Where, x_i and y_i are the rectangular Cartesian coordinates of point i with P as the origin.

The predicted geoid heights (N_P) from the three geoid models denoted as $N_{EGM\ 08-P}$, $N_{EGM\ 96-P}$ and $N_{AGP\ 03-P}$ were determined respectively. The given points were geoid heights at 5' x 5' grid coordinates around each benchmark.

The scheme for obtaining the geoid height of a benchmark P which lies within a 5' x 5' grid cell is depicted in Figure 3. The symbols N_1, N_2, N_3 and N_4 in Figure 3 denote geoid heights at the grid intersections (ϕ_i, λ_i) where $i = (1,2,3,4)$.

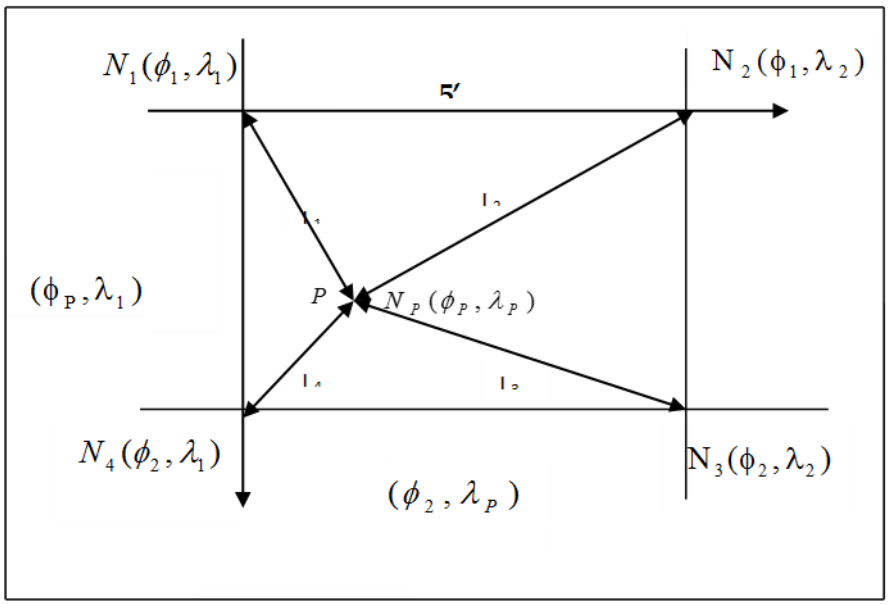

Figure 3: Prediction boundaries of 5' x 5' geoid height grids at all selected benchmarks using Weighted Mean Approach.

These predicted geoid heights were later denoted as N_{EGM08}, N_{EGM96}, N_{AGP03} and N_{TZG13}. For the purpose of geoid heights validation results, the predicted geoid heights from the EGM08, EGM96, AGP03 and the TZG13 geoid models respectively were computed and the results are shown in Table 3.

4.3. Computations and comparison of predicted geoid models against GPS/levelling geoid heights

Computations of geoid heights from Geoid Models were done. The differences of geoid heights from the GPS/levelling derived geoid heights and those predicted from the geoid models at co-located benchmarks provided discrete geometric control validation as illustrated in Table 4.

4.4. Summary of geoid heights differences

Table 5 shows the summary of the predicted geoid height differences results from the four geoid models (two being the global and others being local) at maximum, minimum, mean, root mean square as well as standard deviation respectively.

.

Table 3: Predicted geoid heights results from EGM08, EGM96, AGP03 and the NTZG13 Geoid Models

Benchmark Name	**Predicted Geoid heights (Units in meters)**			
	$N_{EGM08-P}$	$N_{EGM96-P}$	$N_{AGP03-P}$	$N_{TZG13-P}$
FBM Dar-Aux	-27.755	-28.136	-27.364	-27.306
FBM Kwala	-26.163	-26.649	-25.272	-25.708
IBM 3/54_Kilosa – Aux	-21.255	-21.486	-19.924	-19.091
IBM 5/47_Dodoma-Aux	-20.182	-20.293	-19.126	-19.517
FBM Kondoa	-18.968	-19.157	-18.082	-18.192
FBM Tabora	-17.997	-19.035	-17.948	-18.078
FBM Shinyanga	-19.575	-20.095	-19.1998	-19.113
FBM Mwanza-Aux	-17.610	-17.792	-16.874	-16.914
FBM Makuyuni	-19.018	-19.218	-18.352	-18.549
IBM A 24/51_Moshi-Aux	-18.641	-17.098	-18.165	-18.136
IBM 27/55 Korogwe-Aux	-23.518	-23.921	-22.622	-23.031
FBM Maweni	-26.944	-27.589	-26.296	-26.305
IBM Wami	-26.728	-26.918	-25.506	-26.337

Table 4: GPS/levelling-derived geoid heights against the predicted geoid heights from the four Geoid Models

Benchmark Name	Geoid Heights from GPS/Leveling	Geoid Heights from Models				Differences in Geoid Heights			
	N_{GPS}	N_{EGM08}	N_{EGM96}	N_{AGP03}	N_{TZG13}	N_{GPS}-N_{EGM08}	N_{GPS}-N_{EGM96}	N_{GPS}-N_{AGP03}	N_{GPS}-N_{TZG13}
FBM Dar	-26.522	-27.755	-28.136	-27.364	-27.306	1.233	1.614	0.842	0.784
FBM Kwala	-25.032	-26.163	-26.649	-25.272	-25.708	1.131	1.617	0.240	0.676
IBM 3/54_Kilosa –Aux	-20.145	-21.255	-21.486	-19.924	-19.091	1.110	1.341	-0.221	-1.054
IBM 5/47_Dodoma-Aux	-18.858	-20.182	-20.293	-19.126	-19.517	1.324	1.435	0.268	0.659
FBM Kondoa	-17.605	-18.968	-19.157	-18.082	-18.192	1.363	1.552	0.477	0.587
FBM Tabora	-16.998	-17.997	-19.035	-17.948	-18.078	0.999	2.037	0.950	1.080
FBM Shinyanga	-18.396	-19.575	-20.095	-19.1998	-19.113	1.179	1.699	0.804	0.717
FBM Mwanza-Aux	-16.392	-17.610	-17.792	-16.874	-16.914	1.218	1.400	0.482	0.522
FBM Makuyuni	-17.855	-19.018	-19.218	-18.352	-18.549	1.163	1.363	0.497	0.694
IBM A 24/51_Moshi-Aux	-17.609	-18.641	-17.098	-18.165	-18.136	1.032	-0.511	0.556	0.527
IBM Korogwe-Aux	-22.479	-23.518	-23.921	-22.622	-23.031	1.039	1.442	0.143	0.552
FBM Maweni	-25.790	-26.944	-27.589	-26.296	-26.305	1.154	1.799	0.506	0.515
IBM Wami	-25.336	-26.728	-26.918	-25.506	-26.337	1.392	1.582	0.170	1.001

5. Discussion

The results obtained in this research shows that there are differences between GPS/levelling derived geoid heights and those obtained from the four geoid models. The geoid height differences from the GPS/levelling geoid heights and those from EGM08 model range from 0.999 m to 1.392 m. The geoid height differences from EGM96 model and GPS/levelling geoid heights ranges from -0.511 m to 2.037 m while the geoid height differences from AGP03 model against GPS/levelling geoid heights range from -0.221 m to 0.950 m. The differences from TZG13 model versus GPS/levelling geoid heights range from -1.054 to 1.080 m. Figure 4 depicts graphically the geoid height differences from the geoid models based on the standard GPS/levelling derived geoid heights in Tanzania. Table 5 provides summary of predicted geoid height differences.

Table 5: Summary of the predicted geoid height differences results

Geoid Models	Min	Max	Mean	RMS	SD= s
EGM08(Nmax = 2190)	0.999	1.392	1.192	± 1.186	± 0.120
EGM96(Nmax = 360)	-0.511	2.037	1.402	± 1.530	± 0.586
AGP03	-0.221	0.950	0.440	± 0.538	± 0.310
TZG13	-1.054	1.080	0.558	± 0.747	± 0.717

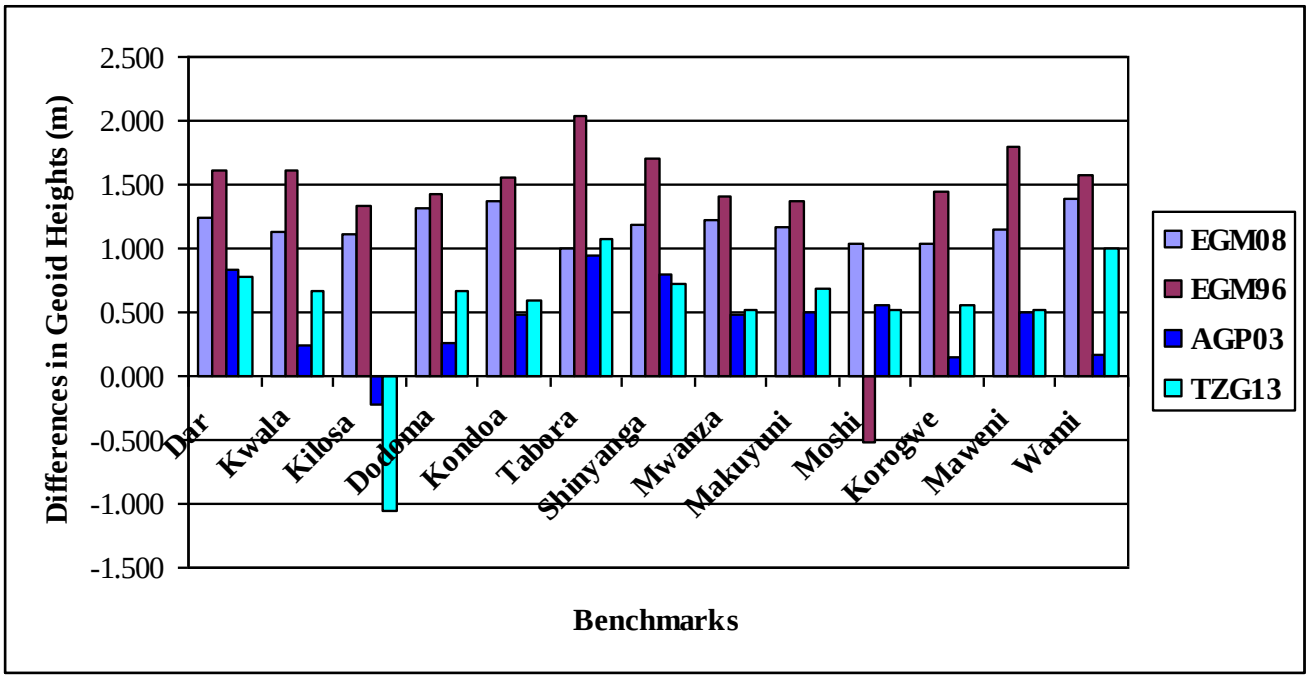

Figure 4: Comparisons of absolute differences of the predicted geoid heights from each model based on GPS/levelling derived geoid heights

The mean differences are 1.180 m, 1.413 m, 0.440 m and 0.558 m; the RMS differences are ±1.186 m, ±1.530 m, ± 0.540 m and 0.747 m; the sample standard deviations are ± 0.120 m, ± 0.586 m, ±0.310 m and 0.717 from EGM08, EGM96, AGP03 and TZG13 respectively as represented graphically in Figure 5.

6. Conclusions

The results of these comparisons of the Geoid models against the GPS-Levelling derived geoid heights over 13 TPLN benchmark shows that among the developed geoid models EGM08, EGM96, AGP03 and the TZG13, the AGP03 model is the best geoid model that fits the GPS and levelling data in Tanzania at present.

The mean differences of 0.440 m and the RMS of ± 0.538 m lead to the conclusion that the AGP03 geoid model is a better model for GPS/Levelling in Tanzania than other three geoid models.

Thus the EGM08 geoid model does not produce geoid heights that are closer to GPS/levelling geoid heights; rather the AGP03 geoid model does so. The major contribution may however come from the higher wavelength of 5' which improves the consistence

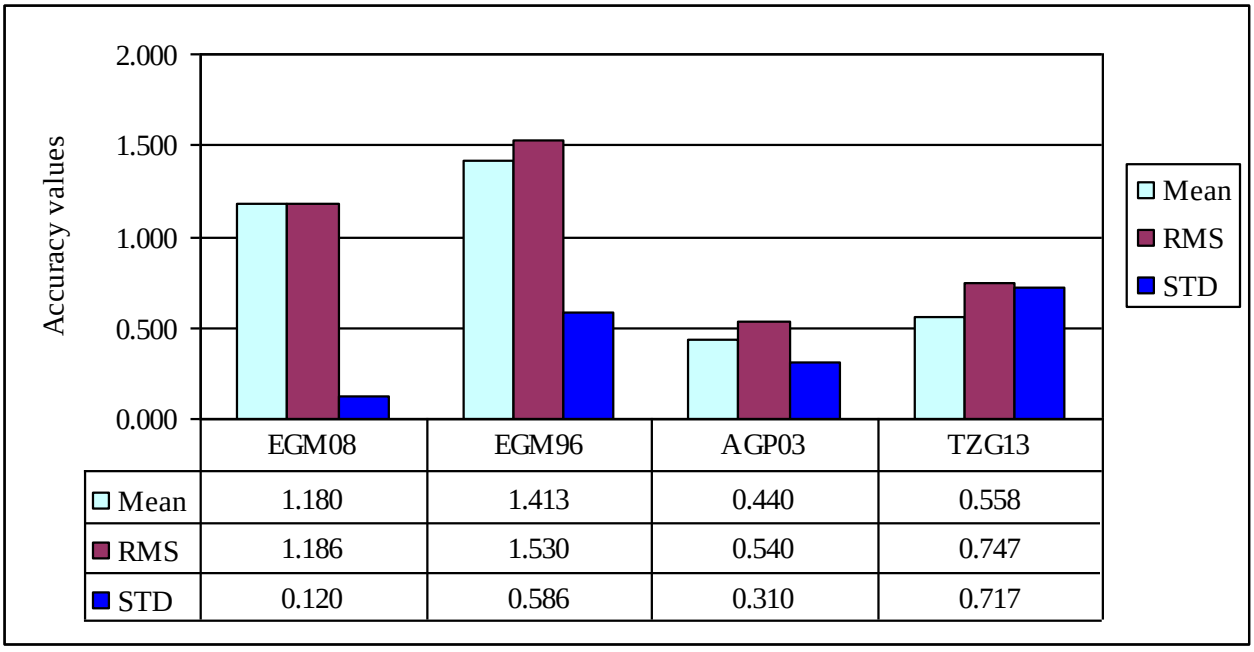

	EGM08	EGM96	AGP03	TZG13
Mean	1.180	1.413	0.440	0.558
RMS	1.186	1.530	0.540	0.747
STD	0.120	0.586	0.310	0.717

Figure 5: Accuracy evaluation of geoid models due to comparisons at independent test benchmarks in the area of interest

between the AGP03 and the GPS/levelling geoid heights such that its shorter wavelength of 5' during its computations and the fact that Stoke's formula is more sensitive to short wavelength components of geoid heights than the higher degree (> 360) spherical harmonics in the EGM08. Thus, the results obtained from point-wise validation have revealed that the AGP03 geoid model performs exceedingly better than other models over the area of interest. The TZG13 which was expected to be the best model as tested in the 13 TPLN benchmarks, does not provide the best accuracy as compared to AGP03.

Acknowledgement

I would like to express my gratitude to the Survey and Mapping Division of the Ministry of Lands, Housing and Human Settlements Development, especially Mr. Shija Wachawandeka for providing me the TPLN orthometric heights as well as the GPS observation data of the benchmarks covering the study area. I am also grateful for the unlimited support from Prof. Peter Morgan (the time when he was working for establishing the Tanzania Geodetic Network) for a free computation of the geoid heights from EGM08 model without which access to the EGM08 datasets would be very difficult during the study. Also, I thank Dr. Ulotu Prosper for providing me geoid heights from the TZG13 model for the 13 TPLN benchmarks. Eventually, many thanks are extended to the reviewers of this study.

References

Deus, D. (2007). Determination of transformation parameters between the Tanzania national levelling datum and the geoid. Master's Thesis, Ardhi University. Dar es salaam, Tanzania.

Hofmann, B and H. Moritz (2006). Physical Geodesy, Second corrected edition, Springer Wien New York.

John, S and P.E. Ulotu (2000). Earth's gravity field and its application in Geodesy, Lecture Notes, Ardhi University, Tanzania.

Kiamehr, R and L.E. Sjöberg (2005). Comparison of the qualities of recent global and local gravimetric geoid models in Iran, Royal Institute of Technology, Geodesy Group, SE-100 44 Stockholm, Sweden.

Lambeck, K and R. Coleman. (1983). The Earth's shape and gravity field: A report of progress from 1958 to 1982. Geophysical Journal of the Royal Astronomical society, 74, 25-54.

Lemoine, F.G., S.C. Kenyon, J.K. Factor, R.G. Trimmer, N.K. Pavlis, D.S. Chinn, C.M. Cox, S.M. Klosko, S.B. Luthcke, M.H. Torrence, Y.M. Wang, R.G. Williamson, E.C. Pavlis, R.H. Rapp and T.R Olson (1998). The development of the joint NASA GSFC and the National Imagery and Mapping Agency (NIMA) geopotential model EGM96, NASA/TP-1998-206861.

Mayunga, S. (2016). Towards a New Geoid Model of Tanzania Using Precise Gravity Data, Journal of Environmental Science and Engineering, A (5), 267-276.

Merry, C.L. (2003). The African Geoid model Project and its relevance to the unification of African vertical reference frames (AFREF). 2nd FIG Regional conference, Marrakech, Morocco, December 2-5, 2003.

Roman, D., Y.M. Wang, J. Saleh and X. Li (2010). Geodesy, Geoids and Vertical Datums: A Perspective from the U. S National Geodetic Survey. FIG Congress 2010. Sidney, Australia.

Pal, S., S. Narayan, T.J. Majumdar and U. Kumar. (2016). Structural mapping over the 85 E Ridge and surroundings using EIGEN6C4 high-resolution global combined gravity field model:an integrated approach. Mar Geophys Res. DOI 10.1007/s11001-016-9274-3.

Pavlis, N.K., S.A. Holmes, S.C Kenyon and J.K. Factor (2008). An Earth Gravitational Model to degree 2160: EGM2008, presented at the 2008 general assembly of the European Geosciences Union, Vienna, Austria, April 13-18, 2008.

Rapp, R.H. (1996). Use of potential coefficient models for geoid undulation determinations using a spherical harmonic representation of the height anomaly/geoid undulation difference, Journal of Geodesy, 71, 282-289.

Ulotu, P.E. (2009). Geoid Model of Tanzania from sparse and varying gravity data density by the KTH method, Doctoral Dissertation in Geodesy PhD Thesis, Division of Geodesy, KTH - Stockholm Sweden.

Yilmaz, N and C. Karaali (2010). Comparison of global and local gravimetric geoid models in Turkey, Scientific Research and Essays, 5(14), 1829-1839.

Journal of Geomatics Vol 12 No. 2 October 2018

enSVM: A classification framework using ensemble of SVMs

Vikas Sharma[1], Dibyajyoti Chutia[1], Diganta Baruah[2], Jonali Goswami[1], Udayan Baruah[2] and P.L.N. Raju[1]
[1]North Eastern Space Applications Centre, Department of Space, Government of India, Umiam, Shillong, Meghalaya - 793103, India
[2]Information Technology Department, Sikkim Manipal Institute of Technology, Majhitar, East Sikkim -737136, India
Email: d.chutia@nesac.gov.in

(Received: Oct 15 2018; in final form: Oct 25, 2018)

Abstract: Empirically, Support Vector Machines (SVMs) have been reported with higher performance on many benchmark datasets including remotely sensed (RS) data. In SVMs, it is prerequisite to obtain a large decision boundary by representing the data points in a n-dimensional feature space using kernel methods. SVMs work well with a minimal number of training samples when appropriate kernels are used to optimize the hyperplane. In addition, SVMs are being used to build ensemble classification methods. The capability of SVM for constructing a set of the diverse base classifier is not yet fully exploited for classification of RS data. The main objective of this work is to develop an ensemble of SVMs (enSVM) with enhanced predictive ability with minimal number of base classifiers. The proposed enSVM is a collection of SVMs as base classifier where each of the base classifiers is assigned independently a random subspace of features to build the predictive model. Each individual classifier cast a unique vote and the final classification is based on the majority of votes of all the base classifiers. An investigation was carried out on the two sets of satellite data of QuickBird and Landsat Enhanced Thematic Mapper Plus (Landsat ETM+) sensors pertaining to different landscape with different land cover classes. It was observed that the enSVM outperformed the SVM, Maximum Likelihood Classifier (MLC), Multi Layer Perceptron (MLP) and achieved comparable results with the most powerful random forest (RF) classifier.

Keywords: Classification, Support Vector Machines, Ensemble, Random subspace, enSVM

1. Introduction

Remote sensing (RS) community paying confident attention to ensemble methods as they have shown significant potential to classify heterogeneous, high dimensional, noisy, missing, and complex RS datasets (Opitz and Maclin, 1999; Han et al., 2012; Huang et al., 2013; Chutia et al., 2015; Chutia et al., 2017; Rawat et al., 2018). The focal intuition of ensemble principle is to create multiple hypotheses generated by weak learners to achieve higher classification accuracy by combining or aggregating their predictions (Opitz and Maclin, 1999). Diversity in multiple hypotheses is prerequisite for ensemble methods. Empirically, ensemble methods tend to produce better results when there is a significant diversity among the models. Diversity can be achieved through the fusion of different classifiers, randomization of training data, and randomization in feature space etc. (Hansen and Salamon, 1990; Kuncheva and Whitaker, 2003; Brown et al., 2004).

Bagging (Breiman, 1996) and Boosting (Freund and Schapire, 1996) are more commonly used ensembles methods in machine learning applications. Bagging being a variant of meta classifier combines the predictions of base classifiers for improving the unstable estimation and the predictive accuracy of the classifiers. It uses the bootstrap technique for randomization of the training data. Bagging creates the small random bags with the replacement of training dataset from the original datasets in order to create the diversity among the base classifiers. It is very popular and more frequently used in decision tree algorithms (DT, Quinlan, 1986) as it avoids the overfitting and reduces the variance [Chan et al., 2001]. However, the boosting algorithm reduces the bias with the variance to achieve higher classification accuracy. It learns from the errors and assigns the corresponding weights to each weak base classifier in order to get better predictive accuracy. In boosting, AdaBoost (Freund and Schapire, 1996) is the most popular and successful version that follows the weight adjustment procedure to classify a novel instance. In every iteration, Adaboost increase the weights on the misclassified instance and decreases the weights on correctly classified instances in order to give a chance to misclassified or unclassified data (Freund and Schapire, 1996; Chan et al., 2001). The main drawback of bagging model is that they suffer from the overfitting while dealing with the noisy data. On the other hand, the large number of outliers (highest weight instance) can reduce the performance of AdaBoost (Freund and Schapire, 1999). For overcoming overfitting problem Breiman proposed random forest (RF) algorithm in 2001 (Breiman, 2001). Currently, the RF has been successfully implemented in various applications (Casanova et al., 2014; Yang et al., 2008; Goldstein et al., 2010; Sylvester et al., 2017). The RF is based on the principal of bagging, where a number of DT are independently constructed as a base classifier through random sampling of the training dataset. The major concern in RF is the selection of appropriate size of the base classifiers; number of random subset of trees. In the current scenario, rotation forest (Rodriguez et al., 2006) is getting popular and found comparable with RF in many instances (Peijun et al., 2015; Xia et al., 2014; Rawat et al., 2018). Unlike RF, rotation forest splits the features into several disjoint subsets and apply the data transformation on each subset using principal component analysis (PCA, Jolliffe, 1986). In the second stage, new training dataset for the DT is formed by concatenating the linear extracted features contained in each subset. Thus, rotation forest enhances the classification accuracy with diversity within the ensemble (Rodriguez et al., 2006; Du et al., 2015; Kuncheva and Rodriguez, 2007; Liu and Huang, 2008). Comparatively, rotation forest is a

complex model but it can provide excellent performance. However, RF is most stable and can provide consistently higher predictive accuracy with the noisy data and low computation cost.

Recently, the Random committee is found as an important platform for combining the base classifiers. Random committee constructs an ensemble of base classifiers and averages their results (Witten and Frank, 2005). The results of all base classifiers are based on the same data, but they are initialized by the different random number seed (Lira et al., 2007; Tatsis et al., 2013). On the other hand, random subspace creates diversity in the training data through feature space. The final prediction is the majority of votes of individual predictor. In recent times, an ensemble of traditional classifiers is in trend in various fields (Rahman et al. 2016; Kenduiywo et al., 2017; Liu et al., 2016; Yu et al., 2015; Sharma et al., 2018; Chutia et al., 2014; Vyškovský et al., 2016; Han et al, 2012; Lv et al., 2017). SVMs now effectively used as a base classifier in ensemble methods (Claesen et al., 2014; Sørensen and Nielsen, 2018; Wandekoken et al., 2011; Lo et al., 2015). Ensemble classifiers with DTs algorithm are mostly preferred as their capability already established on many benchmark data. However, appropriateness of traditional classifier in building ensemble approach needs attention.

1.2 Motivation

Nonparametric classifiers like SVMs are highly productive. But, the performance of SVMs are highly influenced by the selection of kernel parameters. A number of ensemble methods as illustrated in the earlier section have been proposed where DT classifiers have been used as base classifiers in most of the instances. However, the potential of SVMs with suitable kernel parameter and appropriate ensemble methods for erecting a set of the diverse hypothesis is not yet fully explored for RS data classification.

1.3 Objectives

The primary objective of this work is to develop an efficient and effective classification framework using ensemble technique for classification of RS imagery with the following contributions:

1) Selection of appropriate kernel parameters for SVM classifier;
2) To develop an ensemble of SVMs using random subspace method (enSVM);
3) To assess the performance of the enSVM in comparison with the MLP, MLC, RF and SVM.

Rest of the research article summarized as follows: the Section II gives the detailed information about the characteristics of datasets used in the investigation. The framework of the proposed enSVM is illustrated in the Section III. The analysis on the experimental results discussed in the Section IV followed by the concluding remark in the Section V.

2. Dataset used

To assess the predictive ability of the proposed framework, the investigation was carried out on the moderate resolution Landsat ETM+ (Test site-I) and high resolution QuickBird (Test site-II) multispectral sensors datasets. The more details about the respective satellite sensors are given in the Table 1 followed by a description on the test sites.

Table 1: Detailed information of both test sites

Particulars	Landsat ETM+	QuickBird
Satellite Name	Landsat 7	Digital Globe
Spectral Resolution	0.45µm - 0.90µm	0.45µm - 0.90 µm
Number of bands	04	04
Temporal Resolution	16 days	1-3.5 days
Spatial Resolution	30 meter	0.65 meter
Swath	183 km	16.4 Km

2.1 Test site-I

The Test site-I is pertaining to Sontipur area of Assam, India comprised of five major classes including the river Brahmaputra. The site is topographically plain terrain dominated by agricultural crop land followed by forest tree clad area, scrub forest, and sand nearby river Brahmaputra. Details of the classes with respective train and test samples for Test site-I is given in Table 2.

Table 2: Details of classes with train and test samples for test site-I

Class Name	Train sample	Test sample
River/Waterbody-Perennial	3165	1513
Forest tree clad area	259	1119
Agriculture cropland	870	1114
Sand	225	1809
Scrub Forest	118	1502
Total number of samples	4637	7057

2.2 Test site-II

The Test site-II is anurban area of Shillong, capital of Meghalaya state of India representing the five major classes. The site-II is topographically hilly terrain and surrounded by pine trees followed by urban residential areas, open scrub, open surfaces, and shadows. Further information about the classes and their respective train and test samples can be found in the Table 3.

Table 3: Details of classes with train and test samples for test site–II

Class Name	Train sample	Test sample
Urban residential areas	980	1485
Pine trees	845	1103
Shadows	975	958
Open scrub	909	756
Open surfaces	1078	1312
Total number of samples	4787	5614

The satellite image of the Test site-I and Test site-II are shown in a and b respectively of Figure 1.

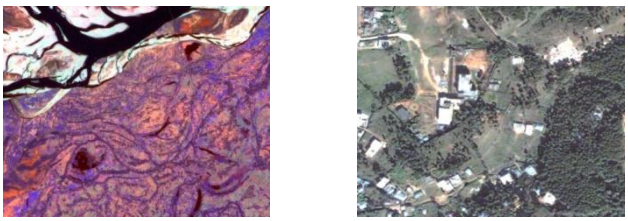

a) Test site-I (Landsat ETM+) **b)** Test site-II (QuickBird)

Figure 1: Satellite images of test sites

3. Methodology

The proposed enSVMis based on the principle of bagging, where each of the base classifier is initialized independently with a randomly selected subset of features. A set of SVMs are used as base classifier and each of the individual SVM casts a vote based on the decision boundary of hyperplane defined by the random subspace of the features. The final classification result is the majority of voting of all the SVM base classifiers.

The entire approach is comprised of the three major components- i) selection of kernel parameter for SVM, ii) building of enSVM framework using random subspace and iii) assessment of enSVM using a set of accuracy assessment parameters.

3.1 Selection of kernel parameters for SVMs

SVM is a nonparametric classifier that uses the hyperplane to separate the data into the predefined classes. It tries to find a hyperplane with the help of support vectors and creates the decision boundary with a maximum distance between two classes.

For an instance, D is the set of all input data, and X_n is the input space with target class $Y_n$then-

$$D(x) = Sign\left(\sum_i^n . \alpha_i y_i (x_i . x) + b\right) (1)$$

SVM uses the kernel function to optimize the hyperplane for classification of multiclass data. Selection of kernel parameters is one of the important aspectsin SVMs. Kernel functions are being used to reduce the time complexity of SVMs by using the inner product of two transformed data vectors in the feature space (Cortes and Vapnik, 1996; Sharma et al., 2016).
Popular kernels those can be used with SVMs are given below.

Linear kernel :$K(x_i, x_j) = x_i^T . x_j$ (2)

Polynomial kernel :$K(x_i, x_j) = (r + \gamma x_i^T . x_j)^d, \gamma > 0$ (3)

RBF kernel :$K(x_i, x_j) = \exp(-\gamma \|x_i - x_j\|^2), \gamma > 0$ (4)

Sigmoid kernel :$K(x_i, x_j) = tan\, h\,(\gamma x_i^T . x_j + r)$(5)

where, x_i = support vector of length m, T = Transformation, γis the gamma function, d = degree of polynomial, and$r$ = bias. The more information about the SVM can be found in Cortes &Vapnik 1996 (Cortes and Vapnik, 1996).

A number of studies suggested that the polynomial kernel can achieve better predictive accuracy than the other kernels for classification of satellite datasets (Sharma et al. 2016; Kumar et al., 2018; Akbari et al., 2012). An investigation was carried out to assess the comparative performance of SVM classifier with all four kernels on both the datasets. It was observed that SVM with the polynomial kernel outperformed the SVM with other kernels with Kappa Index Analysis (KIA) =0.77 and Overall Accuracy (OA) =82.38% for Test site - I dataset and KIA=0.86 and OA=88.64% for Test site - II [Table 4]. Based on the experimental results as specified in Table 4 it is proposed to use SVM with the polynomial kernel as a base classifier for building the enSVM.

Table 4: Comparative assessment of kernels

Kernels	Test site-I			Test site-II		
	OA (%)	KIA	T_r (sec)	OA (%)	KIA	T_r (sec)
Linear	81.46	0.76	0.52	87.27	0.82	7.71
Polynomial	82.38	0.77	0.14	88.64	0.86	1.48
RBF	78.71	0.70	0.50	86.58	0.83	8.46
Sigmoid	76.19	0.67	1.30	85.34	0.82	22.77

3.2 Building enSVM using random subspace

Random subspace creates the diversity in the features space by creating random subspace of features for each base classifier in order to achieve higher predictive accuracy (Ho, 1998). In enSVM model, training dataset has been feed to the random subspace algorithm where a set of training dataset defined by a set of random features was created based on the size of the enSVM. Then each of the randomly generated training datasets is provided to each of the SVM.

Let, p_K is a collection of SVM classifiers, $enSVM \rightarrow \{p(x, s_k^r), k = 1, \ldots, K\}$ of sizeK, where $p(x, s_k^r)$is each individual base classifier trained by a random subspace of feature $s_k^r \in F^R$drawn with replacement.$F^R$is the original set of feature sets of the training datasets T with R number of features and r is the number of features in s_k^r where $r < R$ and $s_{k=i}^r \neq s_{k=j}^r \; \forall\, k$. Each of the SVM base classifiers is represented as $p(x, s_k^r)$ with s_k^rrandomly selected predictors. Each individual $p(x, s_k^r)$ casts a vote for an unknown input x independetly. Let $\hat{C}_{s_k^r}(x)$ is class prediction of each $p(x, s_k^r)$, the final classification of input x is the majority of the voting of all the $p(x, s_k^r)$ classifiers i.e.,$\hat{C}_{s_k^r}(x) = \text{majority vote}\,\{\hat{C}_{s_k^r}(x)\}_1^K$.More detailed information about the random subspace method can be found in (Ho, 1998).

4. Results and Discussions

All experiments were executed in the High Performance Cluster Computing (HPC) environment with 20 core Intel (R) Xeon (R) CPU E5-2680 V2 processor and 48 GB

RAM system configuration. The training samples of Test site - I associated with 80 features whereas 142 features were associated with Test site - II dataset. Random subspace (space=0.50) was used to create diversity among the base classifiers by creating a set of training datasets with a random subspace of optimal features.

A set of parameters such as KIA, Receiver Operating Characteristic (ROC), and Time Complexity (T_r) have been identified for performance analysis. A detailed discussion on the experimental observations are summarized in the context of the following:

1) The optimal size of enSVM;
2) Performance of enSVM against training size;
3) Comparison with other counterparts like MLC, MLP, SVM, and RF.

4.1 Optimal size of enSVM

The size of enSVM (K) or the optimal number of the base classifier is an important parameter of the enSVM. The overall performance of the predictive model is highly affected by the size of the K. The enSVM was executed with K=1 with an increment of 1 till K=30 or it achieved the highest accuracy. Afterwards, the enSVM was executed with K=10 with an increment counter of 10 maximum up to 200 or till it achieved the highest accuracy. It was observed that the enSVM achieved the highest accuracy at K=7 for Test site - I and at K=16 for Test site – II (Figure 2). The red color depicts the experimental observation of the OA on Test site - I against the variable size of K; whereas, the OA of enSVM for the Test site - II is represented by the blue colour. For Test site – I, enSVM was able to give highest accuracy with the 7 base classifier. The performance of enSVM was found higher and consistent on the high spatial resolution satellite dataset (Test site - II) as compared to the moderate spatial resolution dataset (Test site - I). It was also found that the larger size of K cannot ensure the higher performance rather the model can achieve better performance with a minimal size of K. The challenge was to find the optimal value for K. The following two observations are highlighted below:

1) The performance of enSVM is not directly proportional to the higher value of K. However, larger size of K can cause higher computational expenses.
2) During the execution of enSVM, each of the individual SVMs was initialized with a random subspace of feature. The diversity of model is not determined by the size of K rather it depends on the degree of randomization of the feature assign to each SVM.

4.2 Performance of enSVM against training size

SVM has been found effective classification option where the size of the training dataset is limited. It is required to assess the impact of the training data size on the performance of enSVM. The performance of enSVM against different size of the training dataset are given in the Table 5. It was observed that the performance of the enSVM is increased when the training size is large, because the same dataset is splitted into the train and test datasets. For example, enSVM achieved OA=88.58% with KIA=0.85 for Test site - I and OA= 96.22% with KIA=0.94 for Test site - II respectively when the model was trained by 10% of the dataset and tested with the remaining 90%. Similarly, it achieved the highest performance with OA=93.11 for Test site-I and OA=99.19% with KIA=0.98 for Test site-II when the training and test ratio was 90:10. Even though, the performance of enSVM with less training dataset yields slightly lesser accuracy as compared to the larger size of training dataset but this can be accepted when the training dataset is very limited. The remaining part of experiment was carried out with the independently generated train and test datasets as mentioned in the Section - II. There are two major observations can be made here:

1) Like SVM, enSVM can also perform satisfactory when there is a lack of sufficient training dataset.
2) The evaluation of the actual predictive ability the classifier should be trained and tested with the independently generated training and test datasets.

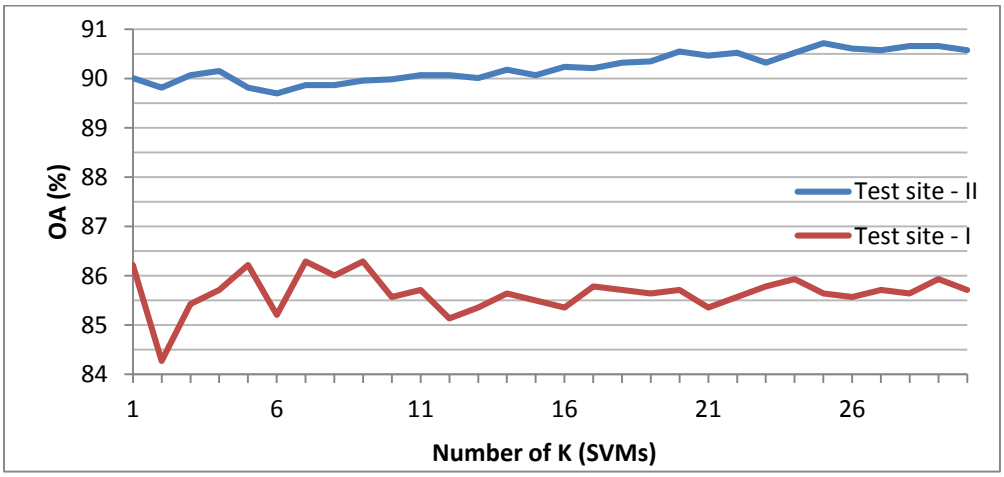

Figure 2: Overall Accuracy (OA) versus number of K (SVMs)

Table 5: Overall Accuracy (OA) versus size of training data

Datasets	Accuracy Parameters	Training data size (%)								
		10	20	30	40	50	60	70	80	90
Test site - I	OA(%)	88.58	90.83	91.79	92.06	92.77	93.16	93.59	93.83	93.11
	KIA	0.85	0.88	0.89	0.90	0.90	0.914	0.91	0.92	0.91
Test site - II	OA(%)	96.22	98.08	98.26	98.52	98.87	98.78	98.92	99.19	99.19
	KIA	0.94	0.97	0.97	0.97	0.98	0.98	0.98	0.98	0.98

Table 6: Comparative assessment of classifier

Classifiers	Test site - I				Test site - II			
	OA	KIA	ROC	t (sec)	OA	KIA	ROC	t (sec)
SVM	82.38	0.77	0.91	0.13	88.64	0.86	0.96	1.39
enSVM	85.50	0.81	0.95	1.26	91.99	0.89	0.98	11.0
MLC	81.70	0.77	0.91	0.02	85.57	0.81	0.97	0.05
MLP	83.30	0.78	0.93	26.5	89.99	0.87	0.98	13.1
RF	84.34	0.79	0.94	0.03	90.24	0.88	0.98	0.10

4.3 Comparison with other counterparts i.e., MLC, MLP, SVM, and RF

The enSVM was executed with the optimal number of K i.e. 7 for Test site-I and 16for Test site - II as illustrated in the earlier section. A set of other counterparts of enSVM such as SVM, MLC, MLP, and RF have been utilized for classification of both the datasets. The comparative performance of all the classifiers are given in the Table6.The final classified outputs of enSVM on both the datasets sites are depicted in Figure 3 and Figure 4. It was found that the enSVM outperformed all the classifiers for both the datasets sites with KIA =0.81 for Test site - I and K=0.89 for Test site - II [Table 6]. The performance of enSVM was significantly enhanced than a single SVM classifier (K =0.77 for Test site - I and K=0.86for Test site - II) (Table 4). In addition, RF was found comparatively effective; it can create more diversity among the base classifiers through bagging and random selection of the best feature at each node. Comparatively enSVM suffers from little computational expenses due to the size of the ensemble (Table 6). The performance of MLP is higher than the MLC; however it causes large computational expenses during the training phase. The ensemble approach can provide higher performance with the traditional powerful classifiers like SVM. However, enSVM can create comparatively less diversity than RF. It will be more sensitive when there is little noise in the data and a random subspace method fails to assign the relevant subspace of features to each individual base classifier. However, if appropriate kernel parameter is selected for SVM, enSVM can performance than other powerful classifier like RF.

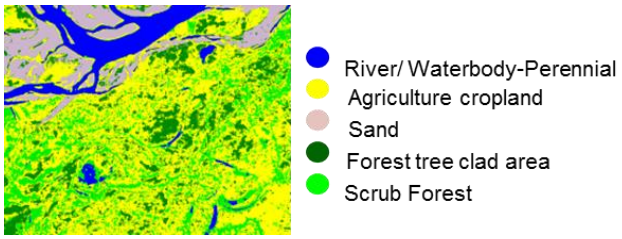

Figure 3:Classified image of test site-I with legends

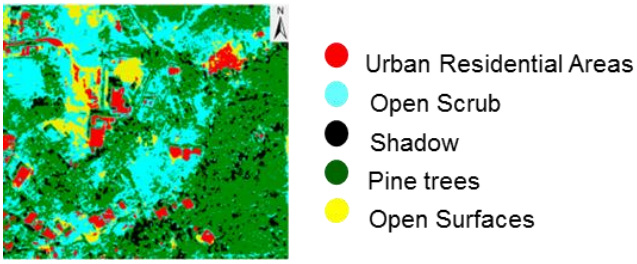

Figure 4: Classified image of test site-II with legends

5. Conclusion

The proposed enSVM is based on the principle of bagging of training dataset in feature dimension where each individual SVM classifier decides the final classification based on the majority of their votes. The performance depends on the random subspace of relevant feature set assigned to each SVM classifier. The observations achieved during the investigation were found quite encouraging. However, random subspace of feature could be defined from the optimal set of relevant features using a feature selection technique in order to enhance the predictive ability as well as the computational complexity.

Acknowledgment

The authors would like to thanks North Eastern Space Applications Centre (NESAC), Department of Space, Government of India, Shillong, Meghalaya for providing the scientific environment, necessary data, High-Performance Cluster Computing (HPC) facility with necessary infrastructure during this research study.

References

Breiman, L. (1996). Bagging Predictors, Machine Learning, 24(2), 123-140 https://doi.org/10.1023/A:1018054314350

Breiman, L. (2001). Machine Learning, 45(1), 5-32 https://doi.org/10.1023/A:1010933404324.

Brown, G., J. Wyatt, R. Harris.andX. Yao. (2004). Diversity creation methods: a survey and categorisation, Information Fusion, 6(1), pp.5-20. https://doi.org/10.1016/j.inffus.2004.04.004.

Casanova, R., S. Saldana, E.Y. Chew, R.P. Danis, C.M. Greven and W.T. Ambrosius. (2014). Application of random forests methods to diabetic retinopathy classification analyses, PLOS ONE, 9(6), pp. 1-8.https://doi.org/10.1371/journal.pone.0098587.

Chan, J., C. Huang and R. Defrie. (2001). Enhanced algorithm performance for land cover classification from remotely sensed data using bagging and boosting,IEEE Transactions on Geoscience and Remote Sensing, 39(3), 663-695.doi: 10.1109/36.91112.

Chutia, D.,D.K. Bhattacharyya, R.Kalita, J. Goswami, S.S. Puyam and S. Sudhakar (2014). A model on achieving higher performance in the classification of hyperspectral satellite data: A case study on Hyperion data, Applied Geomatics, 6. doi:10.1007/s12518-014-0134-z.

Chutia, D., D.K. Bhattacharyya, K.K. Sarma, R. Kalita and S. Sudhakar. (2015). Hyperspectral remote sensing classifications: A perspective survey, Transactions in GIS, 20(4), 463-490. doi:10.1111/tgis.12164.

Chutia, D., D.K. Bhattacharyya, J. Sarma and P.L.N. Raju. (2017). An effective ensemble classification framework using random forests and correlation basedfeature selection technique, Transaction in GIS, 21(6), 1165-1178.https://doi.org/10.1111/tgis.12268.

Claesen, M., F.D. Smet, J.A.K. Suykens and B.D Moor. (2014). EnsembleSVM: A library for ensemble learning using support vector machines, Journal of Machine Learning Research, 14, 141-145.

Cortes, C and V. Vapnik. (1996). Support-Vector Networks, Machine Learning, 20(3),273–297. doi:10.1007.BF00994018.

Du, P., A. Samat, B. Waske, S. Liu and Z. Li. (2015). Random Forest and Rotation Forest for fully polarized SAR image classification using polarimetric and spatial features, ISPRS Journal of Photogrammetry and Remote Sensing, 105, 38-53. doi.10.1016/j.isprsjprs.2015.03.002.

Freund, Y and R.E. Schapire. (1996). Experiments with a new boosting algorithm. Proceedings 13th International Conference on Machine Learning, pp. 148–156.

Freund, Y. and. R.E.Schapire. (1999). A Short introduction to boosting, Journal of Japanese Society for Artificial Intelligence, 14(5), pp.771-780.

Goldstein, BA., A.E. Hubbard, A. Cutle and L.F. Barcellos. (2010). An application of Random Forests to a genome-wide association dataset: Methodological considerations & new findings. 49(11), 1471-2156. https://doi.org/10.1186/1471-2156-11-49.

Han, M., X. Zhu and W. Yao. (2012). Remote sensing image classification based on neural network ensemble algorithm, Neurocomputing,.78, 133-138.

Hansen, L. K and P. Salamon. (1990). Neural network ensembles, IEEE Transactions on Pattern Analysis and Machine Intelligence, 12(10), 993-1001. doi: 10.1109/34.58871.

Ho, T.K. (1998). The random subspace method for constructing decision forests, IEEE Transaction on Pattern Analysis and Machine Intelligence, 20(8), 832–844.

Jolliffe, I.T. (1986). Principal Component Analysis. Ed. Springer-Verlag, New Work

Kenduiywo, BK., D. Bargiel and U. Soergel. (2017). Higher order dynamic conditional random fields Ensemble for crop type classification in radar images, in IEEE Transactions on Geoscience and Remote Sensing, 55(8),4638-4654.

Kumar, R.A., D. Chutia, J. Goswami, V. Sharma and P.L.N. Raju. (2018). Fusion of Hyperion and RapidEye data sets and comparison of classification accuracy over the Dhemaji and Lakhimpur districts of Assam India, Journal of Geomatics (JoG), 12, 35-46.

Kuncheva, L.I and C. Whitaker. (2003). Measures of diversity in classifier ensembles, Machine Learning, 51, 181-207.

Kuncheva, L.I and J.J. Rodriguez. (2007). An experimental study on rotation forest ensembles, Multiple Classifier Systems, 4472,459–468.

Lo, S.L., R. Chiong and D. Cornforth. (2015). Using support vector machine ensembles for target audience classification on Twitter, PLOS ONE, 10(4): e0122855.

Lira, M.M.S., R.R.B. Aquino, A.A. Ferreira, M.A. Carvalho, O.N. Neto and G.S.M. Santos. (2007). Combining multiple artificial neural networks using random committee to decide upon electrical disturbance classification, International Joint Conference on Neural Networks, pp. 2863-2868.

Liu, K.H and D.S. Huang. (2008). Cancer classification using rotation forest, Computers in Biology and Medicine, 38(5), 601–610. doi:10.1016/j.compbiomed.2008.02.007.

Liu, Y., D. Pi and Q. Cheng. (2016). Ensemble kernel method: SVM classification based on game theory, Journal of Systems Engineering and Electronics, 27(1), 251-259.doi: 10.1109/JSEE.2016.00025.

Opitz, D and R. Maclin. (1999). Popular ensemble methods: An empirical study, Journal of Artificial Intelligence Research, 11, 169-198.doi: 10.1613/jair.614.

Quinlan, J.R. (1986). Induction of decision trees, Machine Learning, 1, 81-106.

Rahman, M.M., M.M. Islam, K. Murase and X. Yao. (2016). Layered ensemble architecture for time series forecasting, IEEE Transactions on Cybernetics, 46(1), 270-283.

Rawat, U., V. Sharma, D. Chutia, N. Nishant, U. Baruah, U and P.L.N. Raju. (2018). Random forest versus rotation forest – A comparative assessment towards classification of satellite data, 5th IEEE International Conference on Computing for Sustainable Global Development, 14th - 16th March, Proceedings of the 12th INDIACom; pp. 1732—1736. INDIACom-2018; IEEE Conference ID: 42835.

Rodriguez, J.J., L.I. Kuncheva and C.J. Alonso. (2006). Rotation Forest: A new classifier ensemble method, IEEE Transactions on Pattern Analysis & Machine Intelligence,28, 1619-1630. doi:10.1109/TPAMI.2006.211.

Sharma, V., D. Baruah, D. Chutia, P.L.N. Raju and D.K. Bhattacharya. (2016). An assessment of support vector machine kernel parameters using remotely sensed satellite data, IEEE International Conference on Recent Trends in Electronics, Information & Communication Technology (RTEICT), 1567-1570. doi:10.1109/RTEICT.2016.7808096.

Sharma, V., N. Choudhury, R. Mandal, D. Chutia, U. Baruah and R. Kumar. (2018). An empirical study on traditional classifiers for remotely sensed satellite data classification,5th IEEE International Conference on Computing for Sustainable Global Development, 14th - 16th March, Proceedings of the 12th INDIACom; pp. 2032—2036. INDIACom-2018; IEEE Conference ID: 42835.

Sørensen, L and M. Nielsen. (2018). Ensemble support vector machine classification of dementia using structural MRI and mini-mental state examination, Journal of Neuroscience Methods,302, 66-74. doi: 10.1016/j.jneumeth.2018.01.003.

Sylvester, E.V.A., P. Bentzen, I.R. Bradbury, M. Clément, J. Pearce, J. Horne and R.G. Beiko. (2017). Applications of random forest feature selection for fine- scale genetic population assignment, Evolutionary Applications, 11, 153–165. https://doi.org/10.1111/eva.12524

Tatsis, V.A., C. Tjortjis and P. Tzirakis. (2013). Evaluating data mining algorithms using molecular dynamics trajectories, International Journal of Data Mining and Bioinformatics,8(2), 169–187.doi:10.1504/IJDMB.2013.055499.

Vyškovský, R., D. Schwarz. E. Janoušová and T. Kašpárek. (2016). Random subspace ensemble artificial neural networks for first-episode schizophrenia classification,Federated Conference on Computer Science and Information Systems (FedCSIS), Gdansk, pp.317-321.DOI:10.15439/2016F333.

Wandekoken, E.D., F.M. Varejão, R. Batista and T.W. Rauber. (2011). Support vector machine ensemble based on feature and hyperparametervariation for real-world machine fault diagnosis, soft computing in industrial applications, Advances in Intelligent and Soft Computing, Springer, 96, 271-282. https://doi.org/10.1007/978-3-642-20505-7_24.

Witten, I.H and E. Frank. (2005). Data Mining: Practical machine learning tools and techniques, San Francisco: CA: ELSEVIER, 2nd ed., chapter.7 and 10.

Huang, X and L. Zhang. (2013). An SVM ensemble approach combining spectral, structural, and semantic features for the classification of high-resolution remotely sensed imagery, IEEE Transactions on Geoscience and Remote Sensing, 51(1), 257-272. doi: 10.1109/TGRS.2012.2202912.

Yang, BS., X. Di and T. Han. (2008). Random forests classifier for machine fault diagnosis, Journal of Mechanical Science and Technology, 22(9), 1716–1725. https://doi.org/10.1007/978-1-84628-814-2_82.

Yu, Z., L. Li, J. Liu and G. Han. (2015). Hybrid adaptive classifier ensemble, IEEE Transactions on Cybernetics, 45(2), 177-190. doi: 10.1109/TCYB.2014.2322195.

Reviewers for Journal of Geomatics, Volume 12 No. 1 and 2

Editorial Board places on record its sincere gratitude to the following peers for sparing their valuable time to review papers of the Journal of Geomatics, Volume 12.

Dr. A.S. Rajawat
Chief Editor

Mr Amitabh	Mr S Manthira Moorthi	Mr KN Chaudhari
Dr CP Singh	Dr Sameer Saran	Mr JG Patel
Mr Manish Parmar	Mr Hrishikesh Kumar	Mr Ritesh Agrawal
Mr TVR Murthy	Dr Sreejith KM	Dr I Yilmaz
Dr PLN Raju	Dr C Prakasam	Dr DR Rajak
Mr J Venkatesh	Dr Sandip Oza	Prof TO Idowu
Mr C Patnaik	Dr. Shard Chander	Prof KK Sharma
Mr RJ Bhanderi	Prof Milap Chand Sharma	Prof AL Ramanathan
Dr Alpana Shukla	Dr Sheetal H Shukla	Dr Pratima Singh
Dr Abha Chhabra	Mr Sudhanshu Raghubanshi	Dr Kaushik Gopalan
Dr I.V. Muralikrishna	Mr TP Srinivasan	Prof Anupam Kumar Singh
Dr Markand Oza	Dr VN Sridhar	Mr KLN Sastry
Mr Pankaj Bodani	Dr TJ Majumdar	Dr CM Kishtawal

Author Index

INDIAN SOCIETY OF GEOMATICS: AWARDS

National Geomatics Award for Excellence

This award has been instituted to recognize outstanding and conspicuously important contribution in promoting geomatics technology and applications at the country level. The contributions should have made major impact on the use of this technology for national development.
Areas of contribution considered for the award are:

1. Geographical Information System
2. Global Positioning System
3. Photogrammetry
4. Digital Cartography
5. Applications of Geomatics

The award shall consist of Rs. 50,000/- in cash, a medal and citation.

Eligibility

Any citizen of India, engaged in activities related to geomatics technology and its applications is eligible for this award. The prize is awarded on the basis of work primarily done in India.

The age limit for awardees is 45 years or above as on June 30 of the year of award.

Selection

A duly constituted Award Committee will evaluate all nominations received. The committee shall consist of eminent experts in the field of geo-spatial technology, to be identified by the Executive Council, ISG. The committee shall forward selected name/s to ISG – EC for approval and announcement. Apart from those persons, whose nominations have been received, the Committee may consider any person or persons who, in their opinion, have made outstanding contributions to development of geo-spatial technology and applications.

The award can be withheld in any year if, in the opinion of the committee, no candidate is found suitable in that particular year.

Presentation of the Award

The award shall be presented during the Annual Convention of ISG. Local Hospitality shall be taken care by ISG & Air fare (low cost) may be reimbursed if awardees request for it.

How to make Nomination

The nominations can be proposed by Head of a major research institute/ centre; Vice-Chancellor of a university; Secretary of Government Scientific Departments; President of a National Academy, President, Indian Society of Geomatics / Indian Society of Remote Sensing / Indian National Cartographic Association / ISG fellow or two life members of the society with more than 10-year-old membership.

A candidate once nominated would be considered for a total period of two years. Nomination should be sent in the prescribed format to Secretary, ISG.

The last date for receiving nominations shall be September 30 or otherwise extended.

Format for nomination of Geomatics Award for Excellence

1. Name of the Nominee
2. Postal Address
3. Academic Background (Bachelor degree onwards)
4. Field of Specialisation
5. Important positions held (in chronological order)
6. Professional Experience including foreign assignments.
7. Important Awards / Honours
8. Important Publications/Patents: (A set of ten most important publications to be enclosed with this form)
9. Contributions of Nominee based on which the nomination is sent (in 1000 words, also provide a statement in 50 words which may be used for citation.):
10. Other Relevant Information:

Proposer:

Signature
Name
Address
Phone/ Fax
E-mail
Life Membership No. (in case of ISG Member):

Place & Date

Endorsed by (in case nomination is by 2 ISG Life members)

Signature
Name
Address
Phone/ Fax
E-mail
Life Membership No. (in case of ISG Member):

Place & Date
(The proposer should give a brief citation of the nominee's work)

National Geomatics Award

National Geomatics Award to be given each year: a) for original and significant contribution in Geomatics technology, b) for innovative applications in the field of Geomatics. Each award comprises a medal, a citation and a sum of Rs 25,000/- The guidelines for these awards are available on ISG website.

ISG Chapter Award for Best Performance

The best chapter award will be given to an active chapter of Indian Society of Geomatics, which has made significant contribution to further the mandate and goal of the society. The award consists of a citation and medal

President's Appreciation Medal for Contribution to the ISG

This award will be given to a member of the society, who has made noteworthy contribution to the growth of the ISG (its main body or any chapter). The Award consists of a Medal and a Citation.

Prof. Kakani Nageswara Rao Endowment Young Achiever Award

Indian Society of Geomatics instituted a new award from year 2013 named "Prof. Kakani Nageswara Rao Endowment Young Achiever Award", to encourage young researchers/scientists/academicians pursuing research in the field of geospatial technology/applications. The award carries a cash prize of Rs. 10,000/- along with a citation.

NATIONAL GEOMATICS AWARD

Indian Society of Geomatics has instituted two National Geomatics Awards to be given each year for (a) Original and significant contribution in Geomatics technology, (b) Innovative application(s) in the field of Geomatics. Each award comprises a medal, a citation and a sum of Rs. 25,000/-.

The guidelines for the award are as under

Areas of contribution considered for the award (both technology and applications)

1. Geographical Information System
2. Global Positioning System
3. Photogrammetry
4. Digital Cartography
5. Remote Sensing

Eligibility

Any citizen of India engaged in scientific work in any of the above-mentioned areas of research is eligible for the award.

The awards are to be given for the work largely carried out in India.

- First award will be given for original contribution in the field of Geomatics technology supported by publications in a refereed journal of repute.
- Second award will be given for carrying out innovative application(s). Supported by publications in rear reviewed Journals of repute.
- The contribution for the first award should have been accepted by peers through citation of the work.
- Work based on the applications of existing technologies will not be considered for the first award.
- The work should have made impact on the overall development of Geomatics.

How to Send Nomination

Nominations should be sent in the prescribed format, completed in all aspects to the Secretary, Indian Society of Geomatics, Space Applications Centre Campus, Ahmedabad 380 015 by August 31, 2017.

Selection Process

An expert committee, consisting of at least three members, constituted by the Executive Council of the Indian Society of Geomatics, will scrutinize the nominations and recommend the awardees' names to the Executive Council. The Council will decide on the award based on the recommendations.

FORMAT FOR AWARD NOMINATION

1. Name of the Candidate:
2. Present Position:
3. Positions held earlier (chronological order):
4. Academic qualifications (Bachelor's degree onwards):
5. Names of at least three Indian Scientists/Technologist in the area as possible referees *:
6. Brief write up on the work (500 words) for which award is claimed:
7. Publication(s) on the above work (reprint(s) to be enclosed):
8. List of other publications of the candidate:
9. Citation of the work for which award is claimed:
10. Impact of the work (for which award is claimed) on the development in the field of Geomatics (500 words):
11. Whether the work has already won any award? If so, give details:

The Applications in the above format (five copies) should be submitted (by Registered Post or Speed Post) to

The Secretary, Indian Society of Geomatics,
Space Applications Centre Campus,
Ahmedabad-380015

so as to reach by September 30, 2018

*ISG is, however, not bound to accept these names and can refer the nomination to other experts/peers

INDIAN SOCIETY OF GEOMATICS: FELLOWS

Shri Pramod P. Kale, Pune
Dr George Joseph, Ahmedabad
Dr A.K.S. Gopalan, Hyderabad
Dr Prithvish Nag, Varanasi
Dr Baldev Sahai, Ahmedabad
Shri A.R. Dasgupta, Ahmedabad
Dr R.R. Navalgund, Bengaluru
Shri Rajesh Mathur, New Delhi
Dr Ajai, Ahmedabad
Prof P. Venkatachalam, Mumbai
Dr Shailesh Nayak
Prof I.V. Murli Krishna
Prof SM Ramasamy, Tiruchirapalli
Dr Ashok Kaushal, Pune
Shri A.S. Kiran Kumar, Bengaluru
Prof. P.K. Verma, Bhopal
Maj. Gen. Siva Kumar, Hyderabad

INDIAN SOCIETY OF GEOMATICS: PATRON MEMBERS

P-1 Director, Space Applications Centre (ISRO), Jodhpur Tekra Satellite Road, Ahmedabad - 380 015
P-2 Settlement Commissioner, The Settlement Commissioner & Director of Land Records-Gujarat, Block No. 13, Floor 2, Old Sachivalay, Sector-10, Gandhinagar – 382 010
P-3 Commissioner, Mumbai Metropolitan Region Development Authority, Bandra-Kurla Complex, Bandra East, Mumbai - 400 051
P-4 Commissioner, land Records & Settlements Office, MP, Gwalior - 474 007
P-5 Director General, Centre for Development of Advanced Computing (C-DAC), Pune University Campus, Ganesh Khind, Pune - 411 007
P-6 Chairman, Indian Space Research Organization (ISRO), ISRO H.Q., Antariksha Bhavan, New BEL Road,Bengaluru 560 231
P-7 Director General, Forest Survey of India, Kaulagarh Road, P.O. I.P.E., Dehra Dun – 248 195
P-8 Commissioner, Vadodara Municipal Corporation, M.S. University, Vadodara - 390 002
P-9 Director, Centre for Environmental Planning and Technology (CEPT), Navarangpura, Ahmedabad - 380 009
P-10 Managing Director, ESRI INDIA, NIIT GIS Ltd., 8, Balaji Estate, Sudarshan Munjal Marg, Kalkaji, New Delhi - 110 019
P-11 Director, Gujarat Water Supply and Sewerage Board (GWSSB), Jalseva Bhavan, Sector – 10A, Gandhinagar - 382 010
P-12 Director, National Atlas & Thematic Mapping Organization (NATMO), Salt Lake, Kolkata - 700 064
P-13 Director of Operations, GIS Services, Genesys International Corporation Ltd., 73-A, SDF-III, SEEPZ, Andheri (E), Mumbai - 400 096
P-14 Managing Director, Speck Systems Limited, B-49, Electronics Complex, Kushiaguda, Hyderabad - 500 062
P-15 Director, Institute of Remote Sensing (IRS), Anna University, Sardar Patel Road, Chennai - 600 025
P-16 Managing Director, Tri-Geo Image Systems Ltd., 813 Nagarjuna Hills, PunjaGutta, Hyderabad - 500 082
P-17 Managing Director, Scanpoint Graphics Ltd., B/h Town Hall, Ashram Road, Ahmedabad - 380 006
P-18 Secretary General, Institute for Sustainable Development Research Studies (ISDRS), 7, Manav Ashram Colony, Goplapura Mod, Tonk Road, Jaipur - 302 018
P-19 Commandant, Defense institute for GeoSpatial Information & Training (DIGIT), Nr. Army HQs Camp, Rao Tula Ram Marg, Cantt., New Delhi - 110 010
P-20 Vice President, New Rolta India Ltd., Rolta Bhavan, 22nd Street, MIDC-Marol, Andheri East, Mumbai - 400 093
P-21 Director, National Remote Sensing Centre (NRSC), Deptt. of Space, Govt. of India, Balanagar, Hyderabad - 500 037
P-22 Managing Director, ERDAS India Ltd., Plot No. 7, Type-I, IE Kukatpalli, Hyderabad - 500 072
P-23 Senior Manager, Larsen & Toubro Limited, Library and Documentation Centre ECC Constr. Gp., P.B. No. 979, Mount Poonamallee Road, Manapakkam, Chennai - 600 089.
P-24 Director, North Eastern Space Applications Centre (NE-SAC), Department of Space, Umiam, Meghalaya 793 103
P-25 Progamme Coordinator, GSDG, Centre for Development of Advanced Computing (C-DAC), Pune University Campus, Pune – 411 007
P-26 Chief Executive, Jishnu Ocean Technologies, PL-6A, Bldg. No. 6/15, Sector – 1, Khanda Colony, New Panvel (W), Navi Mumbai – 410 206
P-27 Director General, A.P. State Remote Sensing Applications Centre (APSRAC), 8th Floor, "B" Block, Swarnajayanthi Complex, Ameerpet, Hyderabad- 500 038
P-28 Director, Advanced Data Processing Res. Institute (ADRIN), 203, Akbar Road, Tarbund, Manovikas Nagar P.O., Secunderabad –500 009
P-29 Managing Director, LEICA Geosystems Geospatial Imaging Pvt. (I) Ltd., 3, Enkay Square, 448a Udyog Vihar, Phase-5, Gurgoan- 122 016
P-30 Director, Defense Terrain Research Limited (DTRL), Ministry of Defense, Govt. of India, Defense Research & Development Organisation, Metacafe House, New Delhi – 110 054
P-31 Chairman, OGC India Forum, E/701, Gokul Residency, Thakur Village, Kandivali (E), Mumbai – 400 101
P-32 Managing Director, ML Infomap Pvt. Ltd., 124-A, Katwaria Sarai, New Delhi – 110 016
P-33 Director, Rolta India Limited, Rolta Tower, "A", Rolta Technology Park, MIDC, Andheri (E), Mumbai – 400 093
P-34 Director, State Remote Sensing Applications Centre, Aizawl – 796 012, Mizoram

Instructions for Authors

The journal covers all aspects of Geomatics – geodata acquisition, pre-processing, processing, analysis and publishing. Broadly this implies inclusion of areas like GIS, GPS, Photogrammetry, Cartography, Remote Sensing, Surveying, Spatial Data Infrastructure and Technology including hardware, software, algorithm, model and applications. It endeavors to provide an international forum for rapid publication of developments in the field – both in technology and applications.

A manuscript for publication must be based on original research work done by the author(s). It should not have been published in part or full in any type of publication nor should it be under consideration for publication in any periodical. Unsolicited review papers will not be published.

The Editorial Board or the Indian Society of Geomatics is not responsible for the opinions expressed by the authors.

Language

The language of the Journal will be English (Indian). However, manuscripts in English (US) and English (British) are also acceptable from authors from countries located outside India.

Manuscript Format

Each paper should have a title, name(s) of author(s), and affiliation of each of the authors with complete mailing address, e-mail address, an abstract, four to six keywords, and the text. The text should include introduction/background, research method, results, discussion, followed by acknowledgements and references. The main text should be divided in sections. Section headings should be concise and numbered in sequence, using a decimal system for subsections. Figures, images and their captions should be inserted at appropriate points of the text. Figures, images and tables should fit in two column format of the journal. If absolutely necessary, figures, images and tables can spread across the two columns. Figures and images, however, should not exceed half a page in height. A title should be provided for each Table, Image and Figure. All figures and images should be in 600 dpi resolution and sized as per column/margin width. Authors must ensure that diagrams/figures should not lose easy readability upon reduction to column size. The SI (metric) units and international quantities should be used throughout the paper. In case measurements are given in any other system, equivalent measurements in SI (metric) units should be indicated in brackets.

Use MS Word with English (UK/US) or English (Indian) dictionary. The page size should be A4 paper, with 2 cm margin on all sides. Title, authors and affiliation should be centred. Abstract should be justified across margins. The manuscript text should be in two columns of 8.2 cm each with a gutter of 6mm between them. Use only Times New Roman fonts. Title should be 12 points bold. Authors and affiliation should be 9 points. All other text including headings should be 10 points. Heading numbering scheme should be decimal e.g. 1, 1.1, 1.2.3, etc. Headings should be in bold.

Normally length of a published paper should be about 6-10 pages in A4 size including figures. Use of illustrations in colour should be restricted and resorted to only where it is absolutely necessary and not for enhancing the look of the paper. If the number of colour illustrations exceeds five, authors' institution may be asked to reimburse the extra cost involved, which at current rates is about Rs. 2500 per coloured figure/diagram/plate/illustration.

Submission of Manuscript

Submissions should be in electronic form via email. The manuscript may be sent by email to drajai1953@gmail.com. In exceptional cases hard copy submission in camera ready form may be allowed with the prior permission of the Chief Editor. Submission in any other form will be returned to the author. To speed up the review process, authors are advised to provide a list of three probable reviewers with their institutional address and e-mail IDs.

Guidelines for Citing References

Names of all cited publications should be given in full. No abbreviations should be used. Following procedure is to be adopted.

Journal Publications

Bahuguna, I.M. and A.V. Kulkarni (2005). Application of digital elevation model and orthoimages derived from IRS-1C Pan stereo data in monitoring variations in glacial dimensions, Journal of the Indian Society of Remote Sensing, 33(1), 107- 112. (to be referred to in the text as Bahuguna and Kulkarni (2005) or if more than two sets of authors are to be referred to, as (Bahuguna and Kulkarni, 2005; Jain et al., 1994)) When more than two authors are to be referred to, use Jain et al. (1994). However, in References, all authors are to be mentioned.

Publication in a Book

Misra, V.N. (1984). Climate, a factor in the rise and fall of the Indus Civilization – Evidence from Rajasthan and Beyond in Frontiers of the Indus Civilization (B.B. Lal and S.P. Gupta: Chief Editors) Books and Books, New Delhi, pp. 461-489

Papers Published in Seminar/ Symposium Proceedings

Jain, A., A.R. Shirish, M. Das, K. Das, M.C. Porwal, and P.S. Roy (1994). Remote Sensing and Geographic Information System – An approach for the assessment of biotic interference in the forest ecosystem. Proceedings. 15th Asian Conference on Remote Sensing, Bangalore, November 17-23, 1994, pp. 65-72.

Books

Possehl, Gregory L. (1999). Indus Age: The beginnings. Oxford and IBH Publishing Corporation, New Delhi.

Reviewing

Each paper will be reviewed by three peers. Papers forwarded by members of the Editorial or Advisory Boards along with their comments would get processed faster and may be reviewed by two referees only.

Sample format for Authors is available in downloadable form at ISG website: www.isgindia.org/JOG/Sample_format.doc

Copyright

The copyright of the paper selected for publication will rest with the Indian Society of Geomatics. Corresponding author shall be required to sign a copyright assignment form, on behalf of all authors, once the paper is selected for publication. Authors are, however, at liberty to use this material elsewhere after obtaining permission from the Indian Society of Geomatics.

If the authors have used any copyright material in their manuscript, it is understood that they have obtained permission from the owner of the copyright material and they should convey the same along with the manuscript to the Chief Editor.

Certificate of Original Work

The authors will also provide a certificate that the paper is an original work, not published or being considered for publication elsewhere.

In the event the certificate turns out to be false, the Journal shall ban the author(s) from publishing in the Journal for a period of five years and inform the same to all other related publications.

Reprints

Authors will be allowed to download the (PDF) of their paper from ISG Website www.isgindia.org, No hard copy reprints will be provided

Journal of Geomatics

Advertisement Rates

	1 Issue	4 Issues
Back Cover Page in colour	**Rs. 25,000**	**Rs. 80,000**
Inside Cover Page in colour	**Rs. 20,000**	**Rs. 64,000**
Full Page inside in colour	**Rs. 15,000**	**Rs. 48,000**
Full Page inside in B/W	**Rs. 10,000**	**Rs. 32,000**

Advertisement Details

Mechanical Details
Double Spread/Center Spread (42 x 29.7) cm
Full page bleed (21 x 29.7) cm
Full page non-bleed (19 x 27.7) cm

Art Requirements

Negatives: Art must be right reading, emulsion, down. Film must be supplied in one piece per color, each identified by color. Camera-ready art is accepted for black & White adds; however, film is preferred. Electronic Files are also accepted.

Electronic File Requirements: All material must be received before ad close dates.

Software: Adobe illustrator 9.0 (saved as EPS). Adobe Photoshop CS (saved as EPS or TIFF). Please convert higher versions down. If you can only supply an IBM format, the file must be in viewable EPS or TIFF format with fonts embedded as that format.

Colour Ads: Colour separations must be provided, right reading, emulsion down. Please note that files using RGB or Pantone colours (PMS) must be converted to CMYK before we receive files.

Indian Society of Geomatics

To,
The Secretary, Indian Society of Geomatics
6202, Space Applications Centre (ISRO)
AHMEDABAD – 380 015. INDIA

Sir,
I want to become a Member/ Life Member/ Sustaining Member/ Patron Member/ Foreign Member/ Student Member of the Indian Society of Geomatics, Ahmedabad for the year _____. Membership fee of Rs. _____ /- is being sent to you by Cash/ DD/ Cheque. (In case of DD/ Cheque No._____dated_____drawn on Bank _____ . I **agree to abide by the Constitution of the Society.**

Date:

Place: **Signature**

- Name: Mr/Ms/Mrs/Dr_____
- Address: _____

_____PIN: _____
Phone: _____ Fax: _____Email: _____ • Date of Birth _____
•Qualifications_____
__
- Specialisation: _____
- Designation: _____ Organisation. _____
- Membership in other Societies: _____
- Mailing Address: _____

_____PIN: _____

Proposed by:
(Member's Name and No)

Signature of Proposer

For Office Use: A/P/L Member No.		Receipt No.		Date:	

Indian Society of Geomatics (ISG), Room No. 6202 Space Applications Centre (ISRO), Ahmedabad-380015, Gujarat. Url: www.isgindia.org Phone: +91-79 26916202
Email: secretary@isgindia.org or sasharma@sac.isro.gov.in Fax +91-79-26916287

MEMBERSHIP FEES

Sr. No.	Membership	Life/Patron Membership fees		Annual Subscription
	Category	₹ Indian	US $ Foreign	₹ Indian
1.	Annual Member	10	---	300
2.	Life Member a) Admitted below 45 years of age	2500	250	
	b) Admitted after 45 years of age	2000	200	
3.	Sustaining Member	---	---	2000
4.	Patron Member	50000	3000	---
5.	Student Member	10	---	100

MEMBERSHIP GUIDELINES

- Subscription for Life Membership is also accepted in two equal instalments payable within duration of three months, if so desired by the applicant. In such a case, please specify that payment will be in instalments and also the probable date for the second instalment (within three months of the first instalment).
- A Member of the Society should countersign application of membership as proposer.
- Subscription in DD or Cheque should be made out in the name of **'Indian Society of Geomatics'** and payable at Ahmedabad.
- Direct deposit in ISG A/Cs must include bank fee RS. 25/- for cash payment.
- Financial year of the Society is from April 1 to March 31.
- For further details, contact Secretary, Indian Society of Geomatics at the address given above.
- ISG has chapters already established at the following places. Ahmedabad, Ajmer, Bhagalpur, Bhopal, Chennai, Dehradun, Delhi, Hissar, Hyderabad, Jaipur, Ludhiana, Mangalore, Mumbai, Mysore, Pune, Shillong, Trichi, Srinagar, Vadodara, Vallabh Vidya Nagar, Visakhapatnam and Trivandrum. Applicants for membership have the option to contact Secretary/Chairman of the local chapter for enrolment. Details can be found at the website of the Society: www.isgindia.org.
- Journal of the Society will be sent to Life Members by softcopy only.

Indian Society of Geomatics (ISG), Room No. 6202 Space Applications Centre (ISRO),

Ahmedabad-380015, Gujarat. Url: www.isgindia.org Phone: +91-79 26916202

Email: secretary@isgindia.org or sasharma@sac.isro.gov.in Fax +91-79-26916287

Geomatics Revealed

IGiS

Integrated GIS & IP Software

VERSION 2.0

MAKE IN INDIA

National Awards on Technology
By The Former President of India,
Dr. A. P. J. Abdul Kalam

Launch of IGiS Version 2.0
By Padam Shri AS Kiran Kumar, Chairman, ISRO and
Shri Tapan Mishra, DIRECTOR, SAC, ISRO.

What's new in IGiS

IGiS Version 2.0 is full of enhancements which you'll appreciate every day. New advanced GIS/IP and SAR modules are vital now a days. New COM Based Architecture makes you even more productive. The more you do with IGiS Version 2.0, the more you'll wonder how you ever did without it.

Enhancements in IGiS Version 2.0

- Advanced GIS / Image Processing
- Microwave SAR Analysis
- Meteorological Analysis
- COM Based Scalable Architecture
- New Ribbon Bar GUI
- Python Customization
- OGC Standards

Product Development Partner

इसरो isro
Government of India | Department of Space
Indian Space Research Organisation - (ISRO)

SGL Scanpoint Geomatics Ltd.
www.scanpointgeomatics.com

Scanpoint Geomatics Ltd.
Corporate Office : 12, Abhishree Corporate Park, Iskcon - Ambli Road, Ahmedabad - 380 058. Gujrat (India)
[P] +91 2717 297096-98 [F] +91 2717 297039 [E] info@scanpointgeomatics.com [W] www.scanpointgeomatics.com

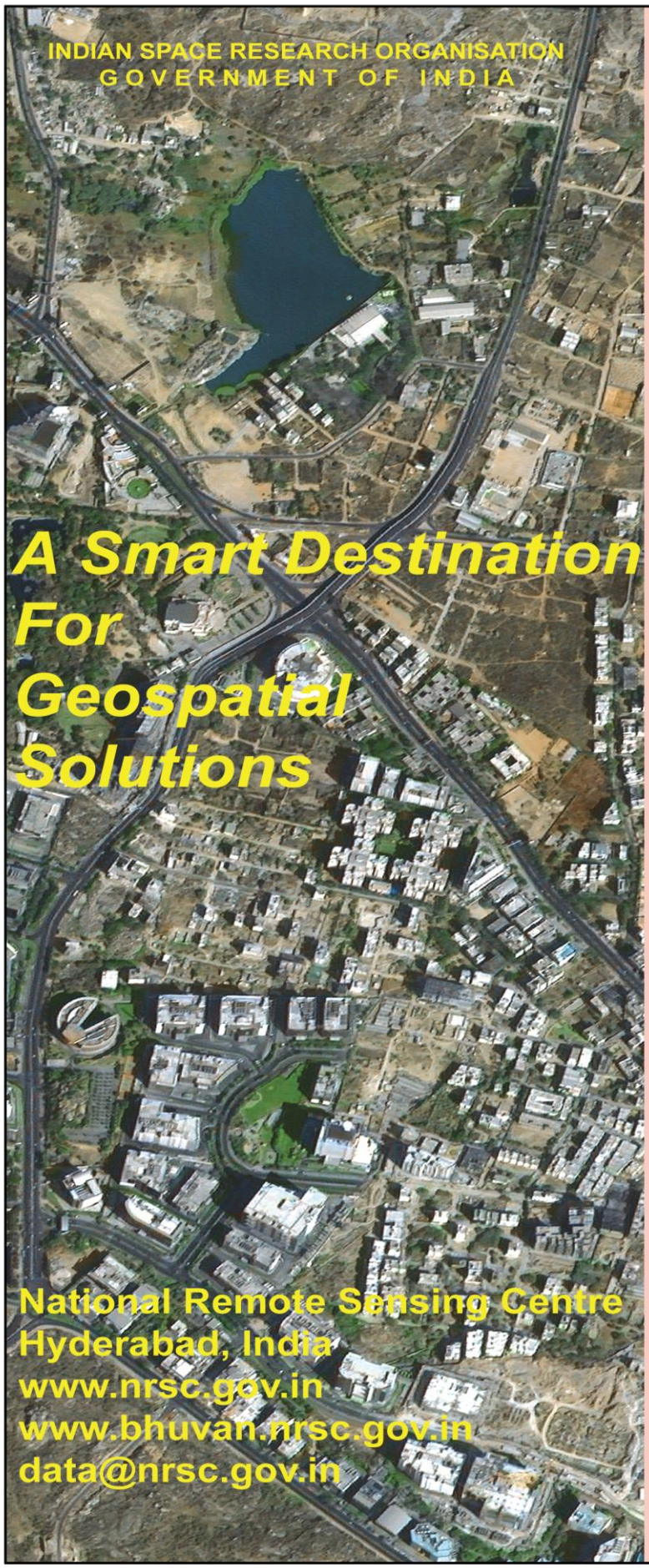

A Smart Destination For Geospatial Solutions

National Remote Sensing Centre
Hyderabad, India
www.nrsc.gov.in
www.bhuvan.nrsc.gov.in
data@nrsc.gov.in

nrsc

इसरो isro

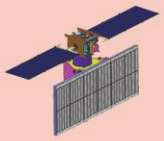

Only Organization in the Country to Acquire & Supply Satellite Data to Users

Aerial Acquisition for Specific User Demands & Disaster Management Support

Open Data & Value Added Products Dissemination Through Bhuvan

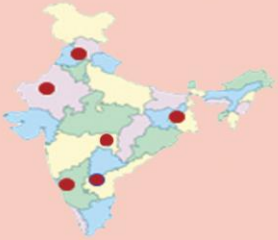

Region Specific Solutions

Capacity Building in Remote Sensing Applications